Genetic regulation of the flowering time of Brassica rapa L.

AYASHA AKTER

(Degree)
博士（農学）

(Date of Degree)
2020-09-25

(Date of Publication)
2021-09-01

(Resource Type)
doctoral thesis

(Report Number)
甲第7888号

(URL)
https://hdl.handle.net/20.500.14094/D1007888

Doctoral Dissertation

Genetic regulation of the flowering time of *Brassica rapa* L.

(*Brassica rapa* 種の開花時期の遺伝的制御)

AYASHA AKTER

July 2020

Kobe University

Graduate School of Agricultural Science

Chapter I

General Introduction

During the life cycle of plants, the change from vegetative to reproductive growth is a major developmental transition in flowering plants. Flowering is the process where a transformation of the vegetative stem primordia into floral primordia occurs due to biochemical changes. In most plants, once the transition from vegetative to reproductive growth begins, it cannot be reversed. Thus, the proper timing of this transition is advantageous to ensuring the successful propagation of offspring. Internal (endogenous cues) and external (environmental stimuli) factors both play important roles in flowering time. As plants are sessile organisms, plants are greatly affected by environmental conditions such as day length (photoperiodism) and temperature. Photoperiodism is controlled via the photoreceptor proteins phytochrome and/or cryptochrome, responsible for sensing red/far-red and blue light, respectively (Más et al. 2000). As daylight and night-time are part of a continuous 24-hour cycle, increases to the length of night-time subsequently shorten the length of daylight exposure that a plant receives. As such, we typically refer to photoperiod requirements as either long day (LD) or short day (SD), with respect to the length of time that a plant receives daylight. As this photoperiod signal is also tied to the annual cyclical seasonal changes, LD, coinciding with the spring and summer seasons, and SD, associated with the autumn and winter seasons both play roles in the floral development of several plant species (Corbesier et al. 2005). A further distinction may be made within such requirements, classifying them as either facultative or obligate photoperiod requirements. In contrast to obligate photoperiod requirements, where obligate photoperiodic plants absolutely require a long or short enough critical night length prior to flowering, facultative photoperiodic plants are more likely to flower when kept in the proper photoperiodic conditions. The regulation of flowering to changes in temperature is known as vernalization. Vernalization is the process, which accelerates flowering in response to the prolonged cold of winter. Many plants have a vernalization requirement, that is, they actively repress flowering until after an exposure to prolonged cold, in order to align seed production with the favorable environmental conditions of spring. The presence of certain photoperiods and ambient temperatures after vernalization are also important (Henderson and Dean, 2004; Kim et al. 2009).

Brassica is a genus in the family of Brassicaceae and includes 37 species of flowering plants, many of which are important both economically and as agricultural crops with members such as broccoli, brown mustard, brussels sprouts, cabbage, cauliflower, Chinese cabbage,

kale, kohlrabi, rape, rutabaga, and turnip. The crops from this genus are sometimes known as cole crops. Three members of the genus *Brassica*, *Brassica rapa*, *Brassica nigra*, and *Brassica oleracea* are denoted as the A, B, and C genomes, respectively. These three species share a unique genomic relationship, known as the "Triangle of U" (U 1935). Allotetraploids between these three species contain two complete diploid genomes derived from the two different parental species, one diploid genome from each parent. The agriculturally important allotetraploid *Brassica napus* (canola or rapeseed) is derived from the interspecific hybridization of the A and C genomes of *B. rapa* and *B. oleracea*, respectively. With the advent of genomic sequencing, the genetic relationship between three diploid species, *B. rapa*, *B. nigra*, and *B. oleracea*, in the *Brassica* genus has been elucidated further, revealing that they are descended from a common hexaploid ancestor that underwent a whole genome triplication (WGT) event roughly 15.9 million years ago (MYA), with speciation divergence occurring approximately 4.6 MYA (Cheng et al. 2014)

Different cultivated varieties of the diploid species of *B. rapa* exhibit extreme developmental and morphological diversity, and from the organs consumed they are generally divided into leafy, turnip, and oil types. *B. rapa* crops are normally grown in two seasons, autumn and spring and their flowering habits are generally controlled by day length and/or temperature. *B. rapa* is a facultative LD plant. Although LD photoperiod conditions accelerate its flowering, it can also flower under SD photoperiod conditions (Falik et al. 2014). *B. rapa* is a leafy vegetable and flowering time is a very important developmental trait because bolting can occur before plants reach the harvest stage such as Chinese cabbage and pak choi, which markedly impairs the product value; this mostly occurs due to low temperatures at the beginning of cultivation and longer day lengths during the growing period in the spring season. For breeding late-bolting leafy *B. rapa* cultivars, the genetic dissection of flowering time control is very important. *B. oleracea* (cabbage) has become established as an important human food and one of the most important vegetable crops in the Brassicaceae family, which is plant-vernalization-responsive type (Ito et al. 1966; Friend, 1985). Vernalization can be classified into two types, seed-vernalization-responsive and plant-vernalization-responsive according to the age of the plant at which it vernalizes in response to low temperature (Friend, 1985). In the plant-vernalization-responsive type, biennial plants grow vegetatively in the first year and flower in the following year after winter. Cabbage normally requires low temperatures about 6 to 8 weeks in duration that is initiated at the stage of 7 to 9 leaves or when the stem diameter reaches 6 mm for flowering initiation (Ito et al. 1966; Friend, 1985). The differences in the

mechanisms involved in vernalization and flowering between seed- and plant-vernalization-responsive types is of agronomic and scientific interest to understand. As such attempts have been made to transfer the seed-vernalization character from Chinese cabbage (*B. rapa*) into cabbage (*B. oleracea*) (Hossain et al. 1990), and the plant-vernalization character from cabbage (*B. oleracea*) into Chinese cabbage (*B. rapa*) (Shea et al. 2018). *B. napus* is an important oilseed crop in the temperate regions of the world. The production of seed in canola depends on flowering time, thus the adaptation of flowering time is important for breeding. In *B. napus*, the natural variation in flowering time in response to vernalization was characterized into three groups, spring type, winter type, and semi-winter type (Raman et al. 2016).

A. thaliana is a small dicotyledonous species used as a model organism for studying plant biology belonging to the family Brassicaceae. In *A. thaliana*, over 180 genes are implicated in flowering time control and these genes are categorized into six major pathways that control flowering time, including the photoperiod/circadian clock pathway, vernalization pathway, ambient temperature pathway, age pathway, autonomous pathway, and gibberellin pathway (Srikanth and Schmid, 2011; Andres and Coupland, 2012). It is a much-studied model for vernalization and the transition to the reproductive phase of *A. thaliana* occurs by two related events, the bolting transition (flower stalk elongates) and the floral transition (first flower appears). Brassicaceae includes many perennial species such as *Arabis alpina* and *Arabidopsis halleri*, and the respective *A. thaliana* orthologous gene is key regulator of flowering transition with seasonal gene expression (Pouteau and Albertine, 2009; Wang et al. 2009; Aikawa et al. 2010).

Two key genes, *FRIGIDA* (*FRI*) and *FLOWERLING LOCUS C* (*FLC*), have been identified by map-based cloning of naturally occurring early flowering accessions of *A. thaliana*. Rapid cycling accessions have mutations in *FRI*, and loss-of-function mutations have originated independently (Johanson et al. 2000). The functional *FRI* gene acts upstream of the *FLC* expression within the vernalization pathway. FRI acts as a scaffold protein interacting with FRIGIDA LIKE 1 (FRL1), FRIGIDA ESSENTIAL 1 (FES1), SUPPRESSOR OF FRIGIDA 4 (SUF4), and FLC EXPRESSOR (FLX). These proteins assemble to form a large protein complex, FRIGIDA-containing complex (FRI-C), with SUF4 directly binding to the *FLC* promoter and FRI-C activating *FLC* expression (Choi et al. 2011).

The *FLC* gene is a floral repressor that contains a MADS box transcriptional regulator protein domain and maintains a plant's vegetative growth until exposure to prolonged cold is experienced. Within the vegetative apical meristem, *FLC* interacts with several important

genes during vegetative growth by inhibiting the activation of a set of genes required for the transition of the apical meristem to inflorescence, ultimately determining the plant's reproductive fate (Sheldon et al. 1999; Michaels and Amasino, 1999; Whittaker and Dean, 2017). At the molecular level, *FLC* blocks flowering by binding to genes that promote flowering and repressing their transcription. Initially, three flowering-time genes, *FLOWERING LOCUS T* (*FT*), *SUPPRESSOR OF OVEREXPRESSSON OF CONSTANS 1* (*SOC1*), and *FLOWERING LOCUS D* (*FD*) were reported to be targeted by FLC, with FLC binding to the promoters of *SOC1* and *FD* and to the first intron of *FT* (Searle et al. 2006; Helliwell et al. 2006). Later, more putative *FLC* targeted genes were identified at the whole genome level by chromatin immunoprecipitation sequencing (ChIP-seq) using antiserum raised against the FLC protein without the conserved MADS domain. About 500 *FLC* binding sites, mostly located in the promoter region of genes containing one CArG box (the known target of MADS-box proteins) were identified (Deng et al. 2012). Two genes (*FT* and *SOC1)* that function downstream of the flowering activator CONSTANS (CO) in the photoperiod pathway were identified as being negatively regulated by *FLC* (Kim et al. 2009; Andres and Coupland, 2012).

Epigenetic regulation is defined as changes in gene activities that are inherited through cell divisions without alteration of the DNA sequence. Epigenetic regulation is crucial for the development and adaptation of plants to a changing environment (Richards, 2011; Fujimoto et al. 2012). DNA methylation and histone modification are the best examples of epigenetic modifications. The vernalization response is one example of epigenetic regulation, and *FLC* expression is regulated by chromatin modification (Dennis and Peacock, 2007; Groszmann et al. 2011). *FLC* is expressed before prolonged cold exposure, and H3K4me3 or H3K36me3 is associated with activation of *FLC* expression (Ko et al. 2010).

Plant homeodomain (PHD) finger protein (*VERNALIZATION INSENSITIVE 3,* VIN3) induces during the exposure to cold, which acts to establish the initial repression of *FLC* (Sung and Amasino, 2004). Moreover, VIN3, VRN5, VIN3/VRN5-like 1 (VEL1) interact with VRN2 protein and form PHD-PRC2 complex (Sung and Amasino, 2004; Wood et al. 2006; De Lucia et al. 2008). Vernalization reduces the *FLC* repression, which is associated with the enrichment of H3K27me3 mediated by the PHD-PRC2 mechanism (De Lucia et al. 2008). During exposure to cold, H3K27me3 is enriched in chromatin at the transcription start sites of *FLC*, later H3K27me3 modification extends across the *FLC* gene due to warm temperature (Finnegan and Dennis, 2007). A stable maintenance of repression requires PRC2, although the initial

transcriptional repression of *FLC* is PRC2-independent (Gendall et al. 2001). After cold exposure the maintenance of *FLC* silencing under warm conditions is therefore mediated by PHD-PRC2 spreading H3K27me3 over the *FLC* locus. Additionally, LIKE HETEROCHROMATIN PROTEIN 1 (LHP1), associated with H3K27me3, and VRN1 are also required for the maintenance of stable *FLC* repression (Leavy et al. 2002; Sung et al. 2006; Mylne et al. 2006). The first intron, promoter region, and exon 1 are important for the regulation of *FLC* expression by prolonged cold treatments (Sheldon et al. 2002).

Advanced technologies such as tiling arrays or RNA-sequencing, use high-throughput sequencing to enable the discovery of long non-coding transcripts. It has been shown that some long non-coding RNAs (lncRNAs) are involved in the regulation of gene expression through interactions with associated proteins. In A. thaliana, cold induced long noncoding RNAs (lncRNAs) such as COOLAIR, COLDAIR, and COLDWRAP are involved in vernalization (Heo and Sung, 2011; Kim and Sung, 2017; Swiezewski et al. 2009). COLDAIR and COLDWRAP play a role in the recruitment of the PRC2 complex to *FLC* following cold exposure.

Recently, the whole genome sequences of the diploid species, *B. rapa*, *B. nigra*, and *B. oleracea*, and the allotetraploid species, *B. napus* and *B. juncea* have been determined. From these genome sequences, it is already known that there are multiple *FLC* paralogs in the genus *Brassica*. Four *FLC* paralogs, Bra009055 (*BrFLC1*), Bra028599 (*BrFLC2*), Bra006051 (*BrFLC3*), and Bra022771 (*BrFLC5*) were found in the reference genome of *B. rapa*, Chiifu-401-42, but Bra022771 is possibly a pseudogene because of deleted two exons .Two *BoFLC* (Bol008758, Bol043693) paralogs are found in the *B. oleracea* var. *capitata* homozygous line 02-12, while four *BoFLC* paralogs are found in TO1000DH3, a doubled haploid derived from a rapid cycling *B. oleracea*.

In *B. rapa*, several QTLs were identified for flowering time (VFR1, 2, and 3 in non-vernalized condition and FR1, 2, and 3 in vernalized condition) from a cross between an annual and a biennial oil seed cultivar (Teutonico and Osborn, 1994; Osborn et al. 1997), which covers the region of *BrFLC1* and *BrFLC2* (Kole et al. 2001; Schranz et al. 2002). Eight QTLs for flowering with one major QTL, which co-localized with *BrFLC2*, were detected using a multi-population derived from several parental lines (rapid cycling, Chinese cabbage, yellow sarson, pak choi, and a Japanese vegetable turnip variety) (Lou et al. 2007). QTL analyses also showed the co-localization of a major QTL with *BrFLC2* using other parental combinations between pak choi and yellow sarson (Zhao et al. 2010; Xiao et al. 2013). Over many years' QTL analysis

have shown a major QTL of flowering time co-localized with *BrFLC2*. QTL analysis was performed in two different conditions, greenhouse and open field using an F_2 population derived from a cross between an extremely late bolting line (Nou 6 gou, and PL6) and early bolting line (A9709) of Chinese cabbage. Five QTLs were detected, but within two condition QTLs did not map in the same position. Among the five QTLs, three QTLs were co-localized with *BrFTa* (greenhouse), *BrFLC1* (open field), and *BrFLC5* (open field) (Kakizaki et al. 2011). In Chinese cabbage, an F_2 population was derived from the cross of an early bolting commercial F_1 varieties, 'Early', and an extremely late bolting line, 'Tsukena No. 2', where QTLs for bolting time after vernalization co-localized with the late bolting alleles of *BrFLC2* and *BrFLC3.* In the extremely late bolting of 'Tsukena No. 2', large insertions were found in the first intron of *BrFLC2* and *BrFLC3*, suggesting that weak repression of *BrFLC2* and *BrFLC3* transcripts by vernalization results in these insertions (Kitamoto et al. 2014). In addition, this group successfully developed new F_1 hybrids of Chinese cabbage by introducing these two *FLC* alleles from Tsukena No. 2 (Kitamoto et al. 2017).

In *B. oleracea*, QTL analysis identified a major QTL covering *BoFLC2*, while *BoFLC1*, *BoFLC3*, and *BoFLC5* were not linked, using a population derived from a DH line of broccoli, Green Comet, and a DH line of cabbage, Reiho (Okazaki et al. 2007). Due to deletion of a single base in exon 4 leading to a frame-shift mutation, suggesting that *BoFLC2* contributes to the control of flowering time in Green Comet (non-vernalization type) (Okazaki et al. 2007). Another group conducted QTL analysis using the population derived from a rapid cycling line of *B. oleracea* var. *alboglabra* (A12DHd) and the broccoli variety, Green Duke. *BoFLC2* is not responsible for the flowering time difference between the two lines because these two lines bear non-functional copies of *BoFLC2;* there is a single base deletion in exon 4 and deletion in the A12DH in Green Duke (Razi et al. 2008). The association between flowering time (under both glasshouse and field conditions) and a QTL at *BoFLC2* has been shown using the population of two purple sprouting broccoli lines (E5 and E9); E9 requires longer cold periods than E5 to head (Irwin et al. 2016). Through allelic variation and sequence polymorphisms, *BoFLC2* was shown to be a major determinant of heading date variation and vernalization response and alters the sensitivity and silencing dynamics of its expression (Irwin et al. 2016). In *B. rapa*, hybridized introgression of *BoFLC2* from a plant-vernalized *B. oleracea* cultivar did not alter the vernalization phenotype in the derived F_2BC_3 offspring, however the duration of cold required for successful vernalization leading to flowering was increased; suggesting that the duration of cold experienced is altered by allelic variation, while the difference in the

developmental stage at which vernalization will occur between the two species is possibly controlled by another mechanism (Shea et al. 2018).

In *B. rapa* grown under normal conditions, all four *BrFLC* paralogs were expressed in the leaves. The expression of *BrFLC* genes was reduced after vernalization, and the repression was stably maintained after returning to ambient temperatures. Before cold treatment, only *BrFLC1* showed accumulation of both H3K4me3 and H3K36me3 modifications, while three of the *BrFLC* paralogs (*BrFLC2, BrFLC3, and BrFLC5*) had only H3K4me3. After four weeks of cold treatment, the accumulation of H3K27me3 was observed in *BrFLC1, BrFLC2,* and *BrFLC3,* and H3K27me3 was maintained after returning to a warm temperature (Kawanabe et al. 2016). The first intron, the promoter region, and exon 1 are important for *FLC* repression in *A. thialiana* (Sheldon et al. 2002), and lncRNA COLDAIR is expressed from the mid-region of first intron (Tsai et al. 2010; Heo and Sung 2011). Although insertions in the first intron cause a weak repression of *BrFLC2* and *BrFLC3* transcripts by vernalization in *B. rapa*, the regions having sequence similarity to the vernalization response element in the first intron or COLDAIR in *A. thaliana* were not detected in the first intron of all *B. rapa* paralogs (Kitamoto et al. 2014). At least, COLDAIR-like transcripts in *B. rapa* were not detected. By contrast, COOLAIR-like transcripts were detected only from *BrFLC2*, and these transcripts were induced by cold treatment. The plant growth cycle was shortened by the over-expression of *FLC* natural antisense transcripts (COLDAIR-like) resulting in decreased flowering time and *FLC* expression, suggesting that the activity of the *BrFLC2* gene was suppressed by *BrFLC* NATs during cold condition (Li et al. 2016). *BoFLC2* was shown to be a major determinant of heading date variation and vernalization response through allelic variation; sequence polymorphisms in *BoFLC2* alter the sensitivity and silencing dynamics of its expression (Irwin et al. 2016).

Understanding the molecular mechanism(s) responsible for vernalization in the control of flowering is important for the breeding of high bolting resistance in *B. rapa* and *B. oleracea* leafy vegetables. Recent studies on vernalization using *Arabidopsis thaliana,* one of the model organisms used for studying plant biology and the first plant to have its entire genome sequenced, provided key insight into the molecular mechanism of vernalization. The knowledge derived from *A. thaliana* research has been useful for understanding the molecular mechanism of vernalization in the genus *Brassica*. The aim of the dissertation is to identify the sequences important for vernalization, termed vernalization responsive elements (VREs), within the genus *Brassica*; and to examine any sequence polymorphisms that may exist with

respect to the vernalization response. This will help to identify important regions and explicate their relationship to sensitivity of vernalization. If there are any correlations, they will be useful for producing different expected lines or variety, and serve as important tools for breeding in the genus *Brassica* including *B. rapa*.

Chapter II

The role of *FRIGIDA* and *FLOWERING LOCUS C* genes in flowering time of *Brassica rapa* leafy vegetables

Abstract

There is a wide variation of flowering time among lines of *Brassica rapa* L.. Most *B. rapa* leafy (Chinese cabbage etc.) or root (turnip) vegetables require prolonged cold exposure for flowering, known as vernalization. Premature bolting caused by low temperature leads to a reduction in the yield/quality of these *B. rapa* vegetables. Therefore, high bolting resistance is an important breeding trait, and understanding the molecular mechanism of vernalization is necessary to achieve this goal. In this study, we demonstrated that *BrFRIb* functions as an activator of *BrFLC* in *B. rapa*. We showed a positive correlation between the steady state expression levels of the sum of the *BrFLC* paralogs and the days to flowering after four weeks of cold treatment, suggesting that this is an indicator of the vernalization requirement. We indicate that *BrFLCs* are repressed by the accumulation of H3K27me3 and that the spreading of H3K27me3 promotes stable *FLC* repression. However, there was no clear relationship between the level of H3K27me3 in the *BrFLC* and the vernalization requirement. We also showed that if there was a high vernalization requirement, the rate of repression of *BrFLC1* expression following prolonged cold treatments was lower.

Keywords: *Brassica rapa*, epigenetics, high bolting resistance, histone modification, *FLOWERING LOCUS C*, *FRIGIDA*, vernalization requirement

Introduction

Flowering is an event that transitions a plant from vegetative to reproductive growth, and is regulated by both internal and external factors (Bloomer and Dean, 2017; Shea et al. 2018). Because plants use the energy accumulated during the vegetative growth period for the reproductive growth phase to propagate offspring, flowering is a crucial developmental process in a plant's life cycle (Bloomer and Dean, 2017; Shea et al. 2018). Flowering time is also important for the yield of crops or vegetables, and the regulation of flowering time is an important goal of plant breeding (Bloomer and Dean, 2017; Itabashi et al. 2018). Changes to flowering time can broaden the area or the period of suitable cultivation, and lead to tolerance against changing climatic conditions (Bloomer and Dean, 2017; Shea et al. 2018).

Many plant species require prolonged cold exposure, generally encountered during the course of winter, before flowering and setting seed. Without exposure to a prolonged cold period, flowering is blocked. This process is known as vernalization, which is derived from the Latin word *vernalis*, meaning 'of, relating to, or occurring in the spring' (Chouard, 1960). Variation in the requirement for vernalization exists in plant species (Bloomer and Dean, 2017; Kim et al. 2009; Johanson et al. 2000). A vernalization requirement is an evolutionary adaptation to temperate climates, preventing flowering before encountering a winter season and ensuring flowering occurs under the more favorable weather conditions of spring (Bloomer and Dean, 2017; Shea et al. 2018; Leijten et al. 2018). Vernalization requirement is also important for the quantity and quality of crop production (Bloomer and Dean, 2017; Shea et al. 2018; Leijten et al. 2018). In vegetative crops, early bolting and flowering caused by a low vernalization requirement can limit the potential for increase in yield or devalue the products (Shea et al. 2018; Itabashi et al. 2018).

The molecular mechanism of vernalization has been studied extensively in *Arabidopsis thaliana*, and an abundance of information about its mechanism has been discovered. In *A. thaliana*, the two genes, *FRIGIDA* (*FRI*) (Johanson et al. 2000) and *FLOWERING LOCUS C* (*FLC*) (Lee and Amasino, 1995; Michaels and Amasino, 1999; Sheldon et al. 1999), are the major determinants of flowering time (Bloomer and Dean, 2017; Kim et al. 2009). *FRI* is one of the causative genes of natural variation of vernalization in *A. thaliana*, and FRI acts as a positive regulator of *FLC* (Johanson et al. 2000). Another flowering regulator, *FLC*, encodes a MADS-box transcription factor and acts as a floral repressor (Lee and Amasino, 1995; Michaels and Amasino, 1999; Sheldon et al. 1999). *FLC* is expressed

before cold exposure and its expression is repressed by vernalization (Sheldon et al., 2000). Cold exposure induces the formation of a plant homeodomain-polycomb repressive complex 2 (PHD-PRC2) that results in an increased abundance of tri-methylation of the 27th lysine of histone H3 (H3K27me3) at the nucleation region of the *FLC* locus (Bastow et al. 2004; De Lucia et al. 2008). Upon return to warm conditions, H3K27me3 spreads over the entire *FLC* gene and silencing of *FLC* is maintained Finnegan and Dennis, 2007; Angel et al. 2011).

Varieties of *Brassica rapa* L. include Chinese cabbage (var. *pekinensis*), pak choi (var. *chinensis*), komatsuna (var. *perviridis*), turnip (var. *rapa*), and oilseed (var. *oleifera*). *B. rapa* is closely related to *A. thaliana*, both being members of the *Brassicaceae* family. Bolting caused by low temperature leads to a reduction in the yield and quality of the harvested products of leafy vegetables such as Chinese cabbage, pak choi, and komatsuna or root vegetables such as turnip. Therefore, a line highly resistant to bolting (i.e., possessing a high vernalization requirement) is desirable for the breeding of *B. rapa* cultivars (Shea et al. 2018; Itabashi et al. 2018). Comparative genetic and physical mapping and genome sequencing studies have revealed that the *B. rapa* genome has undergone a whole-genome triplication, which results in multiple copies of paralogous genes (Wang et al. 2011; Cheng et al. 2012; Tang et al. 2012). Flowering time genes have been characterized and there are two *FRI* paralogs in *B. rapa* Schiessl et al. 2017; Wang et al. 2017). *B. rapa* has four *FLC* paralogs (*BrFLC1*, *BrFLC2*, *BrFLC3*, *BrFLC5*) (Schiessl et al. 2017; Wang et al. 2017; Schranz et al. 2002), of which *BrFLC5* is a pseudogene in the reference genome due to the deletion of two exons (Wang et al. 2011; Schranz et al. 2002). *BrFLC* genes are expressed before vernalization and their expression is repressed following vernalization (Shea et al. 2018; Itabashi et al. 2018; Kawanabe et al. 2016). The silencing of the three functional *BrFLC* paralogs is associated with increased H3K27me3 around the transcription start site (Kawanabe et al. 2016). *FLC* paralogs co-localized with quantitative trait loci (QTLs) for flowering time in *B. rapa* (Lou et al. 2007; Li et al. 2009; Zhao et al. 2010; Kakizaki et al. 2011; Kitamoto et al. 2014). Thus, *FLC* genes are considered to be key regulators of the vernalization requirement in *B. rapa* (Shea et al. 2018; Itabashi et al. 2018).

In *B. rapa*, *FRI* gene function has not yet been confirmed, and how the multiple *FLC* genes are involved in the vernalization requirements is not fully understood. In this study, we characterized two *BrFRI* genes, *BrFRIa* and *BrFRIb*, and confirmed *BrFRIb* functions as an activator of *FLC*. The relationship between expression levels of *BrFRI*s (*BrFRIa* + *BrFRIb*) or *BrFLC*s (*BrFLC1* + *BrFLC2* + *BrFLC3* + *BrFLC5*) and days to flowering was examined. We

also examined the expression levels of *BrFLC* genes and the accumulation of H3K27me3, before and after prolonged cold treatment, in two lines that vary in their vernalization requirements. Our results suggest that the steady state of the sum of functional *BrFLC* expression levels and the level of reduction of this expression by vernalization are key factors in determining the vernalization requirement in *B. rapa*.

Methods

Plant materials and growth conditions

Nine *B. rapa* lines (RJKB-T02, RJKB-T17, 'Harunosaiten', 'Harusakari', 'Natsumaki 50nichi', 'Yellow sarson', BRA2209, Homei, and Osome) were used as plant materials to examine days to flowering after four weeks of cold treatment (Table II- 1). In total, 37 *B. rapa* lines including the above nine lines were used for sequence determination of *BrFRI* genes. Genetic distances among 33 of the 37 lines have been examined[28] and these 33 lines all need vernalization for flowering (Fig. II-1, Table II-1).

Seeds were surface sterilized and grown on agar solidified Murashige and Skoog (MS) plates with 1 % (w/v) sucrose under long day (LD) conditions (16 h light) at 22 °C. For vernalizing cold treatments, 14-days seedlings on MS plates were treated for 2, 3, 4, 5, 6, or 8 weeks at 4 °C under LD conditions (16 h light) or four weeks at 4 °C and then seven days in normal growth condition.

To examine the flowering time in the nine lines, seeds were surface sterilized and grown on MS plates with 1 % (w/v) sucrose under LD conditions (16 h light) at 22 °C for 14 days, and 14-days seedlings on MS plates were treated for four weeks at 4 °C under LD conditions (16 h light). After cold treatments, the plants were transferred to soil and grown in normal growth conditions. The number of days until the appearance of flower buds was counted and scores were set based on the criteria shown in Table II-2. More than ten plants of each line were used for examining the flowering time.

RNA extraction and RT-PCR/qPCR

Total RNA was isolated from 1st and 2nd leaves using the SV Total RNA Isolation System (Promega). The cDNA was synthesized from 500 ng total RNA using ReverTra Ace qPCR RT Master Mix with gDNA Remover (Toyobo). For RT-PCR, the cDNA was amplified using Quick Taq® HS DyeMix (Toyobo). PCR was performed using the following conditions;

1 cycle of 94 ℃ for 2 min, 25, 30, or 35 cycles of 94 ℃ for 30 s, 58 ℃ for 30 s, and 68 ℃ for 30 s. Primer sequences used for RT-PCR are shown in Table II-3.

RT-qPCR was performed using LightCycler 96 (Roche). cDNA was amplified using FastStart Essential DNA Green Master (Roche). PCR conditions were 95 ℃ for 10 min followed by 40 cycles of 95 ℃ for 10 s, 60 ℃ for 10 s, and 72 ℃ for 15 s, and Melting program (60 ℃ to 95 ℃ at 0.1 ℃/s). After amplification cycles, each reaction was subjected to melt temperature analysis to confirm single amplified products. The expression level of each gene relative to *BrACTIN* (Fujimoto et al. 2006). was automatically calculated using automatic CQ calling according to the manufacturer's instructions (Roche). Data presented are the average and standard error (s.e.) calculated from three biological and experimental replications. Primer sequences used for RT-qPCR are shown in Table II- 3.

Sequencing DNA fragments of *BrFRI* and *BrFLC* genes

The region covering *BrFRIa* or *BrFRIb* was amplified using primers, FRIa-F1/-R1 or FRIb-F1/-R1, respectively, using genomic DNA as templates. DNAs from 37 *B. rapa* lines were used for the direct sequencing of PCR products (Table II- 1). PCR products were treated by illustra ExoProStar (GE Healthcare Life Sciences) and were sequenced using ABI Prism 3130 (Applied Biosystems). Primer sequences used for direct sequencing are shown in Table II-3.

Regions covering the coding sequence of each *BrFLC* paralog in RJKB-T02, RJKB-T17, RJKB-T24, Homei, 'Harunosaiten', and BRA2209, were amplified using cDNA as templates (Table II-1). PCR products were treated by illustra ExoProStar (GE Healthcare Life Sciences) and were sequenced using ABI Prism 3130 (Applied Biosystems). PCR was performed using the following conditions; 1 cycle of 94 ℃ for 2 min, 35 cycles of 94 ℃ for 30 s, 58 ℃ for 30 s, and 68 ℃ for 30 s. Primer sequences used for direct sequencing are shown in Table II-3.

The genomic regions covering *BrFLC1*, *BrFLC2*, and *BrFLC3* and their promoter regions were amplified using genomic DNA as a template in BRA2209. PCR products were then cloned into pGEM®-T Easy vector (Promega). Nucleotide sequences of three clones of PCR products were determined with the ABI Prism 3130 (Applied Biosystems), and the data were analyzed using Sequencher (Gene Codes Corporation, MI, USA). PCR was performed

using the following conditions; 1 cycle of 94 °C for 2 min, 35 cycles of 94 °C for 30 s, 58 °C for 30 s, and 68 °C for 2 min. Primer sequences and their positions used for PCR and sequencing are shown in Fig. II- 2 and Table II-3.

Construction and plant transformation

Using cDNAs from leaves of RJKB-T24, either *BrFRIb* or *BrFLC1, 2,* or *3* cDNA fragments were amplified by RT-PCR using primers designed to add *Bam* HI and *Sac* I restriction sites to the 5'- and 3'-ends (Table II-3), and PCR products were then cloned into pGEM®-T Easy vector (Promega). DNA fragments of *BrFRIb* or *BrFLC1, 2,* or *3* cDNA was inserted into *Bam* HI and *Sac* I restriction sites of pBI121. These constructs were transformed into *Agrobacterium tumefaciens* strain EHA105, and transformation of Columbia-0 (Col) accession in *A. thaliana* was carried out by the floral dip procedure (Clough and Bent, 1998). Transgenic seedlings were selected through resistance to kanamycin on a selection medium.

Seeds of T_2 plants were sown on MS medium with or without four weeks of cold treatment and grown under LD conditions (16 h light) at 22 °C. After growing plants on MS medium, they were transferred to soil and grown under the conditions described above. Flowering time in *A. thaliana* was expressed as the number of rosette leaves at the time of flowering.

Chromatin immunoprecipitation (ChIP)

ChIP experiments were performed as described by Buzas et al. (2011). One gram of non-crosslinked chromatin taken from the 1st and 2nd leaves of Homei and 'Harunosaiten' was used (Table II-1). Mononucleosomes were obtained by MNase digestion and samples were sonicated twice. The samples were incubated with anti-H3K27me3 (Millipore, 07-449) antibodies for 4 h and then with protein A agarose for 2h at 4°C with rotation. The protein A agarose was washed, and immunoprecipitated DNAs were eluted by proteinase K treatment followed by a clean-up using Qiagen PCR cleanup kit (Qiagen). We validated the enrichment of purified immunoprecipitated DNAs by ChIP-qPCR using the previously developed positive and negative control primer sets of H3K27me3 (Table II-3) (Kawanabe et al. 2016). Three independent ChIP experiments were carried out on each sample for biological replicates.

ChIP-qPCR was performed by the same method as the RT-qPCR using the immunoprecipitated DNA as a template. The H3K27me3 level of each *BrFLC* gene relative to *SHOOT MERISTEMLESS* gene (*BrSTM*) (Kawanabe et al. 2016), which has H3K27me3

accumulation, was automatically calculated using automatic CQ calling according to the manufacturer's instructions (Roche). The difference in the amplification efficiency between primer pairs was corrected by calculating the difference observed by qPCR amplifying the input-DNA as a template. Data presented are the average and standard error (s.e.) from three biological and experimental replications. Primer sequences used for ChIP-qPCR are shown in Table II-3.

Amino acid sequence analysis

Using the genome sequences of *BrFRIa* and *BrFRIb* in 37 *B. rapa* lines, predicted amino acid sequences were obtained. The amino acid sequences of BrFRIa and BrFRIb in 37 lines of *B. rapa*, two BoFRI (Irwin et al. 2012), and AtFRI (AF228499.1) were aligned using ClustalW (http://www.ddbj.nig.ac.jp/search/clustalw-j.html). A phylogenetic tree was constructed with the neighbor joining method (Saitou and Nei, 1987), and the bootstrap probabilities of 1,000 trials were calculated.

Results

Variation of the days to flower after prolonged cold treatment

To determine the duration of prolonged cold treatment, we determined the days to flowering after prolonged cold treatment. We examined the percentage of plants that had flowered in two early (Homei and RJKB-T02) and two late flowering lines (RJKB-T17 and BRA2209) with different durations of cold treatments, i.e., two, three, four, or five weeks. After two weeks of cold treatment, no line flowered within 100 days (Fig. II- 3). All plants of two early flowering lines flowered after three weeks of cold treatment, while no plant of two late flowering lines flowered (Fig. II-3). In two late flowering lines, four of six plants of RJKB-T17 flowered following four weeks of cold treatment, while no plant in BRA2209 flowered following four weeks of cold treatment (Fig. II-3). Following five weeks of cold treatment, all lines flowered even though there were differences in days to flowering (Fig. II-3). From these data, we determined that four weeks of cold treatment is suitable for detecting differences in vernalization requirement among the *B. rapa* lines.

Next, we examined the days to flower after four weeks of cold treatment in nine *B. rapa* lines. Scores were used for the evaluation of flowering time, because some plants in the late flowering line did not flower within 100 days (see Methods). 'Yellow Sarson' and Homei were

early flowering, while Osome, BRA2209, RJKB-T17, and 'Harunosaiten' were late flowering (Fig. II-4).

Functional analysis of *FRIGIDA* in *B. rapa*

As the early flowering phenotype in some *A. thaliana* accessions is due to the loss of function of *AtFRI*, we examined the sequence variation in *BrFRI* genes using 37 lines of *B. rapa* including the nine lines whose flowering time had been assessed (Fig. II-4, Table II-1). In the reference genome, Chiifu-401-42, there are two *FRI* genes, *BrFRIa* (Bra029192, A03) and *BrFRIb* (Bra035723, A10). The *BrFRIa* sequence in the reference genome is comprised of three exons and showed sequence similarity to *AtFRI* and *BoFRIa*. BoFRIa[32] and AtFRI[7] have already been shown to be a functional activator of *FLC*, considering that *BrFRIa* in Chiifu-401-42 is functional; sharing a high sequence similarity to BoFRIa stands to reason that BrFRIa may perform a similar function. The nucleotide sequence of *BrFRIa* in 37 lines was determined by direct sequencing. There was a high sequence similarity of the amino acid sequence of BrFRIa among 37 *B. rapa* lines (from 97.8 % to 100.0 %) (Table II- 4). The amino acid sequence identities between BrFRIa and AtFRI were from 56.8 % to 57.5 % and being from 87.9 % to 88.1% between BrFRIa and BoFRIa (Figs. II- 5, 6, Table II- 4). Lines showing different flowering times had identical amino acid sequences of BrFRIa (Fig. II-4, Table II-4), indicating that the differences of vernalization requirements among the nine *B. rapa* lines are not due to amino acid sequence variation in BrFRIa.

In contrast, the annotated *BrFRIb* (Bra035723), termed *BrFRIbΔ,* is comprised of two exons, and appears to lack the 3rd exon (Fig. II- 7). We mapped RNA-seq reads that was previously performed (Shimizu et al. 2014) using 14-day leaves in RJKB-T23 and RJKB-T24 on the region covering *BrFRIbΔ* and found another ORF, which contains three exons (Fig. II-8), suggesting that an unannotated functional copy of *BrFRIb* is present in the reference genome sequence. As further evidence of this, transformation of the annotated *BrFRIbΔ* driven with the 35S CaMV promoter into the Col accession of *A. thaliana*, which lacks AtFRI function, did not complement the AtFRI function (Fig. II- 9), indicating that the annotated BrFRIbΔ is non-functional.

We examined whether a newly identified BrFRIb in this study is functional. We transformed *BrFRIb* into the Col accession of *A. thaliana*, and 14 independent T_1 plants were obtained. The flowering time segregated in T_2 plants that were derived from three independent T_1 plants, and the flowering times of T_2 plants with the transgene were later than the T_2 plants

without the transgene or wild type Col (Student *t*-test, $p < 0.01$) (Fig. II-10A). We also found that T_2 plants from some T_1 lines did not flower even when the rosette leaf number was greater than 45. We confirmed the induction of *AtFLC* expression in these late flowering transgenic plants (Fig. II-10B). T_2 seeds were treated with cold for four weeks, and then examined for flowering time. The flowering time in T_2 plants with the transgene was the same as without the transgene (Fig. II-10A). Repression of *AtFLC* by cold treatment was observed in T_2 plants with the transgene (Fig. II-10B, C), indicating that *AtFLC* induced by *BrFRIb* is suppressed by cold treatment. These results indicate that BrFRIb functioned like AtFRI.

We determined the nucleotide sequence of *BrFRIb* in 37 lines by direct sequencing. There was a high sequence similarity of the amino acid sequence of BrFRIb among *B. rapa* lines (from 95.8 % to 100.0 %) (Fig. II-6, Table II- 4). The amino acid sequence identity between BrFRIb and AtFRI were from 59.9 % to 60.3 % and being from 85.8 % to 87.4 % between BrFRIb and BoFRIb (Figs. II-5, 6, Table II-4). The amino acid sequence identities ranged from 63.1 % to 64.3 % between BrFRIa and BrFRIb (Table II- 4). Like BrFRIa, lines showing different flowering time had identical amino acid sequences of BrFRIb (Fig. II-4, Table II- 4), indicating that the difference of vernalization requirement among nine *B. rapa* lines is not due to the amino acid sequence variation of *BrFRIb*.

Next, we examined whether transcription levels of *BrFRI* genes contribute to the difference of vernalization requirement. We examined the transcription levels of *BrFRIa*, *BrFRIb*, or *BrFRI*s (*BrFRIa* + *BrFRIb*) by RT-qPCR in 14-days leaves of the nine lines whose flowering time had been measured (Fig. II-4, Fig. II-11A-C). Expression in 'Yellow sarson' was the lowest, while RJKB-T17 and BRA2209 had the highest expression levels in *BrFRI*s, with expression levels in BRA2209 being 6.8 times higher than that in 'Yellow sarson' (Fig. II-11C). There was a moderate correlation between *BrFRI*s expression level and flowering time but it was not statistically significant ($r = 0.56$, $p > 0.05$) (Fig. II-11D). There was no correlation between *BrFRIa* or *BrFRIb* expression level and flowering time (Fig. II- 12).

Three FLOWERING LOCUS C paralogs function as floral repressors in *B. rapa*

We examined whether *BrFLC* is a key regulator of the differences in vernalization requirements for *B. rapa*. First, we confirmed all three *BrFLC*s (*BrFLC1*, *BrFLC2*, and *BrFLC3*) function as floral repressors. Transformation of a 35S promoter::*BrFLC1*cDNA, 35S promoter::*BrFLC2*cDNA, or 35S promoter::*BrFLC3*cDNA construct into the Col accession of *A. thaliana*, where *AtFLC* was not expressed because of loss of function of AtFRI, revealed

that transgenic plants with overexpressed *BrFLC1*, *BrFLC2*, or *BrFLC3* showed late flowering (Fig. II- 13), confirming that all three *BrFLC*s function as floral repressors like AtFLC.

Second, we examined the amino acid sequences of the three functional BrFLC paralogs (BrFLC1, BrFLC2, and BrFLC3) in RJKB-T24, which was the line used for testing the 35S promoter::*BrFLC* constructs. The amino acid sequence of the early flowering lines, RJKB-T02 and Homei, and the late flowering lines, RJKB-T17, 'Harunosaiten', and BRA2209, were also examined. A comparison of the amino acid sequences for each BrFLC paralog showed no sequence differences between lines, indicating that any difference in flowering time is not due to amino acid sequence variation.

Third, we examined the expression levels of *BrFLC* genes in the nine *B. rapa* lines whose flowering time had been measured (Fig. II-4, Table II-1) using a primer set that can amplify all four *FLC* genes. The lowest level of *BrFLC*s was in early flowering RJKB-T02 and the highest in late flowering RJKB-T17; the expression level in RJKB-T17 was 3.6 times higher than in RJKB-T02 (Fig. II-14A). The expression levels of *BrFRI*s and *BrFLC*s showed a weak correlation ($r = 0.23$, $p > 0.05$) (Fig. II- 15). There was a high correlation between *BrFLC*s expression level and flowering time ($r = 0.73$, $p < 0.05$) (Fig. II-14B), suggesting that the expression level of *BrFLC*s before cold treatment is associated with the vernalization requirement.

Variation of the vernalization response in *BrFLC*s

Of nine *B. rapa* lines whose flowering time had been measured, two early (RJKB-T02, Homei) and two late flowering (BRA2209, 'Harunosaiten') lines were selected to examine the *BrFLC*s expression in different durations of cold treatments. A decrease in *BrFLC*s expression levels in response to four weeks of cold treatment was from 15.8 % to 47.8 %, with the weakest repression observed in BRA2209 (Fig. II-16A, B). The rate of repression of *BrFLC*s expression by four weeks of cold treatment was not related to the expression level of *BrFLC*s before cold treatment (Fig. II-16A, B). *BrFLC* expression levels after four weeks of cold treatment in BRA2209 and 'Harunosaiten' were higher than that in RJKB-T02 and Homei ($p < 0.05$; Tukey-Kramer test) (Fig. II-16A). This difference was related to the difference of flowering time after four weeks of cold treatment (Fig. II-4). *BrFLC*s expression levels were reduced following the cold treatment length in all four lines (Fig. II-16A). The rate of decrease in *BrFLC*s expression level was lowest in BRA2209 (Fig. II-16B).

Histone modification spreads at the *BrFLC* locus upon a return to normal growth conditions after vernalization

We selected two lines (Homei, 'Harunosaiten') to examine the relationship between H3K27me3 levels at the *BrFLC* loci and differences in the vernalization requirements. Homei showed low levels of *BrFLC*s expression before cold treatment and an early flowering phenotype after four weeks of cold treatment, whereas 'Harunosaiten' showed high levels of *BrFLC*s expression before cold treatment and late flowering phenotype after four weeks of cold treatment (Fig. II-4, 16). In both lines, the expression levels of *BrFLC*s decreased following the four weeks of cold treatments and transcriptional repression was maintained upon return to normal temperature (Fig. II-17). At the end of four weeks of cold treatment, H3K27me3 accumulation was observed around the transcription start site (TSS) of the 1st exon of *BrFLC* in both lines. The accumulation of H3K27me3 levels in the region around the TSS was maintained in both lines seven days after returning to normal growth conditions (Fig. II-18). In the 5th exon regions, H3K27me3 levels slightly increased, but were lower relative to the TSS in both lines at the end of four weeks of cold treatment (Fig. II-18). In both lines, H3K27me3 levels increased seven days after returning to normal growth conditions (Fig. II-18); the spreading of H3K27me3 regions in the *BrFLC* loci was observed in Homei and 'Harunosaiten' after seven days of normal growth conditions following four weeks of cold treatment (Fig. II-18). The accumulation of H3K27me3 was similar between Homei and 'Harunosaiten', suggesting that the level of H3K27me3 at the *BrFLC* loci does not explain the difference in vernalization requirement between these lines.

Characterization of three functional *BrFLC* paralogs in BRA2209

We found that the rate of repression of *BrFLC*s expression by cold treatment was low in BRA2209, and this line showed a high vernalization requirement (Fig. II-4, 16). We examined the expression level in each *BrFLC* paralog in BRA2209 using paralog specific primer sets (Kakizaki et al. 2011). Before cold treatment, *BrFLC1* had the highest expression among the four paralogs (Fig. II-19). After four weeks of cold treatment, *BrFLC1* still had the highest expression level and the suppression rate of *BrFLC1* following four weeks of cold treatment was lower than that of other *BrFLC* paralogs (Fig. II-19).

The full lengths of the genic regions of *BrFLC1*, *BrFLC2*, and *BrFLC3* in BRA2209 were determined. In *BrFLC1*, there was a 410 bp deletion, including part of the 7th exon (31 bp of the 3' region including stop codon) and a downstream region (Fig. II- 20). Except for two

SNPs in the 5th intron, the other exon and intron regions were identical to the reference sequence. There were three SNPs in the 963 bp region upstream of the TSS, and no sequence differences in the 497 bp region downstream from the deleted region in *BrFLC1* of BRA2209 (Fig. II-20). In *BrFLC2*, there were several substitutions and indels in promoter and intron regions, but no substitutions in the exon regions (Fig. II-20). In *BrFLC3*, the promoter region had some sequence differences in comparison to the reference genome and there were some substitutions and indels in the intron regions. However, the coding sequence was identical to the reference genome (Fig. II-20).

Discussion

High bolting resistance is an important trait for leafy vegetables in *B. rapa*, and previous reports showed that *FLC* is a key gene for vernalization (Itabashi et al. 2018; Shea et al. 2018). Co-localization of flowering time QTLs with the *BrFLC1* or *BrFLC2* gene suggests that the loss-of-function of *BrFLC* causes early flowering (Itabashi et al. 2018; Shea et al. 2018). Our study and a previous study revealed that all three *BrFLC*s function as floral repressors (Kim et al. 2007). The loss-of-function of one of the *BrFLC* paralogs can result in early flowering, implying that the expression of *BrFLC* paralogs works to repress flowering in a quantitative manner (Itabashi et al. 2018; Shea et al. 2018).

From the reference genome sequence of *B. rapa*, two *BrFRI* genes were identified. *BrFRIa* has three exons and is similar to the functional *FRI* genes found in other species, while the annotated *BrFRIb* in the reference genome (*BrFRIbΔ*) has two exons and appears to be truncated in the C-terminus. As the C-terminus is critical in AtFRI function (Risk et al. 2010), BrFRIbΔ could be non-functional. Indeed, transformation of *BrFRIbΔ* into the *A. thaliana* Col accession did not complement the early flowering phenotype. However, we found a third exon by mapping RNA-seq reads against the reference genome. Complementation using this new ORF, termed *BrFRIb*, confirmed it to be functional, and transformation of *BrFRIb* into Col delayed flowering. In addition, *BrFRIb* induced *AtFLC* transcription and induced *AtFLC*, which was suppressed by four weeks of cold treatment, indicating that BrFRIb has the same function as AtFRI. We did not find mutations leading to a major defect in the translated protein in any of 37 varieties of *B. rapa*, and the amino acid sequences of BrFRIa or BrFRIb among these varieties were more than 95 % identical. In *B. oleracea*, BoFRIa has been confirmed to be functional by a complementation experiment (Irwin et al. 2012), and has about 88 % amino

acid sequence identity to BrFRIa, suggesting that BrFRIa is functional. We consider that both BrFRIa and BrFRIb are functional activators of the floral repressor gene *FLC* in *B. rapa*.

In our study, the nine lines of *B. rapa* did not show any positive correlation between the expression levels of the *BrFRI*s and *BrFLC*s before cold treatment. These results suggest there is no strong correlation between the expression levels of *FRI* and *FLC* before vernalization in the genus *Brassica*.

There was variation in the flowering time after four weeks of cold treatment among nine lines of *B. rapa*, suggesting that a cold treatment of four weeks in duration is not saturating for promoting flowering in some lines. In *A. thaliana*, the variation of flowering time is due to naturally occurring loss-of-function mutations, which have originated independently and result in early flowering accessions (summer annual habit) (Johanson et al. 2000; Le Corre et al. 2002; Gazzani et al. 2003; Shindo et al. 2005; Méndez-Vigo et al. 2011). It is unlikely that sequence variation in the coding sequences of *BrFRIa* or *BrFRIb* influences flowering time variation or the vernalization requirement, because the amino acid sequences are highly conserved and there were no differences in the amino acid sequence between lines showing different flowering times. The absence of an association between *BrFRI* expression levels and vernalization requirement in this study and the low number of reports showing an association between flowering time QTL and *FRI* in the genus *Brassica* (Wang et al. 2011) suggest that the variation of vernalization requirement in *B. rapa* is not greatly influenced by sequence or transcriptional variation of *BrFRI*.

All three *BrFLC*s function as floral repressors; this has been confirmed by other groups in *B. rapa* (Kim et al. 2007) or *B. napus* (Tadege et al. 2001). These results suggest that we should consider not only each paralogous *BrFLC* transcript, but also the sum of the three paralogous *BrFLC* transcripts as an important factor for the vernalization requirement. There is a positive correlation between the expression levels of *BrFLC* paralogs before cold treatment and the days to flowering after four weeks of cold treatment. This suggests that the expression levels of *BrFLC* genes before cold treatment may be an indicator of the duration of cold required for vernalization. The rate of suppression of *BrFLC*s expression by cold treatment was similar among lines except for BRA2209. Generally, if the rate of repression of *BrFLC* expression is similar among varieties, the expression level before cold treatment is predictive of duration of cold required for vernalization. As a longer cold period will be required to suppress *BrFLC*s expression in lines having a higher *BrFLC*s expression prior to cold treatment,

the positive correlation between the expression levels of *BrFLC*s before cold treatment and days to flowering after four weeks of cold treatment supports this idea. However, our experiment assessed nine lines, and we need to verify this possibility by analyzing additional lines.

In BRA2209, expression levels of *BrFLC*s before cold treatment were not as high as in other lines, but the rate of repression of *BrFLC*s expression by cold treatment was low, especially of *BrFLC1*, leading to higher expression levels of *BrFLC*s after four weeks of cold treatment, consistent with the late flowering phenotype. An extremely late bolting line of *B. rapa* has a long insertion in the 1st intron of *BrFLC2* and *BrFLC3*, and the rate of decrease in the expression of *BrFLC2* and *BrFLC3* is low, indicating a weak vernalization response (Kitamoto et al. 2014). We did not identify any sequence difference in the 1st intron of *BrFLC1* between BRA2209 and the reference genome. In contrast, we found a 401 bp deletion covering part of the 7th exon and downstream regions in *BrFLC1* of BRA2209, suggesting that the 3' region of *BrFLC1* might include a sequence important for the response to prolonged cold.

We have shown that *FLC* chromatin is enriched with the active histone marks, H3K4me3 and H3K36me3, prior to cold treatment, and that these histone marks are replaced with the repressive histone mark, H3K27me3, during cold exposure (Kawanabe et al. 2016), suggesting that chromatin change is important for the repression of *FLC* in the vernalization of *B. rapa*. In *A. thaliana*, increasing the duration of cold quantitatively enhances the stability of *AtFLC* repression, and the necessary period of cold treatment varied among accessions. In two different accessions of *A. thaliana* (*FRI* Col and Lov-1), the accumulation of H3K27me3 at the entire *FLC* locus, upon transfer of the plants back to warm conditions after cold treatment, was faster in the accession that requires a shorter period of cold (*FRI* Col) than in the accession that needs a longer period of cold (Lov-1) (Coustham et al. 2012). When treated with four weeks of cold, an enrichment of H3K27me3 was observed around the TSS of the *BrFLC* loci, but not at the region covering the 5th exon in either line. Upon returning to warm conditions after cold exposure, H3K27me3 accumulation occurred at both TSS and the 5th exon regions in both lines, suggesting that H3K27me3 spreads from the 5' to 3' direction in *BrFLC* genes to maintain *FLC* repression. The spreading of H3K27me3 in the *BrFLC* locus is similar to the spreading reported in *A. thaliana* (Finnegan et al. 2007; Angel et al. 2011; Coustham et al. 2012). Unlike the distinct difference in H3K27me3 accumulation reported in *A. thaliana*, we did not find a difference in the accumulation patterns of H3K27me3 at the *BrFLC* loci between early and late flowering lines of *B. rapa*.

Taken together, two factors, the steady state expression levels of *BrFLC*s and the sensitivity of the repression of *BrFLC*s by cold treatment, are important for the vernalization requirement in *B. rapa*. Further study will be required to identify whether variations of these two factors are regulated by *cis* or *trans*.

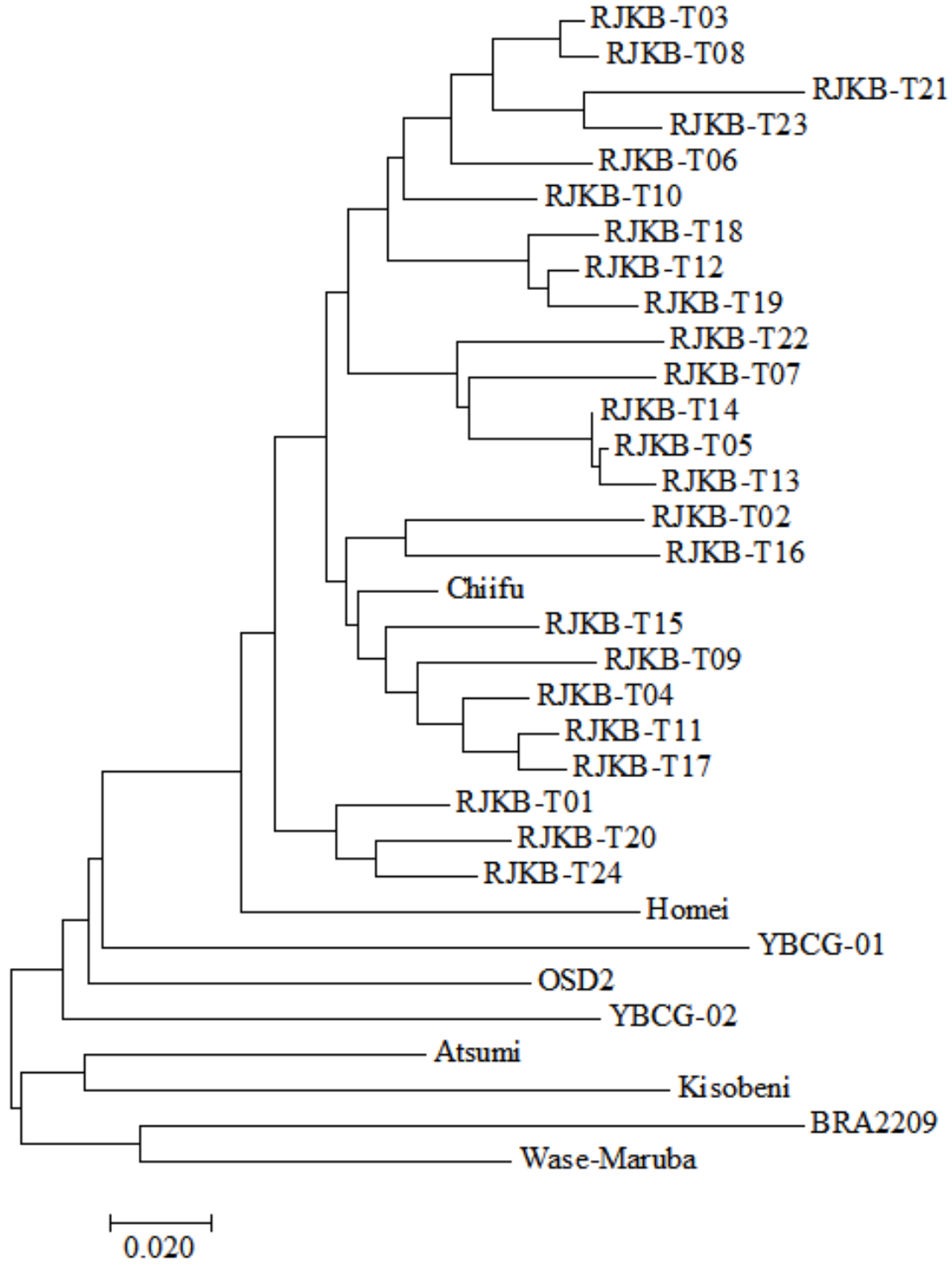

Figure II-1. A phylogenetic tree of the 33 lines in *B. rapa* based on genetic distance calculated by Kawamura et al. 2016. Additional lines have been included in the analysis. Green, yellow, and blue arrows indicate the Chinese cabbage (var. *pekinensis*), komatsuna (var. *perviridis*) and turnip (var. *rapa*) lines, respectively.

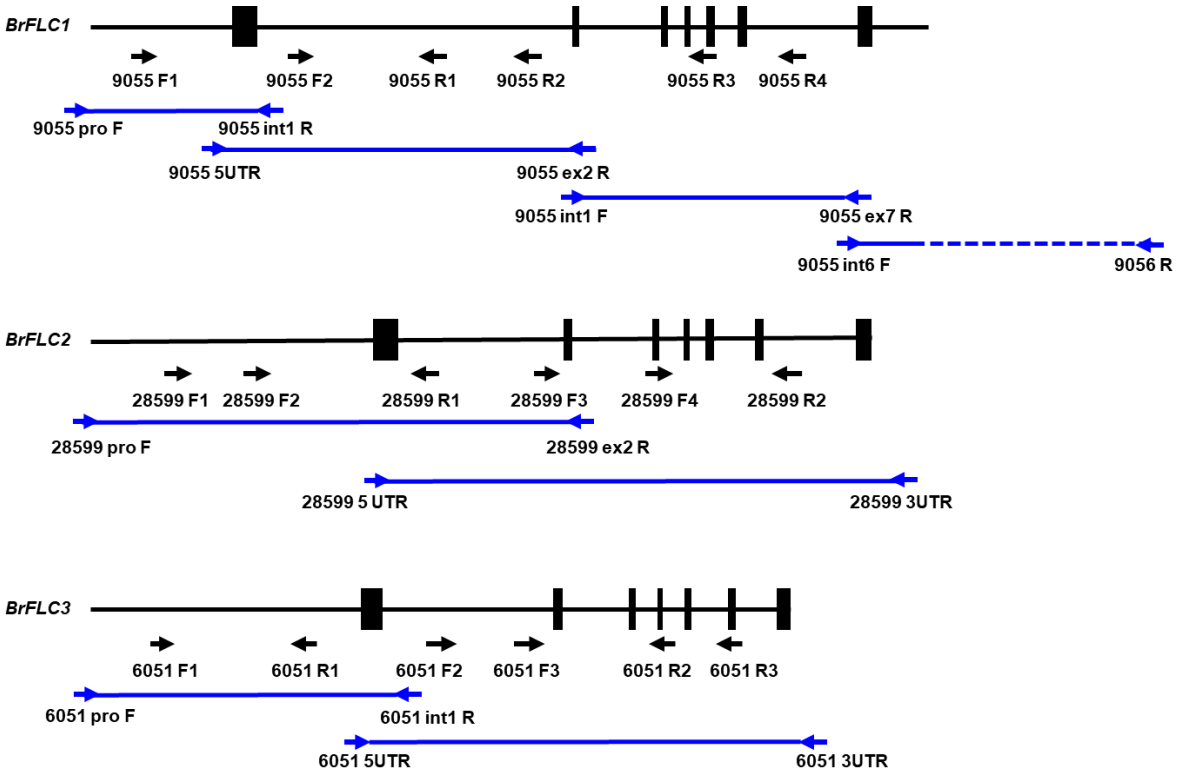

Figure II- 2. Position of primers used for determining the *BrFLC1*, *BrFLC2*, and *BrFLC3* in BRA2209. Blue lines represent the regions amplified by PCR. Black arrows represent the primers used for sequencing.

A

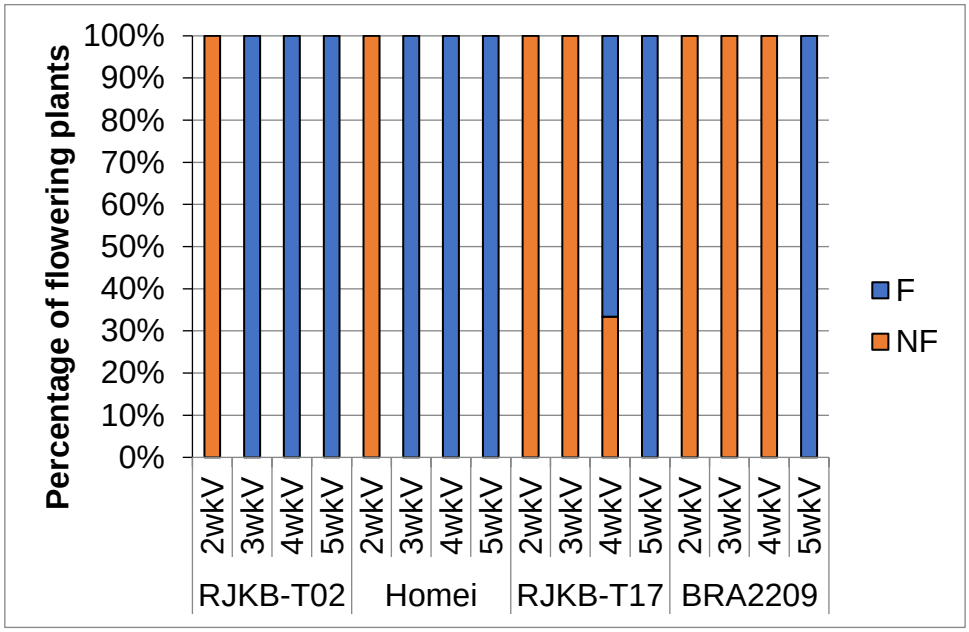

B

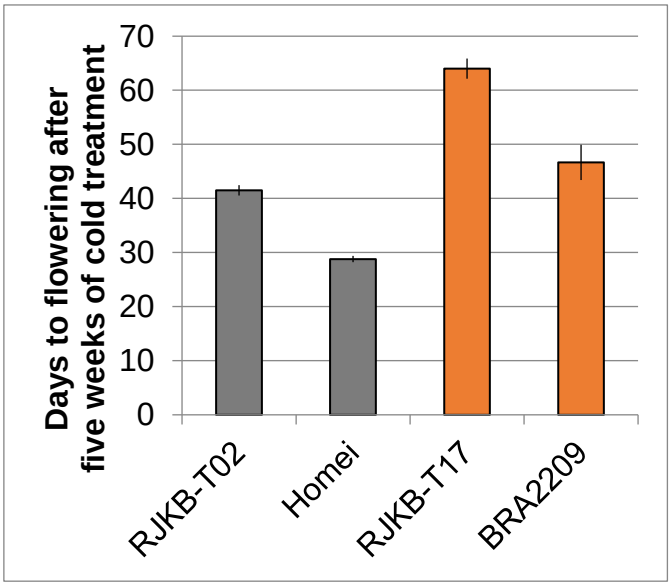

Figure II-3. The percentage of the plants that flowered after 2, 3, 4, or 5 weeks of cold treatment (A). 'F' represents the percentage of plants that flowered within 100 days after cold treatment. 'NF' represents the percentage of plants that did not flower after more than 100 days after cold treatment. (B) The days to flowering after five weeks of cold treatment. More than four plants were examined.

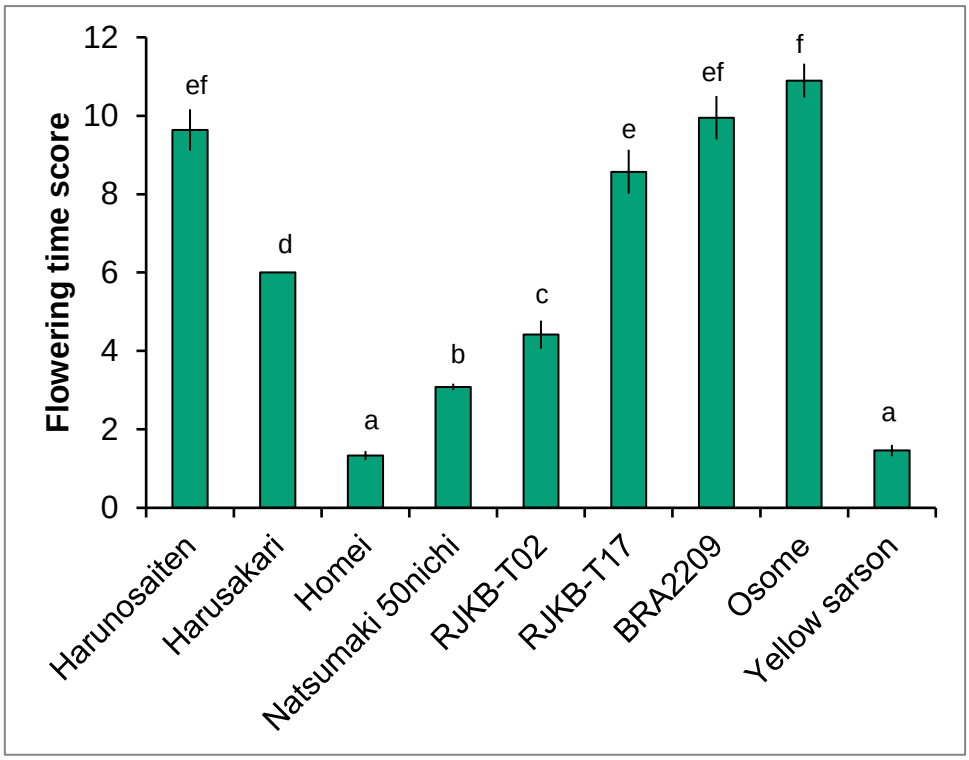

Figure II-4. Flowering time score represented by the expected value of number of days from sowing to bolting in nine *B. rapa* lines. Data presented are the average and standard error (s.e.) from more than ten plants. Letters above the bars indicate significant differences at $p < 0.05$ (Tukey-Kramer test).

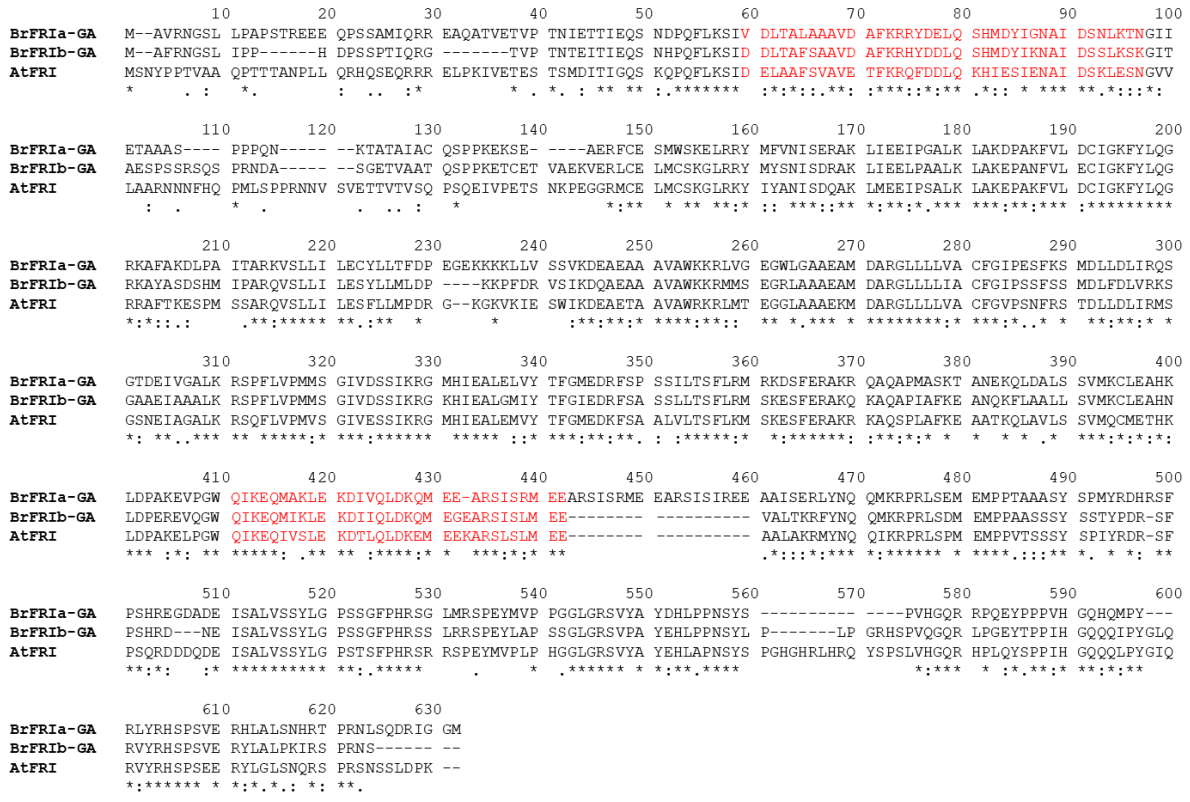

Figure II-5. Comparison of the predicted amino acid sequences between BrFRIa (Group A), BrFRIb (Group A), and functional AtFRI (AF228499.1). The coiled-coil domains are represented in red

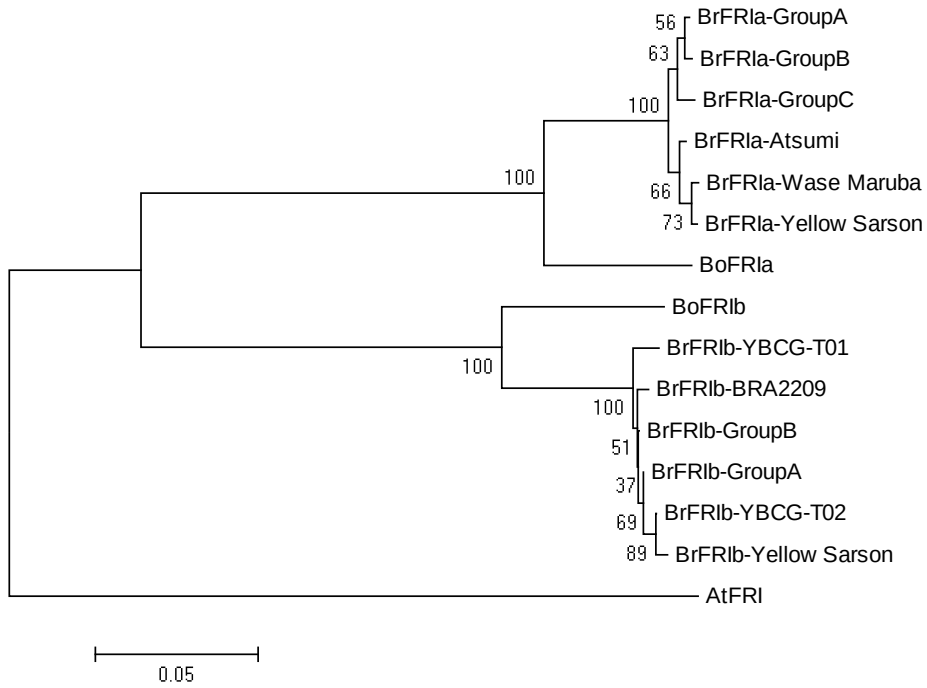

Figure II-6. Phylogenetic tree of amino acid sequences of coding region of *FRIb* genes. Bootstrap values with 1,000 replicates are indicated at the node of the phylogenetic trees. The lines involved in BrFRIa-Group A, B, and C and BrFRIb-Group A and B are shown in Table II-4.


```
                10         20         30         40         50         60         70         80         90        100
BrFRIbΔ M-AFRNGSLI PPHDPSSPTI QRG------- -------TVP TNTEITIEQS NHPQFLKSID DLTAFSAAVD AFKRHYDDLQ SHMDYIKNAI DSSLKSKGIT
AtFRI   MSNYPPTVAA QPTTTANPLL QRHQSEQRRR ELPKIVETES TSMDITIGQS KQPQFLKSID ELAAFSVAVE TFKRQFDDLQ KHIESIENAI DSKLESNGVV
        *  :        *  .:.* : **               * . *. :*** ** ::******** :*:***.**: :***::**** .*:: *:*** **.*:*:*:.

               110        120        130        140        150        160        170        180        190        200
BrFRIbΔ AESPSSRSQS -----PRNDA SGETVAATQS PPKETCETVA EKVE--RLCE LMCSKGLRRY MYSNISDRAK LIEELPAALK LAKEPANFVL ECIGKFYLQG
AtFRI   LAARNNNFHQ PMLSPPRNNV SVETTVTVSQ PSQEIVPETS NKPEGGRMCE LMCSKGLRKY IYANISDQAK LMEEIPSALK LAKEPAKFVL DCIGKFYLQG
          : ... :.      ***:. * **..:... *.:*    .: :* *  *:** ********:* :*:****:** *:**:*:*** ******:*** :*********

               210        220        230        240        250        260        270        280        290        300
BrFRIbΔ RKAYASDSHM IPARQVSLLI LESYLLMLDP KKPFDRVS-- IKDQAEAAAV AWKKRMMSEG RLAAAEAMDA RGLLLLIACF GIPSSFSSMD LFDLVRKSGA
AtFRI   RRAFTKESPM SSARQVSLLI LESFLLMPDR GKGKVKIESW IKDEAETAAV AWRKRLMTEG GLAAAEKMDA RGLLLLVACF GVPSNFRSTD LLDLIRMSGS
        *:*::.:* *  .******** ***:*** *   *   ::.   ***:**:*** **:**:*:**  ***** *** ******:*** *:**.* * * *:**:* **:

               310        320        330        340        350        360        370        380        390        400
BrFRIbΔ AEIAAALKRS PFLVPMMSGI VDSSIKRGKH IEALGMIYTF GIEDRFSASS LLTSFLRMSK ESFERAKQKA QAPIAFACPF FTH------- ----------
AtFRI   NEIAGALKRS QFLVPMVSGI VESSIKRGMH IEALEMVYTF GMEDKFSAAL VLTSFLKMSK ESFERAKRKA QSPLAFKEAA TKQLAVLSSV MQCMETHKLD
        ***.*****  *****:*** *:****** * **** *:*** *:**:***:  :*****:*** *******:** *:*:**  .   .:

               410        420        430        440        450        460        470        480        490        500
BrFRIbΔ ---------- ---------- ---------- ---------- ---------- ---------- ---------- ---------- ---------- ----------
AtFRI   PAKELPGWQI KEQIVSLEKD TLQLDKEMEE KARSLSLMEE AALAKRMYNQ QIKRPRLSPM EMPPVTSSSY SPIYRDRSFP SQRDDDQDEI SALVSSYLGP

               510        520        530        540        550        560        570        580        590        600
BrFRIbΔ ---------- ---------- ---------- ---------- ---------- ---------- ---------- ---------- ---------- ----------
AtFRI   STSFPHRSRR SPEYMVPLPH GGLGRSVYAY EHLAPNSYSP GHGHRLHRQY SPSLVHGQRH PLQYSPPIHG QQQLPYGIQR VYRHSPSEER YLGLSNQRSP

BrFRIbΔ ---------
AtFRI   RSNSSLDPK
```

Figure II-7. Comparison of the predicted amino acid sequences between BrFRIbΔ, AtFRIΔ, and functional AtFRI (AF228499.1). The coiled-coil domains are represented in red.

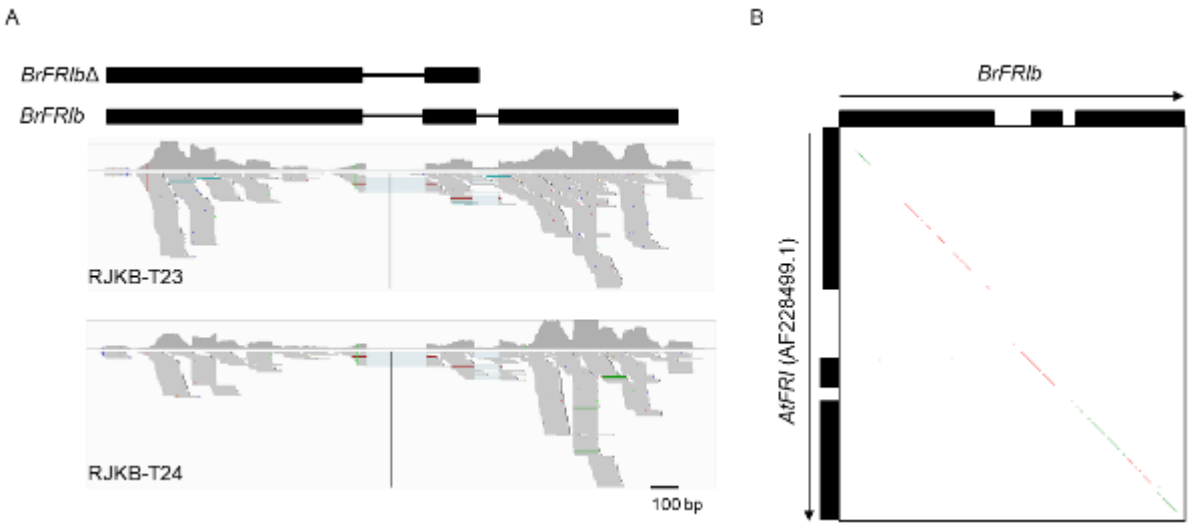

Figure II-8. The detection of new ORF in *BrFRIb*. (A) Mapping by RNA-seq reads of RJKB-T23 and RJKB-T24 against reference *B. rapa* genome (Shimizu et al. 2014). (B) Harr plot analysis of the regions covering *FRI* sequences between *A. thaliana* (AF228499.1) and *B. rapa* (*BrFRIb*, reference genome). Each dot-plot shows the positions where 16 out of 20 nucleotides match in the two sequences.

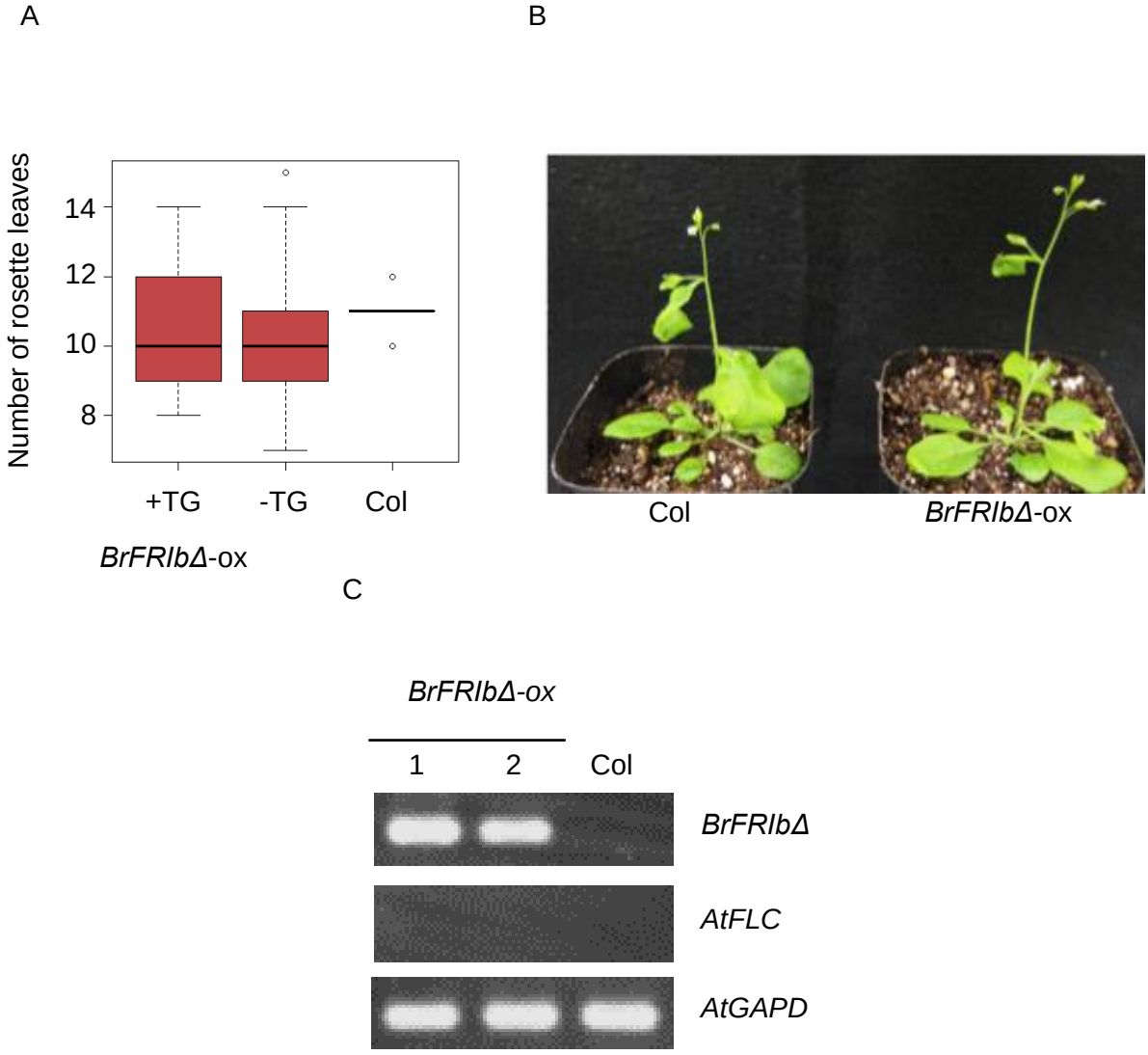

Figure II-9. Overexpression of *BrFRIbΔ* did not change the flowering time. (A) Number of rosette leaves at flowering is shown in the y-axis and the plant lines are shown in the x-axis. T_2 plants derived from three independent T_1 plants were used. There was no significant difference in rosette leaf number between T_2 plants overexpressing *BrFRIbΔ* and Col (Student's *t*-test, $p > 0.05$). -TG shows the absence of transgenes (TG). (B) Flowering-time phenotype of Col and T_2 plants overexpressing *BrFRIbΔ* (C) RT-PCR analysis of *BrFRIbΔ* and *AtFLC* transcripts using leaves without cold treatment. *AtGAPD* was used as a control to demonstrate equal RNA loading.

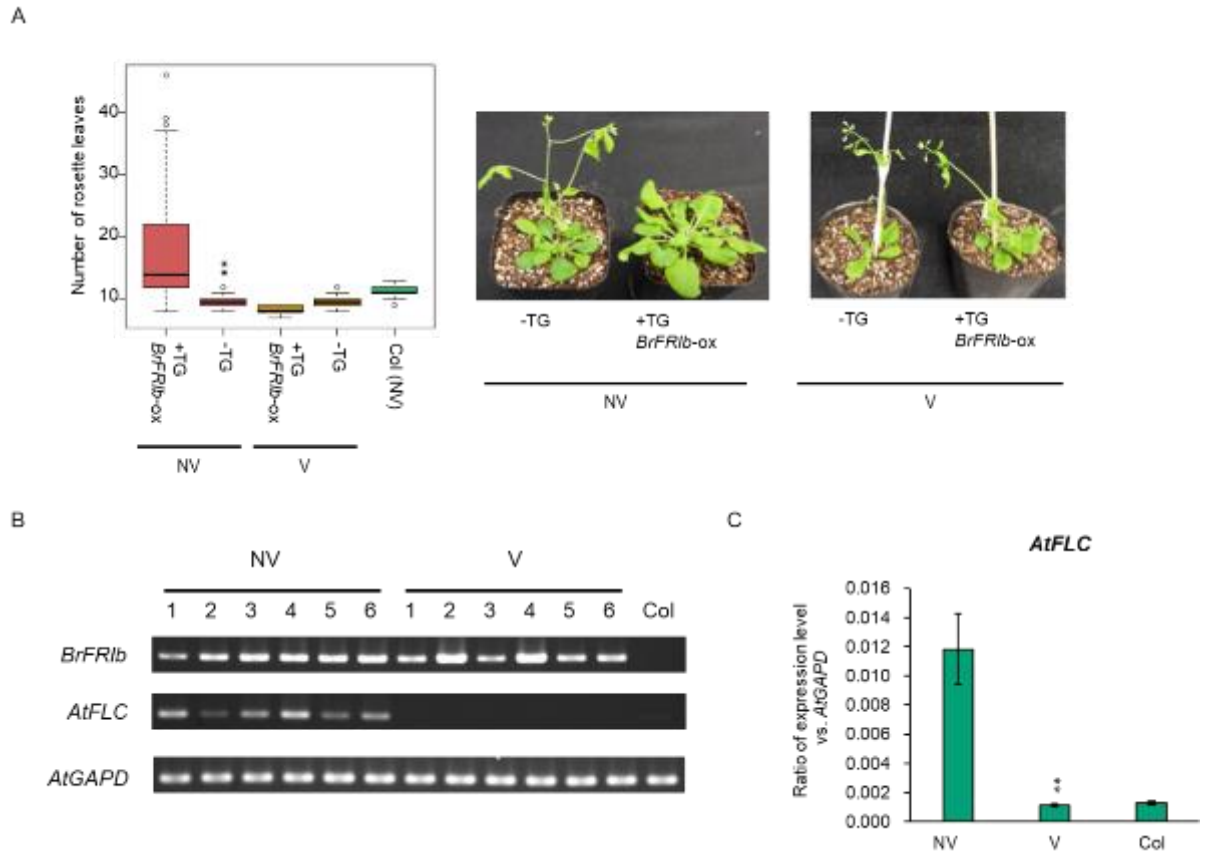

Figure II-10. Overexpression of *BrFRIb* causes late flowering and induce *AtFLC* expression. (A) Number of rosette leaves and flowering-time phenotypes in T_2 plants with overexpressing *BrFRIb* with (V) or without vernalization (NV). +TG and -TG show the presence and absence of transgenes (TG), respectively. **, $p < 0.01$ (Students *t*-test) (B) RT-PCR analysis showing transcription of *BrFRIb* and *AtFLC* before and after four weeks of cold treatment. Non-vernalized Col line is included as a control. *AtGAPD* was used as a control to demonstrate equal RNA loading. NV, non-vernalized; V, vernalized. (C) RT-qPCR analysis of *AtFLC* with (V) and without (NV) four weeks of cold treatment. *AtFLC* expression level relative to *AtGAPD* is shown in the y-axis. Non-vernalized Col line is included as a control. Data presented are the average and standard error (s.e.) from three biological and experimental replications. **, $p < 0.01$ (Students *t*-test)

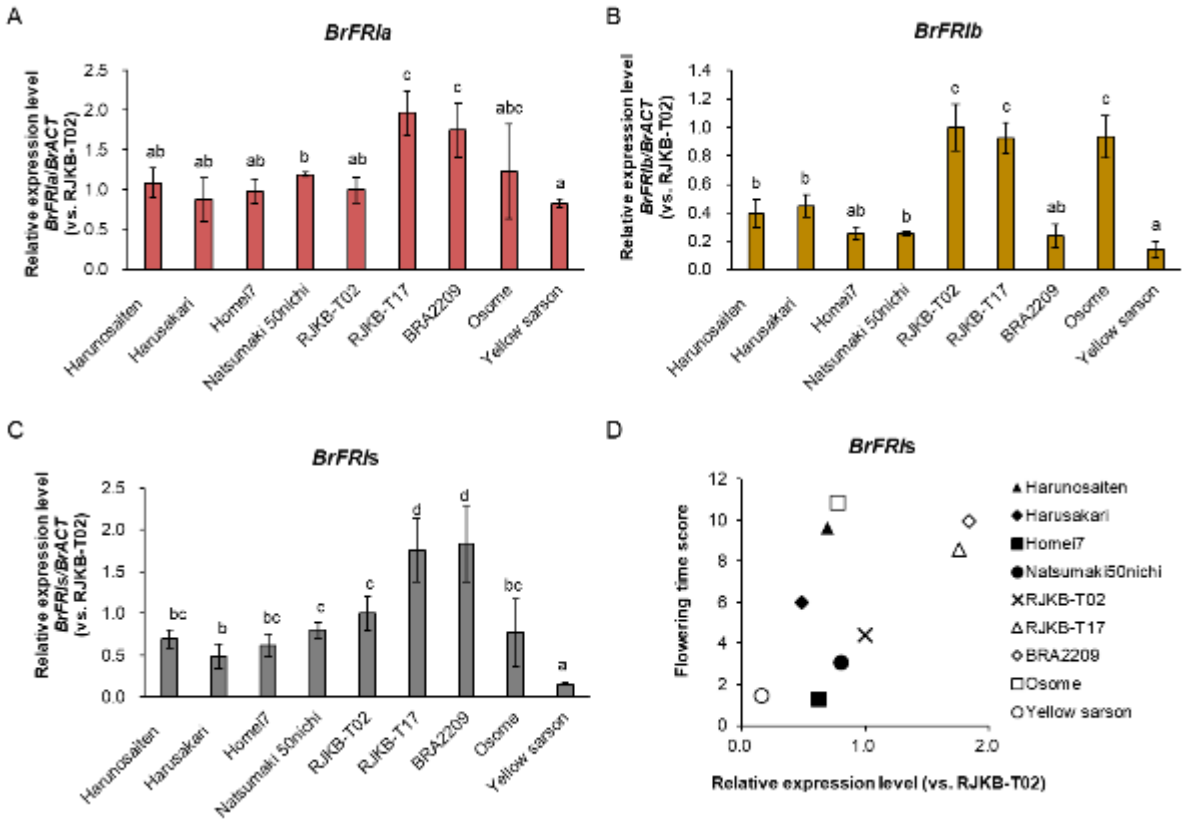

Figure II-11. The relationship between the expression levels of *BrFRI* and flowering time. (A-C) There is variation of the expression levels of *BrFRIa*, *BrFRIb*, or *BrFRIs* (*BrFRIa* + *BrFRIb*) among nine *B. rapa* lines. Expression level of each gene relative to *BrACTIN* (*BrACT*) is calculated, and the y-axis shows the ratio against RJKB-T02. Data presented are the average and standard error (s.e.) from three biological and experimental replications. Letters above the bars indicate significant differences at $p < 0.05$ (Tukey-Kramer test). (D) The relationship between the expression levels of *BrFRIs* and flowering time score in nine *B. rapa* lines.

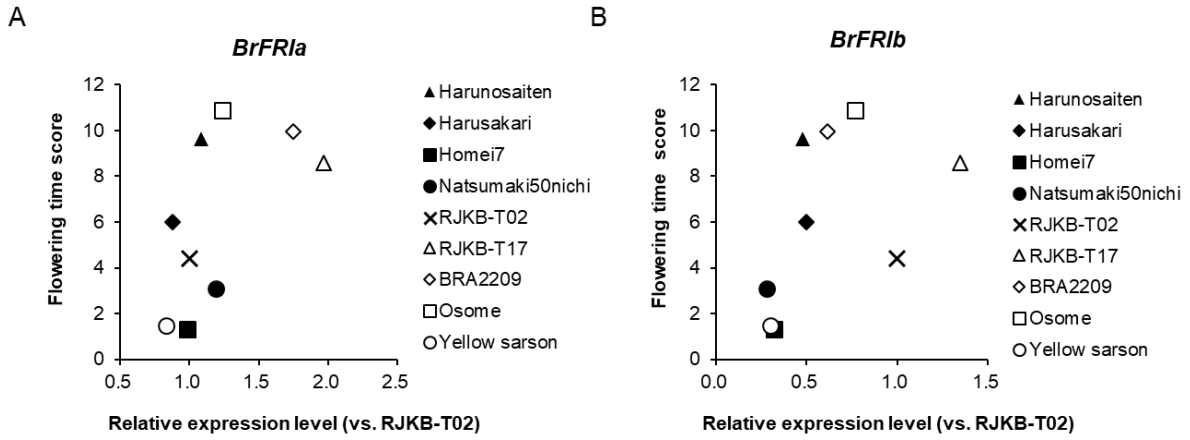

Figure II-12. The steady state expression levels of *BrFRI* is not associated with days to flower after four weeks of cold treatment. Expression level of each gene relative to *BrACTIN* is calculated, and the ratio against RJKB-T02 is used. The correlation coefficient between *BrFRIa* (A) or *BrFRIb* (B) and flowering time score are 0.59 ($p > 0.05$) or 0.49 ($p > 0.05$), respectively.

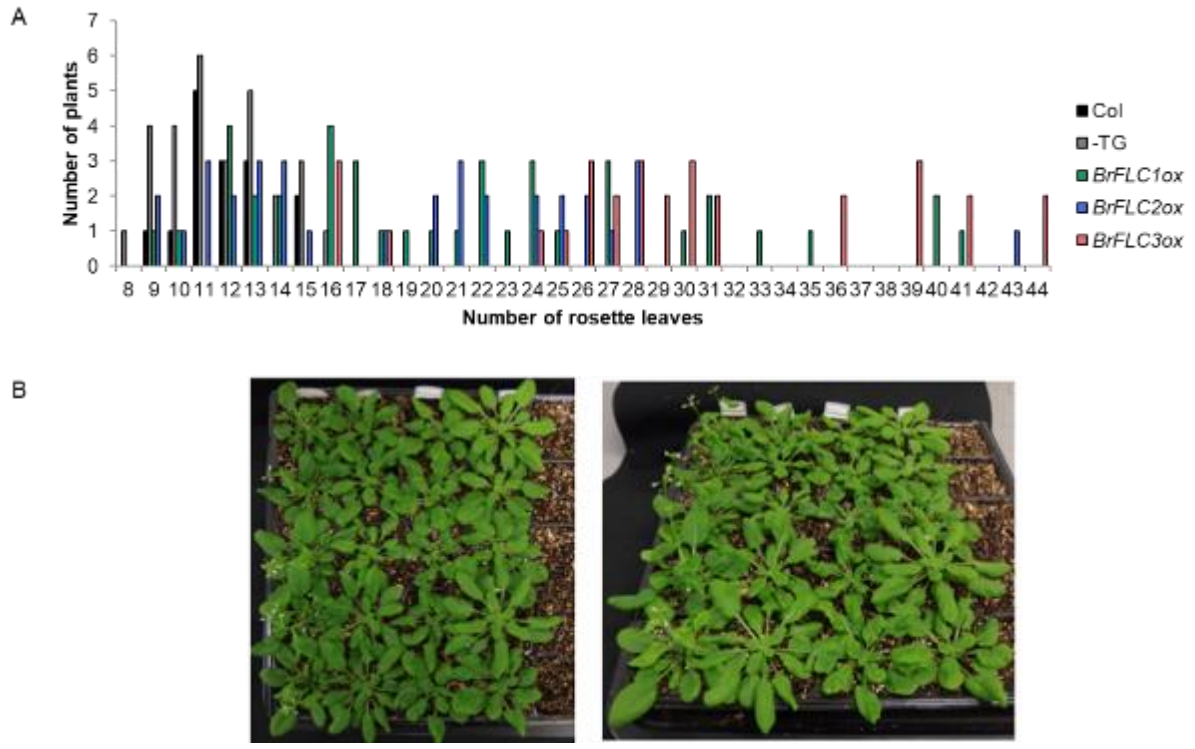

Figure II-13. Overexpressed *BrFLC1*, *BrFLC2*, or *BrFLC3* causes late flowering. (A) Distribution of the flowering time. Arrows represent the average number of rosette leaves in each line. (B) Flowering-time phenotype of Col and T_2 plants overexpressing *BrFLC1*, *BrFLC2,* or *BrFLC3*.

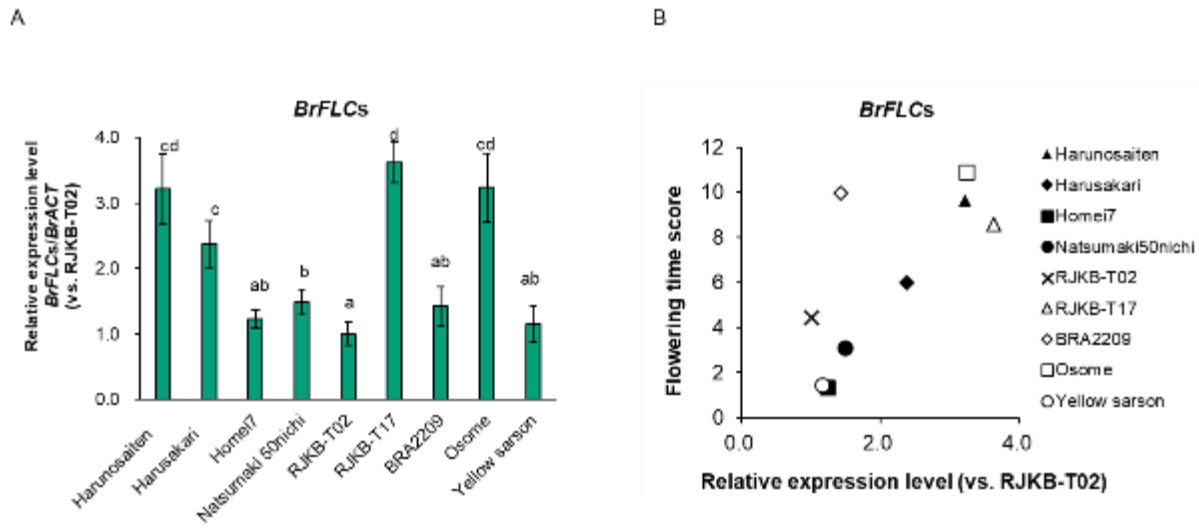

Figure II-14. The relationship between the expression level of *BrFLCs* and flowering time. (A) There is variation of the expression levels of *BrFLC*s (*BrFLC1* + *BrFLC2* + *BrFLC3* + *BrFLC5*) among nine *B. rapa* lines. Expression level of each gene relative to *BrACTIN* (*BrACT*) is calculated, and the y-axis shows the ratio against RJKB-T02. Data presented are the average and standard error (s.e.) from three biological and experimental replications. Letters above the bars indicate significant differences at $p < 0.05$ (Tukey-Kramer test). (B) The steady state expression level of *BrFLC*s is associated with days to flower after four weeks of cold treatment. The correlation coefficient between *BrFLC*s and flowering time score is 0.73 ($p < 0.05$) and if remove the BRA2209 data (outlier) being 0.91 ($p < 0.05$).

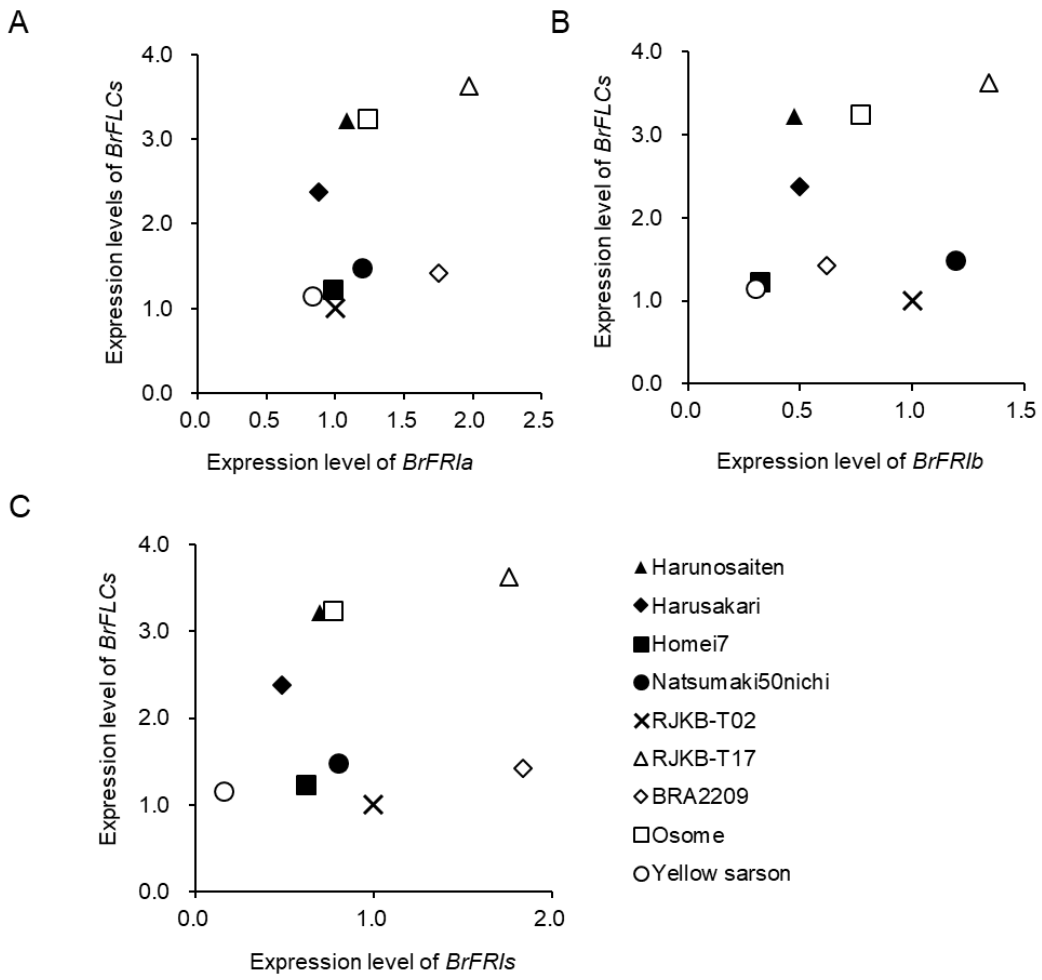

Figure II-15. The relationship between the expression levels of *BrFRIa* (A), *BrFRIb* (B) or *BrFRI*s (C) and *BrFLC*s in nine *B. rapa* lines. Expression level of each gene relative to *BrACTIN* is calculated, and the ratio against RJKB-T02 is used. The correlation coefficient between *BrFRIa*, *BrFRIb*, or *BrFRI*s and *BrFLC*s are 0.42 ($p > 0.05$), 0.48 ($p > 0.05$), or 0.23 ($p > 0.05$), respectively.

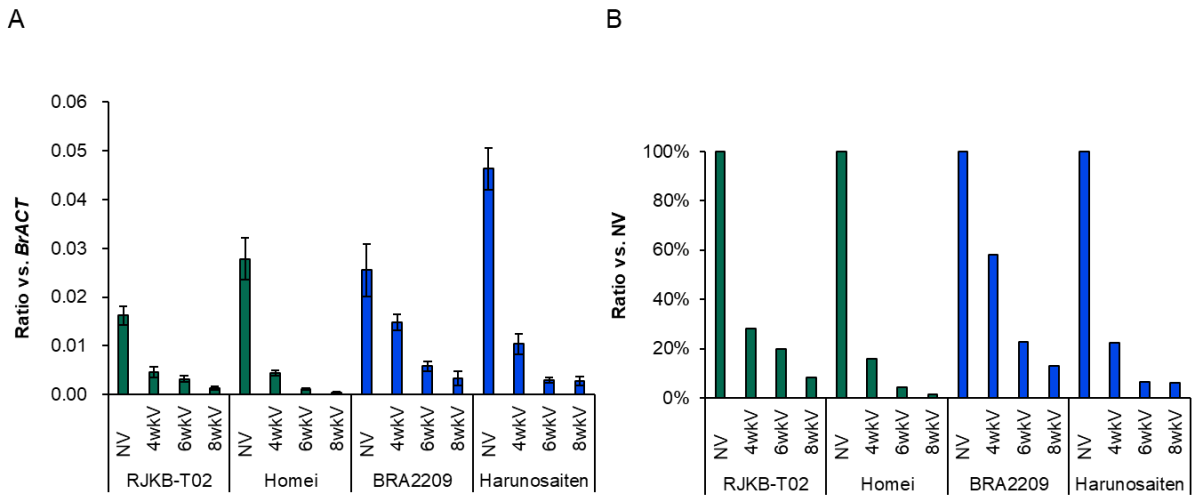

Figure II-16. Variation of *BrFLC* repression by cold treatment. (A) Expression pattern of *BrFLC*s (*BrFLC1* + *BrFLC2* + *BrFLC3* + *BrFLC5*) in four *B. rapa* lines before (NV) and after 4, 6, and 8 weeks of cold treatments (4wkV, 6wkV, and 8wkV, respectively). Y-axis represents the relative expression level of *BrFLC*s compared to *BrACTIN* (*BrACT*). Data presented are the average and standard error (s.e.) from three biological and experimental replications. (B) The ratio of the expression level after cold treatment compared to before cold treatment.

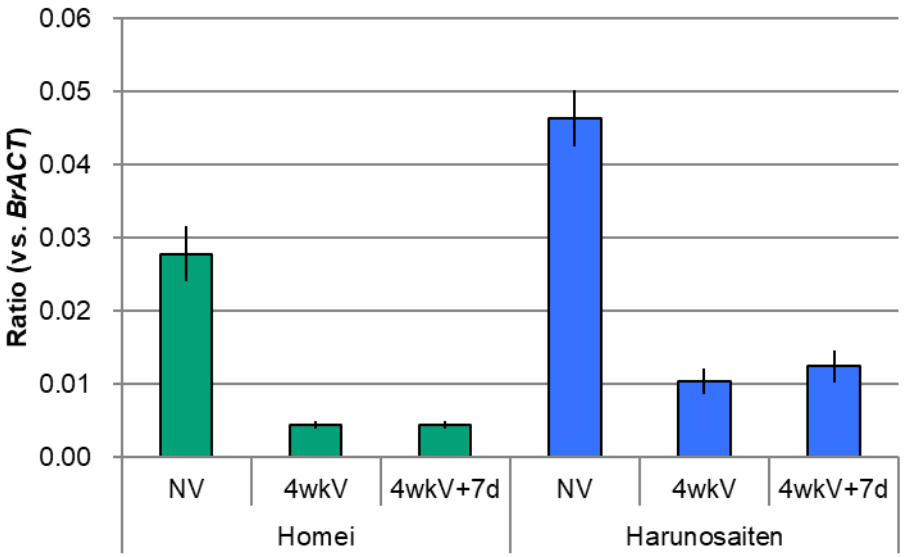

Figure II- 17. Expression pattern of *BrFLC*s (*BrFLC1* + *BrFLC2* + *BrFLC3* + *BrFLC5*) in Homei and 'Harunosaiten' before and after four weeks of cold treatments. Expression level relative to *BrACTIN* (*BrACT*) is calculated. Data presented are the average and standard error (s.e.) from three biological and experimental replications. NV, non-vernalized; 4wkV, four weeks of cold treatment; 4wkV+7d, four weeks of cold treatment and then seven days normal growth condition.

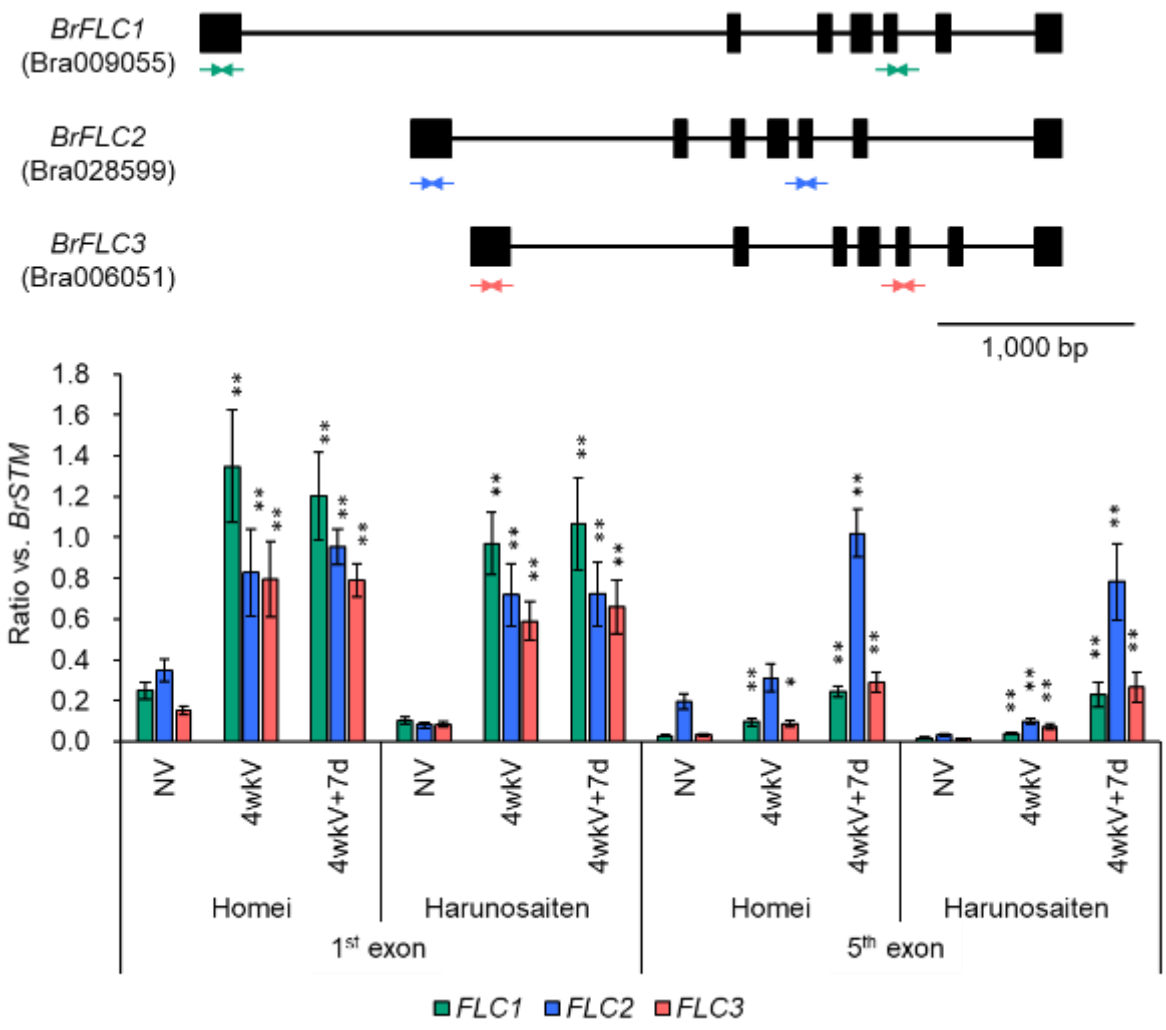

Figure II-18. ChIP-qPCR using H3K27me3 antibodies of *BrFLC* genes before and after four weeks of cold treatment. Upper panel is the gene structure of three *BrFLC* paralogs. Black boxes represent exon and arrows represent the primer position for ChIP-qPCR. Bottom panel shows the level of H3K27me3 in three *BrFLC*s before and after four weeks of cold treatment. Y-axis represents the ratio compared to *BrSTM*, which is an H3K27me3-marked gene. Data presented are the average and standard error (s.e.) from three biological and experimental replications. Statistical tests between NV and 4wkV or between NV and 4wkV+7d are shown (Student *t*-test, *; $p < 0.05$, **; $p < 0.01$). NV, non-vernalized; 4wkV, four weeks of cold treatment; 4wkV+7d, four weeks of cold treatment and then seven days normal growth condition.

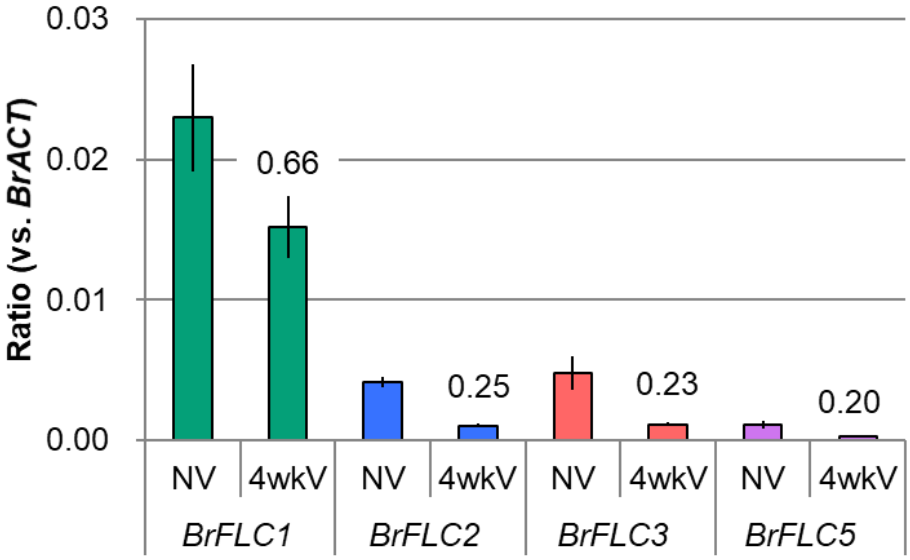

Figure II-19. Expression pattern of *BrFLC* genes in BRA2209 before (NV) and after four weeks of cold treatments (4wkV). Expression level of each *BrFLC* paralog relative to *BrACTIN* (*BrACT*) is calculated. Data presented are the average and standard error (s.e.) from three biological and experimental replications. The ratio of the expression level after cold treatment compared to before cold treatment are shown above the bars. NV, non-vernalized; 4wkV, four weeks of cold treatment.

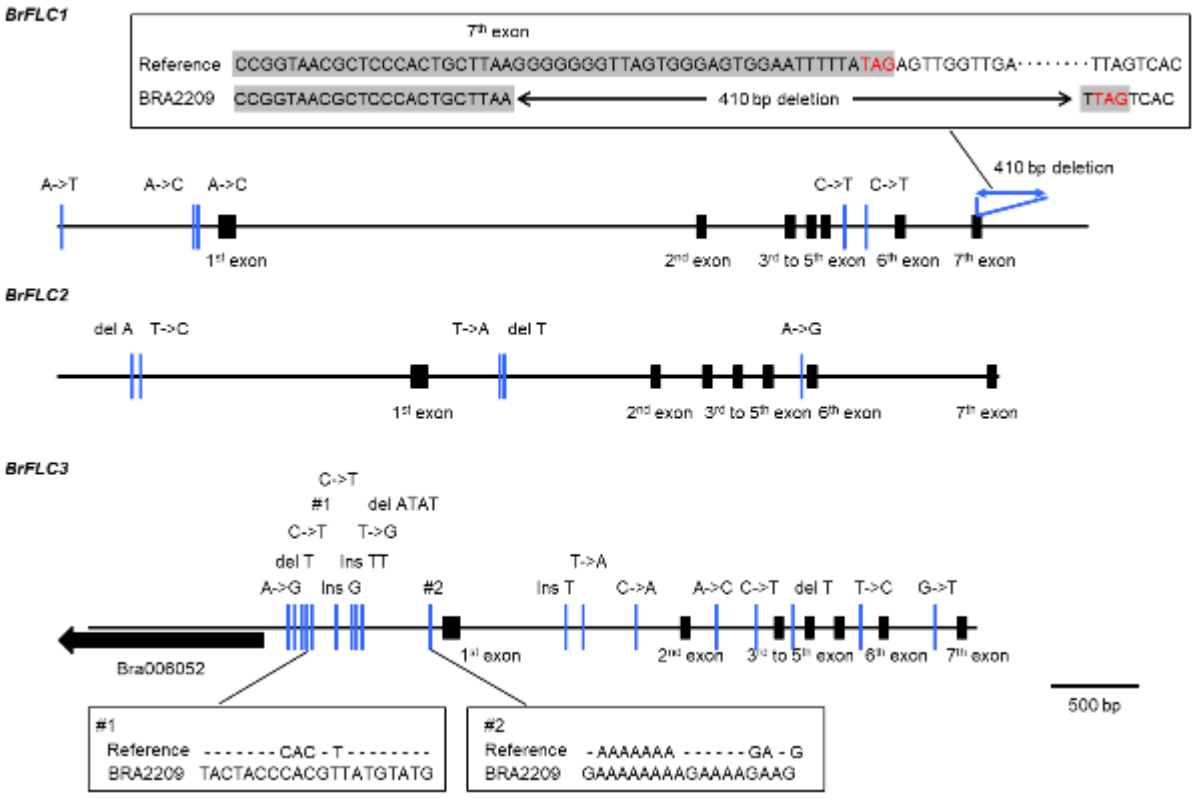

Figure II-20. Genome structure of *BrFLC1*, *BrFLC2*, and *BrFLC3* in BRA2209. Blue lines represent the position of substitutions or indels. del, deletion; ins, insertion.

Table II-1. Plant materials

	Name	Type	Variety	Flowering time	*BrFRI* sequence	Genetic distance	*BrFLC* sequence	*BrFRI* expression	*BrFLC* expression	*BrFLC* expression following vernalization	ChIP
1	Harunosaiten	Commercial cultivar (Watanabe Seed Co., Ltd)	Chinese cabbage (var. *pekinensis*)	✔	✔		✔	✔	✔	✔	✔
2	Harusakari	Commercial cultivar (Watanabe Seed Co., Ltd)	Chinese cabbage (var. *pekinensis*)	✔	✔			✔	✔		
3	Natsumaki 50nichi	Commercial cultivar (Watanabe Seed Co., Ltd)	Chinese cabbage (var. *pekinensis*)	✔	✔			✔	✔		
4	Chiifu	Commercial cultivar	Chinese cabbage (var. *pekinensis*)		✔	✔					
5	Yellwo sarson	Commercial cultivar	Oilseed (var. *oleifera*)	✔	✔			✔	✔		
6	Homei	Doubled haploid line	Chinese cabbage (var. *pekinensis*)	✔	✔	✔	✔	✔	✔	✔	✔
7	BRA2209	Doubled haploid line	Turnip (var. *rapa*)	✔	✔	✔	✔	✔	✔	✔	
8	Atsumi	Doubled haploid line	Turnip (var. *rapa*)		✔	✔					
9	Kisobeni	Doubled haploid line	Turnip (var. *rapa*)		✔	✔					
10	Osome (OSD2)	Doubled haploid line	Komatsuna (var. *perviridis*)	✔	✔	✔		✔	✔		
11	Wase-Maruba	Doubled haploid line	Komatsuna (var. *perviridis*)		✔	✔					
12	RJKB-T01	Inbred line	Chinese cabbage (var. *pekinensis*)		✔	✔					

13	RJKB-T02	Inbred line	Chinese cabbage (var. *pekinensis*)	✔	✔	✔	✔	✔	✔	✔	✔
14	RJKB-T03	Inbred line	Chinese cabbage (var. *pekinensis*)		✔	✔					
15	RJKB-T04	Inbred line	Chinese cabbage (var. *pekinensis*)		✔	✔					
16	RJKB-T05	Inbred line	Chinese cabbage (var. *pekinensis*)		✔	✔					
17	RJKB-T06	Inbred line	Chinese cabbage (var. *pekinensis*)		✔	✔					
18	RJKB-T07	Inbred line	Chinese cabbage (var. *pekinensis*)		✔	✔					
19	RJKB-T08	Inbred line	Chinese cabbage (var. *pekinensis*)		✔	✔					
20	RJKB-T09	Inbred line	Chinese cabbage (var. *pekinensis*)		✔	✔					
21	RJKB-T10	Inbred line	Chinese cabbage (var. *pekinensis*)		✔	✔					
22	RJKB-T11	Inbred line	Chinese cabbage (var. *pekinensis*)		✔	✔					
23	RJKB-T12	Inbred line	Chinese cabbage (var. *pekinensis*)		✔	✔					
24	RJKB-T13	Inbred line	Chinese cabbage (var. *pekinensis*)		✔	✔					
25	RJKB-T14	Inbred line	Chinese cabbage (var. *pekinensis*)		✔	✔					
26	RJKB-T15	Inbred line	Chinese cabbage (var. *pekinensis*)		✔	✔					
27	RJKB-T16	Inbred line	Chinese cabbage (var. *pekinensis*)		✔	✔					
28	RJKB-T17	Inbred line	Chinese cabbage (var. *pekinensis*)	✔	✔	✔	✔	✔	✔		
29	RJKB-T18	Inbred line	Chinese cabbage (var. *pekinensis*)		✔	✔					
30	RJKB-T19	Inbred line	Chinese cabbage (var. *pekinensis*)		✔	✔					
31	RJKB-T20	Inbred line	Chinese cabbage (var. *pekinensis*)		✔	✔					
32	RJKB-T21	Inbred line	Chinese cabbage (var. *pekinensis*)		✔	✔					
33	RJKB-T22	Inbred line	Chinese cabbage (var. *pekinensis*)		✔	✔					
34	RJKB-T23	Inbred line	Chinese cabbage (var. *pekinensis*)		✔	✔					
35	RJKB-T24	Inbred line	Chinese cabbage (var. *pekinensis*)		✔	✔	✔				
36	YBCG-01	Inbred line	Komatsuna (var. *perviridis*)		✔	✔					
37	YBCG-02	Inbred line	Komatsuna (var. *perviridis*)		✔	✔					

[#] *FLC* expression levels following different duration of cold treatments were examined

Table II-2. Criteria for evaluating flowering time

Score	Days for flowering after four weeks of cold treatment
1	46 =< x =< 50
2	51 =< x =< 55
3	56 =< x =< 60
4	61 =< x =< 65
5	66 =< x =< 70
6	71 =< x =< 55
7	76 =< x =< 80
8	81 =< x =< 85
9	86 =< x =< 90
10	91 =< x =< 95
11	96 =< x =< 100
12	101 =< x

Table II-3. Sequences of primers used in this study

Name	Primer sequences (5'-3')	
RT-PCR/RT-qPCR		
AtGAPD	CTCACTTGAAGGGTGGTGCT	TGGTCATGAGTCCCTCAACA
AtFLC	GTCGCTCTTCTCGTCGTCGTCTC	TGACATTTGATCCCACAAGC
BrActin	CGGTCCAGCTTCGTCATACTCAGCC	AAATGTGATGTGGATATCAGGAAGG
BrFRIa	AGAAGCTTTTGGTTAGTTCTGTG	TCATCAGTACCACTCTGCCTAAT
BrFRIb	AACGGTCACCTTTCCTTGTC	GCTTTCTGTTTTGCCCTCTC
BrFRIa/b	GGCGGCTGCTGTTGCGTGGAAG	CTTGATACTTGAATCAACTATAC
BrFLC1/2/3/5	GACGCARYGGTCTCATYGAGAAAGC	AWCATTARTTYTGTCTTYSTAGCTC
BrFLC1	CTTGAGGAATCAAATGTCGATAA	CCCTTAAGCAGTGGGAGCGTTAC
BrFLC2	AAGCTTGTGGAATCAAATTCTG	TAATAAAGYAGYCGGAGAGTYAC
BrFLC3	GTGGAATCAAATGTCGGTGG	TAATTAAGYAGYGGGAGAGTYAC
BrFLC5	TAATGTTAAAGCTTGTTGAAAGT	TAATTAAGYAGYGGGAGAGTYAC
Sequence of DNA fragments of *BrFRI*a or *BrFRI*b		
BrFRIa-F1/R1	GAGTCAAAAAGATATTAATAGGGCC	GAAATATCAATTACAGATCCTAAGC
BrFRIa-F2/R2	TGAACATCTCTGAGCGAGCC	ATTTCTGACAACCTTGGACG
BrFRIa-F3/R3	GGAGCAAAGAGCTCCGAAGG	GGTGAATGTCTGTATAGACG
BrFRIb-F1/R1	TACATACCTTATCTCTCCGACATC	ACTTCATCACTGATAACAACGCAGC
BrFRIb-F2/R2	CCAAGGCAATTGCACTCTAA	CAACTCGCACAATCGCTCCA
Sequence of the full length coding region in each *FLC* paralog		
BrFLC1	CAAAGCACTGTTGGAGACAGAAGCC	CCAACTCTATAAAAATTCCACTCCC
BrFLC2	TCAAATTAGGGCACAAAGGCTTCTC	GTCACAAGTTTTGGACTTAAGGTGG
BrFLC3	TCAAATTAGGGCACAGAGACCACTT	TTTGATCAGCCCCGTCTAACGGTGG
Sequence of the genic region covering each *FLC*		
BrFLC1		
9055 pro F/9055 int1 R	CTCAGAAGTATTTTAAGACC	CACCGGAGGAGAAGCTGTAG
9055 5UTR / 9055 ex2 R	CAAAGCACTGTTGGAGACAGAAGCC	CCAGGCTGGAGAGAAGAGAA
9055 int1 F / 9055 ex7 R	GTTCATTCTTTCAAGGGTTAGCTG	TCGCACAAGATTACTCTTCTCC
9055 int 6 F/ 9056 R	AGATGGAGAAGAGTAATCTTGTGCG	GCAGAGGTGCGTATGATCTAGCCAT
9055 F1 / R1	TTCGATATGTAAAGGCAAAC	GAAAATTGCAACCCCTTGTC
9055 F2 / R2	ATGGCCATGAGAAATACATG	TAATCAATTTCTAACGCTGG

9055 R3 / R4	CTTTAAGGTTCTCGACAAGC	TCGCACAAGATTACTCTTCTCC
BrFLC2		
28599 pro F/28599 ex2 R	TGATTACGCCAAGCTCGGGAATATATTTCCCCAC	GACCACCCGGGGATCTCAGAGCTTTAAGATCATCAG
28599 5 UTR / 3 UTR	TCAAATTAGGGCACAAAGGCTTCTC	GTCACAAGTTTTGGACTTAAGGTGG
28599 F1 / R1	GGCTCAGTTGCAGTTTTCACC	CATACTTATCGCCGGCGGAG
28599 F2 / R2	CTTCCTACTTCAGACCTCAC	CAGAATGATGTCCAACAACCTG
28599 F3 / F4	GGCTACTAGTTGGTTCTTAG	GGTTCACACCATGAGCTACT
BrFLC3		
6051 pro F / 6051 int1 R	TGATTACGCCAAGCTGCGTCATCCTCATCACCA	GGCTAATAAAGGAAGGCACAGA
6051 5UTR/ 6051 3UTR	TCAAATTAGGGCACAGAGACCACTT	TTTGATCAGCCCCGTCTAACGGTGG
6051 F1 / R1	CAACCATGAGGACACCAGGC	TCCTTCGATTCCACTATAGG
6051 F2 / R2	TCTTCTCTTCTGTGCCTTCC	CAGTATGAAGTCAACGTACC
6051 F3 / R3	GCAATGCACTGCACTCCGGA	ATCCAAAAACCAGAATGCCC
For Construction		
BrFRIb	GGATCCATGGCCTTTCGTAATGGTTC	GAGCTCCTAATGTAAAGAAGGGAC
BrFLC1	GGTCTAGAATGGGGAGGAAGAAACTTGA	GCGAGCTCCTAATAAAGCAGTCGGAGAG
BrFLC2	GGTCTAGAATGGGGAGGAAGAAACTTGA	GCGAGCTCCTATAAAAATTCCACTCCCAC
BrFLC3	GGTCTAGAATGGGGAGGAAGAAACTTGA	GCGAGCTCCTAATTAAGCAGTGGGAGAG
ChIP-qPCR		
BrFWA	CGGCATATGATTCGTTTGTG	CCTGGTTGTGTAGCATGTGG
BrSTM	TGGAGAGTGGTTCCAACAGCACTTC	GGAGCTACTTTGTTGGTGGTGTGAC
Bra013206	GACGAGCACAAGAGTGGTGA	TAATCGCTGTCGCTGTCACT
Bra028913	CCCTGGGAGCAACTCTGTTA	GTGGGAGCAATCCTGATGAC
BrFLC1-ex1-F/R	TGGGGAGGAAGAAACTTGAA	CACCGGAGGAGAAGCTGTAG
BrFLC2-ex1-F/R	CGACAAGTCACCTTCTCCAA	AGAGGAACGGAAGCGAAAAG
BrFLC3-ex1-F/R	TTGAGAACAAAAGTAGCCGACA	GGCTAATAAAGGAAGGCACAGA
BrFLC1-ex5-F/R	TGCTTCCAAGTTTATAGCTA	CTCCTGTTTTAAAGATCAAC
BrFLC2-ex5-F/R	ATCTTACCTTGTGTCGAGAG	AAGGTCAACATGATTATCAC
BrFLC3-ex5-F/R	TCTCGTGTTTGAAAGCCTCA	TGAAGGACAACATGTTCATC

Table II-4. The amino acid sequence identities of FRIs

		BrFRIa						BrFRIb						AtFRI	BoFRIa	BoFRIb
		GA	GB	GC	A	WM	YS	GA	GB	B2	Y1	Y2	YS			
BrFRIa	Group A (GA)		99.4	98.6	98.6	98.4	98.8	63.8	63.8	64.1	63.4	64.0	63.8	57.4	87.9	64.3
	Group B (GB)	99.4		99.1	98.1	97.9	98.3	63.9	63.9	64.2	63.5	64.1	63.9	57.5	87.9	64.2
	Group C (GC)	98.6	99.1		98.4	97.8	97.8	63.9	63.9	64.1	63.5	64.1	63.9	57.1	87.7	64.2
	Atsumi (A)	98.6	98.1	98.4		98.8	98.8	64.0	63.9	64.3	63.6	64.1	64.0	56.9	88.1	64.4
	Wase Maruba (WM)	98.4	97.9	97.8	98.8		99.6	63.5	63.5	63.9	63.1	63.7	63.5	56.8	88.1	64.0
	Yellow Sarson (YS)	98.8	98.3	97.8	98.8	99.6		63.5	63.5	63.9	63.1	63.7	63.5	56.8	87.9	64.0
BrFRIb	Group A (GA)	63.8	63.9	63.9	64.0	63.5	63.5		98.6	96.8	95.8	97.3	97.0	59.9	65.4	86.3
	Group B (GB)	63.8	63.9	63.9	63.9	63.5	63.5	98.6		98.2	97.2	98.4	98.0	59.9	65.4	87.4
	BRA2209 (B2)	64.1	64.2	64.1	64.3	63.9	63.9	96.8	98.2		97.5	98.7	98.4	59.7	65.6	86.7
	YBCG-T01 (Y1)	63.4	63.5	63.5	63.6	63.1	63.1	95.8	97.2	97.5		97.7	97.3	59.4	65.0	85.8
	YBCG-T02 (Y2)	64.0	64.1	64.1	64.1	63.7	63.7	97.3	98.4	98.7	97.7		99.6	59.7	65.6	86.3
	Yellow Sarson (YS)	63.8	63.9	63.9	64.0	63.5	63.5	97.0	98.0	98.4	97.3	99.6		59.5	65.4	86.2
AtFRI		57.4	57.5	57.1	56.9	56.8	56.8	59.9	59.9	59.7	59.4	59.7	59.5		59.0	57.8
BoFRIa		87.9	87.9	87.7	88.1	88.1	87.9	65.4	65.4	65.6	65.0	65.6	65.4	59.0		66.6
BoFRIb		64.3	64.2	64.2	64.4	64.0	64.0	86.3	87.4	86.7	85.8	86.3	86.2	57.8	66.6	

BrFRIa-Group A; Homei, Harusakari, Harunosaiten, Natsumaki 50nichi, Chiifu, RJKB-T01, T02, T03, T05, T06, T07, T08, T09, T10, T11, T12, T16, T17, T18, T19, T20, T21, T22, T23, T24

BrFRIa-Group B; Osome, YBCG-01, 02, RJKB-T04, 13, 14, 15

BrFRIa-Group C; BRA2209, Kisobeni

BrFRIb-Group A; Homei, Harusakari, Harunosaiten, Natsumaki 50nichi, Atsumi, Chiifu, Kisobeni, Osome, Wase Maruba, RJKB-T01, T03, T05, T06, T07, T08, T09, T10, T12, T13, T14, T16, T18, T19, T20, T21, T22, T23, T24

BrFRIb-Group B; RJKB-T02, T04, T11, T15, T17

Chapter III

The histone modification H3 lysine 27 tri-methylation has conserved gene regulatory roles in the triplicated genome of *Brassica rapa* L.

Abstract

Brassica rapa L. is an important vegetable and oilseed crop. We investigated the distribution of the histone mark tri-methylation of H3K27 (H3K27me3) in the *B. rapa* genome and its role in the control of gene expression at two stages of development (2-day cotyledons and 14-day leaves) and among paralogs in the triplicated genome. H3K27me3 has a similar distribution in two inbred lines, while there was variation of H3K27me3 sites between tissues. Sites that are specific to 2-day cotyledons have increased transcriptional activity, and low levels of H3K27me3 in the gene body region. In 14-day leaves, levels of H3K27me3 were associated with decreased gene expression. In the triplicated genome, H3K27me3 is associated with paralogs that have tissue-specific expression. Even though *B. rapa* and *Arabidopsis thaliana* are not closely related within the Brassicaceae, there is conservation of H3K27me3-marked sites in the two species. Both *B. rapa* and *A. thaliana* require vernalization for floral initiation with *FLC* being the major controlling locus. In all four *BrFLC* paralogs, low-temperature treatment increases H3K27me3 at the proximal nucleation site reducing BrFLC expression. Following return to normal temperature growth conditions, H3K27me3 spreads along all four *BrFLC* paralogs providing stable repression of the gene.

Keywords: histone H3 lysine 27 tri-methylation, vernalization, epigenetics, Brassica, FLOWERING LOCUS C

Introduction

Brassica rapa L. encompasses commercially important vegetable crops including Chinese cabbage (var. *pekinensis*), pak choi (var. *chinensis*), and turnip (var. *rapa*) as well as oilseed crops (var. *oleifera*). The *B. rapa* genome has undergone a whole-genome triplication resulting in multiple copies of paralogous genes. Three subgenomes, the least fractioned subgenome (LF) and two more fractionated subgenomes (MF1 and MF2), are recognized within the *B. rapa* genome (Cheng et al. 2012).

Activity levels of the component genes of the genomes are regulated by transcription factors and epigenetic modifications. The regulation of gene expression by epigenetic modification is crucial for the development and adaptation of plants to changing environments (Fujimoto et al. 2012; Quadrana and Colot, 2016). Epigenetic modifications refer mainly to DNA methylation and covalent modifications of the histone proteins. The tri-methylation of histone H3 lysine 4 (H3K4me3) and H3K36me3 have been associated with transcriptional activation, and H3K9me2 and H3K27me3 with gene silencing (Fuchs et al. 2006; Xiao et al. 2016).

H3K27me3 modification is catalyzed by the POLYCOMB REPRESSIVE COMPLEX 2 (PRC2), which is composed of a subset of the Polycomb group (PcG) proteins (Zheng and Chen, 2011). In *Arabidopsis thaliana*, H3K27me3 sites occur in euchromatin and not in transposable elements or heterochromatin (Turck et al. 2007; Zhang et al. 2007). In plants, H3K27me3 regions are usually limited to single genes, rarely extending into adjacent genes (Zhang et al. 2007; He et al. 2010; Makarevitch et al. 2013). Conservation of H3K27me3 sites between lines has been observed in *A. thaliana*, rice, and maize (He et al. 2010; Moghaddam et al. 2011; Makarevitch et al. 2013). The chromosomal distribution of the H3K27me3 sites in the histones of genomes of different plant species provides data on the possible conservation of H3K27me3 sites and effect on gene activity (Zheng and Chen, 2011). H3K27me3 preferentially marks repressed or lowly expressed genes in *A. thaliana*, rice, and maize (Liu et al. 2010; Chen and Zhou, 2013). The level of H3K27me3 can vary between tissues at the same gene locus (Zhang et al. 2007; Weinhofer et al. 2010; Bouyer et al. 2011; Lafos et al. 2011; Makarevitch et al. 2013).

In *A. thaliana*, *FLOWERING LOCUS C* (*FLC*) is a key determinant of vernalization, which is the acquisition or acceleration of the ability to flower by a prolonged low temperature treatment (Chouard, 1960). *FLC* encodes a MADS box DNA binding protein, which acts as a

floral repressor of *SUPPRESSOR OF CONSTANS OVEREXPRESSION 1* (*SOC1*) and *FLOWERING LOCUS T* (*FT*) (Michaels and Amasino, 1999; Sheldon et al. 1999; Helliwell et al. 2006). Without prolonged cold exposure, *FLC* is expressed. With cold exposure chromatin structure at *FLC* is remodeled from an active to a repressed state. H3K27me3 levels are increased following vernalization, this is catalyzed by the VERNALIZATION (VRN) complex, one of several PRC2 complexes, and *FLC* expression is reduced (Dennis and Peacock, 2007; Groszmann et al. 2011). The FLC protein belongs to a MADS-box protein family, which contains five other members, MADS AFFECTING FLOWERING 1-5 (MAF1-MAF5). *MAF1-MAF4* are repressed by vernalization, and the repression in each case associated with an increase of H3K27me3 level (Sheldon et al. 2009).

The control of flowering is a critical property for the Chinese cabbage crop (Itabashi et al. 2018). Chinese cabbage is generally vernalization-sensitive and can respond to cold exposure during seed germination (Lin et al. 2005; Shea et al. 2018a; Su et al. 2018). In the absence of vernalization, most Chinese cabbage lines do not bolt before six months after sowing (Su et al. 2018). There are four *FLC* paralogs (*BrFLC1*, *BrFLC2*, *BrFLC3*, and *BrFLC5*) in the genome (Wang et al. 2011), and all can be repressed by vernalization treatment in some Chinese cabbage lines (Kim et al. 2007; Kakizaki et al. 2011; Kawanabe et al. 2016; Li et al. 2016).

In the present study, two inbred lines of Chinese cabbage, RJKB-T23 (T23) and RJKB-T24 (T24) show high sequence similarity to the reference genome of *B. rapa* var. *pekinensis* Chiifu-401-42 version 1.5 (Wang et al. 2011), have similar genetic distances to the reference genome (Shea et al. 2018b), and are parents of the commercial F_1 hybrid cultivar, 'W77'. We compared the distribution of H3K27me3 in the cotyledons and earliest leaves of these parental inbred lines to investigate the role of H3K27me3 in tissue specific gene expression. We found more similarity of distribution between the two parental lines than between different tissues within a line. In paralogous gene families and 14-day tissue, the presence of H3K27me3 was associated with tissue specific gene expression. We showed that H3K27me3 plays an important role in the regulation of *FLC* paralogous genes in the vernalization process of *B. rapa*.

Materials and methods

Plant materials and growth conditions

Two Chinese cabbage inbred lines (*B. rapa* var. *pekinensis*), RJKB-T23 (T23)/R09 and RJKB-T24 (T24)/S11 (Kawamura et al. 2016; Takahashi et al. 2018), and the C24 accession of *A. thaliana* were used. The genetic relationship between RJKB-T23 and RJKB-T24 is shown in Fig. III-1. *B. rapa* seeds were surface sterilized and grown on agar solidified Murashige and Skoog (MS) plates with 1 % (w/v) sucrose under long day (LD) condition (16h light) at 22 °C. Plants were harvested at 2 and 14 days after sowing (2 days; cotyledons (2d-C), 14 days; 1st and 2nd leaves (14d-L)) for expression and ChIP analyses (Fig. III-2). *A. thaliana* seeds were surface sterilized and grown on MS with 3 % (w/v) sucrose agar medium. After a 2-day stratification period at 4°C, seedlings were grown at 22°C under LD condition (16h light) for 12 days.

They do not flower for more than four months without vernalization. For vernalizing cold treatments in T24, seeds were surface-sterilized and placed on agar solidified MS plates with 1 % (w/v) sucrose for four weeks at 4°C under LD condition (16h light). Plant materials were harvested at the end of four weeks cold treatment (cotyledons/BrV1) at which time the developmental stage was similar to seedlings at 2 days after sowing under normal growth conditions (2d-C). After four weeks vernalization, seedlings were grown for 12 days using normal growth condition (1st and 2nd leaves/BrV2) at which time the developmental stage was similar to seedlings at 14 days after sowing under normal growth conditions (14d-L).

The C24 accession of *A. thaliana* is a vernalization sensitive and seed-vernalization-responsive type (Fujimoto et al. 2012b). For vernalization, C24 seeds were exposed to 4°C for four weeks then grown at 22°C under LD for 10 days (V) at which time the developmental stage was similar to seedlings at 12 days after sowing under normal growth conditions (NV).

Chromatin immunoprecipitation sequencing (ChIP-seq)

ChIP experiments were performed as described by Buzas et al. (2011). One gram of cotyledons or 1st and 2nd leaves of *B. rapa* or seedlings of *A. thaliana* was used for ChIP analysis, and anti-H3K27me3 (Millipore, 07-449) antibodies were used. In *B. rapa*, before the ChIP-seq, we validated the enrichment of purified immunoprecipitated DNAs by qPCR using the positive and negative control primer sets of H3K27me3 previously developed (Fig. III-3, Table III-1) (Kawanabe et al. 2016). Purified immunoprecipitated DNA and input DNA in *B. rapa* were sequenced by Hiseq2000 (36bp single-end). ChIP DNA fragments and input DNA in *A. thaliana* were sequenced by Illumina with an Illumina Genome Analyzer (GAII). Low quality reads or adapter sequences were purged from the ChIP-seq reads using cutadapt version 1.7.1

and Trim Galore! version 0.3.7. The reads were mapped to the *B. rapa* reference genome v.1.5 (http://brassicadb.org/brad/) or to the *A. thaliana* reference genome (TAIR 10) using Bowtie2 version 2.2.3 (Table III-2, III-3). The two replicates of 14-day 1st and 2nd leaves in *B. rapa* showed high correlation (Fig. III-4), thus these two data sets were combined. The mapped reads on the interspersed repeat regions (IRRs), such as the transposable elements (TEs) detected by RepeatMasker, were examined.

ChIP-qPCR was performed using a LightCycler Nano (Roche). The immunoprecipitated DNA was amplified using FastStart Essential DNA Green Master (Roche). PCR conditions were 95°C for 10 min followed by 40 cycles of 95°C for 10 s, 60°C for 10 s, and 72°C for 15 s, and Melting program (60°C to 95°C at 0.1°C/s). After amplification cycles, each reaction was subjected to melt temperature analysis to confirm single amplified products. Data presented are the average and standard error (SE) from three biological and experimental replications. Enrichment of H3K27me3 marks was calculated by comparing the target gene and non-H3K27me3-marked genes by qPCR using immunoprecipitated DNA as a template. The difference between primer pairs was corrected by calculating the difference observed by qPCR amplifying the input-DNA as a template. Primer sequences used in this study are shown in Table III-1.

Detection of H3K27me3 peaks by model-based analysis for ChIP-seq (MACS)

We performed peak calling on alignment results using MACS 2 2.1.0 and identified the regions having H3K27me3 peaks. The MACS callpeak was used with the following options (effective genome size: 2.30e+08, band width: 200, model fold: 10-30, tag size: 36). The cutoff of *p*-value, 1.00e-05, was used to call significant peaks. H3K27me3-marked genes were defined as genes that had a more than 200 bp length peak within a genic region (exon-intron) including 200bp upstream and downstream. The number of H3K27me3 peaks in *B. rapa* and *A. thaliana* is shown in Table III-4 and III-5, respectively. We validated H3K27me3-marked genes by ChIP-qPCR of genes that have been identified previously (Fig. III-5) (Kawanabe et al. 2016).

Identification of differentially marked H3K27me3 genes

To statistically identify the difference of H3K27me3 genic regions between lines, tissues, or between non-vernalized and vernalized samples, mapped reads on a target region that contains a gene, 200 bp upstream and 200 bp downstream were counted. The number of ChIP-seq reads mapped on a target region was then normalized with signal extraction scaling

(SES) method (Diaz et al. 2012). Statistical significance of differences between samples was determined by Fisher's exact test. The regions that showed significant differences of H3K27me3 level were selected with more than |log2|=2.0, *q*-value < 0.05 and, with significant H3K27me3 peaks.

Calculation of tissue specificity by T-value

We used RNA-seq datasets that contain root, stem, leaf, flower, silique and callus samples (Tong et al. 2013). The tissue specificity index T (T-value) was computed in each gene according to the formula as described in Tong et al. 2013.

Identification of SNPs in *B. rapa* genes

We performed whole genome resequences in T23 and T24 (Shea et al. 2018b). The reads of two lines were mapped to the *B. rapa* reference genome v.1.5 using Bowtie2 version 2.2.3. We used Picard v.2.9.0 'MarkDuplicates' command to remove duplication. Samtools v1.7 'mpileup' command with -q 20 -Q 30 options and bcftools v1.7 'call' command with -p 0.9 -v -c -O z options were performed to make VCF files. The identification of SNPs was performed using bcftools 'view' command with -v snps -g hom options. SNPs that have more than 10 reads were used for subsequent analyses. The number of SNPs per nucleotide length was measured for each gene.

Gene Ontology analysis

Analysis for enrichment of gene functional ontology terms was completed using the gene ontology (GO) tool agriGO (Du et al. 2010) following the methods described by Shimizu et al. 2014. Statistical tests for enrichment of functional terms used the hypergeometric test and false discovery rate (FDR) correction for multiple testing to a level of 1 % FDR.

RNA extraction and qPCR

Total RNA was isolated from cotyledons (2d-C, BrV1) or 1st and 2nd leaves (14d-L, BrV2) using the SV Total RNA Isolation System (Promega). cDNA was synthesized from 500 ng total RNA using ReverTra Ace qPCR RT Master Mix with gDNA Remover (Toyobo). qPCR was performed by the same methods as the ChIP-qPCR using the cDNA as a template. The relative expression level of each gene relative to *ACTIN* (Fujimoto et al. 2006) was automatically calculated using automatic CQ calling according to the manufacturer's

instructions (Roche). Data presented are the average and SE from three biological and experimental replicates. Primer sequences used in this study are shown in Table III-1.

In BrV1 and BrV2, the region covering part of the *BrFLC* gene was amplified using primers, which can amplify all BrFLC paralogs (*BrFLC1*, *BrFLC2*, *BrFLC3*, *BrFLC5*), using cDNA as templates. PCR was performed using the following conditions; 1 cycle of 94 °C for 2 min, 35 cycles of 94 °C for 30 s, 58 °C for 30 s, and 68 °C for 30 s. Primer sequences used for RT-PCR are shown in Table III-1.

RNA sequencing (RNA-seq)

RNA-seq using 2-day cotyledons and 14-day leaves with two replicates was performed in T23 and T24 (100 nt read length with paired end on an Illumina HiSeq^{TM} 2000) conditions. The numbers of clean reads and the percentage of mapped reads are shown in Table III-6. Low quality reads were filtered using FaQCs Version 1.34 (Lo and Chain, 2014). HISAT2 (Kim *et al*., 2015) was used to align the sequence data sets to Brapa_sequence_v1.5 (http://brassicadb.org/brad/). Cuffdiff was used for the gene expression levels scored by fragments per kilo-base per million (FPKM) and identification of differentially expressed genes (DEGs) with two criteria, two-fold difference (log2 ratio ≥ 1.0) and 95% confidence. The level of gene expression was categorized into seven groups using log2 score of FPKM, e.g., Group-6 (highest), log2 score of FPKM (x) is greater than 9.0; Group-5, 6.0<=x<9.0; Group-4, 3.0<=x<6.0; Group-3, 0.0<=x<3.0; Group-2, -3.0<=x<0.0; Group-1, x<-3.0; Group-0, no read (lowest) (Kawanabe et al. 2016; Takahashi et al. 2018b).

Results

The two parental lines of *B. rapa* have conserved sites of H3K27me3 but H3K27me3 differ between tissues

The diversity and conservation of H3K27me3 distribution between parental lines of the commercial F_1 hybrid cultivar of Chinese cabbage (T23 and T24) were determined. The presence of H3K27me3 marks on the chromatin of 2-day cotyledons (2d-C) and 14-day leaves (14d-L) in the parental lines was mapped by chromatin immunoprecipitation sequencing (ChIP-seq) (Table III-2). Reads mapped in the genic regions were classified into 2 kb upstream, exon, intron, and 2 kb downstream segments. The proportions of reads in each of these segments were similar to those in the input DNA (Fig. III- 6, Table III-7), suggesting there is no preferential location of H3K27me3 in any of the coding or regulating regions. H3K27me3

was enriched in the transcribed region in both 2-day cotyledon and 14-day leaf samples in both lines, especially around the transcription start sites (Fig. III-7A). The percentage of reads in the interspersed repeat regions (IRRs) (transposable elements and repeats) was lower than in the input DNA (Table III-2). There was no enrichment in IRR sequences or their flanking regions (Fig. III-7B).

We found a similar pattern of H3K27me3 distribution in the parental lines in two different tissues (2-day cotyledons and 14-day leaves) at the whole genome level (Fig. III-8A). We defined an H3K27me3-marked gene as having a peak of more than 200 bp within the genic region, which includes 200 bp upstream and downstream sequences (see Materials and methods). 17,027 H3K27me3-marked genes were common to the two parental lines in the 2-day cotyledons, and 10,456 H3K27me3-marked genes in the 14-day leaf samples were present in both lines (Fig. III-9A, Table III-8). The 2-day cotyledon sample contained most of the marked 14-day genes as well as 2-day cotyledon specific sites (Fig. III-9B). 7,930 H3K27me3-marked genes were present in 2-day cotyledon and 14-day leaf samples in both lines and were termed H3K27me3 stably marked genes. In these genes, H3K27me3 was enriched throughout the transcribed region (Fig. III-7C).

We compared H3K27me3 levels by the number of ChIP-seq reads that had been normalized using single extraction scaling (see Materials and methods) (Diaz et al. 2012). The two parental lines showed few differences in H3K27me3 distribution in the same tissue contrasting to the differences between 2-day cotyledons and 14-day leaves (Fig. III-9C, D, Table III-9). In genic regions, the correlation coefficient between tissues was lower than between lines (Fig. III-8B).

At 14 days but not 2 days, genes marked with H3K27me3 had lower levels of transcription

There were higher numbers of H3K27me3-marked genes in 2-day cotyledons compared to 14-day leaves (Table III-9). We examined whether these differences affected the transcriptome. We assigned genes into seven groups on the basis of their expression level in 14-day leaves of the two lines (Kawanabe et al. 2016; Du et al. 2010; Lo et al. 2014). Using the same criteria, we also categorized gene expression levels from a transcriptome of 2-day cotyledon material in each of the two lines (Fig. III-10).

In both the 2-day cotyledon and 14-day leaf samples in both lines, the proportion of H3K27me3-marked genes classified into each of the seven activity groups differs significantly from the distribution in the total transcriptome (Chi-squared test, $p < 10^{-10}$) (Fig. III-10). In the

2-day cotyledon samples, H3K27me3-marked genes were less frequently classified in Group-0 to -3 (low expression levels) and more frequently in Group-4 to -6 (high expression levels) (Fig. III-10). The average transcription level of H3K27me3-marked genes was higher than that of genes without H3K27me3 or in all of the genes in the two lines (Fig. III-11). In contrast, in 14-day leaf material H3K27me3-marked genes had decreased numbers in Group-4 to -6 and increased numbers in Group-0 to -3 (Fig. III-10). The average transcription level of H3K27me3-marked genes was lower than that of genes without H3K27me3 or the total genes in both lines (Fig. III-11). The average transcription level of H3K27me3 stably marked genes was lower than that of genes without H3K27me3 or than total genes in both tissues and lines (Fig. III-11); the lower expression level could be due to the highly enriched H3K27me3 mark throughout gene body regions (Fig. III-7C).

Contrary to expectation, H3K27me3-marked genes in 2-day cotyledons showed higher gene expression than those without marks (Fig. III-11). These genes included 9,700 genes that had H3K27me3 only in 2-day cotyledons. The overall level of H3K27me3 was lower in the 2-day sample than in the 14-day sample, and H3K27me3 marks were significantly lower in the 3' regions (Fig. III-7D). Genes having H3K27me3 marks only in 2-day cotyledons were further decreased in the H3K27me3 level in the 3' regions (Fig. III-7E). The expected negative correlation between H3K27me3-marked genes and reduced expression was masked in the 2-day data because there are both highly expressed genes with a low level of H3K27me3 and lowly expressed genes with a higher level of H3K27me3.

H3K27me3 is associated with tissue-specific gene expression

In genes having different levels of H3K27me3 in the parental lines, 33.1% (241 of 729 genes in 2-day cotyledons) and 22.3% (200 of 898 genes in 14-day leaves) of genes showed differential expression levels (Table III-10). From 7.8% to 12.7% of these genes showed a negative correlation between H3K27me3 levels and expression levels between lines (Table III-10). There was a high proportion of genes with parallel levels of expression and of H3K27me3 (Table III-10), suggesting that the difference in expression between lines does not result from a difference in H3K27me3 level. In genes with different levels of H3K27me3 between tissues, approximately 60% of genes showed differential expression (Table III-10). The genes (from 13.3% to 19.8%) showed a negative correlation between a difference of H3K27me3 levels and expression levels between tissues, especially in genes showing higher H3K27me3 levels in 14-day leaves than in 2-day cotyledons (Table III-10).

A tissue specificity index, T-value, which interpolates the entire range between 0 for housekeeping genes and 1 for strictly one-tissue-specific genes, was calculated using the transcriptome data from six different tissues in *B. rapa* (Tong et al. 2013). We found H3K27me3-marked genes showed significantly higher average T-values compared with total genes (Fig. III-12), suggesting that H3K27me3 has a role in tissue specific gene expression.

Comparison of H3K27me3 states between paralogous genes in *B. rapa*

We compared H3K27me3 locations between paralogs in 14-day leaf samples using 5,439 and 1,675 genes with two or three syntenic copies (Cheng et al. 2012). Among the 1,675 three-copy sets, 265 had H3K27me3 in all three copies, 164 had H3K27me3 in at least two copies, 262 had H3K27me3 in at least one copy, and 984 sets did not have H3K27me3 in any copies (Fig. III-13A). Among the 5,439 two-copy pairs, 796 pairs had H3K27me3 in both copies, 938 pairs had H3K27me3 in one copy, and 3,705 pairs did not have H3K27me3 in any copies (Fig. III-13A). Totally, 1,225 pairs (= 265 + 164 + 796) showed conservation of H3K27me3 among paralogs, termed paralogous-conserved H3K27me3-marked genes, and 1,200 pairs (= 262 + 938) showed H3K27me3 in one of the paralogs, termed copy-specific H3K27me3-marked genes (Fig. III-13A).

Gene Ontology (GO) analysis showed that genes categorized into ‘Transcription factor activity’, ‘Regulation of metabolic process’, and ‘Developmental process’ were overrepresented in paralogous-conserved H3K27me3-marked genes compared with copy-specific H3K27me3-marked genes (Fig. III-13B, Table III-11). Genes categorized into ‘Plasma membrane’ and ‘Vacuole’ were overrepresented in copy-specific H3K27me3-marked genes compared with paralogous-conserved H3K27me3-marked genes (Fig. III-13B, Table III-11).

We examined whether a difference in H3K27me3 states between paralogs was associated with a different level of gene activity. Between paralogous pairs, the average expression levels of genes with H3K27me3 marks was lower than those without H3K27me3 in 14-day leaves of both T23 and T24 (Fig. III-14), indicating that the presence of H3K27me3 results in a difference of gene expression level between paralogous pairs. There was no difference in T-values between paralogous-conserved and copy-specific H3K27me3-marked genes, and T-values were higher than that in total genes (Fig. III-12). Between paralogous pairs, the average T-values of genes with H3K27me3 was significantly higher than that without H3K27me3 (Fig. III-12, Fig. III-15), suggesting an association of H3K27me3 with tissue specific gene expression differences between paralogous pairs.

Some genes marked with H3K27me3 are shared between *B. rapa* and *A. thaliana*

To gain information about conservation of H3K27me3 states beyond *B. rapa*, we compared the genes marked with H3K27me3 in *B. rapa* and *A. thaliana*. Of 10,456 genes, which had H3K27me3 in the 14-day leaf samples in both *B. rapa* lines (Fig. III-9A), 9,769 (93.4 %) had sequence homology to putatively orthologous genes in *A. thaliana*. This was reduced to 6,207 genes in *A. thaliana* following the removal of genes where two or three *B. rapa* genes showed sequence similarity to one *A. thaliana* gene. In *A. thaliana*, 5,333 genes identified as having H3K27me3 marks in 12-day seedlings in the C24 accession (At-data 1) (Deng et al. 2013), and 5,118 genes (At-data 2), which were selected by Berke and Snel (2014). About 80% of genes overlapped between the two data sets (At-data 1 and At-data 2). Between orthologous genes of *B. rapa* and *A. thaliana*, 2,409 of 6,207 genes (38.8 %) had H3K27me3 in both *B. rapa* and the two data sets of *A. thaliana*, these were termed species-conserved H3K27me3-marked genes. 3,097 of 6,207 genes (49.9 %) had H3K27me3 in only *B. rapa*, these were termed *Br*-specific H3K27me3-marked genes (Fig. III-13C).

Genes categorized into ‘Transcription factor activity’ and ‘Regulation of metabolic process’ tended to be overrepresented in species-conserved H3K27me3-marked genes compared with *Br*-specific H3K27me3-marked genes (Fig. III-13D, Table III-12). In contrast, genes categorized into ‘Plasma membrane’, ‘Transporter activity’, ‘Kinase activity’, ‘Response to stress’, and ‘Response to abiotic stimulus’ tended to be overrepresented in *Br*-specific H3K27me3-marked genes compared with species-conserved H3K27me3-marked genes (Fig. III-13D, Table III-12).

Both species-conserved and *Br*-specific H3K27me3-marked genes showed high tissue specificity (Fig. III-12). Genes having H3K27me3 tended to have a lower SNP number per length in each gene (mutation rates) than total genes as did species-conserved H3K27me3-marked genes relative to *Br*-specific H3K27me3-marked genes in T23 but not in T24 (Fig. III-16).

Higher H3K27me3 levels in 14-day leaves are associated with decreased post-embryonic gene expression

H3K27me3 plays an important role in tissue specific gene expression. We identified genes showing different H3K27me3 states just after germination (2-day cotyledons) and more than 10 days after germination (14-day leaves) in *B. rapa* (Table III-9). We compared the

H3K27me3 levels between germinating seeds and 12-day seedlings (At-data 1) in C24 accession of *A. thaliana* (Table III-13) (Deng et al. 2013; Zhu et al. 2017).

Four genes showed higher H3K27me3 levels in 2-day cotyledons than in 14-day leaves in both *B. rapa* lines and in *A. thaliana*, in germinating seeds than in 12-day seedlings (Table III-13). Sixty-four genes showed higher H3K27me3 levels in 14-day leaves than in 2-day cotyledons in both *B. rapa* lines and in *A. thaliana*, in 12-day seedlings than in germinating seeds (Table III-13), and these genes tended to be categorized into 'Seed maturation', 'Seed dormancy', 'Seed development' and 'Post-embryonic development' (Table III-14). Genes categorized into 'Post-embryonic development' tended to have lower expression levels in 14-day leaves than in 2-day cotyledons in *B. rapa* (Table III-15), suggesting H3K27me3 is involved in silencing of embryogenic expression in 14-day leaves relative to their activity levels in 2-day cotyledons.

Change of H3K27me3 state after vernalization treatment in *B. rapa*

Vernalization involves regulation of gene expression of *FLC* by H3K27me3 (Dennis and Peacock, 2007; Groszmann et al. 2011; Itabashi et al. 2018). We confirmed H3K27me3 accumulation at the *FLC* locus by a comparison of the whole genome level of H3K27me3 states between non-vernalized (NV) and upon return to 22°C after vernalization (V) in the C24 accession of *A. thaliana*. In the genome, only *FLC* showed an increased H3K27me3 level following return to 22°C after vernalization in *A. thaliana* (Table III-16).

We examined H3K27me3 states in non-vernalized (2d-C, 14d-L), vernalized (BrV1), and following return to 22°C after vernalization (BrV2) in T24 (*B. rapa*). Between non-vernalized and vernalized samples at similar developmental stages, H3K27me3 levels at the whole genome level had correlation coefficients of 0.97 and 0.99 (Fig. III-8C). Some genes showed increased H3K27me3 levels following vernalization including the four *BrFLC* paralogs (Table III-16, III-17). Following four weeks vernalization (BrV1) H3K27me3 increased at the first exon and part of the first intron (nucleation site) in all four *FLC* paralogs (Fig. III-17). Following a return to 22 °C after vernalization (BrV2), an increase of H3K27me3 was observed in all four *FLC* paralogs, which started at the nucleation site and spread 5' to 3' along the genes (Fig. III-17). Expression levels of the total amount of the four *FLC* paralogs were downregulated in BrV1 and BrV2 compared with the unvernalized 2d-C and 14d-L, respectively (Fig. III-18). *VERNALIZATION INSENSITIVE 3* (*VIN3*) and *SOC1* were highly

induced in BrV1 and BrV2, respectively, and the expression level of *FT* was upregulated in BrV1 and BrV2 (Fig. III-18).

Three of five *MAF*-like genes (Bra031888, Bra024350, and Bra024351) showed a spread from 5' to 3' of H3K27me3 similar to that seen in the *FLC* genes following the return to normal conditions after four weeks of cold treatment (Fig. III-17). Expression levels of these three *MAF*-like genes were downregulated following vernalization (Fig. III-18). Increased H3K27me3 levels of Bra006050 and Bra009056 in the sample upon return to 22 °C might be due to the spread of H3K27me3 from the nearby genes, Bra006051 (*BrFLC3*) and Bra009055 (*BrFLC1*) (Fig.III-19); other genes neighboring *FLC* or *MAF* genes did not have increased H3K27me3 levels (Fig. III-20). From the comparison of ChIP-seq data, two genes (Bra032761/CYTOKININ-INDEPENDENT 1 and Bra037899/protein kinase family protein) showed decreased H3K27me3 levels following a return to 22°C after vernalization in both *B. rapa* and *A. thaliana* (Table III-16).

Discussion

The location of H3K27me3 sites was conserved between the two *B. rapa* lines. The sites of H3K27me3 modification are less conserved between tissues than between lines, especially in genic regions. Genes with H3K27me3 marks have tissue specific expression, suggesting a role for H3K27me3 in regulation of gene expression during development.

The H3K27me3-marked genes in 14-day leaves showed lower expression levels on average than total gene expression levels, but the H3K27me3-marked genes in 2-day cotyledons showed higher expression levels than the average level of gene expression. This was especially the case in 2-day cotyledon specific H3K27me3-marked genes. Genes that are H3K27me3-marked in both 2-day cotyledons and 14-day leaves had lower expression levels on average than the total genes in both tissues. The level of H3K27me3 in 2-day cotyledon specific H3K27me3-marked genes was lower around the 3' region, while H3K27me3 stably marked genes showed a higher enrichment of H3K27me3 throughout the gene body region, suggesting that the low level of H3K27me3 present in 2-day cotyledon specific H3K27me3-marked genes is not sufficient to repress gene expression. In general, there is an association between H3K27me3 marks on a gene and lower expression. In the 2-day cotyledons, this relationship did not hold. This finding is probably because of the early developmental time used; none of the analyses in other species used such early material.

Genes that showed higher levels of H3K27me3 in 14-day leaves compared to 2-day cotyledons showed an overrepresentation in the category of 'Post-embryonic development'. These genes had lower expression levels in 14-day leaves than in 2-day cotyledons, suggesting a role in reducing the expression of genes concerned with embryo development at this time. In maize and *A. thaliana* 34% of orthologs were marked (Makarevitch et al. 2013). In maize and rice 70% of orthologs are similarly marked (Makarevitch et al. 2013). The data suggest that genes having important functions such as regulation of transcription factor gene expression or metabolic process also have conservation of H3K27me3 marks.

Approximately 30% of the pairs of paralogous genes in *B. rapa* had H3K27me3 in more than one copy. A similar situation holds with most pairs of syntenic genes in maize and *A. thaliana* (Makarevitch et al. 2013; Berke et al. 2014) The tissue specificity of gene expression was higher in paralogous pairs marked with H3K27me3 than in those without H3K27me3 marks and expression levels were lower in the marked genes. These findings suggest that the different distribution of H3K27me3 between paralogous genes may be involved in their sub-functionalization.

Environmentally related changes at the *FLC* locus involve H3K27me3 marks. In *A. thaliana* H3K27me3 has functional roles associated with the activity level of *FLC* (Dennis and Peacock, 2007; Groszmann et al. 2011; Itabashi et al. 2018). Plants treated for four weeks at 4 °C (vernalization) gain H3K27me3 at a site downstream of the transcription start site (the nucleation region), and gene expression ceases. Following return of the plants to 22 °C, H3K27me3 spreads across the entire *FLC* locus stabilizing the lack of expression, allowing expression of the floral promoters, *FT* and *SOC1*, and permitting flowering to occur (Helliwell et al. 2015). In *B. rapa*, *FLC* has a similar role in vernalization (Itabashi et al. 2018; Shea et al. 2018). Three *BrFLC* paralogs (*BrFLC1*, *BrFLC2*, and *BrFLC3*), which might have been generated by whole genome triplication (Fig. III-21), and *BrFLC5* had active transcription before vernalization. Their expression decreased after vernalization; the repressed state was maintained upon return to 22°C after vernalization. Prior to the low temperature treatment in *B. rapa* all four *FLC* paralogs had only background levels of H3K27me3. At the end of four weeks low temperature treatment, H3K27me3 was localized at the proximal nucleation region. H3K27me3 spreads across all of the four *FLC* paralogs upon return to 22°C after vernalization. In both *B. rapa* and *A. thaliana*, there is little change to genome-wide H3K27me3 levels following a return of the plants to 22°C. There are five *MAF*-like genes in *B. rapa* and it is not

clear whether these paralogs were generated by whole genome triplication (Fig. III-21). Spreading of H3K27me3 was also observed in some of the *MAF*-like genes.

In *A. thaliana*, a noncoding RNA COLDAIR molecule derived from the first intron of *FLC* is reported to play a role in the recruitment of PRC2 to *FLC* (Heo et al. 2011). There is no sequence showing similarity to COLDAIR in any of the first introns of the four *FLC* paralogs in *B. rapa* (Kitamoto et al. 2014; Shea et al. 2018) In agreement with Li et al. 2016, we did not find any transcript from the first intron of any of the four *FLC* paralogs in *B. rapa* in vernalized leaves (Shea et al. 2019). COLDAIR and any other noncoding RNAs may not be expressed from the first intron of *FLC* paralogs in *B. rapa* (Shea et al. 2019). A stabilization of repression by the spreading of H3K27me3 marks on return to normal growth condition has been attributed to COLDAIR RNA control but the absence of COLDAIR transcripts in *B. rapa* suggests a reconsideration of this view is needed.

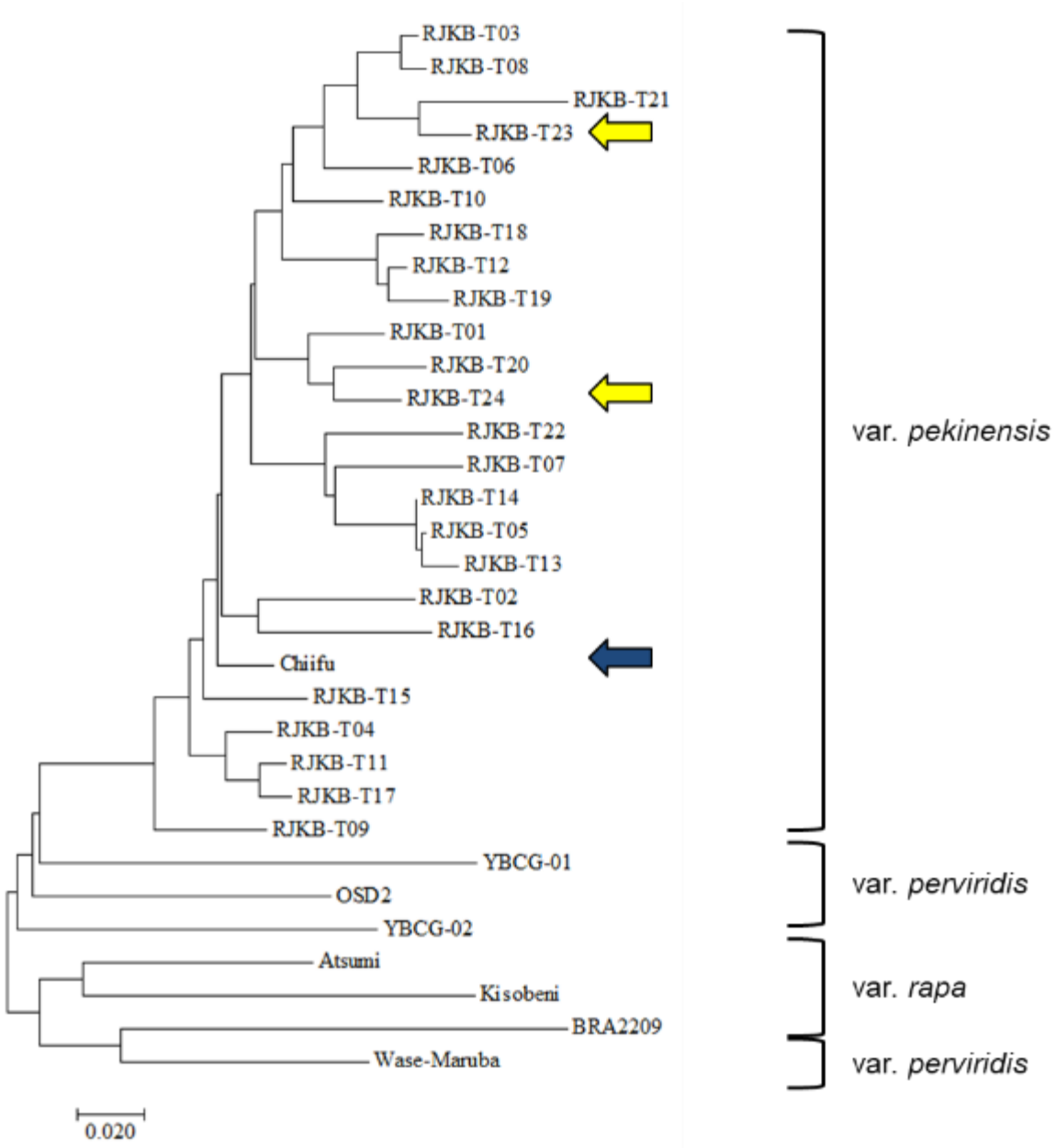

Figure III-1. Genetic distance of lines/cultivars in *B. rapa*. The Chinese cabbage line, Chiifu (blue arrow; reference genome), twenty-four Chinese cabbage (var. *pekinensis*) inbred lines, three turnip (var. *rapa*) lines and four komatsuna (var. *perviridis*) lines were used. Genetic distance was calculated using data described in Kawamura *et al*. 2016.

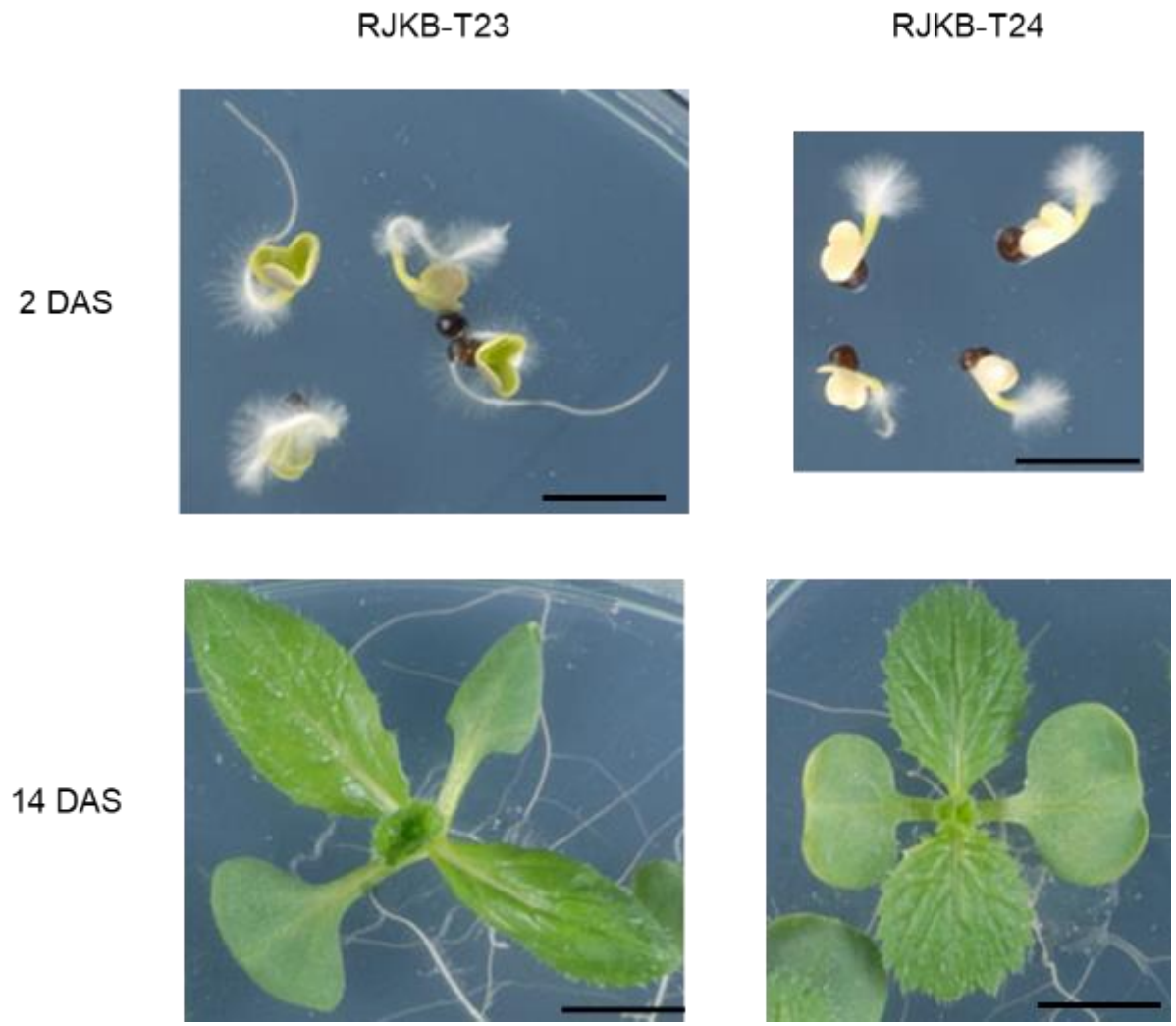

Figure III-2. Plants at 2 days or 14 days after sowing in RJKB-T23 and RJKB-T24. Scale bar represents 1 cm in length.

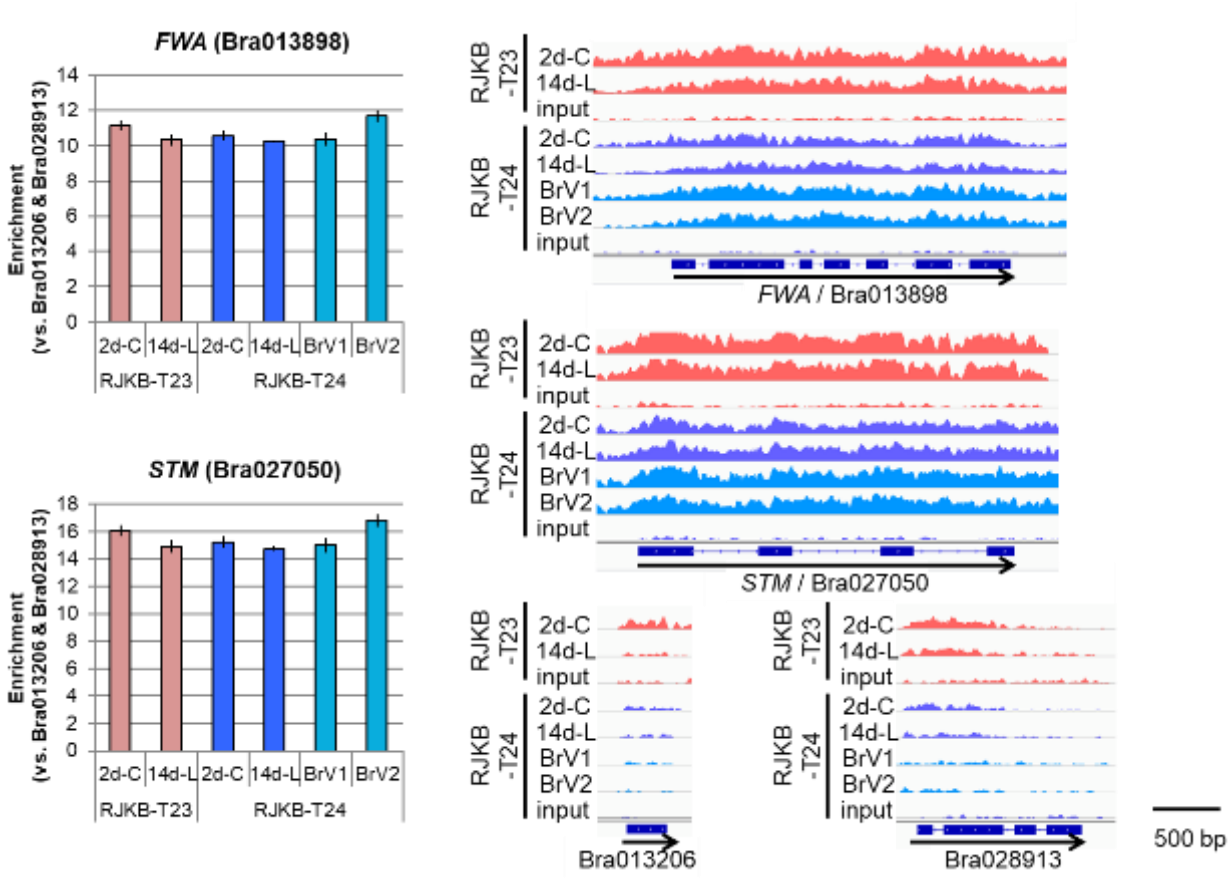

Figure III-3. Validation of the enrichment of purified immunoprecipitated (IP) DNAs by qPCR. *FWA* and *STM* are H3K27me3 marked genes (positive control), and Bra013206 and Bra028913 are low level H3K27me3 marked genes (negative control) (Kawanabe et al. 2016). Values are means ± standard error (s.e.) (three biological and technical replicates) of relative H3K27me3 levels. Visualization of H3K27me3 peaks by Integrative Genomics Viewer (IGV) by ChIP-seq are shown in the right panel.

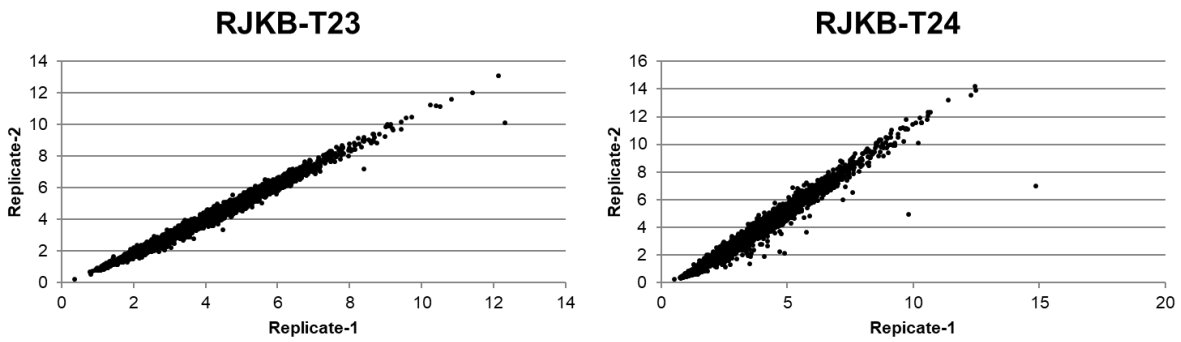

Figure III-4. Comparison of the two replicates for ChIP-seq of 14dL in RJKB-T23 and RJKB-T24. The RPKM of each sliding window per 100 kb was compared between replicate 1 and 2 (n=2,578). Correlation coefficient in each window of the two replicates was 0.99 and 0.98 in RJKB-T23 and RJKB-24, respectively.

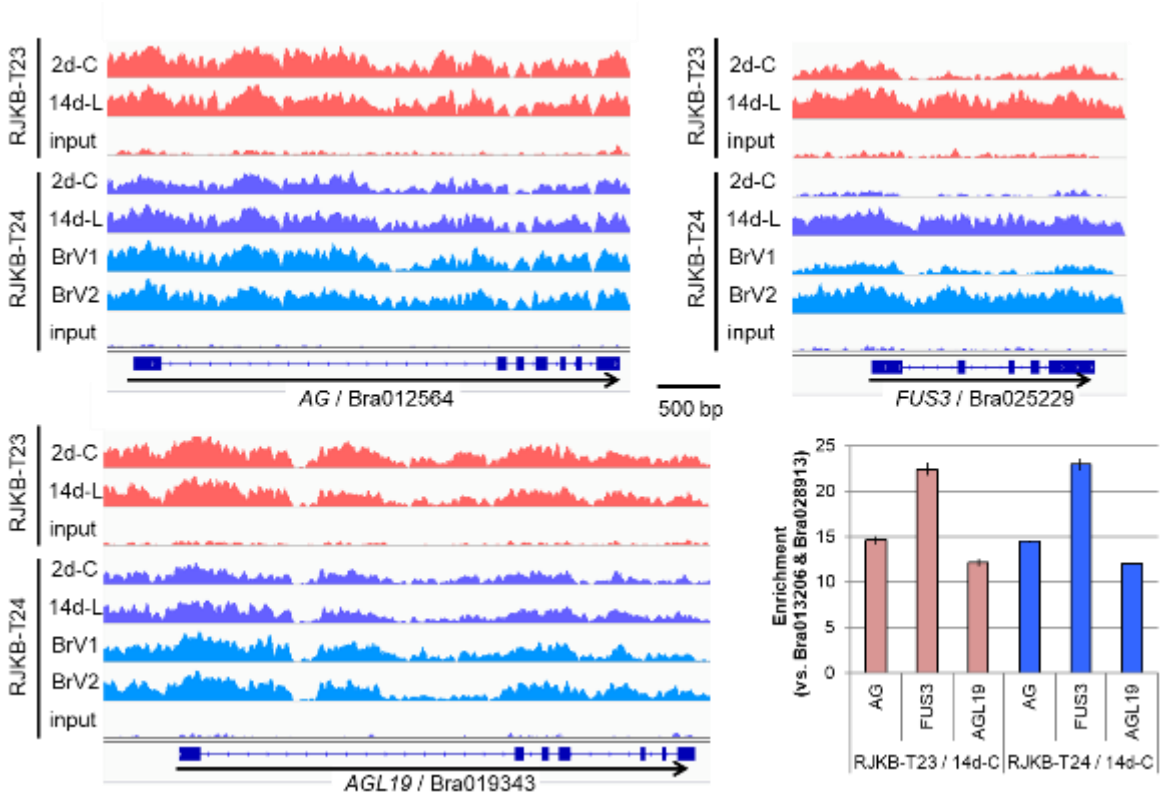

Figure III-5. Validation of the enrichment of purified immunoprecipitated DNAs by qPCR. *AG*, *FUS3*, and *AGL14* are H3K27me3 marked genes reported in Kawanabe et al. 2016. Values are means ± standard error (s.e.) (three biological and technical replicates) of relative H3K27me3 levels. Visualization of H3K27me3 peaks by Integrative Genomics Viewer (IGV) by ChIP-seq are shown.

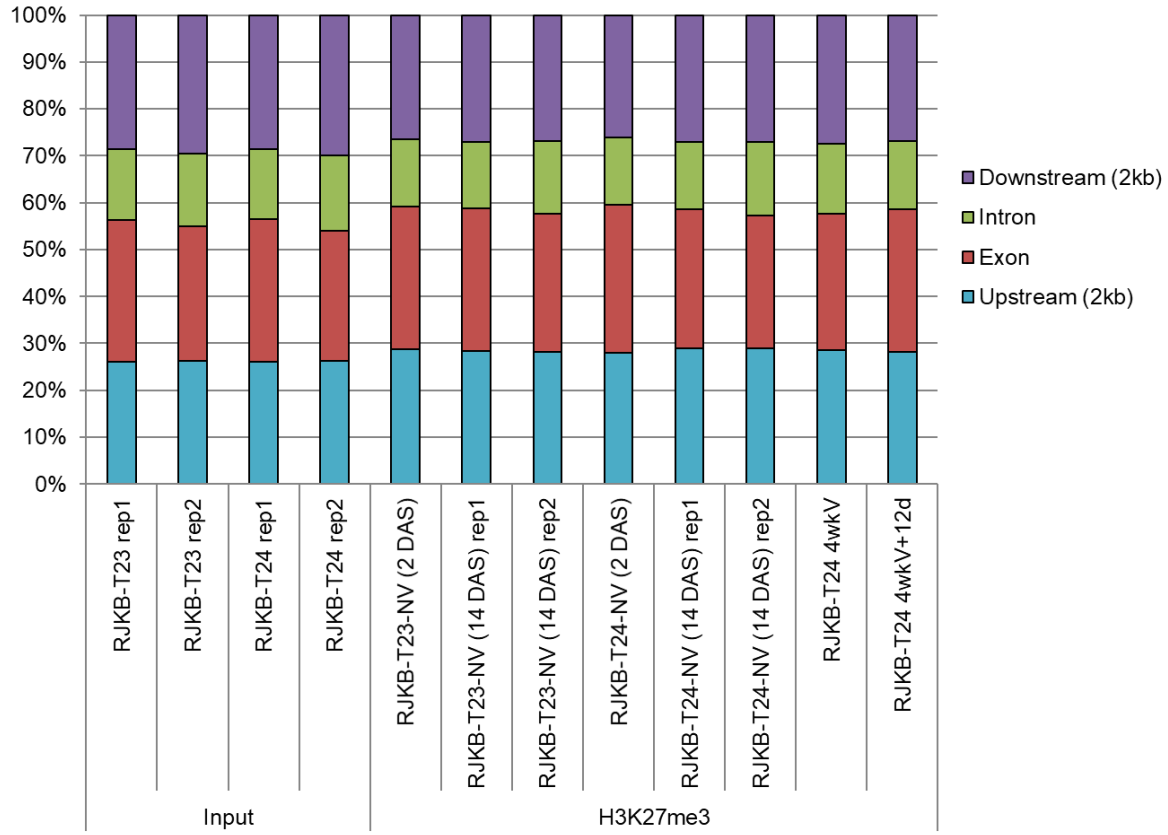

Figure III-6. Mapped reads of input and immunoprecipitated DNA using anti-H3K27me3 antibodies in genic regions classified into 2kb-upstream, exon, intron, and 2kb downstream positions.

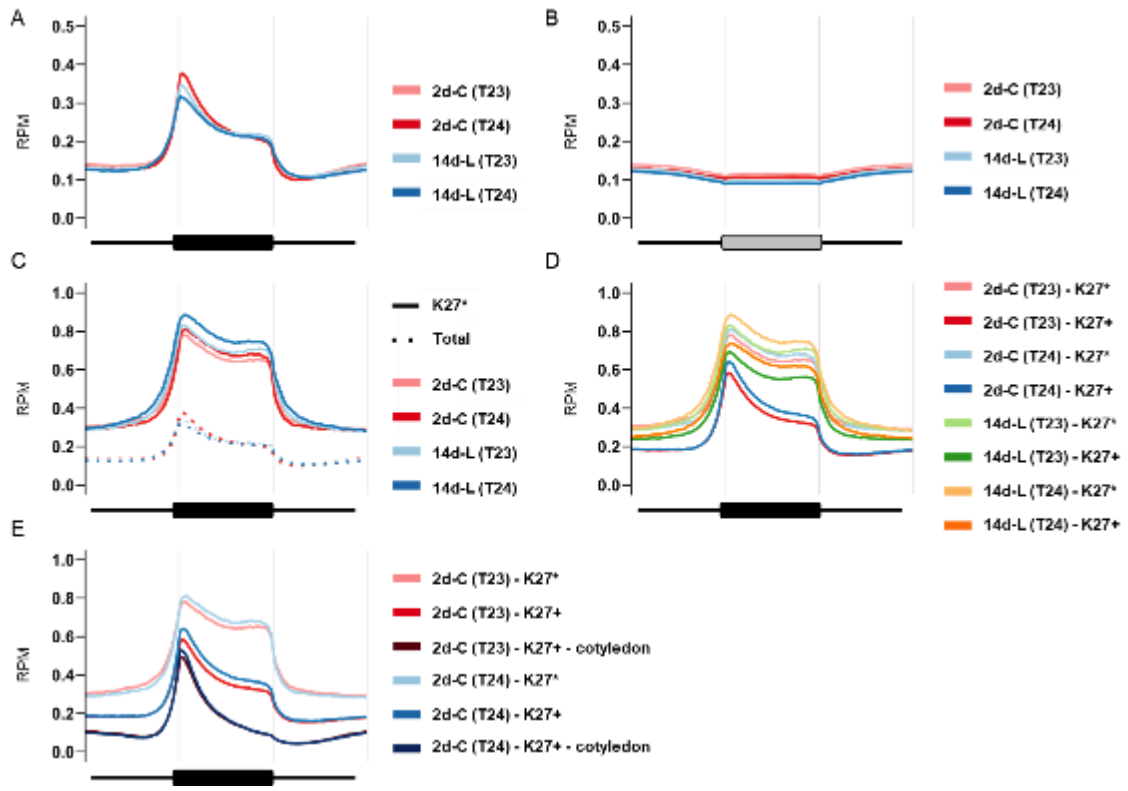

Figure III-7. Metagene plots of H3K27me3 in genic region and interspersed repeat region (IRR). (A, B) H3K27me3 level at genic or IRR region with 1 kb upstream and 1 kb downstream is shown using all genes (A) or all IRRs (B) in 2-day cotyledons (2d-C) and 14-day leaves (14d-L) in RJKB-T23 (T23) and RJKB-T24 (T24). (C, D) H3K27me3 level at genic region in all H3K27me3-marked genes (Total), H3K27me3 stably marked genes (K27*), or H3K27me3-marked genes (K27+) in 2d-C and 14d-L of both lines. (E) H3K27me3 level at genic region in H3K27me3 stably marked genes (K27*), H3K27me3-marked genes (K27+), or 2-day cotyledon specific H3K27me3-marked genes (K27+ - cotyledon) in 2d-C of both lines. RPM; Reads per Million mapped reads.

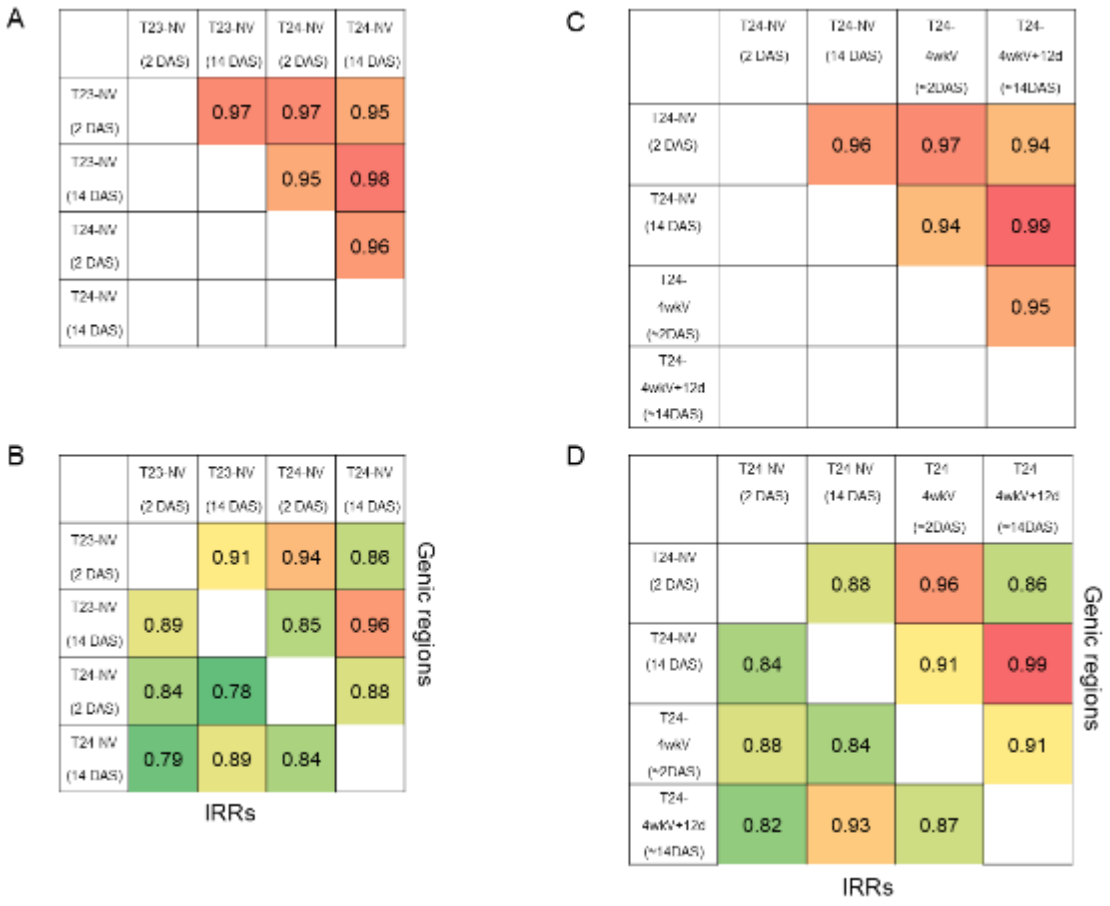

Figure III-8. The comparison of H3K27me3 levels between different tissues or lines (A, B) or between with and without four weeks of cold treatments (C, D). The correlation coefficient of H3K27me3 levels quantified by reads per kilobase million (RPKM) in each sliding window per 100 kb at the whole genome level (n=2,578) (A, C). The bottom panel (B, D) represents the correlation coefficient of RPKM scores in the genic regions (n=39,609) (upper right) or interspersed repeats regions (IRRs) (n=314,881) (lower left).

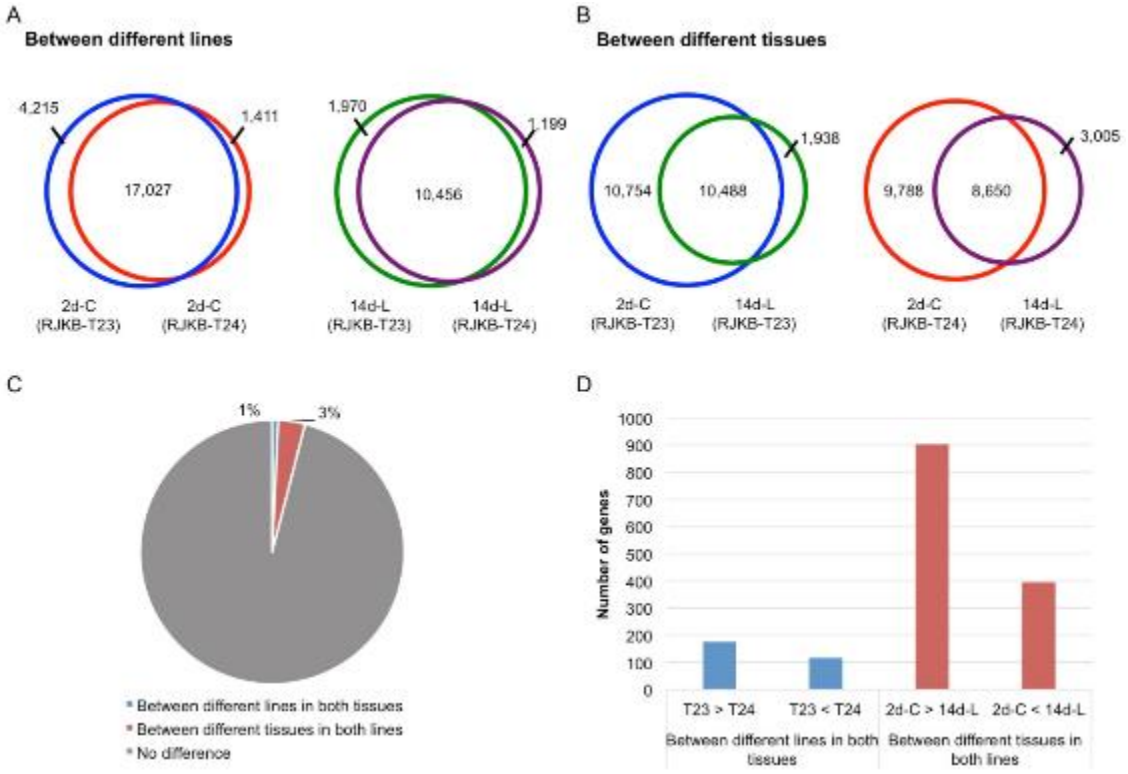

Figure III-9. Comparison of H3K27me3 between lines or between tissues. (A, B) Venn diagram of genes having H3K27me3 in genic regions of 2-day cotyledons (2d-C) and 14-day leaves (14d-L) in RJKB-T23 (T23) compared with RJKB-T24 (T24). (C) Percentage of genes showing different H3K27me3 levels between lines in both tissues or between tissues in both lines. (D) Number of genes showing different H3K27me3-marked genes between lines in both tissues or between tissues in both lines.

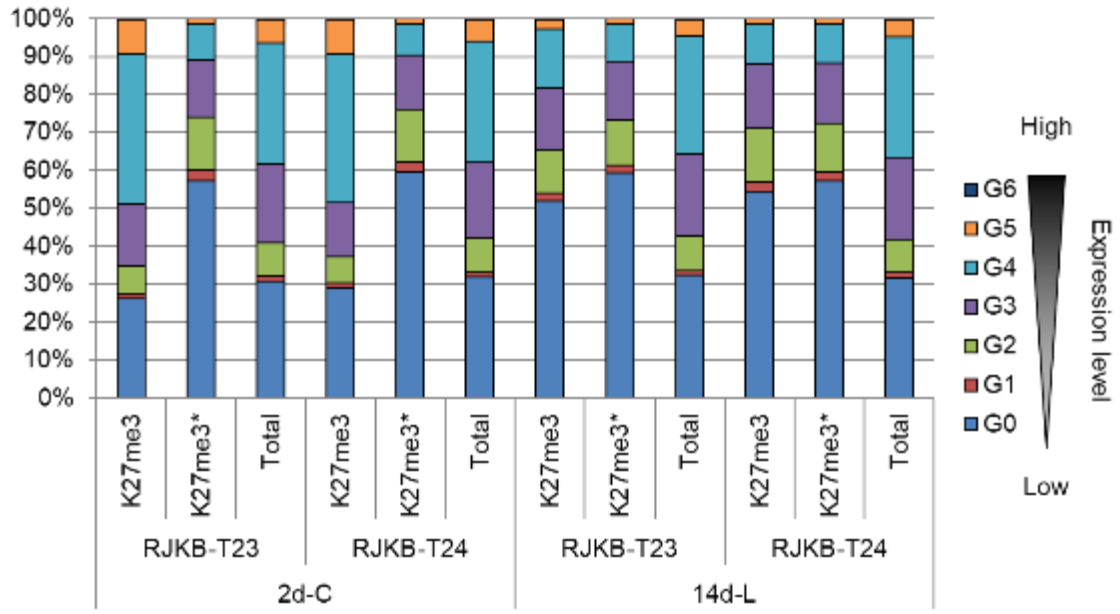

Figure III-10. Classification of genes having H3K27me3 in genic regions into seven groups of expression levels. 'K27+' and 'K27*' represent H3K27me3-marked genes and H3K27me3 stably marked genes, respectively. 'Total' indicates all genes. 2d-C; 2-day cotyledons, 14d-L; 14-day leaves. Group-0, No mapped read; Group-1, $\log_2$ (FPKM)<-3.0; Group-2, -3.0=< $\log_2$ (FPKM)<0.0; Group-3, 0.0=< $\log_2$ (FPKM)<3.0; Group-4, 3.0=< $\log_2$ (FPKM)<6.0; Group-5, 6.0=< $\log_2$ (FPKM)<9.0; Group-6, 9.0=< $\log_2$ (FPKM). FPKM, Fragments Per Kilobase of transcript per Million mapped reads.

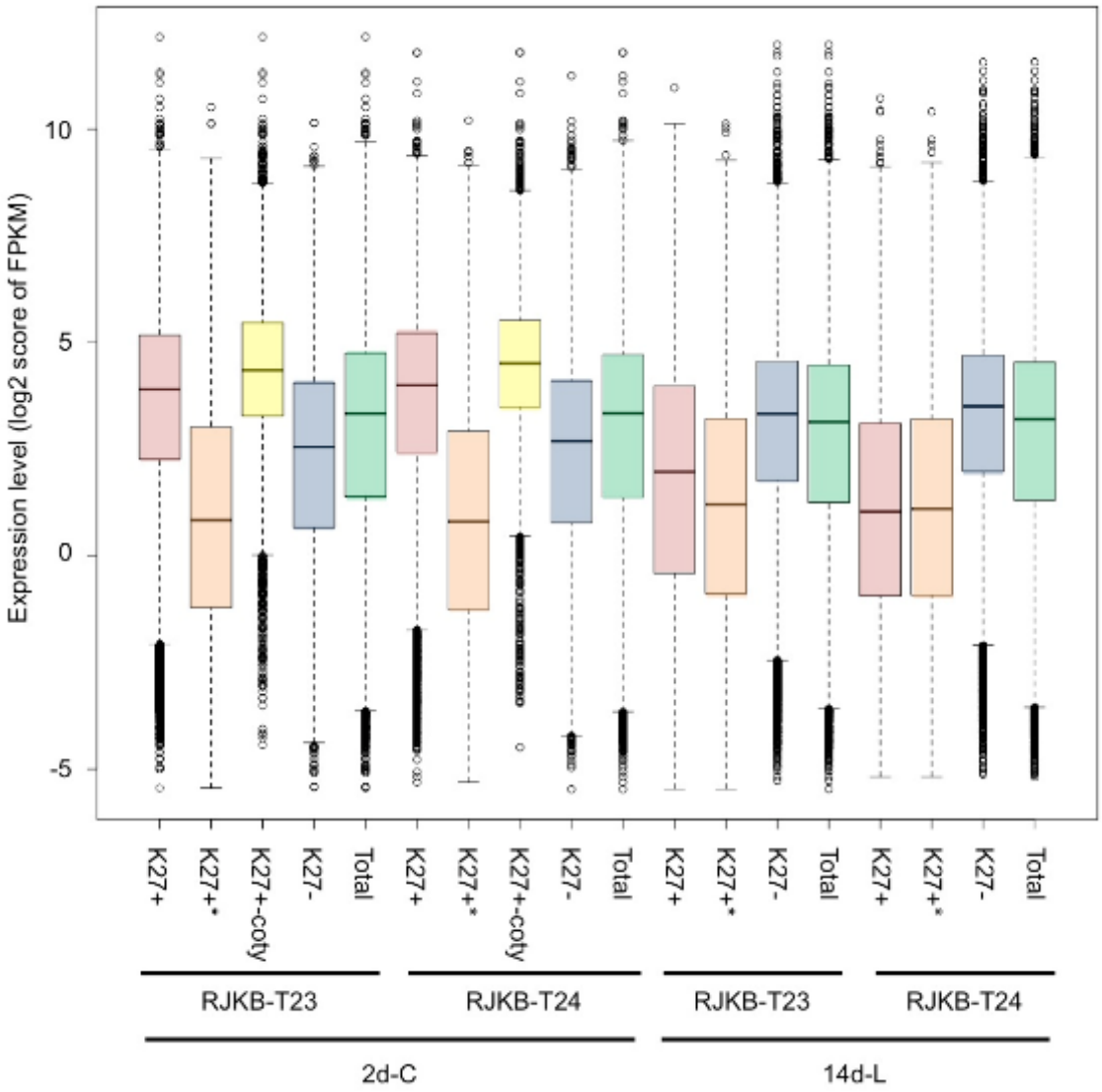

Figure III-11. Box plots of the gene expression levels of log 2 score of FPKM with (+) or without (-) H3K27me3 in genic regions of RJKB-T23 and RJKB-T24. * indicates the log 2 score of FPKM in H3K27me3 stably marked genes. 'Total' indicates the log 2 score of FPKM in all genes (FPKM < 0.01). 'K27+-coty' represents the log 2 score of FPKM in 2-day cotyledon specific H3K27me3-marked genes. FPKM; Fragments Per Kilobase of transcript per Million mapped reads, 2d-C; 2-day cotyledons, 14d-L; 14-day leaves.

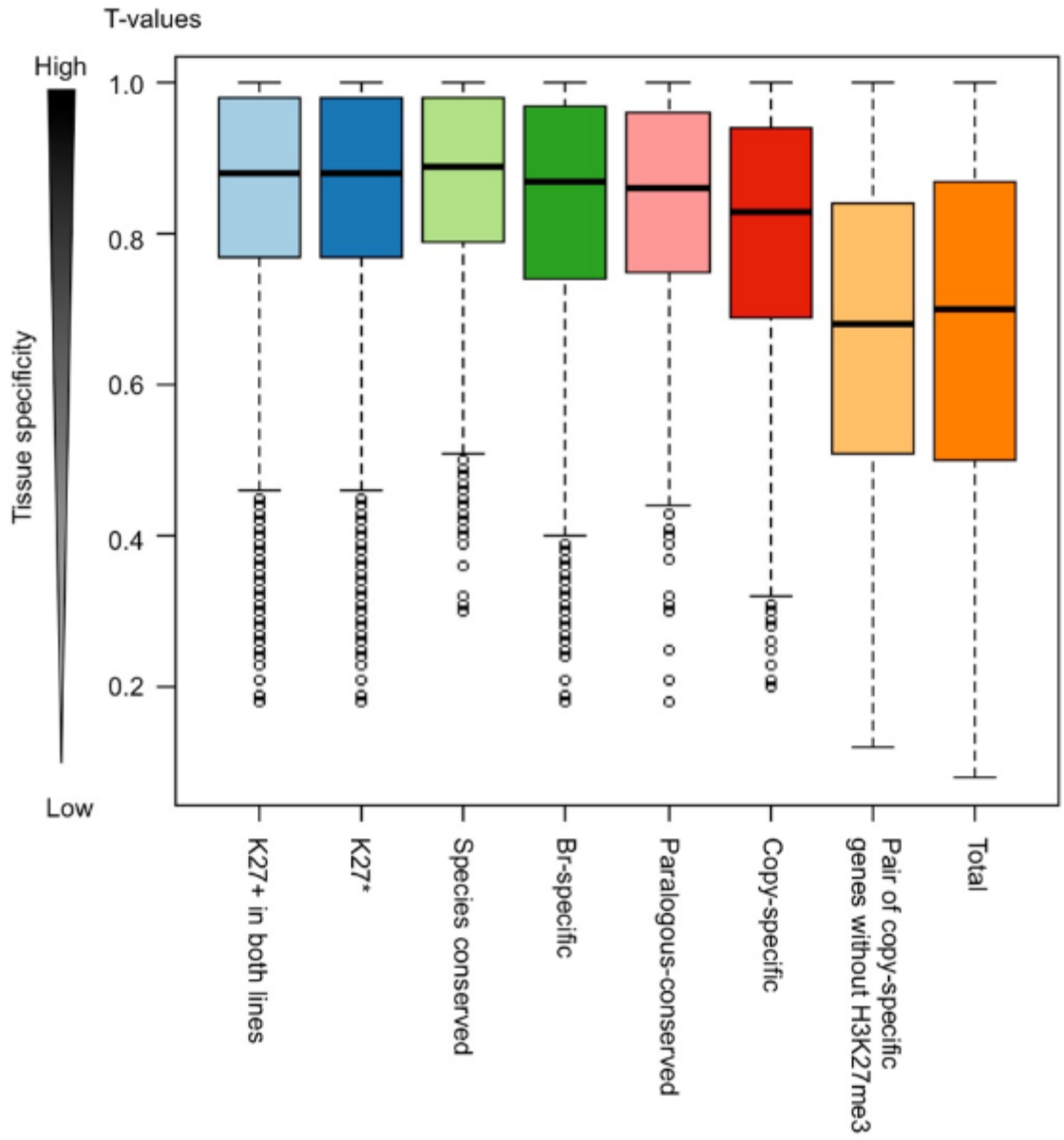

Figure III-12. Tissue specificity of expression in genes having a H3K27me3 mark. A tissue specificity index, T-value, which interpolates the entire range between 0 for housekeeping genes and 1 for strictly one-tissue-specific genes, was calculated using the transcriptome data in six different tissues in *B. rapa.* 'K27+' and 'K27*' represent the H3K27me3-marked genes and H3K27me3 stably marked genes, respectively.

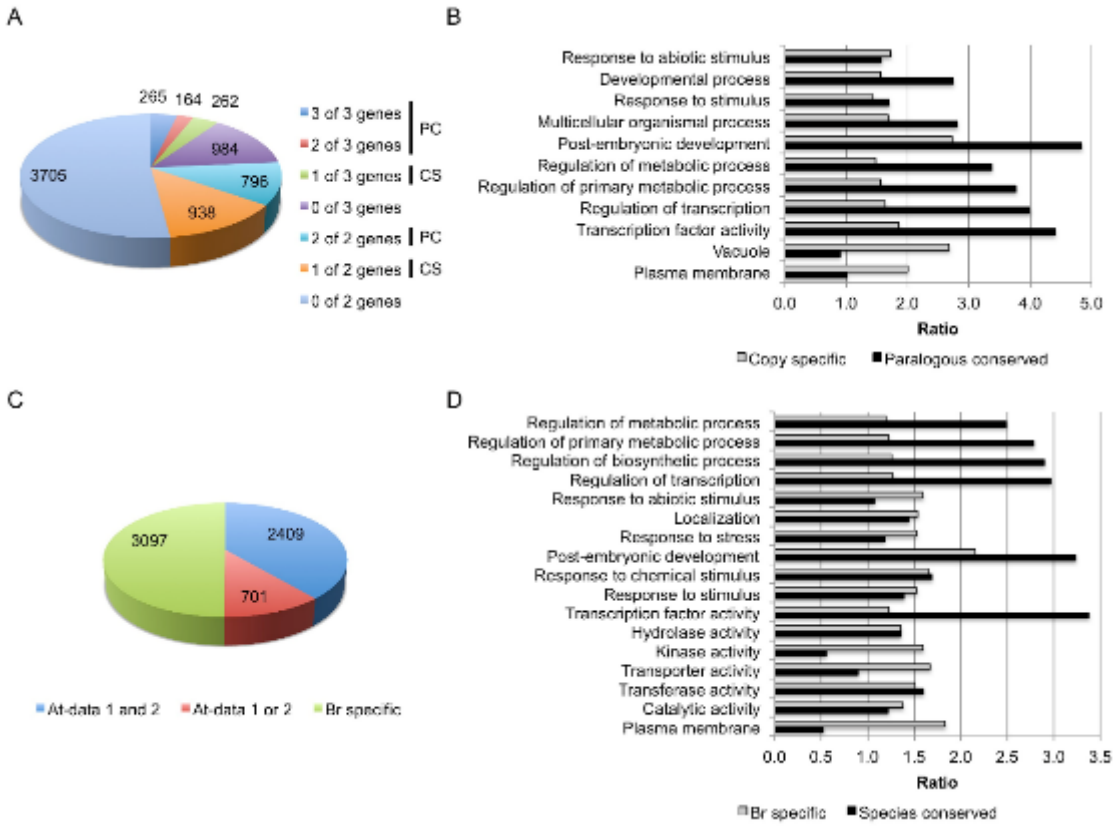

Figure III-13. Analysis of paralogous and species-conserved genes. (A) Classification of paralogous conserved (PC) and copy-specific (CS) H3K27me3-marked genes. (B) Gene ontology (GO) analysis using paralogous-conserved and copy-specific H3K27me3-marked genes. (C) Classification of H3K27me3-marked genes in *B. rapa* (Br). Blue, species-conserved H3K27me3-marked genes; red, single data set of *A. thaliana* (At) genes that overlapped with *B. rapa*, green, *Br*-specific H3K27me3-marked genes. (D) GO analysis using species-conserved and *Br*-specific H3K27me3-marked genes.

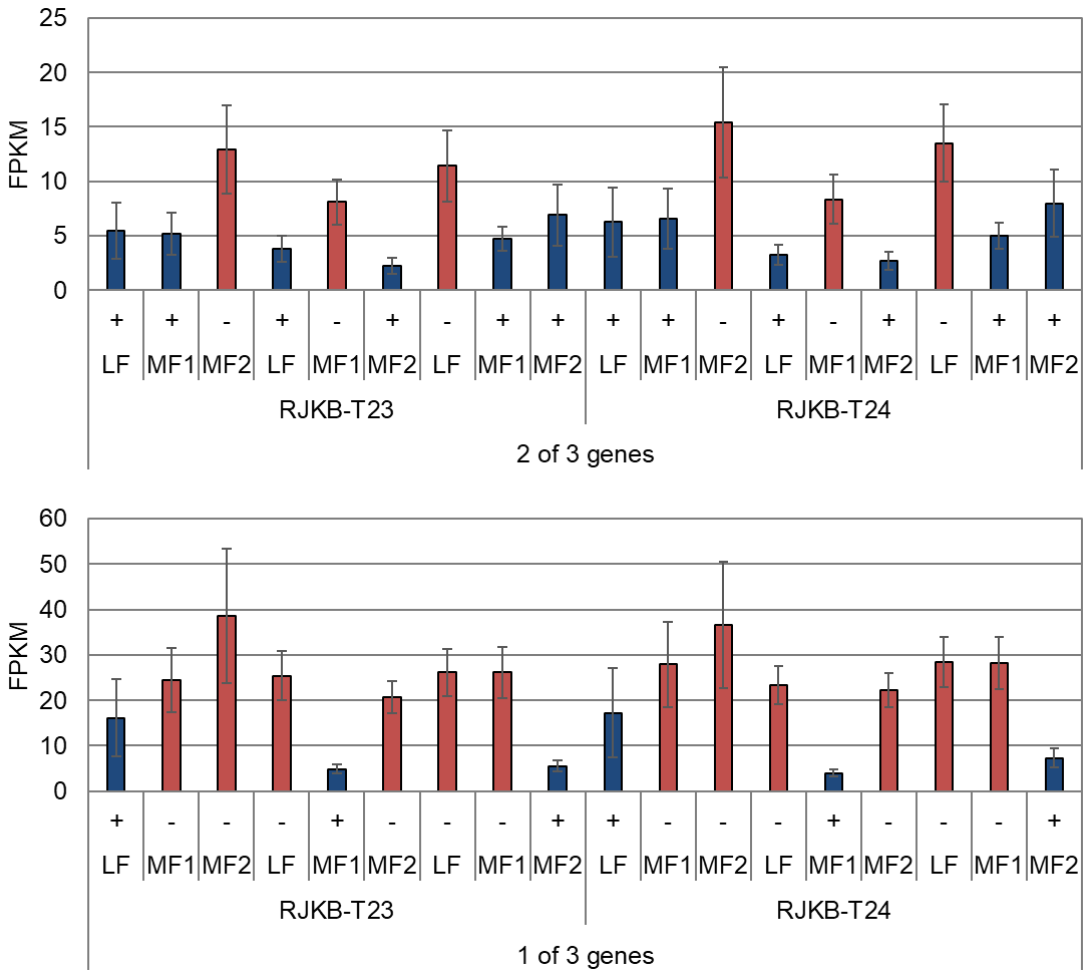

Figure III-14. Comparison of the expression level (FPKM) between paralogous pairs with and without H3K27me3. Values are means ± standard error (s.e.) of FPKM. + and – represent presence and absence of H3K27me3, respectively. *, $p<0.05$; **, $p<0.01$ (Student *t*-test). Least fractionated (LF), medium fractionated (MF1) and most fractionated blocks (MF2).

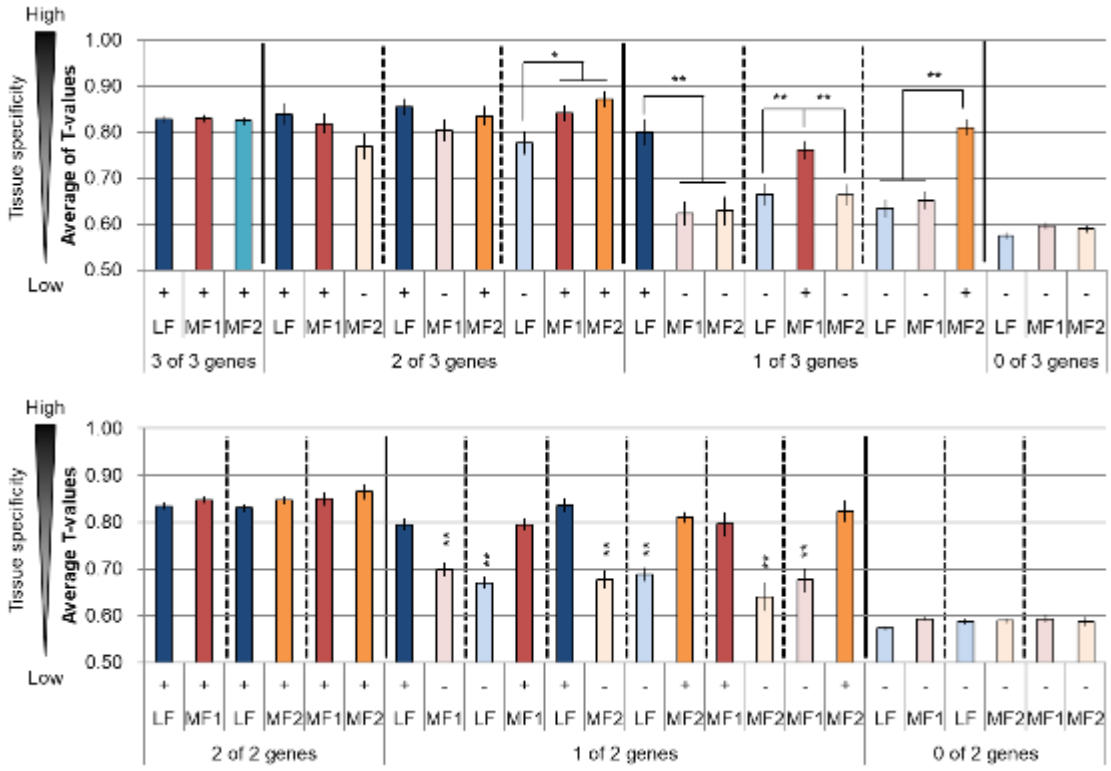

Figure III-15. Comparison of the tissue specificity between paralogous pairs with and without H3K27me3 using T-values. Values are means ± standard error (s.e.) of T-values. + and – represent presence and absence of H3K27me3, respectively. *, $p<0.05$; **, $p<0.01$ (Student *t*-test). Least fractionated (LF), medium fractionated (MF1) and most fractionated blocks (MF2).

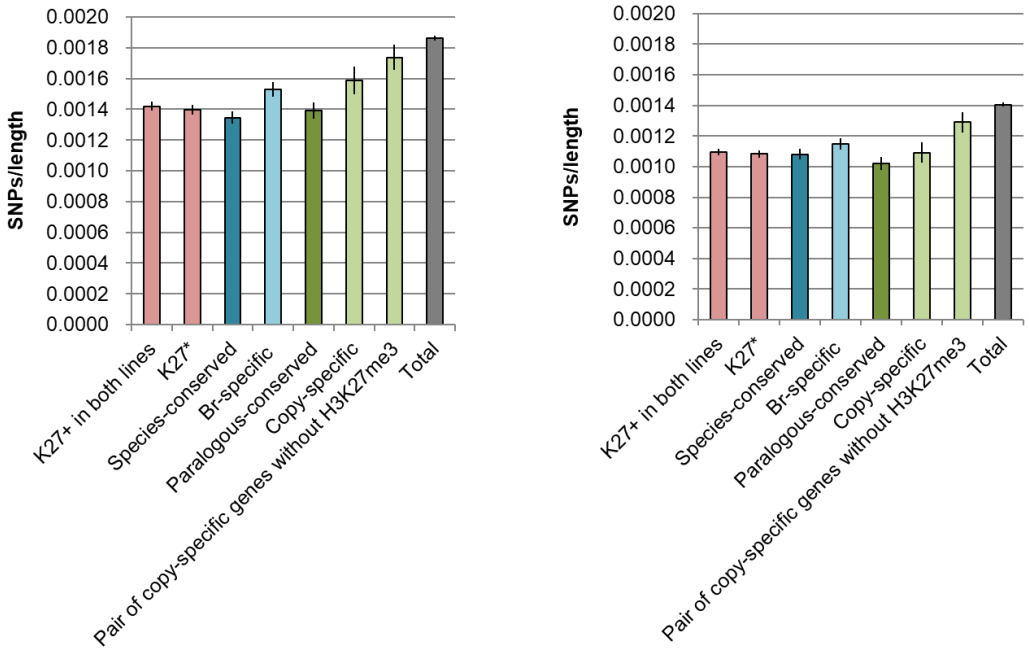

Figure III-16. Comparison of the average mutation rate (SNPs per length) in each gene having a H3K27me3 mark in RJKB-T23 and RJKB-T24. 'n. s.' represents no significant difference. Values are means ± standard error (s.e.) of SNP numbers per length. *, $p < 0.05$ (Student *t*-test). 'K27+' and 'K27*' represent the H3K27me3-marked genes and H3K27me3 stably marked genes, respectively. K27+ in both lines (n=10,456), K27* (n=7,930), Species-conserved (n=4,368), Br-specific (n=4,224), Paralogous-conserved (n=2,715), Copy-specific (n=1,200), Pair of copy-specific genes without H3K27me3 (n=1,462), Total (n=35,198).

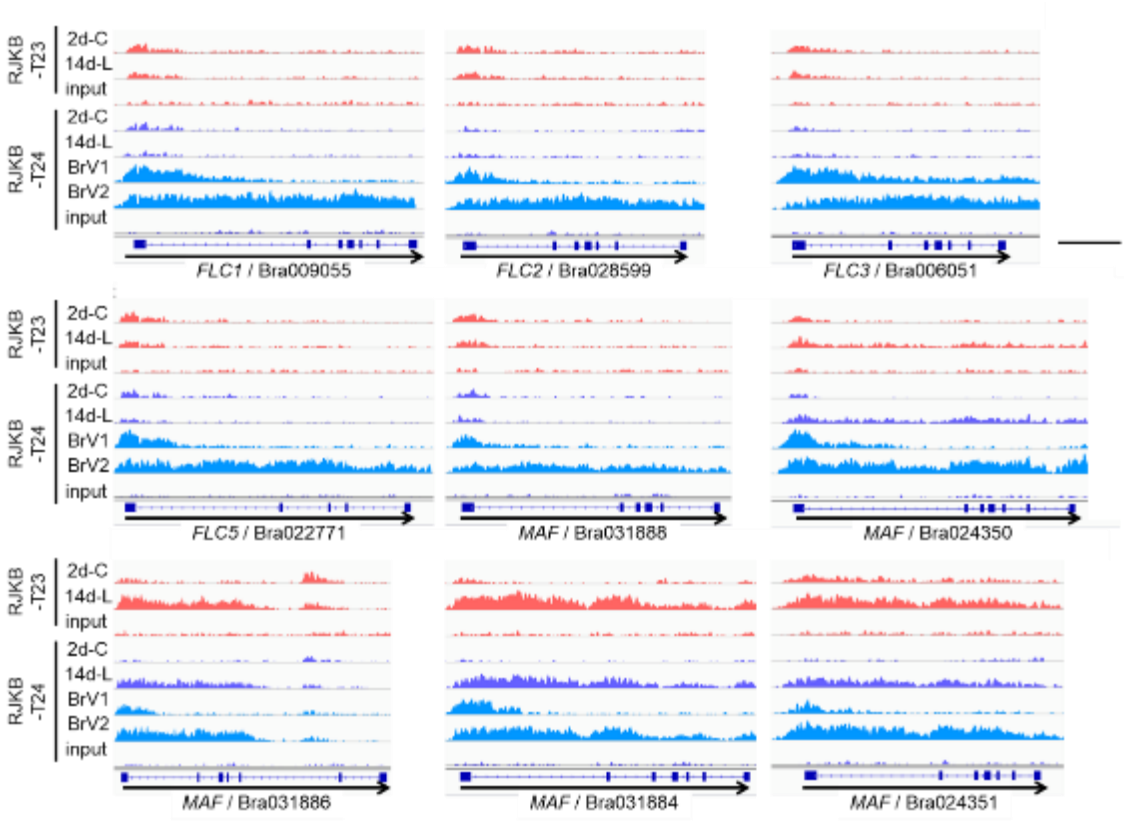

Figure III-17. Visualization of H3K27me3 peaks by Integrative Genomics Viewer (IGV). 2d-C and 14d-L are non-vernalized samples and BrV1 and BrV2 are vernalized samples. 2d-C, 2-day cotyledons; 14d-L,14-day leaves; BrV1, seeds were treated for four weeks at 4°C (vernalization); BrV2, seeds were treated for four weeks at 4°C and plants were transferred to the normal growth conditions for 12 days after vernalization.

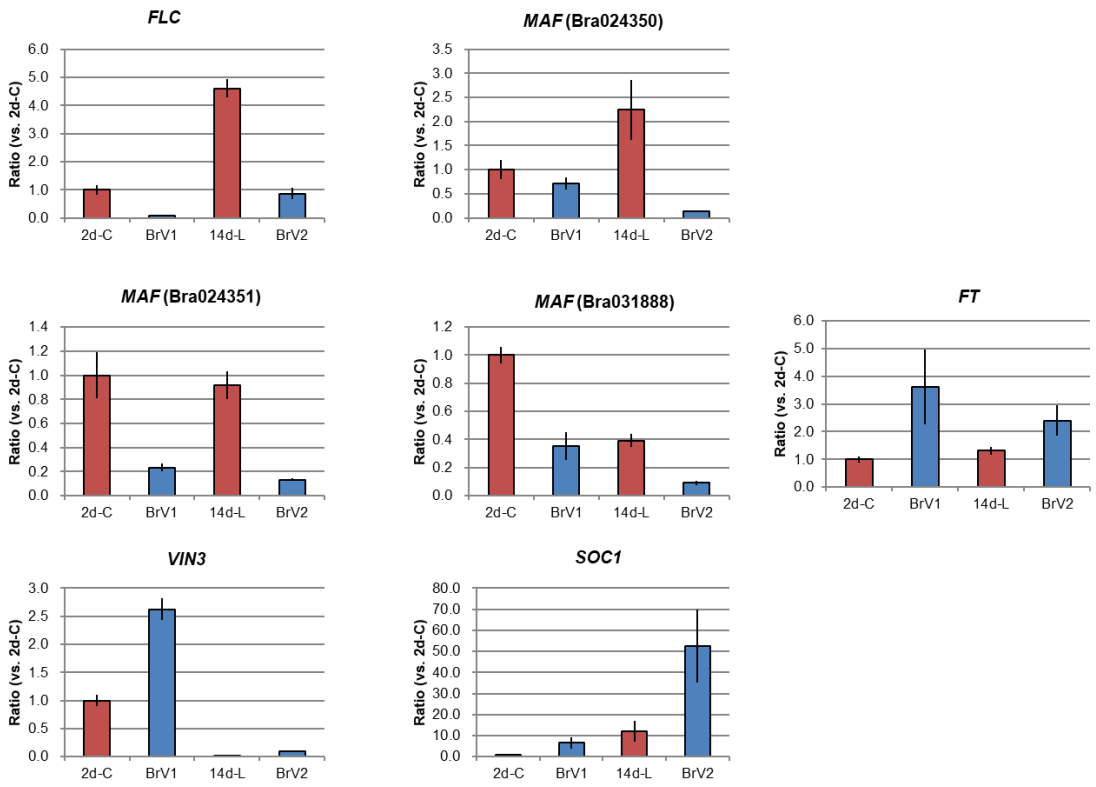

Figure III-18. Expression analysis by qPCR with and without vernalization treatment. Bar graph represents the level of expression among four *FLC* paralogs, *MAF*, *VIN3*, *SOC1*, and *FT*. 2d-C, 2-day cotyledons; 14d-L,14-day leaves; BrV1, seeds were treated for four weeks at 4°C (vernalization); BrV2, seeds were treated for four weeks at 4°C and plants were transferred to the normal growth conditions for 12 days after vernalization. Expression level of each gene relative to *BrACTIN* is calculated, and the y-axis shows the ratio against 2d-C. Data presented are the average and standard error (s.e.) from three biological and experimental replications.

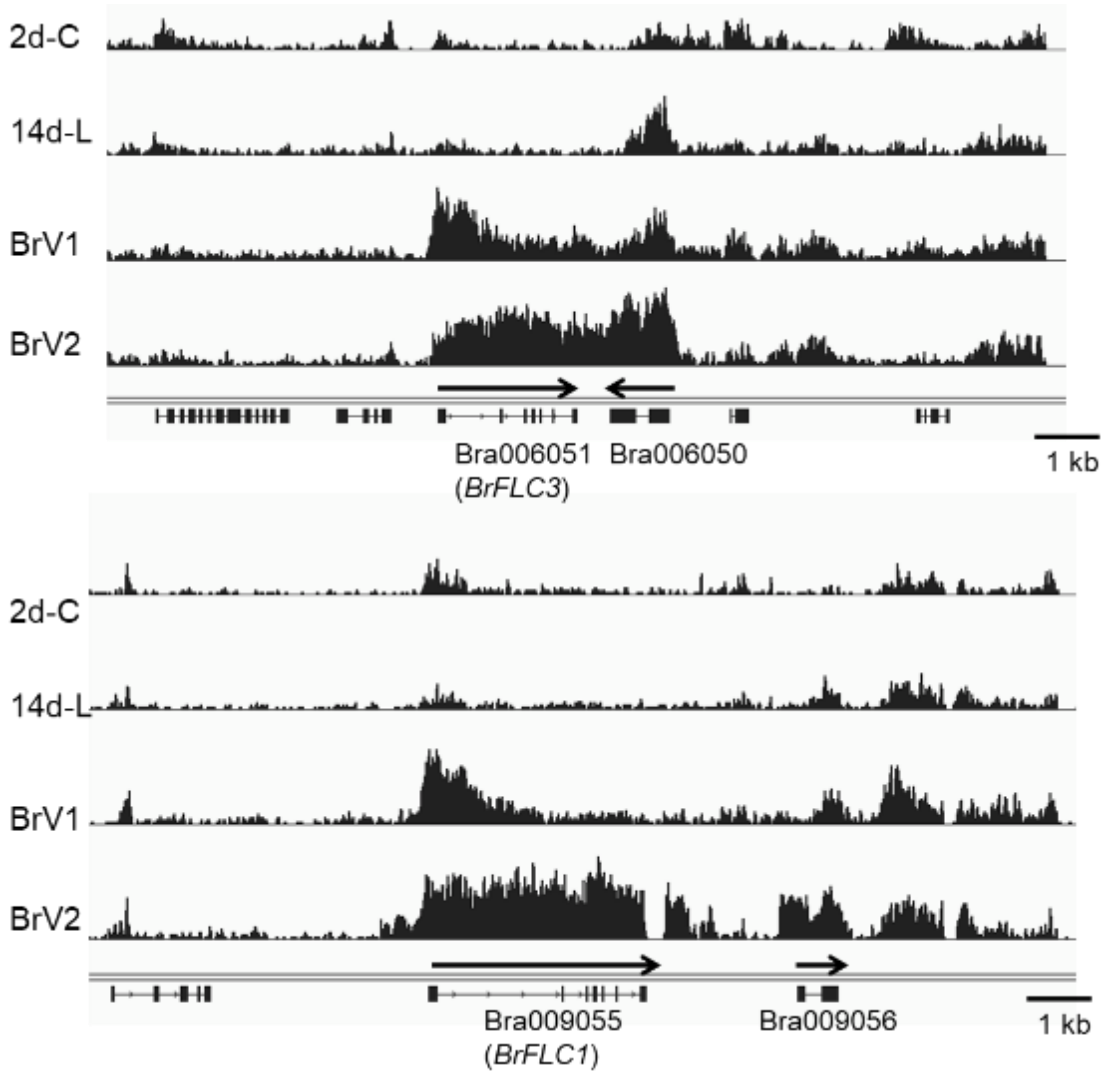

Figure III-19. Visualization of H3K27me3 peaks by Integrative Genomics Viewer (IGV). 2d-C and 14d-L are non-vernalized samples and BrV1 and BrV2 are vernalized samples. 2d-C, 2-day cotyledons; 14d-L,14-day leaves; BrV1, seeds were treated for four weeks at 4°C (vernalization); BrV2, seeds were treated for four weeks at 4°C and plants were transferred to the normal growth conditions for 12 days after vernalization.

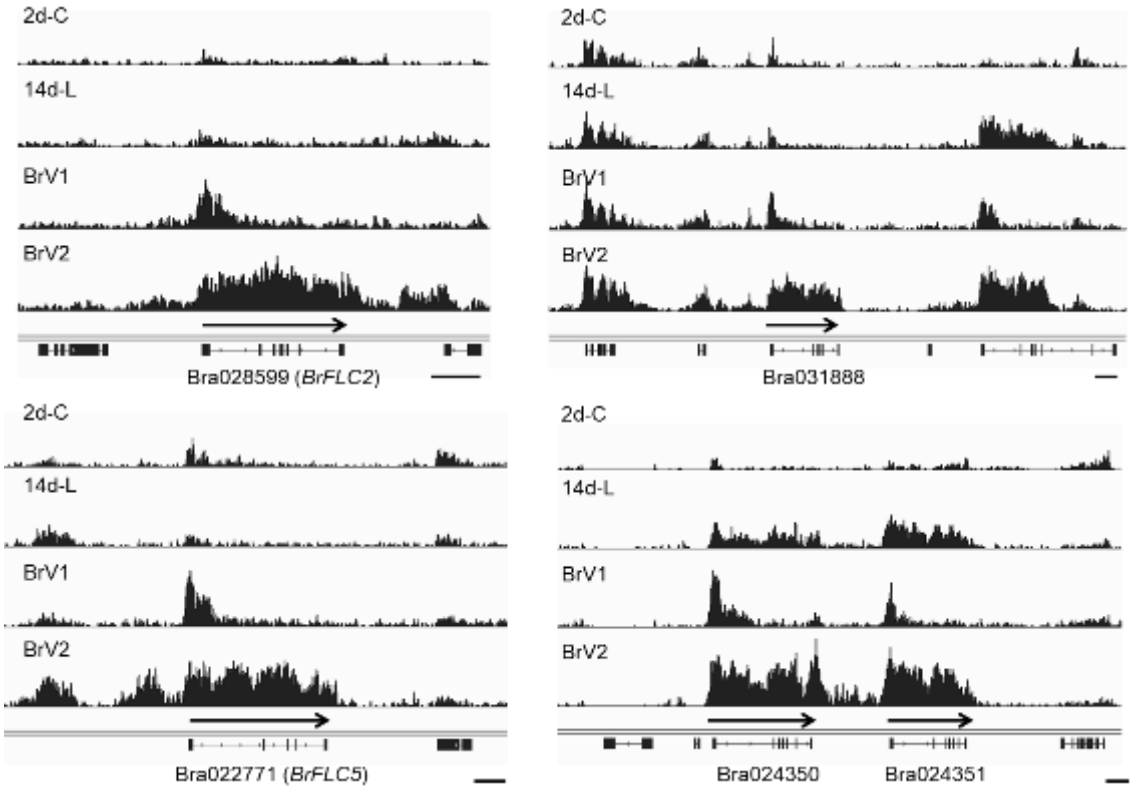

Figure III-20. Visualization of H3K27me3 peaks by Integrative Genomics Viewer (IGV). 2d-C and 14d-L are non-vernalized samples and BrV1 and BrV2 are vernalized samples. 2d-C, 2-day cotyledons; 14d-L,14-day leaves; BrV1, seeds were treated for 4 weeks at 4°C (vernalization); BrV2, seeds were treated for 4 weeks at 4°C and plants were transferred to the normal growth conditions for 12 days after vernalization. Bar represents 1 kb in length.

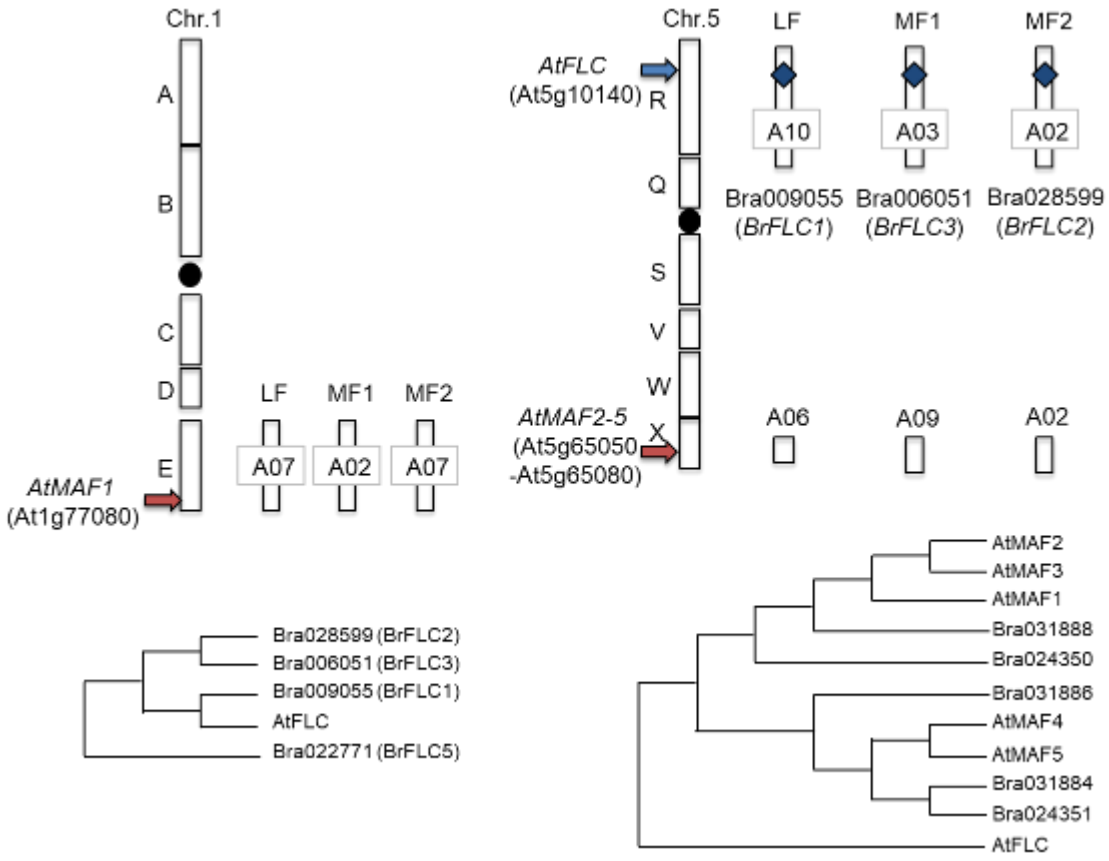

Figure III-21. Representation of the syntenic segments covering *AtFLC* and *AtMAF1-5* and their corresponding three subgenome in *B. rapa*. For analysis of chromosome segments in chromosome 1 and 5 in *A. thaliana,* Cheng et al. 2012 was followed.[1] *AtFLC* has high confidence syntenic gene set in three subgenome of *B. rapa*, while *AtMAF1*, *2*, *3*, *4*, and *5* do not have high confidence syntenic gene set in *B. rapa*. Phylogenetic relationship in FLC or MAF genes in *A. thaliana* and *B. rapa* is shown in bottom panel.

Table III-1. Sequences of primers used for ChIP-qPCR

Name	Primer sequences (5'-3')	
ChIP-qPCR (H3K27me3)		
Positive control		
FWA	CGGCATATGATTCGTTTGTG	CCTGGTTGTGTAGCATGTGG
STM	TGGAGAGTGGTTCCAACAGCACTTC	GGAGCTACTTTGTTGGTGGTGTGAC
Negative control		
Bra013206	GACGAGCACAAGAGTGGTGA	TAATCGCTGTCGCTGTCACT
Bra028913	CCCTGGGAGCAACTCTGTTA	GTGGGAGCAATCCTGATGAC
Validation		
AG	AAATGAGAGGAACAATCCAAGTATG	ACACTAACTGAAGAGCGGTTTGGTC
AGL19	AGATSAAGAGRATAGAGAACGCAAC	GAGCTAGAGAACTCATAGAGTTTGG
FUS3	CCMAGATTATAATCAKCATTACAAC	ATTCTCGACTGAGCCAAAACCCTCG
RT-qPCR		
FLC	GACGCARYGGTCTCATYGAGAAAGC	AWCATTARTTYTGTCTTYSTAGCTC
VIN3	GAGAATKTAGCTTGTAGAGCTGCGC	CGGACCCACATCACCCTCCAGCTTC
SOC1	CCAGCTCCAATATGCAAGATA	CCCAAGAGTTTACGTTTGGA
FT	ACTTGGTTATGGTGGATCC	CCGAGYGYCGGAACAATA
MAF (Bra024350)	TGGTGTAAGTGTAGATTCTC	AGGAACGTCTGCTTCCAAAT
MAF (Bra024351)	CAGTCCAACGCAAGATTGAA	CCAAAACCGTGGTTCTCGTCT
MAF (Bra031888)	GCAATCTTGAAGAACCAAATG	GAATTGTTCTCTCTCCTTCC
Actin	CGGTCCAGCTTCGTCATACTCAGCC	AAATGTGATGTGGATATCAGGAAGG

Table III-2. Sequence data of ChIP-seq in *B. rapa*

Sample	a. Total number of reads	b. Mapped reads	b/a (%)	c. Mapped reads (Unique aligned)	c/a (%)	d. Mapped in A01-A10	d/c (%)	e. Mapped in IRRs	e/c (%)
Input									
RJKB-T23 rep1	30,674,566	27,017,433	88.1%	14,575,541	47.5%	12,405,527	85.1%	6,294,140	43.2%
RJKB-T23 rep2	41,092,509	36,173,019	88.0%	18,713,543	45.5%	16,174,659	86.4%	7,683,962	41.1%
Total (rep1 + rep2)	71,767,075	63,190,452	88.0%	33,289,084	46.4%	28,580,186	85.9%	13,978,102	42.0%
RJKB-T24 rep1	27,342,223	24,058,760	88.0%	12,247,035	44.8%	10,320,865	84.3%	5,369,066	43.8%
RJKB-T24 rep2	37,826,546	33,372,769	88.2%	18,221,789	48.2%	15,809,899	86.8%	7,130,500	39.1%
Total (rep1 + rep2)	65,168,769	57,431,529	88.1%	30,468,824	46.8%	26,130,764	85.8%	12,499,566	41.0%
H3K27me3									
RJKB-T23-NV (2 DAS) (2d-C)	52,880,782	48,859,230	92.4%	27,086,194	51.2%	25,420,526	93.9%	8,851,994	32.7%
RJKB-T23-NV (14 DAS) rep1 (14d-L)	41,820,661	38,823,628	92.8%	23,015,481	55.0%	21,726,425	94.4%	6,749,601	29.3%
RJKB-T23-NV (14 DAS) rep2 (14d-L)	36,653,927	34,618,067	94.4%	22,226,240	60.6%	21,115,898	95.0%	7,438,845	33.5%
Total (rep1 + rep2)	78,474,588	73,441,695	93.6%	45,241,721	57.7%	42,842,323	94.7%	14,188,446	31.4%
RJKB-T24-NV (2 DAS) (2d-C)	21,602,547	19,387,437	89.7%	13,882,370	64.3%	13,005,380	93.7%	4,479,345	32.3%
RJKB-T24-NV (14 DAS) rep1 (14d-L)	24,642,163	22,924,992	93.0%	15,729,508	63.8%	14,857,532	94.5%	4,430,772	28.2%
RJKB-T24-NV (14 DAS) rep2 (14d-L)	36,305,045	34,558,761	95.2%	20,850,733	57.4%	19,999,679	95.9%	6,290,978	30.2%
Total (rep1 + rep2)	60,947,208	57,483,753	94.3%	36,580,241	60.0%	34,857,211	95.3%	10,721,750	29.3%
RJKB-T24 4wkV (BrV1)	34,808,836	30,863,991	88.7%	19,724,454	56.7%	18,358,178	93.1%	6,242,434	31.6%
RJKB-T24 4wkV+12d (BrV2)	30,321,990	28,273,802	93.2%	17,943,792	59.2%	17,087,498	95.2%	4,796,303	26.7%

Table III-3. Sequence data of ChIP-seq in *A. thaliana*

Sample	a. Total number of reads	b. Mapped reads	b/a (%)	c. Mapped reads (Unique aligned)	c/a (%)	d. Mapped in Chr.1-5	d/c (%)	e. Mapped in TEs	e/c (%)
Input									
C24 NV	10,579,095	9,560,022	90.4%	6,513,137	61.6%	6,282,087	96.5%	892,807	13.7%
C24 V	22,861,344	21,297,824	93.2%	14,721,593	64.4%	14,424,566	98.0%	2,009,779	13.7%
H3K27me3									
C24 NV	10,695,290	9,577,431	89.5%	7,220,900	67.5%	7,125,902	98.7%	699,979	9.7%
C24 V	10,132,497	9,386,915	92.6%	6,865,299	67.8%	6,813,607	99.2%	608,638	8.9%
SRX2024391									
Input									
INPUT rep1	20,723,051	19,562,204	0.944	12,126,533	58.5%	11,828,335	97.5%	2,462,841	20.3%
INPUT rep2	20,367,796	19,343,543	0.9497	12,718,442	62.4%	12,356,508	97.2%	2,290,838	18.0%
H3K27me3									
K27me3 rep1	19,953,881	18,222,084	0.9132	10,939,137	54.8%	10,730,095	98.1%	1,432,077	13.1%
K27me3 rep2	18,145,651	16,565,195	0.9129	6,791,531	37.4%	6,584,951	97.0%	1,010,429	14.9%

SRX2024391 is ChIP-seq data in germinating seeds of C24 accession (Zhu *et a*l. 2017)

NV, Non-vernalized

V, upon return to warm conditions after vernalization

Table III-4. Number of peaks identified from ChIP-seq analysis using H3K27me3 antibodies in *B. rapa*

		A01-A10							
	Total	2kb upstream		Exon		Intron		2kb downstream	
	Peaks	Peaks	Number of genes	Peaks	Number of genes	Peaks	Number of genes	Peaks	Number of genes
RJKB-T23-NV (2 DAS) (2d-C)									
Total	47,816	24,128	21,081	26,728	21,913	18,288	14,147	14,794	12,754
in IRRs	19,739	5,673	5,155	6,274	5,346	4,388	3,346	4,753	4,313
RJKB-T23-NV (14 DAS) (14d-L)									
Total	32,526	14,507	12,614	16,656	12,872	11,597	8,209	11,153	9,667
in IRRs	16,348	4,653	4,287	5,307	4,486	3,957	3,081	4,057	3,805
RJKB-T24-NV (2 DAS) (2d-C)									
Total	43,395	20,874	18,062	24,953	19,750	16,690	12,303	13,562	11,314
in IRRs	16,808	4,804	4,326	5,896	4,883	3,882	2,903	4,038	3,640
RJKB-T24-NV (14 DAS) (14d-L)									
Total	23,754	10,752	9,982	12,205	10,158	8,878	7,013	8,678	8,239
in IRRs	14,447	4,144	3,963	4,596	4,131	3,549	2,988	3,695	3,601
RJKB-T24 4wkV (BrV1)									
Total	29,074	12,307	10,435	14,599	11,186	10,002	6,940	9,617	8,207
in IRRs	14,671	4,075	3,714	4,842	4,096	3,460	2,660	3,512	3,231
RJKB-T24 4wkV+12d (BrV2)									
Total	30,951	13,938	11,899	16,236	12,459	11,677	8,142	11,084	9,673
in IRRs	15,761	4,588	4,232	5,552	4,721	4,057	3,129	4,062	3,808

IRR; interspersed repeats region

Table III-5. Number of peaks identified in ChIP-seq analysis using H3K27me3 antibodies in *A. thaliana*

		Chr. 1-5							
	Total	2kb upstream		Exon		Intron		2kb downstream	
	Peaks	Peaks	Number of genes	Peaks	Number of genes	Peaks	Number of genes	Peaks	Number of genes
C24 NV	19,125	9,412	6,382	12,356	6,285	6,920	3,488	8,449	5,708
in TEs	1,208	564	601	445	399	276	241	486	508
C24 V	19,802	9,734	7,153	13,875	7,349	7,850	4,034	8,954	6,417
in TEs	1,274	584	626	491	436	300	258	534	546
SRX2024391	12,138	7,966	8,661	7,197	6,452	4,920	4,321	6,898	7,459
in TEs	3,086	2,137	2,748	1,571	1,803	1,165	1,214	1,790	2,348

SRX2024391 is ChIP-seq data in germinating seeds of C24 accession (Zhu *et a*l. 2017)

Table III-6. Number of mapped RNA sequencing reads at 2-day cotyledons and 14-day leaves of RJKB-T23 and RJKB-T24

Sample	Total number of reads	Mapped reads	(%)
RJKB-T23			
2-day cotyledons rep-1	47,252,005	39,627,335	83.86
2-days cotyledon rep-2	51,844,231	43,070,384	83.08
14-day leaves rep-1	27,386,426	22,818,660	83.32
14-day leaves rep-2	19,888,184	16,587,879	83.41
RJKB-T24			
2-day cotyledons rep-1	50,028,624	41,708,620	83.37
2-days cotyledon rep-2	43,674,941	36,498,416	83.57
14-day leaves rep-1	43,398,832	36,612,692	84.36
14-day leaves rep-2	50,939,899	42,803,366	84.03

Table III-7. Mapped reads in genic region using Input-DNA-seq and ChIP-seq data of RJKB-T23 and RJKB-T24

Sample	a. Mapped reads (Unique aligned)	b. Upstream (2kb)	b/a	c. Exon	c/a	d. Intron	d/a	e. Downstream (2kb)	e/a
Input									
RJKB-T23 rep1	14,575,541	3,104,668	21.3%	3,617,693	24.8%	1,815,451	12.5%	3,410,205	23.4%
RJKB-T23 rep2	18,713,543	4,185,124	22.4%	4,588,848	24.5%	2,498,728	13.4%	4,712,180	25.2%
RJKB-T24 rep1	12,247,035	2,549,482	20.8%	2,971,301	24.3%	1,474,871	12.0%	2,787,697	22.8%
RJKB-T24 rep2	18,221,789	4,192,231	23.0%	4,433,169	24.3%	2,573,304	14.1%	4,778,009	26.2%
H3K27me3									
RJKB-T23-NV (2 DAS) (2d-C)	27,086,194	8,124,571	30.0%	8,519,668	31.5%	4,072,384	15.0%	7,458,267	27.5%
RJKB-T23-NV (14 DAS) rep1 (14d-L)	23,015,481	7,068,465	30.7%	7,574,954	32.9%	3,513,082	15.3%	6,722,707	29.2%
RJKB-T23-NV (14 DAS) rep2 (14d-L)	22,226,240	7,061,660	31.8%	7,374,104	33.2%	3,877,172	17.4%	6,715,249	30.2%
RJKB-T24-NV (2 DAS) (2d-C)	13,882,370	4,108,931	29.6%	4,643,563	33.4%	2,114,726	15.2%	3,828,520	27.6%
RJKB-T24-NV (14 DAS) rep1 (14d-L)	15,729,508	4,920,545	31.3%	5,066,318	32.2%	2,432,701	15.5%	4,625,054	29.4%
RJKB-T24-NV (14 DAS) rep2 (14d-L)	20,850,733	6,927,559	33.2%	6,762,614	32.4%	3,783,487	18.1%	6,474,412	31.1%
RJKB-T24 4wkV (BrV1)	19,724,454	5,723,551	29.0%	5,850,405	29.7%	3,003,627	15.2%	5,487,379	27.8%
RJKB-T24 4wkV+12d (BrV2)	17,943,792	5,612,568	30.0%	6,032,169	31.5%	2,897,528	18.1%	5,320,993	27.5%

Table III-8. Comparison of the H3K27me3-marked genes between tissues and lines

	Total number of Peaks	1	2	3	4	5	6
1. RJKB-T23-NV (2 DAS) (2d-C)	21,242		10,488	17,027	9,130		
2. RJKB-T23-NV (14 DAS) (14d-L)	12,426			9,355	10,456		
3. RJKB-T24-NV (2 DAS) (2d-C)	18,438				8,650	9,909	9,446
4. RJKB-T24-NV (14 DAS) (14d-L)	11,655					9,137	11,088
5. RJKB-T24 4wkV (BrV1)	11,139						9,550
6. RJKB-T24 4wkV+12d (BrV2)	12,580						

Table III-9. Difference of H3K27me3 levels in the genic regions

	Between lines				Between tissues		
	T23 > T24	T23 < T24	Total		2d-C > 14d-L	2d-C < 14d-L	Total
2 DAS (2d-C)	528	201	729	RJKB-T23	1,309	480	1,789
14 DAS (14d-L)	574	324	898	RJKB-T24	6,709	1,443	8,152
Both	175	118	293	Both	903	395	1,298

Table III-10. Number of genes showing difference between H3K27me3 and expression levels

H3K27me3 level		Expression level				
Between different lines		T23 > T24	T23 < T24	Total	(%)	Antagonistic (%)
T23 > T24 (2 DAS)	528	148	41	189	35.8%	7.8%
T23 < T24 (2 DAS)	201	16	36	52	25.9%	8.0%
Total	729	164	77	241	33.1%	
T23 > T24 (14 DAS)	574	69	72	141	24.6%	12.5%
T23 < T24 (14 DAS)	324	41	18	59	18.2%	12.7%
Total	898	110	90	200	22.3%	
Between different tissues		2d-C > 14d-L	2d-C < 14d-L	Total	(%)	Antagonistic (%)
2d-C > 14d-L (T23)	1309	735	174	909	69.4%	13.3%
2d-C < 14d-L (T23)	480	95	41	136	28.3%	19.8%
Total	1789	830	215	1,045	58.4%	
2d-C > 14d-L (T24)	6709	3,449	1,099	4,548	67.8%	16.4%
2d-C < 14d-L (T24)	1443	246	158	404	28.0%	17.0%
Total	8152	3,695	1,257	4,952	60.7%	

Gray highlight reveals the gene number showing antagonistic relationship between H3K27me3 level and expression level

Table III-11. GO function term overrepresented in paralogous-conserved and copy-specific H3K27me3-marked genes

GO accession	Term type	Term	*p* value	FDR
Paralogous-conserved H3K27me3-marked genes				
GO:0003700	F	transcription factor activity	1.70E-102	1.40E-99
GO:0030528	F	transcription regulator activity	3.70E-97	1.50E-94
GO:0003677	F	DNA binding	8.40E-80	2.30E-77
GO:0045449	P	regulation of transcription	6.00E-68	5.30E-65
GO:0009889	P	regulation of biosynthetic process	6.30E-68	5.30E-65
GO:0031326	P	regulation of cellular biosynthetic process	6.30E-68	5.30E-65
GO:0010556	P	regulation of macromolecule biosynthetic process	6.20E-67	4.00E-64
GO:0019219	P	regulation of nucleobase, nucleoside, nucleotide and nucleic acid metabolic process	3.80E-66	1.90E-63
GO:0080090	P	regulation of primary metabolic process	3.50E-65	1.30E-62
GO:0051171	P	regulation of nitrogen compound metabolic process	3.60E-65	1.30E-62
GO:0006350	P	transcription	3.10E-63	9.90E-61
GO:0031323	P	regulation of cellular metabolic process	1.10E-62	3.10E-60
GO:0010468	P	regulation of gene expression	5.60E-61	1.40E-58
GO:0060255	P	regulation of macromolecule metabolic process	6.70E-59	1.50E-56
GO:0019222	P	regulation of metabolic process	7.30E-58	1.50E-55
GO:0065007	P	biological regulation	8.10E-54	1.60E-51
GO:0050794	P	regulation of cellular process	4.50E-47	8.20E-45
GO:0050789	P	regulation of biological process	9.80E-47	1.70E-44
GO:0003676	F	nucleic acid binding	6.20E-39	1.20E-36
GO:0009791	P	post-embryonic development	2.70E-38	4.30E-36
GO:0032502	P	developmental process	1.50E-36	2.30E-34
GO:0032501	P	multicellular organismal process	3.70E-35	5.20E-33
GO:0007275	P	multicellular organismal development	3.90E-35	5.20E-33
GO:0006355	P	regulation of transcription, DNA-dependent	1.30E-33	1.70E-31
GO:0051252	P	regulation of RNA metabolic process	2.80E-33	3.40E-31
GO:0006139	P	nucleobase, nucleoside, nucleotide and nucleic acid metabolic process	6.40E-33	7.50E-31
GO:0006351	P	transcription, DNA-dependent	1.00E-31	1.10E-29
GO:0032774	P	RNA biosynthetic process	1.10E-31	1.20E-29
GO:0048856	P	anatomical structure development	3.00E-31	3.10E-29
GO:0048513	P	organ development	6.20E-30	6.10E-28
GO:0048731	P	system development	6.80E-30	6.40E-28
GO:0006807	P	nitrogen compound metabolic process	4.90E-28	4.50E-26
GO:0009058	P	biosynthetic process	1.60E-27	1.40E-25
GO:0044249	P	cellular biosynthetic process	1.40E-26	1.20E-24
GO:0034645	P	cellular macromolecule biosynthetic process	2.60E-25	2.10E-23

GO:0009059	P	macromolecule biosynthetic process	2.70E-25	2.20E-23
GO:0042221	P	response to chemical stimulus	2.80E-22	2.10E-20
GO:0003006	P	reproductive developmental process	5.80E-21	4.40E-19
GO:0010467	P	gene expression	1.10E-20	8.00E-19
GO:0009908	P	flower development	4.30E-20	3.10E-18
GO:0022414	P	reproductive process	5.40E-19	3.70E-17
GO:0000003	P	reproduction	7.70E-19	5.10E-17
GO:0048608	P	reproductive structure development	4.40E-18	2.90E-16
GO:0048869	P	cellular developmental process	1.00E-17	6.40E-16
GO:0016070	P	RNA metabolic process	3.50E-17	2.10E-15
GO:0010033	P	response to organic substance	1.80E-15	1.10E-13
GO:0048437	P	floral organ development	2.40E-15	1.40E-13
GO:0048569	P	post-embryonic organ development	3.30E-15	1.90E-13
GO:0048438	P	floral whorl development	3.70E-15	2.10E-13
GO:0005488	F	binding	7.50E-15	1.20E-12
GO:0009653	P	anatomical structure morphogenesis	1.90E-14	1.00E-12
GO:0050896	P	response to stimulus	2.10E-14	1.10E-12
GO:0009719	P	response to endogenous stimulus	3.20E-14	1.70E-12
GO:0030154	P	cell differentiation	1.60E-12	8.30E-11
GO:0009725	P	response to hormone stimulus	2.30E-12	1.20E-10
GO:0065008	P	regulation of biological quality	2.20E-11	1.10E-09
GO:0010876	P	lipid localization	4.00E-11	2.00E-09
GO:0005634	C	nucleus	9.90E-11	1.80E-08
GO:0009886	P	post-embryonic morphogenesis	1.70E-10	8.20E-09
GO:0007389	P	pattern specification process	2.20E-10	1.00E-08
GO:0042545	P	cell wall modification	8.20E-10	3.80E-08
GO:0010817	P	regulation of hormone levels	1.80E-09	8.20E-08
GO:0022857	F	transmembrane transporter activity	2.20E-09	3.00E-07
GO:0009739	P	response to gibberellin stimulus	2.90E-09	1.30E-07
GO:0050793	P	regulation of developmental process	3.60E-09	1.60E-07
GO:0048467	P	gynoecium development	5.20E-09	2.30E-07
GO:0051179	P	localization	5.50E-09	2.30E-07
GO:0009887	P	organ morphogenesis	7.60E-09	3.20E-07
GO:0009888	P	tissue development	1.00E-08	4.30E-07
GO:0048466	P	androecium development	1.60E-08	6.20E-07
GO:0048443	P	stamen development	1.60E-08	6.20E-07
GO:0003002	P	regionalization	2.50E-08	9.60E-07
GO:0048827	P	phyllome development	3.00E-08	1.10E-06
GO:0022804	F	active transmembrane transporter activity	4.20E-08	4.80E-06
GO:0030599	F	pectinesterase activity	4.80E-08	4.80E-06
GO:0048440	P	carpel development	5.90E-08	2.20E-06
GO:0048367	P	shoot development	7.30E-08	2.70E-06
GO:0040007	P	growth	8.50E-08	3.10E-06
GO:0022621	P	shoot system development	8.80E-08	3.20E-06

GO:0048589	P	developmental growth	1.00E-07	3.60E-06
GO:0005215	F	transporter activity	1.20E-07	1.10E-05
GO:0006810	P	transport	1.80E-07	6.40E-06
GO:0051234	P	establishment of localization	2.00E-07	7.10E-06
GO:0044238	P	primary metabolic process	2.20E-07	7.70E-06
GO:0048609	P	reproductive process in a multicellular organism	2.40E-07	8.10E-06
GO:0045595	P	regulation of cell differentiation	2.60E-07	8.80E-06
GO:0032989	P	cellular component morphogenesis	2.70E-07	8.90E-06
GO:0000902	P	cell morphogenesis	3.50E-07	1.10E-05
GO:0048468	P	cell development	4.30E-07	1.40E-05
GO:0032504	P	multicellular organism reproduction	4.50E-07	1.40E-05
GO:0009987	P	cellular process	5.20E-07	1.60E-05
GO:0048653	P	anther development	6.60E-07	2.10E-05
GO:0048645	P	organ formation	8.20E-07	2.50E-05
GO:0022622	P	root system development	8.30E-07	2.50E-05
GO:0048364	P	root development	8.30E-07	2.50E-05
GO:0015291	F	secondary active transmembrane transporter activity	9.50E-07	7.70E-05
GO:0016563	F	transcription activator activity	1.10E-06	7.70E-05
GO:0042446	P	hormone biosynthetic process	1.40E-06	4.10E-05
GO:0042445	P	hormone metabolic process	1.70E-06	5.00E-05
GO:0020037	F	heme binding	2.00E-06	0.00013
GO:0004091	F	carboxylesterase activity	2.10E-06	0.00013
GO:0006855	P	multidrug transport	2.40E-06	7.00E-05
GO:0048825	P	cotyledon development	2.90E-06	8.40E-05
GO:0022891	F	substrate-specific transmembrane transporter activity	3.20E-06	0.00019
GO:0015893	P	drug transport	3.60E-06	0.0001
GO:0042493	P	response to drug	4.10E-06	0.00011
GO:0015103	F	inorganic anion transmembrane transporter activity	5.20E-06	0.00028
GO:0010154	P	fruit development	5.40E-06	0.00015
GO:0045596	P	negative regulation of cell differentiation	5.60E-06	0.00015
GO:0048646	P	anatomical structure formation involved in morphogenesis	6.30E-06	0.00017
GO:0010073	P	meristem maintenance	6.40E-06	0.00017
GO:0009826	P	unidimensional cell growth	7.30E-06	0.00019
GO:0060560	P	developmental growth involved in morphogenesis	7.30E-06	0.00019
GO:0044260	P	cellular macromolecule metabolic process	7.50E-06	0.0002
GO:0009699	P	phenylpropanoid biosynthetic process	9.00E-06	0.00023
GO:0016684	F	oxidoreductase activity, acting on peroxide as acceptor	1.00E-05	0.00047
GO:0004601	F	peroxidase activity	1.00E-05	0.00047
GO:0009834	P	secondary cell wall biogenesis	1.10E-05	0.00027
GO:0005506	F	iron ion binding	1.30E-05	0.00057
GO:0016049	P	cell growth	1.40E-05	0.00035

GO:0009733	P	response to auxin stimulus	1.50E-05	0.00037
GO:0042398	P	cellular amino acid derivative biosynthetic process	1.70E-05	0.00042
GO:0010200	P	response to chitin	2.00E-05	0.0005
GO:0048316	P	seed development	2.10E-05	0.00051
GO:0006811	P	ion transport	2.10E-05	0.00051
GO:0019827	P	stem cell maintenance	2.20E-05	0.00051
GO:0048864	P	stem cell development	2.20E-05	0.00051
GO:0046906	F	tetrapyrrole binding	2.20E-05	0.00091
GO:0008361	P	regulation of cell size	2.30E-05	0.00053
GO:0006979	P	response to oxidative stress	2.50E-05	0.00057
GO:0015297	F	antiporter activity	2.50E-05	0.00095
GO:0009055	F	electron carrier activity	2.50E-05	0.00095
GO:0009743	P	response to carbohydrate stimulus	2.60E-05	0.00059
GO:0048863	P	stem cell differentiation	2.60E-05	0.00059
GO:0008152	P	metabolic process	2.60E-05	0.00059
GO:0051239	P	regulation of multicellular organismal process	2.70E-05	0.00059
GO:0032535	P	regulation of cellular component size	2.70E-05	0.00059
GO:0090066	P	regulation of anatomical structure size	2.70E-05	0.00059
GO:0048507	P	meristem development	3.40E-05	0.00075
GO:0031224	C	intrinsic to membrane	3.40E-05	0.003
GO:0009698	P	phenylpropanoid metabolic process	3.50E-05	0.00076
GO:0044237	P	cellular metabolic process	4.30E-05	0.00092
GO:0048366	P	leaf development	4.90E-05	0.001
GO:0016705	F	oxidoreductase activity, acting on paired donors, with incorporation or reduction of molecular oxygen	5.10E-05	0.0019
GO:0009605	P	response to external stimulus	5.30E-05	0.0011
GO:0031225	C	anchored to membrane	5.50E-05	0.0033
GO:0022892	F	substrate-specific transporter activity	5.90E-05	0.002
GO:0016209	F	antioxidant activity	6.30E-05	0.002
GO:0015238	F	drug transmembrane transporter activity	6.30E-05	0.002
GO:0015698	P	inorganic anion transport	6.40E-05	0.0013
GO:0030570	F	pectate lyase activity	6.90E-05	0.0021
GO:0016837	F	carbon-oxygen lyase activity, acting on polysaccharides	6.90E-05	0.0021
GO:0048518	P	positive regulation of biological process	7.50E-05	0.0015
GO:0008509	F	anion transmembrane transporter activity	7.50E-05	0.0022
GO:0009827	P	plant-type cell wall modification	7.90E-05	0.0016
GO:0000904	P	cell morphogenesis involved in differentiation	8.30E-05	0.0017
GO:0044464	C	cell part	9.10E-05	0.0033
GO:0005623	C	cell	9.10E-05	0.0033
GO:0009838	P	abscission	9.30E-05	0.0019
GO:0009900	P	dehiscence	9.30E-05	0.0019
GO:0009901	P	anther dehiscence	9.30E-05	0.0019
GO:0004857	F	enzyme inhibitor activity	9.60E-05	0.0027

Copy-specific H3K27me3-marked genes

GO:0030528	F	transcription regulator activity	2.60E-11	2.20E-08
GO:0009791	P	post-embryonic development	2.70E-11	5.90E-08
GO:0003700	F	transcription factor activity	8.20E-11	3.50E-08
GO:0044464	C	cell part	3.00E-10	6.70E-08
GO:0005623	C	cell	3.00E-10	6.70E-08
GO:0005886	C	plasma membrane	1.40E-09	2.20E-07
GO:0016020	C	membrane	3.90E-09	4.40E-07
GO:0065007	P	biological regulation	5.00E-09	5.40E-06
GO:0003677	F	DNA binding	1.70E-08	5.00E-06
GO:0032501	P	multicellular organismal process	1.90E-07	0.00014
GO:0007275	P	multicellular organismal development	3.40E-07	0.00019
GO:0005488	F	binding	5.20E-07	0.00011
GO:0050789	P	regulation of biological process	1.00E-06	0.00043
GO:0065008	P	regulation of biological quality	1.50E-06	0.00051
GO:0050896	P	response to stimulus	1.60E-06	0.00051
GO:0031225	C	anchored to membrane	1.60E-06	0.00012
GO:0005773	C	vacuole	1.70E-06	0.00012
GO:0050794	P	regulation of cellular process	2.40E-06	0.00066
GO:0032502	P	developmental process	4.90E-06	0.0011
GO:0009628	P	response to abiotic stimulus	5.20E-06	0.0011
GO:0045449	P	regulation of transcription	6.10E-06	0.0012
GO:0010556	P	regulation of macromolecule biosynthetic process	8.30E-06	0.0015
GO:0019219	P	regulation of nucleobase, nucleoside, nucleotide and nucleic acid metabolic process	9.10E-06	0.0015
GO:0009889	P	regulation of biosynthetic process	1.10E-05	0.0016
GO:0031326	P	regulation of cellular biosynthetic process	1.10E-05	0.0016
GO:0006350	P	transcription	1.50E-05	0.002
GO:0051171	P	regulation of nitrogen compound metabolic process	2.00E-05	0.0026
GO:0080090	P	regulation of primary metabolic process	2.60E-05	0.0031
GO:0031323	P	regulation of cellular metabolic process	2.90E-05	0.0033
GO:0009719	P	response to endogenous stimulus	3.80E-05	0.0042
GO:0010033	P	response to organic substance	4.20E-05	0.0044
GO:0010468	P	regulation of gene expression	6.10E-05	0.0061
GO:0042221	P	response to chemical stimulus	6.70E-05	0.0062
GO:0060255	P	regulation of macromolecule metabolic process	6.90E-05	0.0062
GO:0003006	P	reproductive developmental process	8.20E-05	0.0071
GO:0019222	P	regulation of metabolic process	9.20E-05	0.0077

C, Cellular component; F, Molecular function; P, Biological process

Table III-12. GO function term overrepresented in species-conserved and *Br*-specific H3K27me3-marked genes

GO accession	Term type	Term	*p* value	FDR
Species-conserved H3K27me3-marked genes				
GO:0003700	F	transcription factor activity	2.40E-105	3.00E-102
GO:0030528	F	transcription regulator activity	1.60E-95	1.00E-92
GO:0003677	F	DNA binding	2.20E-75	9.10E-73
GO:0045449	P	regulation of transcription	4.50E-63	1.50E-59
GO:0009889	P	regulation of biosynthetic process	2.10E-62	2.30E-59
GO:0031326	P	regulation of cellular biosynthetic process	2.10E-62	2.30E-59
GO:0010556	P	regulation of macromolecule biosynthetic process	1.70E-61	1.40E-58
GO:0019219	P	regulation of nucleobase, nucleoside, nucleotide and nucleic acid metabolic process	7.50E-61	4.90E-58
GO:0051171	P	regulation of nitrogen compound metabolic process	8.60E-60	4.70E-57
GO:0080090	P	regulation of primary metabolic process	1.40E-58	6.40E-56
GO:0006350	P	transcription	2.90E-57	1.20E-54
GO:0031323	P	regulation of cellular metabolic process	2.90E-55	1.10E-52
GO:0010468	P	regulation of gene expression	1.20E-54	4.00E-52
GO:0060255	P	regulation of macromolecule metabolic process	4.10E-52	1.20E-49
GO:0019222	P	regulation of metabolic process	2.50E-49	6.80E-47
GO:0065007	P	biological regulation	4.30E-39	1.10E-36
GO:0050794	P	regulation of cellular process	1.00E-36	2.40E-34
GO:0050789	P	regulation of biological process	2.10E-33	4.60E-31
GO:0009791	P	post-embryonic development	3.80E-30	7.70E-28
GO:0006355	P	regulation of transcription, DNA-dependent	4.10E-27	7.90E-25
GO:0051252	P	regulation of RNA metabolic process	1.00E-26	1.80E-24
GO:0003676	F	nucleic acid binding	1.10E-26	3.50E-24
GO:0007275	P	multicellular organismal development	1.90E-26	3.20E-24
GO:0032502	P	developmental process	4.20E-26	6.80E-24
GO:0032501	P	multicellular organismal process	6.00E-26	9.30E-24
GO:0048513	P	organ development	2.60E-25	3.80E-23
GO:0048731	P	system development	2.80E-25	4.00E-23
GO:0006351	P	transcription, DNA-dependent	5.80E-25	7.80E-23
GO:0032774	P	RNA biosynthetic process	6.30E-25	8.20E-23
GO:0012505	C	endomembrane system	6.90E-25	1.60E-22
GO:0004091	F	carboxylesterase activity	2.10E-23	5.30E-21
GO:0006139	P	nucleobase, nucleoside, nucleotide and nucleic acid metabolic process	1.70E-22	2.20E-20
GO:0048856	P	anatomical structure development	1.60E-21	2.00E-19
GO:0006807	P	nitrogen compound metabolic process	1.20E-19	1.30E-17
GO:0009058	P	biosynthetic process	8.60E-19	9.70E-17

GO:0030599	F	pectinesterase activity	1.70E-18	3.60E-16
GO:0044249	P	cellular biosynthetic process	1.00E-16	1.10E-14
GO:0016491	F	oxidoreductase activity	6.50E-16	1.20E-13
GO:0042545	P	cell wall modification	7.90E-15	8.30E-13
GO:0016684	F	oxidoreductase activity, acting on peroxide as acceptor	1.90E-14	2.70E-12
GO:0004601	F	peroxidase activity	1.90E-14	2.70E-12
GO:0009059	P	macromolecule biosynthetic process	5.70E-14	5.80E-12
GO:0048869	P	cellular developmental process	1.20E-13	1.20E-11
GO:0005488	F	binding	1.40E-13	1.70E-11
GO:0016798	F	hydrolase activity, acting on glycosyl bonds	2.00E-13	2.40E-11
GO:0034645	P	cellular macromolecule biosynthetic process	2.30E-13	2.20E-11
GO:0048438	P	floral whorl development	2.70E-13	2.50E-11
GO:0010033	P	response to organic substance	3.00E-13	2.70E-11
GO:0016209	F	antioxidant activity	4.60E-13	4.70E-11
GO:0009055	F	electron carrier activity	4.80E-13	4.70E-11
GO:0042221	P	response to chemical stimulus	4.90E-13	4.30E-11
GO:0019748	P	secondary metabolic process	6.00E-13	5.10E-11
GO:0009908	P	flower development	6.70E-13	5.60E-11
GO:0005506	F	iron ion binding	8.80E-13	7.90E-11
GO:0009719	P	response to endogenous stimulus	1.10E-12	9.20E-11
GO:0004553	F	hydrolase activity, hydrolyzing O-glycosyl compounds	1.10E-12	9.10E-11
GO:0009653	P	anatomical structure morphogenesis	1.20E-12	9.60E-11
GO:0009886	P	post-embryonic morphogenesis	2.60E-12	2.00E-10
GO:0020037	F	heme binding	2.70E-12	2.20E-10
GO:0007389	P	pattern specification process	6.10E-12	4.70E-10
GO:0004857	F	enzyme inhibitor activity	6.40E-12	4.80E-10
GO:0019825	F	oxygen binding	6.80E-12	4.80E-10
GO:0003006	P	reproductive developmental process	8.50E-12	6.30E-10
GO:0048437	P	floral organ development	8.60E-12	6.30E-10
GO:0000003	P	reproduction	9.90E-12	7.00E-10
GO:0048569	P	post-embryonic organ development	1.20E-11	8.40E-10
GO:0003002	P	regionalization	1.60E-11	1.10E-09
GO:0048608	P	reproductive structure development	1.20E-10	7.90E-09
GO:0005618	C	cell wall	1.50E-10	1.60E-08
GO:0030312	C	external encapsulating structure	2.10E-10	1.60E-08
GO:0046906	F	tetrapyrrole binding	3.30E-10	2.20E-08
GO:0022414	P	reproductive process	3.50E-10	2.30E-08
GO:0030154	P	cell differentiation	3.70E-10	2.40E-08
GO:0022857	F	transmembrane transporter activity	3.90E-10	2.50E-08
GO:0009725	P	response to hormone stimulus	5.30E-10	3.30E-08
GO:0010467	P	gene expression	5.30E-10	3.30E-08
GO:0050896	P	response to stimulus	7.40E-10	4.50E-08
GO:0006629	P	lipid metabolic process	8.10E-10	4.80E-08

GO:0016070	P	RNA metabolic process	9.30E-10	5.40E-08
GO:0050660	F	FAD binding	1.30E-09	7.90E-08
GO:0003824	F	catalytic activity	1.90E-09	1.10E-07
GO:0009887	P	organ morphogenesis	2.00E-09	1.10E-07
GO:0004650	F	polygalacturonase activity	3.60E-09	2.00E-07
GO:0009505	C	plant-type cell wall	8.10E-09	4.80E-07
GO:0022804	F	active transmembrane transporter activity	1.40E-08	7.20E-07
GO:0009888	P	tissue development	1.80E-08	9.80E-07
GO:0048467	P	gynoecium development	1.80E-08	9.80E-07
GO:0015291	F	secondary active transmembrane transporter activity	3.00E-08	1.50E-06
GO:0016788	F	hydrolase activity, acting on ester bonds	3.50E-08	1.70E-06
GO:0046914	F	transition metal ion binding	4.30E-08	2.00E-06
GO:0016143	P	S-glycoside metabolic process	4.40E-08	2.30E-06
GO:0019757	P	glycosinolate metabolic process	4.40E-08	2.30E-06
GO:0019760	P	glucosinolate metabolic process	4.40E-08	2.30E-06
GO:0043167	F	ion binding	4.90E-08	2.10E-06
GO:0043169	F	cation binding	4.90E-08	2.10E-06
GO:0015075	F	ion transmembrane transporter activity	5.90E-08	2.50E-06
GO:0048440	P	carpel development	7.00E-08	3.60E-06
GO:0010817	P	regulation of hormone levels	9.50E-08	4.90E-06
GO:0005215	F	transporter activity	1.10E-07	4.30E-06
GO:0005576	C	extracellular region	1.60E-07	7.50E-06
GO:0048646	P	anatomical structure formation involved in morphogenesis	1.80E-07	8.90E-06
GO:0048827	P	phyllome development	2.00E-07	9.60E-06
GO:0065008	P	regulation of biological quality	2.00E-07	9.60E-06
GO:0045735	F	nutrient reservoir activity	2.30E-07	9.00E-06
GO:0048609	P	reproductive process in a multicellular organism	2.60E-07	1.20E-05
GO:0016787	F	hydrolase activity	2.90E-07	1.10E-05
GO:0016705	F	oxidoreductase activity, acting on paired donors, with incorporation or reduction of molecular oxygen	3.70E-07	1.40E-05
GO:0044238	P	primary metabolic process	4.40E-07	2.10E-05
GO:0016137	P	glycoside metabolic process	4.40E-07	2.10E-05
GO:0032504	P	multicellular organism reproduction	5.70E-07	2.60E-05
GO:0048367	P	shoot development	7.40E-07	3.30E-05
GO:0046872	F	metal ion binding	8.90E-07	3.20E-05
GO:0022621	P	shoot system development	9.20E-07	4.10E-05
GO:0008324	F	cation transmembrane transporter activity	1.10E-06	4.00E-05
GO:0022891	F	substrate-specific transmembrane transporter activity	1.50E-06	5.10E-05
GO:0016829	F	lyase activity	1.50E-06	5.10E-05
GO:0008152	P	metabolic process	1.60E-06	7.00E-05
GO:0042398	P	cellular amino acid derivative biosynthetic process	1.70E-06	7.40E-05
GO:0042446	P	hormone biosynthetic process	2.70E-06	0.00012

GO:0042445	P	hormone metabolic process	2.80E-06	0.00012
GO:0045595	P	regulation of cell differentiation	2.90E-06	0.00012
GO:0051179	P	localization	3.20E-06	0.00013
GO:0005451	F	monovalent cation:hydrogen antiporter activity	3.60E-06	0.00012
GO:0015299	F	solute:hydrogen antiporter activity	4.40E-06	0.00014
GO:0009733	P	response to auxin stimulus	4.70E-06	0.00019
GO:0048825	P	cotyledon development	4.80E-06	0.00019
GO:0048645	P	organ formation	5.20E-06	0.00021
GO:0009699	P	phenylpropanoid biosynthetic process	5.70E-06	0.00022
GO:0015385	F	sodium:hydrogen antiporter activity	5.90E-06	0.00018
GO:0032787	P	monocarboxylic acid metabolic process	6.10E-06	0.00024
GO:0045165	P	cell fate commitment	6.40E-06	0.00025
GO:0010089	P	xylem development	7.40E-06	0.00028
GO:0030234	F	enzyme regulator activity	7.40E-06	0.00022
GO:0006575	P	cellular amino acid derivative metabolic process	8.50E-06	0.00032
GO:0006811	P	ion transport	9.80E-06	0.00036
GO:0065001	P	specification of axis polarity	9.80E-06	0.00036
GO:0045596	P	negative regulation of cell differentiation	1.00E-05	0.00037
GO:0009698	P	phenylpropanoid metabolic process	1.10E-05	0.00038
GO:0008471	F	laccase activity	1.10E-05	0.00031
GO:0016144	P	S-glycoside biosynthetic process	1.20E-05	0.0004
GO:0019758	P	glycosinolate biosynthetic process	1.20E-05	0.0004
GO:0019761	P	glucosinolate biosynthetic process	1.20E-05	0.0004
GO:0046910	F	pectinesterase inhibitor activity	1.50E-05	0.00043
GO:0001708	P	cell fate specification	1.70E-05	0.00057
GO:0015297	F	antiporter activity	1.70E-05	0.00046
GO:0009943	P	adaxial/abaxial axis specification	1.80E-05	0.0006
GO:0019915	P	lipid storage	1.80E-05	0.0006
GO:0005634	C	nucleus	1.90E-05	0.00075
GO:0015491	F	cation:cation antiporter activity	2.10E-05	0.00057
GO:0016847	F	1-aminocyclopropane-1-carboxylate synthase activity	2.10E-05	0.00057
GO:0048466	P	androecium development	2.20E-05	0.00071
GO:0048443	P	stamen development	2.20E-05	0.00071
GO:0015298	F	solute:cation antiporter activity	2.40E-05	0.00065
GO:0048037	F	cofactor binding	2.60E-05	0.00068
GO:0009944	P	polarity specification of adaxial/abaxial axis	3.90E-05	0.0013
GO:0010087	P	phloem or xylem histogenesis	3.90E-05	0.0013
GO:0016138	P	glycoside biosynthetic process	4.30E-05	0.0014
GO:0015103	F	inorganic anion transmembrane transporter activity	4.30E-05	0.0011
GO:0009955	P	adaxial/abaxial pattern formation	5.20E-05	0.0016
GO:0006869	P	lipid transport	5.20E-05	0.0016
GO:0050793	P	regulation of developmental process	5.30E-05	0.0016

GO:0016747	F	transferase activity, transferring acyl groups other than amino-acyl groups	6.10E-05	0.0015
GO:0022892	F	substrate-specific transporter activity	6.60E-05	0.0016
GO:0008610	P	lipid biosynthetic process	6.80E-05	0.0021
GO:0050664	F	oxidoreductase activity, acting on NADH or NADPH, with oxygen as acceptor	8.40E-05	0.002
GO:0010073	P	meristem maintenance	9.50E-05	0.0029
GO:0006725	P	cellular aromatic compound metabolic process	9.50E-05	0.0029
GO:0016114	P	terpenoid biosynthetic process	9.80E-05	0.0029
***Br*-specific H3K27me3-marked genes**				
GO:0003824	F	catalytic activity	7.70E-30	1.40E-26
GO:0050896	P	response to stimulus	7.00E-22	3.20E-18
GO:0044464	C	cell part	2.50E-20	8.80E-18
GO:0005623	C	cell	2.50E-20	8.80E-18
GO:0016020	C	membrane	6.10E-18	1.50E-15
GO:0005886	C	plasma membrane	2.30E-15	4.10E-13
GO:0016740	F	transferase activity	3.80E-15	3.40E-12
GO:0042221	P	response to chemical stimulus	1.90E-14	4.20E-11
GO:0009791	P	post-embryonic development	2.80E-13	4.20E-10
GO:0006950	P	response to stress	2.40E-11	2.60E-08
GO:0005215	F	transporter activity	4.50E-11	2.70E-08
GO:0065007	P	biological regulation	1.70E-10	1.50E-07
GO:0051234	P	establishment of localization	2.80E-10	2.10E-07
GO:0006810	P	transport	3.40E-10	2.20E-07
GO:0016301	F	kinase activity	4.30E-10	1.90E-07
GO:0016772	F	transferase activity, transferring phosphorus-containing groups	5.50E-10	2.00E-07
GO:0051179	P	localization	6.70E-10	3.70E-07
GO:0009628	P	response to abiotic stimulus	4.00E-09	2.00E-06
GO:0022804	F	active transmembrane transporter activity	4.00E-09	1.20E-06
GO:0016787	F	hydrolase activity	5.60E-09	1.40E-06
GO:0022857	F	transmembrane transporter activity	1.00E-08	2.30E-06
GO:0005488	F	binding	1.20E-08	2.40E-06
GO:0032501	P	multicellular organismal process	1.50E-08	6.90E-06
GO:0051704	P	multi-organism process	2.80E-08	1.10E-05
GO:0010033	P	response to organic substance	3.80E-08	1.40E-05
GO:0010876	P	lipid localization	5.00E-08	1.70E-05
GO:0009719	P	response to endogenous stimulus	6.70E-08	2.10E-05
GO:0032502	P	developmental process	9.70E-08	2.90E-05
GO:0007275	P	multicellular organismal development	1.40E-07	3.90E-05
GO:0022892	F	substrate-specific transporter activity	2.90E-07	5.10E-05
GO:0016705	F	oxidoreductase activity, acting on paired donors, with incorporation or reduction of molecular oxygen	4.30E-07	7.10E-05
GO:0043687	P	post-translational protein modification	4.50E-07	0.00012
GO:0009987	P	cellular process	7.10E-07	0.00018

GO:0006468	P	protein amino acid phosphorylation	9.10E-07	0.00022
GO:0010035	P	response to inorganic substance	1.10E-06	0.00026
GO:0065008	P	regulation of biological quality	1.40E-06	0.00029
GO:0009605	P	response to external stimulus	1.60E-06	0.00032
GO:0006629	P	lipid metabolic process	1.70E-06	0.00032
GO:0009725	P	response to hormone stimulus	2.00E-06	0.00036
GO:0005524	F	ATP binding	2.00E-06	0.00029
GO:0016773	F	phosphotransferase activity, alcohol group as acceptor	2.10E-06	0.00029
GO:0050789	P	regulation of biological process	2.40E-06	0.00042
GO:0022891	F	substrate-specific transmembrane transporter activity	2.50E-06	0.00032
GO:0032559	F	adenyl ribonucleotide binding	2.60E-06	0.00032
GO:0048589	P	developmental growth	3.50E-06	0.0006
GO:0016310	P	phosphorylation	4.10E-06	0.00068
GO:0019748	P	secondary metabolic process	4.30E-06	0.00069
GO:0009266	P	response to temperature stimulus	5.90E-06	0.00092
GO:0000904	P	cell morphogenesis involved in differentiation	6.90E-06	0.001
GO:0050794	P	regulation of cellular process	7.00E-06	0.001
GO:0032555	F	purine ribonucleotide binding	7.00E-06	0.00065
GO:0032553	F	ribonucleotide binding	7.00E-06	0.00065
GO:0006464	P	protein modification process	7.20E-06	0.001
GO:0001883	F	purine nucleoside binding	7.50E-06	0.00065
GO:0001882	F	nucleoside binding	7.50E-06	0.00065
GO:0030554	F	adenyl nucleotide binding	7.50E-06	0.00065
GO:0004672	F	protein kinase activity	7.60E-06	0.00065
GO:0006796	P	phosphate metabolic process	8.30E-06	0.0011
GO:0006793	P	phosphorus metabolic process	8.60E-06	0.0011
GO:0006952	P	defense response	1.30E-05	0.0016
GO:0044262	P	cellular carbohydrate metabolic process	1.50E-05	0.0018
GO:0016706	F	oxidoreductase activity, acting on paired donors, with incorporation or reduction of molecular oxygen, 2-oxoglutarate as one donor, and incorporation of one atom each of oxygen into both donors	1.70E-05	0.0014
GO:0009826	P	unidimensional cell growth	1.80E-05	0.0021
GO:0060560	P	developmental growth involved in morphogenesis	1.80E-05	0.0021
GO:0017076	F	purine nucleotide binding	1.80E-05	0.0014
GO:0009607	P	response to biotic stimulus	1.90E-05	0.0021
GO:0051707	P	response to other organism	1.90E-05	0.0021
GO:0040007	P	growth	1.90E-05	0.0021
GO:0044238	P	primary metabolic process	2.30E-05	0.0025
GO:0000166	F	nucleotide binding	2.60E-05	0.0019
GO:0008152	P	metabolic process	2.80E-05	0.0029
GO:0019438	P	aromatic compound biosynthetic process	4.20E-05	0.0043

GO:0019825	F	oxygen binding	4.50E-05	0.0032
GO:0031224	C	intrinsic to membrane	4.90E-05	0.007
GO:0009611	P	response to wounding	5.00E-05	0.0048
GO:0016049	P	cell growth	5.00E-05	0.0048
GO:0009699	P	phenylpropanoid biosynthetic process	5.20E-05	0.0048
GO:0015833	P	peptide transport	5.20E-05	0.0048
GO:0006857	P	oligopeptide transport	5.20E-05	0.0048
GO:0009409	P	response to cold	5.40E-05	0.0049
GO:0030001	P	metal ion transport	5.90E-05	0.0052
GO:0005515	F	protein binding	5.90E-05	0.0041
GO:0042398	P	cellular amino acid derivative biosynthetic process	6.10E-05	0.0053
GO:0016491	F	oxidoreductase activity	7.80E-05	0.005
GO:0015171	F	amino acid transmembrane transporter activity	7.90E-05	0.005
GO:0046943	F	carboxylic acid transmembrane transporter activity	8.40E-05	0.005
GO:0005342	F	organic acid transmembrane transporter activity	8.40E-05	0.005
GO:0046686	P	response to cadmium ion	8.50E-05	0.0072
GO:0010038	P	response to metal ion	9.10E-05	0.0076
GO:0016757	F	transferase activity, transferring glycosyl groups	9.60E-05	0.0055
GO:0008361	P	regulation of cell size	9.80E-05	0.008

C, Cellular component; F, Molecular function; P, Biological process

Table III-13. Difference of H3K27me3 levels between tissues

	gernminating seeds > 12-day seedlings	gernminating seeds < 12-day seedlings	Total
C24	52	641	693
Overlap with *B. rapa*			
2d-C > 14d-L in both lines	4		
2d-C < 14d-L in both lines		64	

Table III-14. GO function term overrepresented in genes showing higher H3K27me3 levels in seedlings of *A. thaliana* and 14-day leaves in *B. rapa*

GO accession	Term type	Term	*p* value	FDR
GO:0010431	P	seed maturation	1.30E-11	9.60E-09
GO:0010162	P	seed dormancy	1.20E-10	2.90E-08
GO:0022611	P	dormancy process	1.20E-10	2.90E-08
GO:0048316	P	seed development	3.90E-10	7.10E-08
GO:0010154	P	fruit development	6.00E-10	8.90E-08
GO:0019915	P	lipid storage	4.30E-09	5.30E-07
GO:0016114	P	terpenoid biosynthetic process	1.00E-08	1.10E-06
GO:0048609	P	reproductive process in a multicellular organism	1.30E-08	1.20E-06
GO:0006721	P	terpenoid metabolic process	2.00E-08	1.60E-06
GO:0032504	P	multicellular organism reproduction	2.50E-08	1.80E-06
GO:0050826	P	response to freezing	1.10E-07	7.00E-06
GO:0048608	P	reproductive structure development	1.50E-07	8.80E-06
GO:0009791	P	post-embryonic development	1.60E-07	8.80E-06
GO:0009790	P	embryonic development	1.70E-07	8.80E-06
GO:0009686	P	gibberellin biosynthetic process	2.10E-07	1.00E-05
GO:0016102	P	diterpenoid biosynthetic process	2.20E-07	1.00E-05
GO:0009756	P	carbohydrate mediated signaling	2.80E-07	1.10E-05
GO:0010182	P	sugar mediated signaling pathway	2.80E-07	1.10E-05
GO:0003006	P	reproductive developmental process	3.20E-07	1.20E-05
GO:0010876	P	lipid localization	3.30E-07	1.20E-05
GO:0009685	P	gibberellin metabolic process	3.60E-07	1.30E-05
GO:0016101	P	diterpenoid metabolic process	3.90E-07	1.30E-05
GO:0071322	P	cellular response to carbohydrate stimulus	4.60E-07	1.50E-05
GO:0009793	P	embryonic development ending in seed dormancy	5.00E-07	1.50E-05
GO:0022414	P	reproductive process	1.10E-06	3.10E-05
GO:0008299	P	isoprenoid biosynthetic process	1.20E-06	3.40E-05
GO:0000003	P	reproduction	1.40E-06	3.90E-05
GO:0006720	P	isoprenoid metabolic process	1.80E-06	4.60E-05

P, Biological process

Table III-15. Transcription levels of genes involved in 'Post-embryonic development' with higher H3K27me3 levels in 14-day leaves than in 2-day cotyledons in *B. rapa*

	2-day cotyledons (FPKM)		14-day leaves (FPKM)			
test_id	RJKB-T23	RJKB-T24	RJKB-T23	RJKB-T24		Discription
Bra015275	0.29	0.15	0.00	0.00	AT1G03880	CRUCIFERIN 2
Bra032359	0.60	0.60	0.31	0.46	AT1G30100	NINE-CIS-EPOXYCAROTENOID DIOXYGENASE 5
Bra008006	2.02	5.02	0.00	0.11	AT1G72100	LEA domain-containing protein
Bra004981	8.63	10.73	0.00	0.00	AT2G40170	EARLY METHIONINE-LABELLED 6 / LATE EMBRYOGENESIS ABUNDANT 6
Bra016868	0.63	0.85	0.00	0.00	AT2G42560	LEA domain-containing protein
Bra001843	283.63	228.71	0.01	0.00	AT3G21720	ISOCITRATE LYASE
Bra031301	1,683.69	1,545.71	0.06	0.00	AT3G21720	ISOCITRATE LYASE
Bra023813	0.67	0.45	0.00	0.00	AT3G22640	cupin family protein
Bra022494	0.00	0.00	0.00	0.00	AT3G22650	CEGENDUO / S-LOCUS F-BOX 61
Bra025229	0.58	0.19	0.03	0.00	AT3G26790	FUSCA3
Bra033021	2.05	0.43	0.09	0.00	AT3G27660	OLEOSIN 4
Bra007239	0.39	0.34	0.00	0.00	AT3G56350	Iron/manganese superoxide dismutase family protein
Bra036282	0.40	0.10	0.97	0.73	AT4G02280	SUCROSE SYNTHASE 3
Bra013489	0.87	0.46	0.04	0.00	AT4G21020	LEA family protein
Bra013866	0.56	0.31	0.00	0.00	AT4G25140	OLEOSIN 1
Bra009026	2.37	2.82	0.62	0.34	AT5G10510	AINTEGUMENTA-LIKE 6 / PLETHORA 3
Bra028584	4.12	7.11	3.84	3.02	AT5G10510	AINTEGUMENTA-LIKE 6 / PLETHORA 3
Bra027542	4.13	7.71	0.06	0.00	AT5G44310	LEA family protein
Bra013338	0.02	0.02	0.02	0.88	AT5G45830	DELAY OF GERMINATION 1
Bra020444	75.43	150.81	1.92	0.63	AT5G57390	AINTEGUMENTA-LIKE 5
Bra031884	1.10	2.54	0.03	0.07	AT5G65070	MADS AFFECTING FLOWERING 4

FPKM, Fragments Per Kilobase of transcript per Million mapped reads
Black box reveals the significantly differential expression level between tissues

Table III-16. Comparison of the H3K27me3 levels between vernalized and non-vernalized samples in *A. thaliana* and *B. rapa*

	NV > V		NV < V	
1. C24 (*A. thaliana*)	379		1	*FLC*
2. 2d-C vs. BrV1	6,712		102	
3. 14d-L vs. BrV2	29		160	
Overlap 1 & 2	18	Bra007436, Bra009639, Bra009992, Bra010662 Bra014228, Bra016924, Bra017905, Bra019857 Bra020171, Bra023292, Bra025591, Bra027656 Bra027868, Bra029749, Bra029769, Bra032088 Bra037484, Bra038650	1	Bra006051 (*BrFLC3*)
Overlap 1 & 3	2	Bra032761, Bra037899	4	Bra006051 (*BrFLC3*), Bra009055 (*BrFLC1*), Bra022771 (*BrFLC5*), Bra028599 (*BrFLC2*)
Overlap 2 & 3	3	Bra022408, Bra029401, Bra027328	2	Bra009056, Bra006051 (*BrFLC3*)

Table III-17. Comparison of the H3K27me3 levels between two different vernalized samples in *B. rapa*

	BrV1 > BrV2	BrV1 < BrV2
BrV1 vs. BrV2	336	2,467
Overlap (2d-C > 14d-L in RJKB-T24)	216	76
Overlap (2d-C < 14d-L in RJKB-T24)	0	1,028

Chapter IV

Gene expression analysis in response to vernalization in Chinese cabbage (*Brassica rapa* L.)

Abstract

Chinese cabbage (*Brassica rapa* L. var. *pekinensis*) is an economically and agriculturally significant leafy vegetable and is extensively cultivated throughout the world. Vernalization is exposure to prolonged cold that alters gene expression and accelerates a transition from the vegetative to reproductive phase. Premature bolting caused by exposure to cold inhibits the head production and reduces the yield in Chinese cabbage, thus developing late bolting line is important for breeding. Therefore, it is critical to identify the genes showing differential expression patterns during cold treatment in Chinese cabbage. However, there are few studies on the transcriptome profiling of different duration of cold treatments in Chinese cabbage. Here, we analyzed the gene expression profiles in a Chinese cabbage inbred line RJKB-T24 given different durations of cold treatments using RNA sequencing. Differentially expressed genes (DEGs) between non-vernalized and vernalized samples tended to be downregulated, and some genes involved in the flowering pathway (including *BrFLC* and *BrMAF* genes) were downregulated following cold treatment. Functional enrichment analysis indicated that some DEGs were involved in the stress response and hormone signaling pathways. For genes involved in the FRI containing complex, a known activator of *FLC* in *Arabidopsis thaliana*, only *BrFRL1* showed changes in expression. In contrast to *A. thaliana*, *BrVIP* and *BrVRN* genes showed different expression patterns between paralogs during cold treatment, suggesting that Chinese cabbage's flowering pathway is somehow different and more complex than in *A. thaliana*. These outcomes provide significant insights into the genetic control of bolting and flowering that occurred during the vernalization of Chinese cabbage.

Key Words: differentially expressed genes, flowering pathway, RNA-sequencing, transcriptome

Introduction

Chinese cabbage (*Brassica rapa* L. var. *pekinensis*) is an important vegetable contributing to our health as a source of beneficial dietary fibers and vitamins. *B. rapa* is the first species in the genus *Brassica* to be sequenced, and a double haploid (DH) line of Chinese cabbage, chiifu-401-42, was examined for sequencing (Wang et al. 2011). Whole genome sequencing of this line shows that *B. rapa* experienced a whole genome triplication (WGT) after speciation between the genera *Brassica* and *Arabidopsis* (Cheng et al. 2012; Wang et al. 2011). Vernalization refers to prolonged exposure to cold temperature, and is usually required to facilitate flowering in Brassicaceae. Because Chinese cabbage can sense low temperatures during seed germination (seed-vernalization-responsive type), it sometimes undergoes early flowering/bolting due to low temperatures that occur during production in the fall (Shea et al. 2018; Su et al. 2018). Premature bolting leads to a decline in the commercial quality and a loss of the market value. For the breeding of Chinese cabbage cultivars, a high bolting resistance is preferred (Shea et al. 2018).

It has been extensively studied how vernalization promotes flowering in *Arabidopsis thaliana*. Two genes, *FRIGIDA* (*FRI*) and *FLOWERING LOCUS C* (*FLC*), play vital roles in the flowering process in *A. thaliana*. *FRI* encodes a novel protein with two coiled-coil domains and is an activator of *FLC* (Johanson et al. 2000). *FLC* encodes a MADS-box transcription factor and acts as a suppressor of flowering (Michaels and Amasino, 1999; Sheldon et al. 1999). During cold treatment, *FLC* expression is decreased and maintained even after being returned to warm conditions. *VERNALIZATION INSENSITIVE 3* (*VIN3*), *VERNALIZATION1* (*VRN1*), *VRN2*, and *VRN5* are identified as regulatory genes of *FLC* expression associated with vernalization (He and Amasino, 2005; Greb et al. 2007; Wood et al. 2006). At the beginning of cold treatment, *VIN3* is activated (Sung and Amasino, 2004), while expression of *VRN1* and *VRN2* does not change during cold treatment (Gendall et al. 2001; Levy et al. 2002). Five MADS-box genes, *MADS AFFECTING FLOWERING1* (*MAF1*) to *MAF5*, belong to the MADS-box protein family containing *FLC* (Alvarez-Buylla et al. 2000; Ratcliffe et al. 2001; 2003) and act as floral repressors (Kim and Sung, 2010; Ratcliffe et al. 2001; Scortecci et al. 2001; 2003; Sheldon et al. 2009). *MAF* genes show temperature-dependent changes in expression; *MAF1-MAF4* are downregulated by vernalization, whereas *MAF5* is upregulated (Ratcliffe et al. 2001; 2003). MAFs also directly interact with each other and produce complexes, which regulate the genes related to floral transition such as *FLOWERING LOCUS T* (*FT*) (Gu et al. 2013).

Transcriptional repression of *FLC* during prolonged cold exposure is associated with changes in histone modifications from active marks (trimethylation of lysine 4 in histone H3 (H3K4me3) or H3K36me3) to a repressive mark (H3K27me3), initiating a conformational change from euchromatin to heterochromatin (Dennis and Peacock, 2007; Groszmann et al. 2011). This is mediated by Polycomb repressive complex 2 (PRC2) components including the Su(z)12 homologue, VRN2, and two plant homeodomain (PHD) finger proteins, VRN5 and VIN3 (Birve et al. 2001; Bastow et al. 2004; De Lucia et al. 2008; Gendall et al. 2001; Sung and Amasino, 2004; Wood et al. 2006). Upon being returned to warm conditions after prolonged cold exposure, the PHD–PRC2 spreads across the *FLC* locus with spreading H3K27me3 marks, and *the* expression of *FLC* is epigenetically silenced (Angel et al. 2011; Finnegan and Dennis, 2007). *VRN1* encodes a DNA-binding protein containing two plant-specific B3 domains, and is required for the increase of H3K27me3 at the *FLC* locus during prolonged cold treatment (Levy et al. 2002; Sheldon et al. 2006).

In Chinese cabbage, the reduced transcription of *FLC* could be an important factor for premature bolting (Itabashi et al. 2018; Shea et al. 2018; Su et al. 2018; Takada et al. 2019). There are four *FLC* paralogs in *B. rapa* and at least three of them act as floral repressors (Kawanabe et al. 2016; Kim et al. 2007; Schranz et al. 2002; Takada et al. 2019). All *FLC* paralogs were downregulated by prolonged cold treatment, and an increased level of H3K27me3 was observed around the first exon in all *FLC* paralogs in Chinese cabbage (Kawanabe et al. 2016; Akter et al. 2019). Following return to normal temperature growth conditions, H3K27me3 spreads along all four *BrFLC* paralogs providing stable repression of the gene (Akter et al. 2019; Takada et al. 2019). Many QTL analyses using populations derived from the crossing of parents with two different flowering times showed co-localization of QTLs and *FLC* genes, suggesting that the different function of *FLC* alleles between lines results in the variation of flowering time (Kakizaki et al. 2011; Kitamoto et al. 2014; Kole et al. 2001; Li et al. 2009; Lou et al. 2007; Osborn et al. 1997; Schranz et al. 2002; Xiao et al. 2013; Zhao et al. 2010).

Innovation of sequencing technology enables us to examine the transcriptome by RNA-sequencing (RNA-seq), providing high accuracy, a wider detection range of transcription, and high reproducibility (Ansorge, 2009; Mortazavi et al. 2008; Saeki et al. 2016). Using this technology, transcriptional changes in response to many kinds of abiotic or biotic stress have been examined in the genus *Brassica* (Long et al. 2015; Miyaji et al. 2017; Wang et al. 2016; Xing et al. 2016; Yong et al. 2014; Zou et al. 2013). This method has also been applied to the

detection of transcriptional changes in Brassicaceae following vernalization in either pak-choi (*B. rapa* var. *chinensis*) or radish (*Raphanus sativus*) (Liu et al. 2017; Sun et al. 2015).

There is no report examining the transcriptome associated with different durations of vernalization treatments in Chinese cabbage. In this study, we analyzed the transcriptome during vernalization by RNA-seq to discover genes responding to the cold treatment and to identify the metabolic pathways involved in cold response in Chinese cabbage. Our study provides an important opportunity to facilitate the research on vernalization mechanisms in *B. rapa*.

Materials and Methods

Plant materials and growth conditions

A Chinese cabbage inbred line, RJKB-T24, was used as a plant material (Kawamura et al. 2016). Seeds were surface sterilized and grown on agar solidified Murashige and Skoog (MS) medium with 1 % (w/v) sucrose under long day (LD) conditions (16 h light) at 22 °C. For cold treatment, 14-day seedlings on MS plates were treated for two (2V), four (4V), or six (6V) weeks at 4 °C under the LD conditions (16 h light) or six weeks at 4 °C and then seven days in normal growth conditions (6V7N). RJKB-T24 did not flower without four weeks of cold treatment even if more than 100 days passed after sowing. When four weeks of cold treatment was applied to 14-day seedlings, flowering occurred 66 days after cold treatment. These results indicate that RJKB-T24 requires vernalization for flowering.

RNA extraction and RT-PCR/qPCR

First and second leaves with (2V, 4V, 6V, 6V7N) or without (NV) cold treatments were used for isolation of total RNAs using the SV Total RNA Isolation System (Promega). The leaves from three individual plants in each condition were harvested as biological replicates. The cDNA was synthesized from 500 ng total RNAs using ReverTra Ace qPCR RT Master Mix with gDNA Remover (TOYOBO Co., Ltd., Osaka JAPAN). The cDNA was PCR amplified using Quick Taq® HS DyeMix (TOYOBO) for RT-PCR. Prior to quantitative real-time RT-PCR (RT-qPCR), the specificity of the primer set for each gene was first tested by electrophoresis of PCR amplified products using QuickTaq®HS DyeMix (TOYOBO) on 2.0 % agarose gel in which single products were observed. Absence of genomic DNA contamination was confirmed by PCR of a no RT control using *BrACTIN* (*BrACT*) gene (Fujimoto et al. 2006). PCR was performed using the following conditions; 1 cycle of 94 °C for 2 min followed by 30

cycles of 94 ℃ for 30 s, 55 ℃ for 30 s, and 68 ℃ for 30 s. Primer sequences used for RT-PCR are shown in Table IV-2.

RT-qPCR was performed by using LightCycler 96 (Roche) and cDNA was amplified using FastStart Essential DNA Green Master (Roche). PCR conditions were 95 ℃ for 10 min followed by 55 cycles of 95 ℃ for 10 s, 60 ℃ for 10 s, and 72 ℃ for 15 s, and melting program (60 ℃ to 95 ℃ at 0.1 ℃/s). After amplification cycles, each reaction was subjected to melt temperature analysis to confirm single amplified products. The expression level of each gene relative to *BrACT* was automatically calculated using automatic CQ calling according to the manufacturer's instructions (Roche). Data presented are the means and standard error (s.e.) calculated from three biological and experimental replications. Primer sequences used for RT-qPCR are shown in Table IV-2. Dunnett's test was performed for statistical test.

RNA-sequencing

RNA-sequencing (RNA-seq) was performed using first and second leaves with (2V, 4V, 6V, 6V7N) or without (NV) cold treatments. Sequence library was prepared as described previously (Nagano et al. 2015). RNA-seq was performed with three replicates of each condition using Illumina Hiseq2000 (single-end sequencing, 50 bp). Sequence data have been submitted to the DDBJ database (http://www.ddbj.nig.ac.jp) under accession numbers DRA009156.

The quality of the RNA-seq libraries was evaluated using the FastQC software (http://www.bioinformatics.babraham.ac.uk/projects/fastqc/). After QC, filtered reads were used for further analysis. Tophat2 (Kim et al. 2013) with the default parameters was used to align RNA-seq reads against the *B. rapa* reference genome downloaded from the Ensemble Genome database (ftp://ftp.ensemblgenomes.org/pub/plants/release-32/fasta/brassica_rapa/dna/Brassica_rapa.IVFCAASv1.dna.toplevel.fa). The levels of gene expression were scored by fragments per kilo-base per million (FPKM) using cufflinks, and cuffdiff was used for identification of differentially expressed genes (DEGs) with and without cold treatments (Trapnell et al., 2012). Analysis for enrichment of gene functional ontology terms was completed using the gene ontology (GO) tool, agriGO (Du et al. 2010) according to the methods, which we previously described (Shimizu et al. 2014). Statistical tests for enrichment of functional terms used the hypergeometric test and false discovery rate (FDR) correction for multiple testing to a level of 5% FDR.

We validated the RNA-seq data by RT-qPCR using 25 genes, and 23 of 25 genes showed similar expression patterns to RNA-seq data (FPKM) (Fig. IV-3, Table IV-3).

Results

Identification of differentially expressed genes between vernalized and non-vernalized samples

We performed the RNA-seq in leaves with and without cold treatments in an inbred line of Chinese cabbage, RJKB-T24, which needs vernalization for flowering. The samples with three different durations of cold treatments, two (2V), four (4V), or six (6V) weeks, and upon return to warm conditions for seven days after six weeks of cold treatment (6V7N) were used. Total reads and mapped reads on the reference genome are shown in Table IV-4. The differentially expressed genes (DEGs) between non-vernalized (NV) and vernalized samples (2V, 4V, 6V, 6V7N) were identified by Tophat/cuffdiff at 95% confidence. Total number of 3,787 (2V vs. NV), 3,543 (4V vs. NV), 2,630 (6V vs. NV), or 3,896 (6V7N vs. NV) DEGs were identified, including 1,169, 1,291, 980, or 946 upregulated and 2,618, 2,252, 1,650, or 2,950 downregulated genes in 2V, 4V, 6V, or 6V7N, respectively (Table IV-1).

Comparing DEGs between the different cold treatment conditions, 345 up and 1,222 downregulated genes overlapped between 2V/NV and 4V/NV, and the number of overlapped upregulated genes decreased between 2V/NV and 6V/NV or between 2V/NV and 6V7N/NV (Fig. IV-1). The number of overlapped downregulated genes decreased between 2V/NV and 6V/NV, whereas it increased between 2V/NV and 6V7N/NV (Fig. IV-1). The numbers of overlapped up and downregulated genes between 4V/NV and 6V/NV were 322 and 934, respectively, and 277 upregulated and 1,207 downregulated genes overlapped between 4V/NV and 6V7N/NV (Fig. IV-1). Between 6V/NV and 6V7N/NV, 211 upregulated and 936 downregulated genes overlapped (Fig. IV-1). There were 128 upregulated and 48 downregulated genes in three conditions (2V/NV, 4V/NV, and 6V/NV), and 646 upregulated and 430 downregulated genes were found in four conditions (2V/NV, 4V/NV, 6V/NV and 6V7N/NV) (Table IV-1).

Transcriptional change in flowering pathway genes following cold treatment

Genes involved in flowering pathways in *B. rapa* have been identified (Wang et al. 2017), and 89 genes mainly involved in vernalization and autonomous pathways were selected in this study (Table IV-5). In our RNA-seq data, the 29 out of 89 genes showed differential

expression in vernalized samples compared with non-vernalized samples for at least one cold treatment condition (Fig. III-9, Table IV-5). More genes showed downregulation rather than upregulation (Fig. IV -2, Table IV-5).

Expression levels of *BrVIN3* (Bra020445) and *SUPPRESSOR OF OVEREXPRESSION OF CO 1* (*BrSOC1*; Bra004928 and Bra039324) had risen by increased durations of cold treatments (Fig. IV-2). By RT-qPCR, the expression of *BrVIN3*s was decreased on return to normal temperature, while the increased expression of *BrSOC1*s had been maintained (Fig. IV-4A). Three *BrFLC* paralogs (*BrFLC1*/Bra009055, *BrFLC2*/Bra028599, *BrFLC3*/Bra006051) and three of five *BrMAF* genes (Bra024350, Bra024351, Bra031888) were downregulated by cold treatment (Fig. III-9), and repression of the expression levels had been maintained after return to normal temperature (Fig. III-9). Downregulation of total amount of four *BrFLC* genes and each three *BrMAF* genes was also confirmed by RT-qPCR (Fig. IV-4B).

From the RNA-seq data, we identified that *BrUBC1* (Bra026833), *BrSEF* (Bra006766), *BrFRL1* (Bra008624), and one of *BrVRN1* (Bra022376) were upregulated by cold treatment (Fig. IV-2, Fig. IV-3). *BrLD* (Bra018540), *BrUBC2* (Bra026582), one of *VERNALIZATION INDEPENDENCE 4* (*BrVIP4*) paralogs (Bra029332), *BrVIP5* (Bra031459), *BrVIP6/BrELF8* (Bra013162), and two of three *BrVRN1* paralogs (Bra037544, Bra001729) showed downregulation by cold treatment (Fig. IV-2). In addition, we found the opposite expression pattern between *BrVIP4* paralogs (Fig. IV-4C) or between *BrVRN1* paralogs (Fig. IV-4D).

Functional annotation of differentially expressed genes after vernalization

To identify the functions of DEGs, GO enrichment analysis was conducted. The up and downregulated genes at different durations of vernalization (2V, 4V, 6V, and 6V7N) were categorized into GO cellular component (CC), GO molecular function (MF), and GO biological process (BP). In upregulated genes in 2V, 4V, 6V, and 6V7N, 25, 64, 93, and 22 categories were overrepresented ($p < 0.0001$, FDR < 0.05), respectively (Tables IV-6-9). Twelve categories were overrepresented in upregulated genes in 2V, 4V, and 6V, and six categories were overrepresented in upregulated genes in all four conditions (Fig. IV-6). In downregulated genes in 2V, 4V, 6V, and 6V7N, 344, 372, 241, and 377 categories were overrepresented ($p < 0.0001$, FDR < 0.05), respectively (Tables IV-6-9). Ten categories were overrepresented in downregulated genes in 2V, 4V, and 6V, and 73 categories were overrepresented in downregulated genes in all four conditions (Fig. IV-6).

The categories related to stress response such as ‘Response to cold’ or response to plant hormone stimulation such as ‘Response to jasmonic acid stimulus’, ‘Response to ethylene stimulus’, or ‘Response to salicylic acid stimulus’ tended to be overrepresented in both up and downregulated genes by cold treatment (Fig. IV-5, Fig. IV-6). The category of ‘Response to heat’ tended to be overrepresented in upregulated genes, while the categories of ‘Small molecule metabolic process’ and ‘Defense response’ tended to be overrepresented in downregulated genes (Fig. IV-5, Fig. IV-6). The category of ‘Regulation of transcription’ was overrepresented in upregulated genes, especially at 4V (Fig. IV-5).

We performed RT-qPCR for examination of the expression of six genes related to stress response. Expression level of *HEAT SHOCK TRANSCRIPTION FACTOR B2A* (*BrHSFB2A*) increased with cumulative time of cold treatment, and its expression decreased when it returned to the normal temperature (Fig. IV-7). Expression level of *HEAT SHOCK PROTEIN 70* (*BrHSP70*) increased with cumulative time of cold treatment, and its expression was maintained when it returned to the normal temperature (Fig. IV-7). *COLD REGULATED 15B* (*BrCOR15B*) showed rapid induction of its expression at low temperature and its expression was undetectable when it returned to the normal temperature (Fig. IV-7). Expression levels of *INDOLE-3-ACETIC ACID INDUCIBLE 28* (*BrIAA28*), *IAA-LEUCINE RESISTANT (ILR)-LIKE GENE 6* (*BrILL6*), and *BrMYB28* were downregulated cumulatively by cold treatment, and repression of the expression was maintained after being returned to normal temperature (Fig. IV-7).

Discussion

Vernalization is one of the major pathways for flowering regulation, and there is a variation of flowering time or vernalization requirements among lines or cultivars of Chinese cabbage (Su et al., 2018). Previous research has revealed that *BrFLC* gene(s) is a key factor for vernalization in Chinese cabbage (Itabashi et al. 2018; Shea et al. 2018; Su et al. 2018; Takada et al. 2019). However, there is limited research showing how the regulators of *BrFLC* genes react in response to vernalization or transcriptional response at whole genome levels during prolonged cold treatment in Chinese cabbage.

In this study, we analyzed the transcriptome using first and second leaves before and after vernalization, and differentially expressed genes tended to be downregulated by cold treatment. During cold treatments, plant growth was slow, but leaf size gradually increased according to the low temperature period. In 6V7N, plant growth speed returned normal when

the temperature was returned to normal growth conditions, and the leaf size of 6V7N was larger than NV. Compared of expression levels in vernalized samples (2V, 4V, 6V, 6V7N) to non-vernalized sample (NV) suggested that to some extent, genes whose expression changed depending on the difference of growth stages were involved, especially in 6V7N. A cold responsive gene *BrCOR15B* was highly induced in response to cold treatment, but rapidly returned to previous expression levels upon a return to normal growth conditions. *BrSOC1* genes were upregulated during cold treatment. In RT-qPCR data, *BrSOC1* expression level in 6V7N was still higher than NV, while RNA-seq data showed similar expression levels between 6V7N and NV. The expression pattern of *BrSOC1* in previous reports in *B. rapa* were similar to the RT-qPCR results (Kawanabe et al. 2016; Akter et al. 2019), suggesting that the RT-qPCR results may be representing the correct expression pattern. *BrVIN3* gene was upregulated and *BrFLC* genes were downregulated during cold treatment, which was consistent with previous studies in *A. thaliana* and *B. rapa* (Deng et al. 2011; Jung et al. 2018; Kawanabe et al. 2016; Sheldon et al. 2000; 2006). These results indicate that we could capture genes whose expression was changed by cold treatment.

GO categories related to stress or stimulus tended to be overrepresented in both up and downregulated genes by cold treatment, but some GO categories showed difference between up and downregulated genes. The category of 'Response to heat' was overrepresented in upregulated genes, and we showed expression levels of *BrHSFB2A* and *BrHSP70* increased during cold treatment. It has already been shown that *Hsf*s and *HSP*s, which are first described as a factor that functions at high temperature conditions, are induced in low temperature (Swindell et al. 2007). These results suggest that upregulation of genes categorized into 'Response to heat' play a role in cold stress response. The category of 'Regulation of transcription' was overrepresented in upregulated genes after four weeks of cold treatment, suggesting that some transcription factors are activated when a sufficient period of cold is applied. In contrast, the categories 'Response to biotic stimulus' and 'Defense response' were overrepresented in downregulated genes. Some studies have reported the cross-talk between biotic stress response and the transition to flowering (Chin et al. 2013; Lyons et al. 2015). The genes categorized into response to plant hormone stimulation tended to change the expression levels by cold treatment. We found the downregulation of genes involved in auxin signaling, and previous studies showed that a decreased IAA hormone was detected after vernalization in *B. rapa* (Huang et al. 2018a). Although we could not distinguish between genes involved in the vernalization response promoting flowering and the physical cold response, some genes

identified in this study could be involved in vernalization response or the transition from vegetative to reproductive phase (e.g. *BrSOC1*).

In *A. thaliana*, regulators of *AtFLC* have been identified (Kim and Sung, 2014). FRI containing complex (FRI-C) including *AtFRI*, *AtFRL1*, *AtFES1*, *AtSUF4*, and *AtFLX* or PAF1 complex including *AtVIP4*, *AtVIP5*, *AtELF7*, and *AtELF8* are known as activators of *AtFLC* expression (Kim and Sung, 2014; Shea et al. 2018). In this study, *BrFRL1* expression levels were increased with cumulative time of cold treatment, while other genes involved in FRI-C did not show any change of their expression levels during cold treatment. Expression of *BrFLC* genes were downregulated with cumulative time of cold treatment, thus the upregulation *BrFRL1* could be independent from the downregulation of *BrFLC* genes during cold treatment. Genes involved in the PAF1 complex showed a change of expression levels during cold treatment in Chinese cabbage. *BrVIP3* and one of two *BrVIP4* showed upregulation by cold treatment, while one of two *BrVIP4*, *BrVIP5*, and *BrVIP6* showed downregulation by cold treatment. In *A. thaliana*, vernalization-associated changes in mRNA for *AtVIP4*, *AtVIP5*, or *AtVIP6* have not been observed (Oh et al. 2004; Zhang and van Nocker, 2002). If the PAF1 complex is also an activator of *BrFLC* genes in Chinese cabbage, the downregulation of the genes involved in PAF1 complex by vernalization results in the downregulation of *BrFLC* genes.

Genes involved in autonomous pathway or components of PHD-PRC2 are known as repressor of *AtFLC* expression in *A. thaliana* (Kim and Sung, 2014; Michaels and Amasino, 2001). Expression levels of *AtVRN1* and *AtVRN2* are not affected by vernalization in *A. thaliana* (Gendall et al. 2001; Levy et al. 2002). However, in this study, expression levels of *BrVRN1* genes changed by cold treatment in Chinese cabbage, and the expression patterns observed during cold treatment were different among the three paralogous genes; two *BrVRN1* genes were downregulated and one *BrVRN1* gene was upregulated. Upregulation of *BrVRN1* by 20 days of cold treatment was also observed in pak choi (Sun et al. 2015). These results suggest that, unlike in *A. thaliana*, it may be necessary to examine the possibility that the suppression of *BrFLC* expression is dependent upon the upregulation of *BrVRN1* by cold in *B. rapa*.

Five *BrMAF* genes were identified in the reference genome of *B. rapa*, but orthologous relationship between *BrMAF* genes in *B. rapa* and *AtMAF1-5* in *A. thaliana* is unable to be determined (Cheng et al. 2012). Two *BcMAF* genes in pak choi, *BcMAF1* (homologous gene,

Bra031884, blastp, 3e-61) and *BcMAF2* (homologous gene, Bra031888, blastp, 2e-74), have been shown to act as floral repressors (Huang et al. 2018b; 2019). In this study, we showed that three of five *BrMAF* genes were downregulated with cumulative time of cold treatment, suggesting that downregulation of *BrMAF* genes is important for promotion of flowering by vernalization. Further research will be required to clarify how much the *BrMAF* genes contribute to the promotion of flowering by vernalization in comparison with *BrFLC* genes.

In this study, we identified differentially expressed genes following cold treatment and some genes involved in flowering pathways showed different expression patterns between Chinese cabbage and *A. thaliana*. In addition, in genes involved in the flowering pathways, we found a difference in expression pattern between paralogous genes during cold treatment in Chinese cabbage, leading to a more complicated flowering pathway in Chinese cabbage than in *A. thaliana*. The findings in *A. thaliana* can mostly be applied to the molecular mechanism(s) of vernalization in Chinese cabbage, but there are some differences compared to *A. thaliana*; for example, cold induced noncoding RNAs were not found in Chinese cabbage (Li et al. 2016; Shea et al. 2019). Further analyses of the genes found in this study will be required to identify the genetic factors involved in vernalization and the molecular mechanism of vernalization in Chinese cabbage.

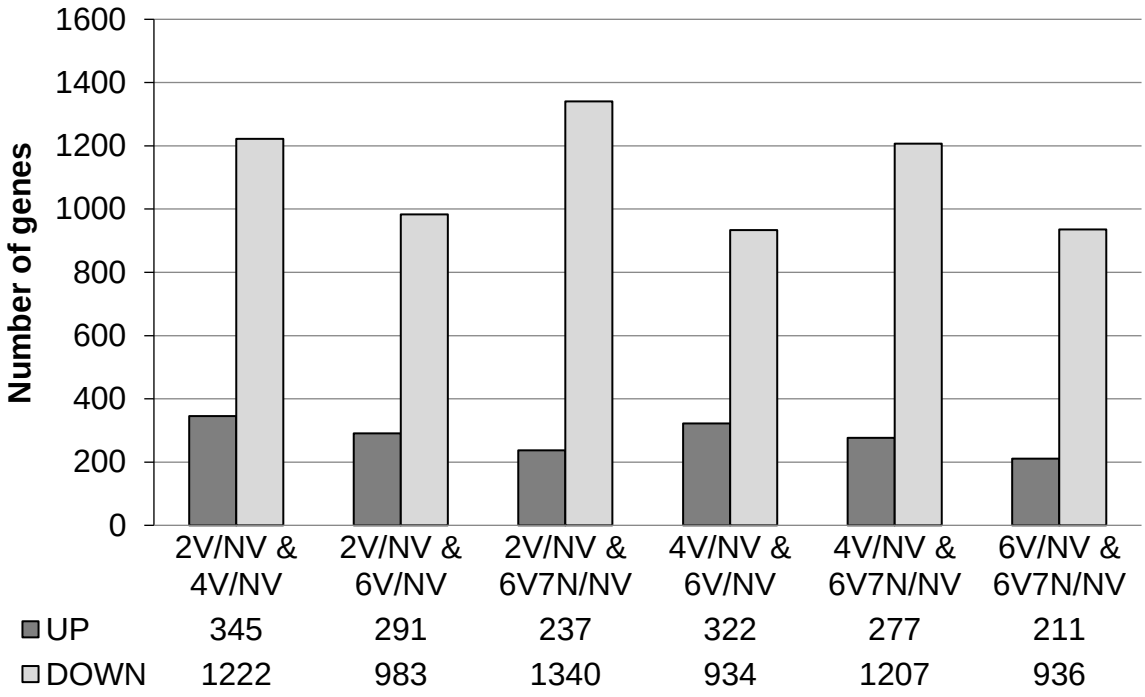

Figure IV-1. The total number of overlapped genes under different vernalization conditions. NV, non-vernalized; 2V, two weeks of cold treatment; 4V, four weeks of cold treatment; 6V, six weeks of cold treatment; 6V7N, six weeks of cold treatment followed by seven days in the normal growth conditions.

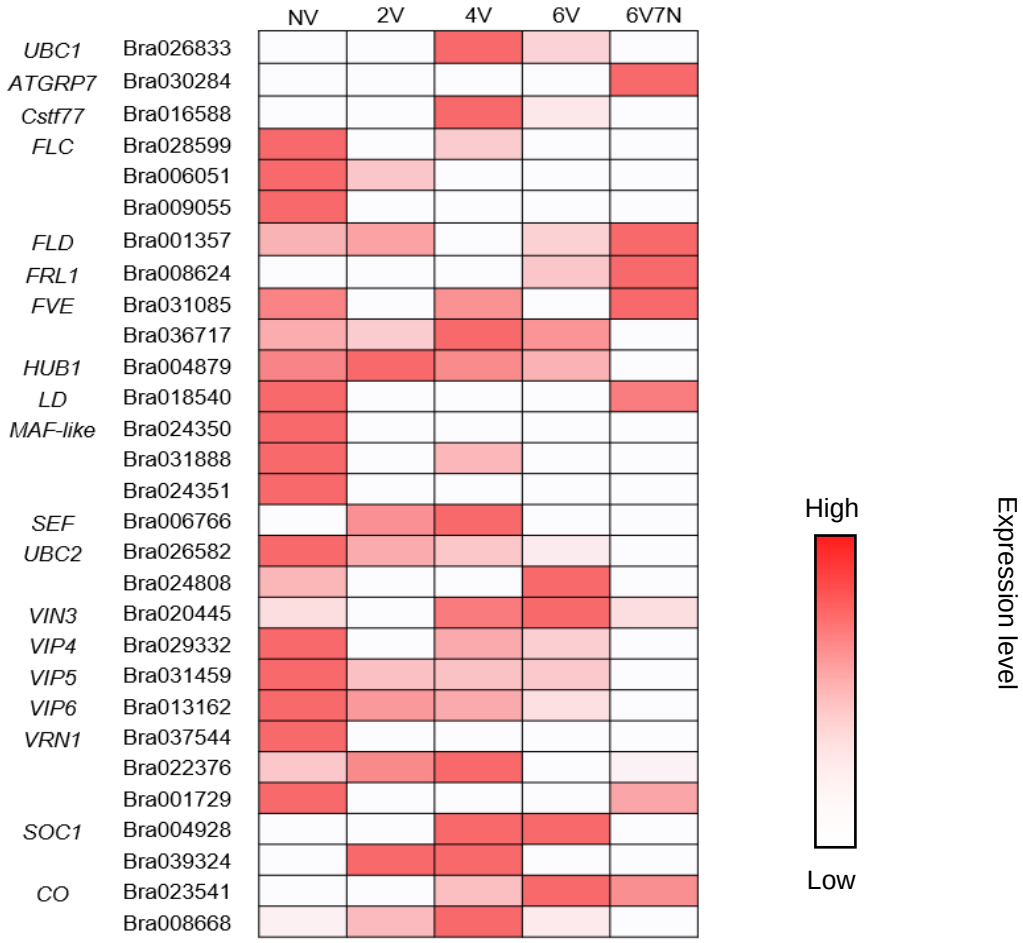

Figure IV-2. Heat map of the expression levels in genes involved in flowering pathway showing up or downregulation by cold treatment. Expression levels (FPKM) higher or lower than the median is shown. NV, non-vernalized; 2V, two weeks of cold treatment; 4V, four weeks of cold treatment; 6V, six weeks of cold treatment; 6V7N, six weeks of cold treatment followed by seven days in the normal growth conditions.

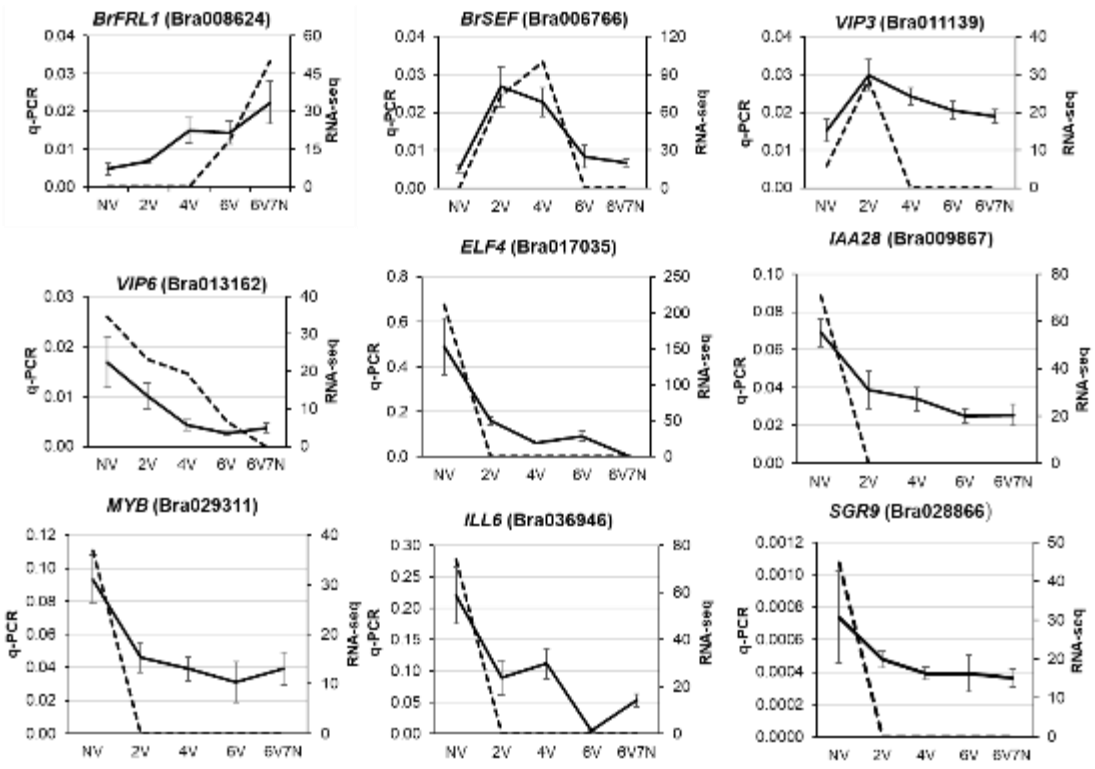

Figure IV-3. The validation of RNA-seq data by RT-qPCR of selected nine genes. Expression level of each gene relative to *BrACTIN* (*BrACT*) is calculated. Data presented are the average and standard error (s.e.) from three biological and experimental replications. From RNA-seq data, fragments per kilo-base per million (FPKM) is shown. Solid black line shows the RT-qPCR in the left Y-axis. The dashed black line shows the RNA-seq (FPKM) in the right Y-axis. NV, non-vernalized; 2V, two weeks of cold treatment; 4V, four weeks of cold treatment; 6V, six weeks of cold treatment; 6V7N, six weeks of cold treatment followed by seven days in the normal growth conditions.

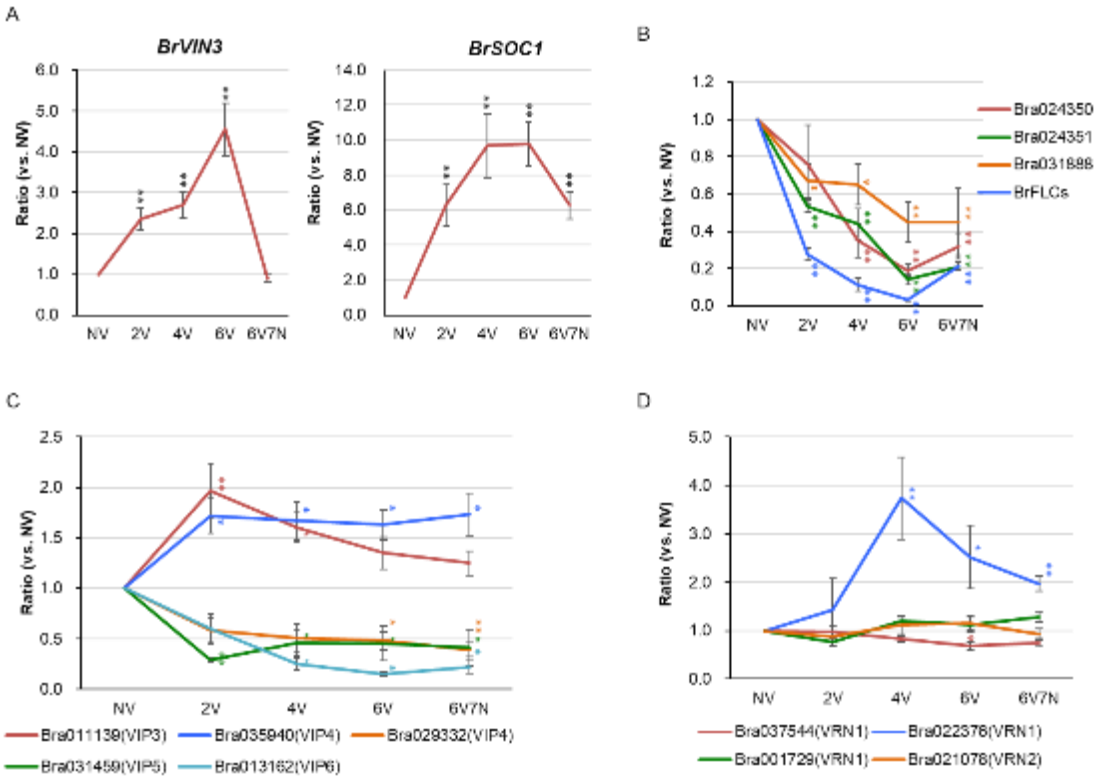

Figure IV-4. The validation of the expression levels by RT-qPCR for selected genes involved in the flowering pathway. The expression levels of each gene relative to *BrACTIN* (*BrACT*) are calculated, and the y-axis shows the ratio of vernalized samples (2V, 4V, 6V, 6V7N) compared with non-vernalized samples (NV). Data presented are the average and standard error (s.e.) from three biological and experimental replications. Statistical tests between non-vernalized and vernalized samples are shown (Dunnett's test, *; $p < 0.05$, **; $p < 0.01$, ***; $p < 0.001$). NV, non-vernalized; 2V, two weeks of cold treatment; 4V, four weeks of cold treatment; 6V, six weeks of cold treatment; 6V7N, six weeks of cold treatment followed by seven days in the normal growth conditions.

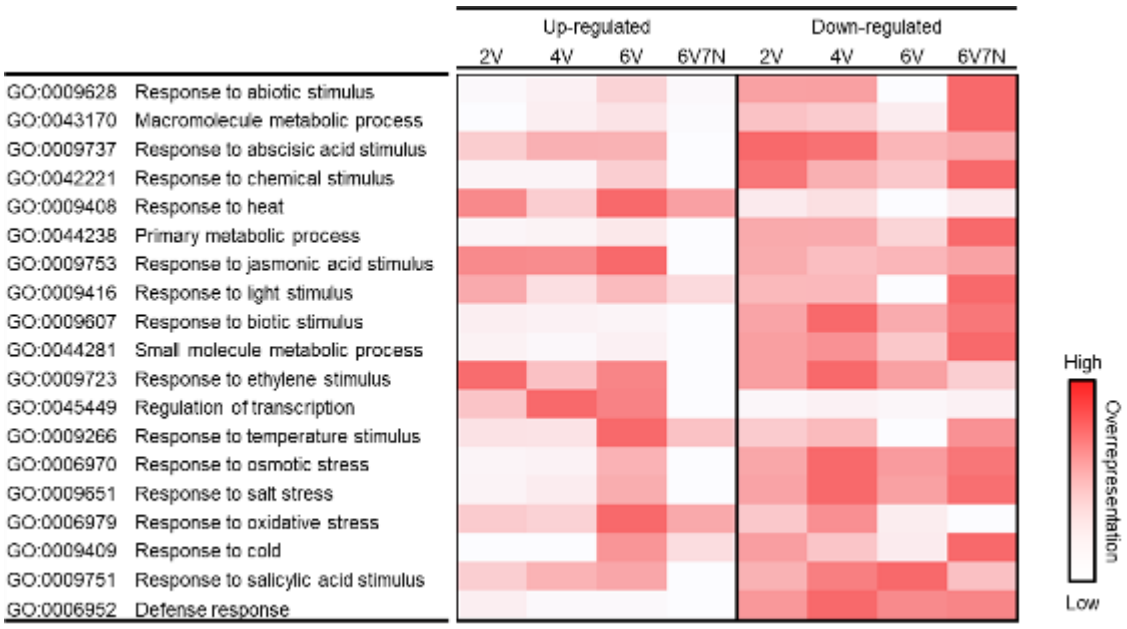

Figure IV-5. The GO enrichment analysis using up or downregulated genes by cold treatment. Log10 score of *p*-value is used for showing overrepresentation. Heat map shows overrepresentation higher or lower than the median. All selected categories belong to GO biological process (BP). NV, non-vernalized; 2V, two weeks of cold treatment; 4V, four weeks of cold treatment; 6V, six weeks of cold treatment; 6V7N, six weeks of cold treatment followed by seven days in the normal growth conditions.

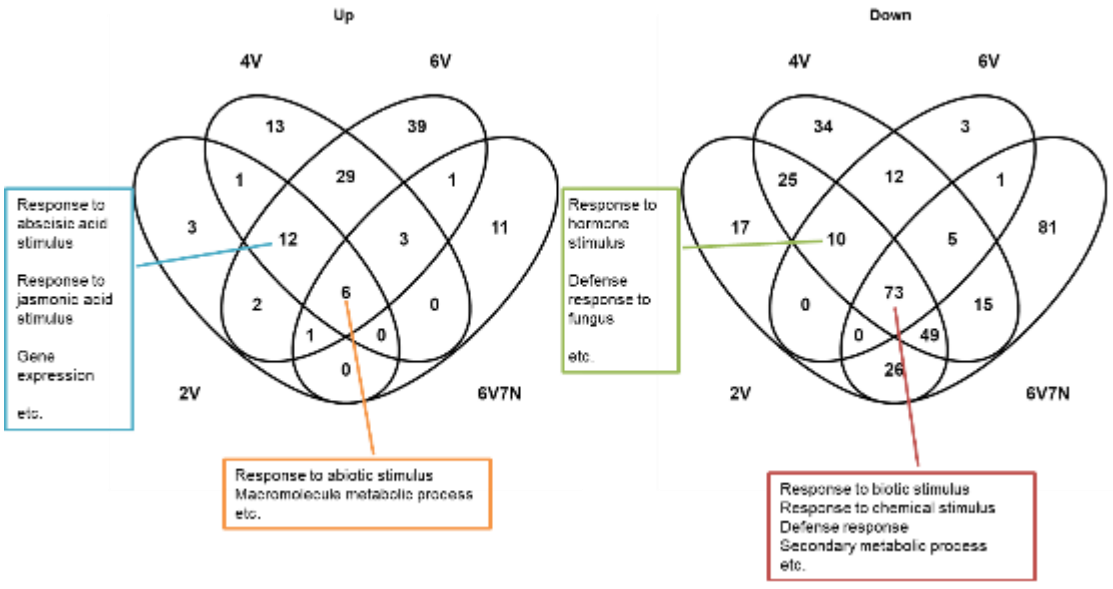

Figure IV-6. Venn diagram of the number of GO terms overrepresented in up and downregulated genes by cold treatments. NV, non-vernalized; 2V, two weeks of cold treatment; 4V, four weeks of cold treatment; 6V, six weeks of cold treatment; 6V7N, six weeks of cold treatment followed by seven days in the normal growth conditions

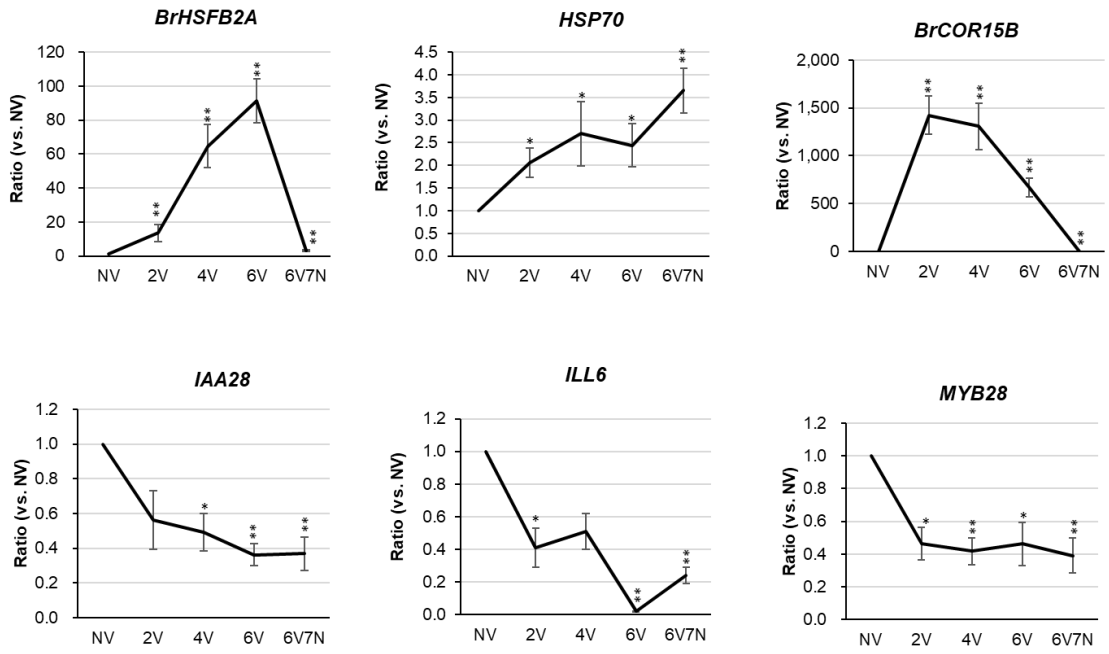

Figure IV-7. The expression patterns of six genes related to stress response measured by RT-qPCR. Expression level of each gene relative to *BrACTIN* (*BrACT*) is calculated. The relative expression levels of vernalized samples (2V, 4V, 6V, 6V7N) compared with non-vernalized samples (NV) were shown. Data presented are the average and standard error (s.e.) from three biological and experimental replications. Dunnett's test was performed for comparing the expression levels between non-vernalized and vernalized samples. *; $p < 0.05$, **; $p < 0.01$, ***; $p < 0.001$. NV, non-vernalized; 2V, two weeks of cold treatment; 4V, four weeks of cold treatment; 6V, six weeks of cold treatment; 6V7N, six weeks of cold treatment followed by seven days in the normal growth conditions.

Table IV-1. Number of differentially expressed genes between vernalized and non-vernalized samples

	Up-regulated in vernalized samples	Down-regulated in vernalized samples
1. 2V vs. NV (2V/NV)	1,169	2,618
2. 4V vs. NV (4V/NV)	1,291	2,252
3. 6V vs. NV (6V/NV)	980	1,650
4. 6V7N vs. NV (6V7N/NV)	946	2,950
Overlapped genes (1, 2, 3)	128	48
Overlapped genes (1, 2, 3, 4)	646	430

NV, non-vernalized samples

2V, samples with two weeks of cold treatment

4V, samples with four weeks of cold treatment

6V, samples with six weeks of cold treatment

6V7N, six weeks of cold treatment followed by seven days in the normal growth conditions.

Table IV-2. Sequences of primers used in this study

Name	Primer sequences (5'-3')	
RT-PCR/RT-qPCR		
Actin	CGGTCCAGCTTCGTCATACTCAGCC	AAATGTGATGTGGATATCAGGAAGG
FLC	GACGCARYGGTCTCATYGAGAAAGC	AWCATTARTTYTGTCTTYSTAGCTC
VIN3	GAGAATKTAGCTTGTAGAGCTGCGC	CGGACCCACATCACCCTCCAGCTTC
SOC1	CCAGCTCCAATATGCAAGATA	CCCAAGAGTTTACGTTTGGA
MAF (Bra024350)	TGGTGTAAGTGTAGATTCTC	AGGAACGTCTGCTTCCAAAT
MAF (Bra024351)	CAGTCCAACGCAAGATTGAA	CCAAAACCGTGGTTCTCGTCT
MAF (Bra031888)	GCAATCTTGAAGAACCAAATG	GAATTGTTCTCTCTCCTTCC
VRN1 (Bra037544)	CGCTGATCCTGAGGAAATAAATTC	TCTGTATAGATAGGATGGTCGT
VRN1 (Bra022376)	TCTGTATAGATAGGATGGTCGT	ATGATTGGTGTGATCCATCCAG
VRN1 (Bra001729)	CATGGACTCTGCATCACACA	TGGGTCATCATCTCTCGGT
VRN2 (Bra021078)	GTGGTCTCGGCTGCTAAGTC	ATCTGCAACGTCATCATCCA
VIP3 (Bra011139)	TTCTGAGGTTTGGGGTATGC	ACGAACTTCTTGCTGCTGGT
VIP4 (Bra029332)	GCTGCGGTTGAAGTGAATGTAG	ATCTTGTCTCCTCTTTGTAA
VIP4 (Bra035940)	TTGAAGTCCACGGTGAGCCTG	ATCTCGTCTCCTCGTTGTAG
VIP5 (Bra031459)	ATGAAACCTCTGCTGCTCGT	AGTCTCCGCCGAGTAGACAA
VIP6 (Bra0131162)	AAGATGAAGACGCCAACACC	GGCATTGTCATTACCCCATC
HSFB2A	ACGGTAACATCTTTGGACTCA	CCGTAGAAACCGTCTTCACA
COR15B	TGATCTACGCCGAKAAAGGT	TGCAGTGTCTTTGGCTTCAA
HSP70	GGTCGGAGGGTGTTCTTACA	AGGTCTAAACTCCCGAACGG
IAA28 (Bra009867)	TGGCCGCCGGTRAGATCATC	GAGTTGGTCAACGGCATGTG
ILL6 (Bra036946)	TGGATGACGTGGAGGCTATC	CCTTGAAGGCTTATGACGGC
MYB28 (Bra029311)	GGTGTGGAAAGAGTTGTAGAC	CTAGGTAAATGTCTCGCTATG
FRL1 (Bra008624)	CTGAGGAGCTTTCGCGTTAC	ACATAAACCTCACCGCCAAG
SEF (Bra006766)	CTTACAAGCACCGACAATCG	GCTTTACGAGCCTCCAAAGC
Bra028866	TGGACTTGCGACGCCGGAAT	TCTACTTCTCCGGCGGCGTT
ELF4 (Bra017035)	GATCGGAATTTCAGACAAGTG	GAAACGCCGATGAGAAATTGG

Table IV-3. Verification of the RNA-seq data by RT-qPCR

Gene ID	Fig. S1	Fig. III-11	Fig.5	Similar expression patten to RNA-seq data
Bra006766 (*BrSEF*)	✓			Yes
Bra008624 (*BrFRL1*)	✓			Yes
Bra009867 (*BrIAA28*)	✓		✓	Yes
Bra011139 (*BrVIP3*)	✓	✓		Yes
Bra013162 (*BrVIP6*)	✓	✓		Yes
Bra017035 (*BrELF4*)	✓			Yes
Bra028866 (*BrSGR9*)	✓			Yes
Bra029311 (*BrMYB28*)	✓		✓	Yes
Bra036946 (*BrILL6*)	✓		✓	Yes
Bra001729 (*BrVRN1*)		✓		No
Bra021078 (*BrVRN2*)		✓		Yes
Bra022376 (*BrVRN1*)		✓		Yes
Bra024350 (*BrMAF*)		✓		Yes
Bra024351 (*BrMAF*)		✓		Yes
Bra029332 (*BrVIP4*)		✓		Yes
Bra031459 (*BrVIP5*)		✓		Yes
Bra031888 (*BrMAF*)		✓		Yes
Bra035940 (*BrVIP5*)		✓		Yes
Bra037544 (*BrVRN1*)		✓		Yes
*BrFLC*s (*BrFLC1*, *2*, *3*, *5*)		✓		Yes
*BrSOC1 (*Bra004928 & Bra039324)		✓		No
*BrVIN3 (*Bra020445)		✓		Yes
BrHSFB2A			✓	Yes
BrCOR15B			✓	Yes
BrHSP70			✓	Yes

Table IV-4. Number of mapped RNA sequencing reads with and without cold treatments

Sample	Total number of reads	Mapped reads	% Mapped reads	NOTEST
NV	22,003,803	14,410,763	65.5%	
2V	8,647,017	5,417,156	62.7%	59.1%
4V	10,159,252	6,651,848	65.5%	58.2%
6V	20,428,247	11,281,787	55.2%	56.7%
6V7N	5,422,918	3,634,309	67.0%	59.8%

NOTEST indicates percentage of genes without enough aligned reads for a differential expression test between vernalized and non-vernalized samples

NV, non-vernalized samples

2V, samples with two weeks of cold treatment

4V, samples with four weeks of cold treatment

6V, samples with six weeks of cold treatment

6V7N, samples upon return to warm conditions for seven days after six weeks of cold treatment

Table IV-5. Expression pattern in genes involved in flowering pathway following cold treatment

			2V	4V	6V	6V7N
VERNALIZATION and AUTONOMOUS PATHWAYS						
UBC1 (UBIQUITIN CONJUGATING ENZYME 1)	AT1G14400	Bra016703				
		Bra026833		UP		
AGL19 (AGAMOUS-LIKE 19)	AT4G22950	Bra019343				
		Bra020826				
ATGRP7	AT2G21660	Bra030284				UP
		Bra031210				
ATH1 (ARABIDOPSIS THALIANA HOMEOBOX 1)	AT4G32980	Bra011403				
		Bra037031				
ATX1 (ARABIDOPSIS TRITHORAX 1)	AT2G31650	Bra021721				
BRI1 (BraSSINOSTEROID INSENSITIVE 1)	AT4G39400	Bra033615				
		Bra011862				
		Bra010684				
CLF (CURLY LEAF)	AT2G23380	Bra032169				
Cstf64 (CLEAVAGE STIMULATION FACTOR 64)	AT1G71800	Bra007985				
		Bra003913				
Cstf77 (CLEAVAGE STIMULATION FACTOR 77)	AT1G17760	Bra016588		UP		
EFS (EARLY FLOWERING IN SHORT DAYS)	AT1G77300	Bra015678				
ELF6 (EARLY FLOWERING 6)	AT5G04240	Bra009474				
		Bra009475				
ELF7 (EARLY FLOWERING 7)	AT1G79730	Bra009582				
EMF1 (EMBRYONIC FLOWER 1)	AT5G11530	Bra023327				
		Bra006104				
		Bra008955				
EMF2 (EMBRYONIC FLOWER 2)	AT5G51230	Bra015200				
		Bra022541				
		Bra029179				
FCA (FLOWERING TIME CONTROL PROTEIN ALPHA)	AT4G16280	Bra038446				
FES (FRIGIDA ESSENTIAL 1)	AT2G33835	Bra005468				
		Bra022958				
		Bra022957				
FLC (FLOWERING LOCUS C)	AT5G10140	Bra028599	DOWN		DOWN	
		Bra006051		DOWN	DOWN	DOWN
		Bra009055	DOWN	DOWN	DOWN	DOWN
		Bra022771				
FLD (FLOWERING LOCUS D)	AT3G10390	Bra001357		DOWN		

FLK (FLOWERING LATE KH MOTIF)	AT3G04610	Bra001111				
FPA	AT2G43410	Bra004761				
		Bra007458				
FRI (FRIGIDA)	AT4G00650	Bra035723				
		Bra029192				
FRL1 (FRIGIDA LIKE 1)	AT5G16320	Bra008624				UP
FVE	AT2G19520	Bra031085	DOWN		DOWN	
		Bra040678				
		Bra036717				DOWN
		Bra011133				
FWA (FLOWERING WAGENINGEN)	AT4G25530	Bra013898				
FY	AT5G13480	Bra006202				
		Bra023416				
HUA2 (HUA is the full name, means flower in Chinese)	AT5G23150	Bra029359				
		Bra013022				
HUB1 (HISTONE MONOUBIQUITINATION 1)	AT2G44950	Bra040332				
		Bra004879				DOWN
HUB2 (HISTONE MONOUBIQUITINATION 2)	AT1G55250	Bra030874				
LD (LUMINIDEPENDENS)	AT4G02560	Bra018540	DOWN	DOWN	DOWN	
MAF1 (MADS AFFECTING FLOWERING 1)	AT1G77080		DOWN	DOWN	DOWN	DOWN
MAF2 (MADS AFFECTING FLOWERING 2)	AT5G65050	Bra024350				
		Bra031888	DOWN		DOWN	DOWN
MAF3 (MADS AFFECTING FLOWERING 3)	AT5G65060					
MAF4 (MADS AFFECTING FLOWERING 4)	AT5G65070	Bra031884				
MAF5 (MADS AFFECTING FLOWERING 5)	AT5G65080	Bra024351	DOWN	DOWN	DOWN	DOWN
PIE1 (PHOTOPERIOD INDEPENDENT EARLY FLOWERING 1)	AT3G12810	Bra034727				
REF6 (RELATIVE OF EARLY FLOWERING 6)	AT3G48430	Bra018060				
SDG26 (SET DOMAIN GROUP 26)	AT1G76710	Bra015723				
SEF (SERRATED LEAVES AND EARLY FLOWERING)	AT5G37055	Bra002649				
		Bra006766	UP	UP		
UBC2 (UBIQUITIN CONJUGATING ENZYME 2)	AT2G02760	Bra026582				DOWN
		Bra024808	DOWN	DOWN		DOWN
		Bra017410				
UBP26 (UBIQUITIN-SPECIFIC PROTEASE 26)	AT3G49600	Bra017972				
		Bra019603				
VIL1 (VERNALIZATION INSENSTIVE 3 LIKE 1) / VRN5 (VERNALIZATION 5)	AT3G24440	Bra015040				

		Bra006824				
VIN3 (VERNALIZATION INSENSITIVE 3)	AT5G57380	Bra020445		UP	UP	
VIP3 (VERNALIZATION INDEPENDENCE 3)	AT4G29830	Bra011139				
VIP4 (VERNALIZATION INDEPENDENCE 4)	AT5G61150	Bra035940				
		Bra029332	DOWN			DOWN
VIP5 (VERNALIZATION INDEPENDENCE 5)	AT1G61040	Bra031459				DOWN
VIP6 (VERNALIZATION INDEPENDENCE 6) / EARLY FLOWERING 8 (ELF8)	AT2G06210	Bra013162				DOWN
VRN1 (VERNALIZATION 1)	AT3G18990	Bra037544	DOWN	DOWN	DOWN	DOWN
		Bra022376		UP		
		Bra001729	DOWN	DOWN		
VRN2 (VERNALIZATION 2)	AT4G16845	Bra021078				
MERISTEM RESPONSE and DEVELOPMENT						
SOC1 (SUPPRESSOR OF OVEREXPRESSION OF CONSTANS)	AT2G45660	Bra000393				
		Bra004928		UP	UP	
		Bra039324	UP	UP		
PHOTOPERIOD PATHWAY, CIRCADIAN CLOCK, LIGHT SIGNALING						
CO (CONSTANS)	AT5G15840	Bra008669				
		Bra023541		UP	UP	UP
		Bra008668	UP	UP	UP	DOWN
FT (FLOWERING LOCUS T)	AT1G65480	Bra022475				
		Bra004117				
		Bra015710				

NV, non-vernalized samples

2V, samples with two weeks of cold treatment

4V, samples with four weeks of cold treatment

6V, samples with six weeks of cold treatment

6V7N, samples upon return to warm conditions for seven days after six weeks of cold treatment

Table IV-6. List of overrepresented GO terms in genes differential expression between 2V and NV

GO accession	Term type	Term	*p* value	FDR
Upregulated (2V > NV) (*p* < 0.0001)				
GO:0009408	BP	response to heat	9.40E-07	0.0034
GO:0044267	BP	cellular protein metabolic process	1.30E-06	0.0034
GO:0009416	BP	response to light stimulus	2.00E-06	0.0034
GO:0009628	BP	response to abiotic stimulus	2.20E-06	0.0034
GO:0009314	BP	response to radiation	2.60E-06	0.0034
GO:0009059	BP	macromolecule biosynthetic process	8.00E-06	0.0089
GO:0044249	BP	cellular biosynthetic process	1.10E-05	0.010
GO:0009058	BP	biosynthetic process	1.30E-05	0.010
GO:0050896	BP	response to stimulus	1.50E-05	0.011
GO:0034645	BP	cellular macromolecule biosynthetic process	1.70E-05	0.011
GO:0007242	BP	intracellular signaling cascade	1.90E-05	0.012
GO:0019538	BP	protein metabolic process	2.30E-05	0.013
GO:0009753	BP	response to jasmonic acid stimulus	2.70E-05	0.013
GO:0023052	BP	signaling	2.80E-05	0.013
GO:0042221	BP	response to chemical stimulus	3.60E-05	0.016
GO:0044260	BP	cellular macromolecule metabolic process	4.70E-05	0.019
GO:0010033	BP	response to organic substance	5.20E-05	0.019
GO:0009719	BP	response to endogenous stimulus	5.20E-05	0.019
GO:0009723	BP	response to ethylene stimulus	5.30E-05	0.019
GO:0009607	BP	response to biotic stimulus	6.40E-05	0.021
GO:0009737	BP	response to abscisic acid stimulus	7.90E-05	0.024
GO:0043170	BP	macromolecule metabolic process	9.00E-05	0.026
GO:0044238	BP	primary metabolic process	9.50E-05	0.026
GO:0010467	BP	gene expression	7.20E-05	0.023
GO:0005794	CC	Golgi apparatus	4.60E-05	0.026
Downregulated (2V < NV) (*p* < 0.00001)				
GO:0044281	BP	small molecule metabolic process	7.60E-23	6.90E-19
GO:0050896	BP	response to stimulus	8.00E-22	3.70E-18
GO:0010033	BP	response to organic substance	1.80E-21	5.60E-18
GO:0044237	BP	cellular metabolic process	2.80E-18	6.40E-15
GO:0044248	BP	cellular catabolic process	5.20E-18	9.60E-15
GO:0009056	BP	catabolic process	1.20E-17	1.80E-14
GO:0043412	BP	macromolecule modification	2.20E-17	2.90E-14
GO:0046483	BP	heterocycle metabolic process	7.50E-17	8.20E-14
GO:0044282	BP	small molecule catabolic process	8.00E-17	8.20E-14
GO:0009987	BP	cellular process	9.20E-17	8.40E-14
GO:0044267	BP	cellular protein metabolic process	2.80E-16	2.30E-13
GO:0006950	BP	response to stress	4.90E-16	3.70E-13
GO:0042221	BP	response to chemical stimulus	1.50E-15	1.10E-12
GO:0006464	BP	protein modification process	2.60E-15	1.70E-12
GO:0009628	BP	response to abiotic stimulus	5.70E-15	3.50E-12
GO:0016043	BP	cellular component organization	9.80E-15	5.60E-12
GO:0043436	BP	oxoacid metabolic process	1.40E-14	7.00E-12
GO:0019752	BP	carboxylic acid metabolic process	1.40E-14	7.00E-12
GO:0006082	BP	organic acid metabolic process	1.60E-14	7.60E-12

GO:0044238	BP	primary metabolic process	2.00E-14	9.10E-12
GO:0042180	BP	cellular ketone metabolic process	3.20E-14	1.40E-11
GO:0019538	BP	protein metabolic process	3.90E-14	1.60E-11
GO:0034641	BP	cellular nitrogen compound metabolic process	4.50E-14	1.80E-11
GO:0051186	BP	cofactor metabolic process	6.90E-14	2.60E-11
GO:0051716	BP	cellular response to stimulus	7.90E-14	2.90E-11
GO:0009607	BP	response to biotic stimulus	1.30E-13	4.50E-11
GO:0008152	BP	metabolic process	1.80E-13	6.10E-11
GO:0044260	BP	cellular macromolecule metabolic process	2.00E-13	6.40E-11
GO:0044265	BP	cellular macromolecule catabolic process	2.30E-13	7.20E-11
GO:0065007	BP	biological regulation	4.10E-13	1.20E-10
GO:0009057	BP	macromolecule catabolic process	4.80E-13	1.40E-10
GO:0071310	BP	cellular response to organic substance	5.60E-13	1.60E-10
GO:0065008	BP	regulation of biological quality	9.40E-13	2.60E-10
GO:0006996	BP	organelle organization	1.60E-12	4.30E-10
GO:0043170	BP	macromolecule metabolic process	1.70E-12	4.40E-10
GO:0009308	BP	amine metabolic process	2.10E-12	5.50E-10
GO:0023052	BP	signaling	2.60E-12	6.30E-10
GO:0048519	BP	negative regulation of biological process	3.50E-12	8.40E-10
GO:0070887	BP	cellular response to chemical stimulus	3.80E-12	8.80E-10
GO:0043687	BP	post-translational protein modification	5.40E-12	1.20E-09
GO:0006807	BP	nitrogen compound metabolic process	8.10E-12	1.80E-09
GO:0006066	BP	alcohol metabolic process	9.00E-12	2.00E-09
GO:0009117	BP	nucleotide metabolic process	1.20E-11	2.60E-09
GO:0006753	BP	nucleoside phosphate metabolic process	1.90E-11	3.90E-09
GO:0044275	BP	cellular carbohydrate catabolic process	2.10E-11	4.30E-09
GO:0006519	BP	cellular amino acid and derivative metabolic process	2.20E-11	4.40E-09
GO:0016052	BP	carbohydrate catabolic process	2.40E-11	4.70E-09
GO:0044106	BP	cellular amine metabolic process	2.60E-11	5.00E-09
GO:0044271	BP	cellular nitrogen compound biosynthetic process	3.30E-11	6.20E-09
GO:0009719	BP	response to endogenous stimulus	4.80E-11	8.80E-09
GO:0006006	BP	glucose metabolic process	5.50E-11	9.80E-09
GO:0055086	BP	nucleobase, nucleoside and nucleotide metabolic process	6.70E-11	1.20E-08
GO:0007242	BP	intracellular signaling cascade	7.80E-11	1.30E-08
GO:0044283	BP	small molecule biosynthetic process	9.20E-11	1.60E-08
GO:0051641	BP	cellular localization	9.90E-11	1.60E-08
GO:0032787	BP	monocarboxylic acid metabolic process	1.10E-10	1.80E-08
GO:0050789	BP	regulation of biological process	1.40E-10	2.20E-08
GO:0046164	BP	alcohol catabolic process	1.40E-10	2.20E-08
GO:0046394	BP	carboxylic acid biosynthetic process	1.50E-10	2.30E-08
GO:0016053	BP	organic acid biosynthetic process	1.50E-10	2.30E-08
GO:0002376	BP	immune system process	1.90E-10	2.80E-08
GO:0006955	BP	immune response	1.90E-10	2.80E-08
GO:0046365	BP	monosaccharide catabolic process	2.00E-10	2.90E-08

GO:0051234	BP	establishment of localization	2.30E-10	3.30E-08
GO:0009058	BP	biosynthetic process	2.30E-10	3.30E-08
GO:0019320	BP	hexose catabolic process	2.40E-10	3.30E-08
GO:0006007	BP	glucose catabolic process	2.40E-10	3.30E-08
GO:0048583	BP	regulation of response to stimulus	2.50E-10	3.30E-08
GO:0006810	BP	transport	2.70E-10	3.60E-08
GO:0051707	BP	response to other organism	3.20E-10	4.20E-08
GO:0046907	BP	intracellular transport	3.20E-10	4.20E-08
GO:0006952	BP	defense response	3.30E-10	4.20E-08
GO:0045087	BP	innate immune response	4.00E-10	5.00E-08
GO:0051179	BP	localization	4.00E-10	5.00E-08
GO:0010817	BP	regulation of hormone levels	4.20E-10	5.20E-08
GO:0051649	BP	establishment of localization in cell	4.70E-10	5.70E-08
GO:0006396	BP	RNA processing	5.90E-10	7.00E-08
GO:0046395	BP	carboxylic acid catabolic process	6.50E-10	7.50E-08
GO:0016054	BP	organic acid catabolic process	6.50E-10	7.50E-08
GO:0023046	BP	signaling process	7.40E-10	8.30E-08
GO:0023060	BP	signal transmission	7.40E-10	8.30E-08
GO:0007165	BP	signal transduction	7.50E-10	8.30E-08
GO:0019748	BP	secondary metabolic process	7.70E-10	8.50E-08
GO:0005996	BP	monosaccharide metabolic process	7.80E-10	8.50E-08
GO:0070727	BP	cellular macromolecule localization	9.40E-10	1.00E-07
GO:0006520	BP	cellular amino acid metabolic process	1.00E-09	1.10E-07
GO:0006605	BP	protein targeting	1.20E-09	1.30E-07
GO:0019318	BP	hexose metabolic process	1.30E-09	1.30E-07
GO:0044249	BP	cellular biosynthetic process	1.30E-09	1.40E-07
GO:0034613	BP	cellular protein localization	2.30E-09	2.30E-07
GO:0009725	BP	response to hormone stimulus	3.20E-09	3.20E-07
GO:0080129	BP	proteasome core complex assembly	3.80E-09	3.80E-07
GO:0006886	BP	intracellular protein transport	5.00E-09	4.90E-07
GO:0043623	BP	cellular protein complex assembly	6.40E-09	6.20E-07
GO:0034621	BP	cellular macromolecular complex subunit organization	7.00E-09	6.80E-07
GO:0006732	BP	coenzyme metabolic process	7.40E-09	7.00E-07
GO:0009310	BP	amine catabolic process	7.90E-09	7.40E-07
GO:0008104	BP	protein localization	8.00E-09	7.50E-07
GO:0009737	BP	response to abscisic acid stimulus	8.40E-09	7.80E-07
GO:0034622	BP	cellular macromolecular complex assembly	1.00E-08	9.30E-07
GO:0009165	BP	nucleotide biosynthetic process	1.50E-08	1.30E-06
GO:0009651	BP	response to salt stress	1.60E-08	1.40E-06
GO:0009309	BP	amine biosynthetic process	1.70E-08	1.50E-06
GO:0006796	BP	phosphate metabolic process	1.70E-08	1.50E-06
GO:0050832	BP	defense response to fungus	1.80E-08	1.50E-06
GO:0006793	BP	phosphorus metabolic process	1.90E-08	1.70E-06
GO:0045184	BP	establishment of protein localization	2.50E-08	2.10E-06
GO:0015031	BP	protein transport	2.50E-08	2.10E-06
GO:0051789	BP	response to protein stimulus	2.70E-08	2.20E-06
GO:0006725	BP	cellular aromatic compound metabolic process	2.70E-08	2.30E-06
GO:0018130	BP	heterocycle biosynthetic process	3.50E-08	2.90E-06
GO:0006511	BP	ubiquitin-dependent protein catabolic process	3.70E-08	3.00E-06

GO:0043933	BP	macromolecular complex subunit organization	3.80E-08	3.10E-06
GO:0009260	BP	ribonucleotide biosynthetic process	4.40E-08	3.50E-06
GO:0070271	BP	protein complex biogenesis	4.50E-08	3.50E-06
GO:0006461	BP	protein complex assembly	4.50E-08	3.50E-06
GO:0006220	BP	pyrimidine nucleotide metabolic process	4.60E-08	3.50E-06
GO:0009793	BP	embryonic development ending in seed dormancy	4.60E-08	3.50E-06
GO:0006970	BP	response to osmotic stress	4.80E-08	3.70E-06
GO:0032502	BP	developmental process	4.90E-08	3.70E-06
GO:0051788	BP	response to misfolded protein	5.00E-08	3.70E-06
GO:0009218	BP	pyrimidine ribonucleotide metabolic process	5.10E-08	3.80E-06
GO:0065003	BP	macromolecular complex assembly	5.60E-08	4.10E-06
GO:0043632	BP	modification-dependent macromolecule catabolic process	5.90E-08	4.30E-06
GO:0019941	BP	modification-dependent protein catabolic process	5.90E-08	4.30E-06
GO:0055082	BP	cellular chemical homeostasis	7.60E-08	5.50E-06
GO:0009620	BP	response to fungus	8.00E-08	5.80E-06
GO:0043248	BP	proteasome assembly	8.10E-08	5.80E-06
GO:0070838	BP	divalent metal ion transport	8.10E-08	5.80E-06
GO:0048367	BP	shoot development	1.10E-07	7.30E-06
GO:0022621	BP	shoot system development	1.10E-07	7.30E-06
GO:0071495	BP	cellular response to endogenous stimulus	1.10E-07	7.50E-06
GO:0006221	BP	pyrimidine nucleotide biosynthetic process	1.10E-07	7.70E-06
GO:0008652	BP	cellular amino acid biosynthetic process	1.40E-07	9.70E-06
GO:0050794	BP	regulation of cellular process	1.50E-07	9.90E-06
GO:0009743	BP	response to carbohydrate stimulus	1.50E-07	1.00E-05
GO:0048878	BP	chemical homeostasis	1.50E-07	1.00E-05
GO:0009259	BP	ribonucleotide metabolic process	1.70E-07	1.10E-05
GO:0051603	BP	proteolysis involved in cellular protein catabolic process	1.70E-07	1.10E-05
GO:0006873	BP	cellular ion homeostasis	1.90E-07	1.20E-05
GO:0007154	BP	cell communication	2.00E-07	1.30E-05
GO:0009657	BP	plastid organization	2.00E-07	1.30E-05
GO:0009220	BP	pyrimidine ribonucleotide biosynthetic process	2.10E-07	1.30E-05
GO:0080134	BP	regulation of response to stress	2.20E-07	1.40E-05
GO:0031347	BP	regulation of defense response	2.30E-07	1.40E-05
GO:0009790	BP	embryonic development	2.30E-07	1.50E-05
GO:0044262	BP	cellular carbohydrate metabolic process	2.90E-07	1.80E-05
GO:0042445	BP	hormone metabolic process	2.90E-07	1.80E-05
GO:0007275	BP	multicellular organismal development	3.00E-07	1.80E-05
GO:0044255	BP	cellular lipid metabolic process	3.10E-07	1.90E-05
GO:0051704	BP	multi-organism process	3.60E-07	2.20E-05
GO:0033554	BP	cellular response to stress	4.20E-07	2.50E-05
GO:0044257	BP	cellular protein catabolic process	4.30E-07	2.60E-05
GO:0032501	BP	multicellular organismal process	4.50E-07	2.70E-05
GO:0009063	BP	cellular amino acid catabolic process	4.80E-07	2.80E-05

GO:0005975	BP	carbohydrate metabolic process	5.60E-07	3.30E-05
GO:0006139	BP	nucleobase, nucleoside, nucleotide and nucleic acid metabolic process	5.70E-07	3.30E-05
GO:0010154	BP	fruit development	5.80E-07	3.40E-05
GO:0019725	BP	cellular homeostasis	7.00E-07	4.00E-05
GO:0048316	BP	seed development	7.50E-07	4.30E-05
GO:0033036	BP	macromolecule localization	7.60E-07	4.30E-05
GO:0010629	BP	negative regulation of gene expression	7.90E-07	4.40E-05
GO:0048856	BP	anatomical structure development	8.30E-07	4.70E-05
GO:0030163	BP	protein catabolic process	8.60E-07	4.80E-05
GO:0009617	BP	response to bacterium	8.80E-07	4.90E-05
GO:0042440	BP	pigment metabolic process	9.30E-07	5.10E-05
GO:0009791	BP	post-embryonic development	9.40E-07	5.10E-05
GO:0005829	CC	cytosol	1.20E-20	1.10E-17
GO:0044422	CC	organelle part	2.30E-19	7.60E-17
GO:0044446	CC	intracellular organelle part	2.40E-19	7.60E-17
GO:0016020	CC	membrane	7.10E-19	1.70E-16
GO:0005886	CC	plasma membrane	7.70E-17	1.50E-14
GO:0043234	CC	protein complex	2.70E-14	4.40E-12
GO:0032991	CC	macromolecular complex	2.80E-11	3.80E-09
GO:0044425	CC	membrane part	3.60E-11	4.30E-09
GO:0044444	CC	cytoplasmic part	1.00E-09	1.10E-07
GO:0031090	CC	organelle membrane	1.20E-09	1.20E-07
GO:0005794	CC	Golgi apparatus	1.70E-09	1.40E-07
GO:0009536	CC	plastid	2.70E-09	2.10E-07
GO:0044459	CC	plasma membrane part	2.90E-09	2.10E-07
GO:0009507	CC	chloroplast	5.60E-09	3.80E-07
GO:0009506	CC	plasmodesma	9.90E-09	5.90E-07
GO:0055044	CC	symplast	9.90E-09	5.90E-07
GO:0005911	CC	cell-cell junction	1.20E-08	6.50E-07
GO:0030054	CC	cell junction	1.80E-08	9.70E-07
GO:0005737	CC	cytoplasm	2.10E-08	1.10E-06
GO:0044435	CC	plastid part	2.40E-08	1.10E-06
GO:0044434	CC	chloroplast part	3.90E-08	1.70E-06
GO:0070013	CC	intracellular organelle lumen	1.30E-07	5.30E-06
GO:0043233	CC	organelle lumen	1.30E-07	5.30E-06
GO:0005730	CC	nucleolus	1.80E-07	6.90E-06
GO:0031974	CC	membrane-enclosed lumen	1.80E-07	6.90E-06
GO:0031981	CC	nuclear lumen	2.50E-07	9.20E-06
GO:0005773	CC	vacuole	5.40E-07	1.90E-05
GO:0044428	CC	nuclear part	1.00E-06	3.40E-05
GO:0005515	MF	protein binding	9.50E-13	1.70E-09
GO:0003824	MF	catalytic activity	1.90E-10	1.70E-07
GO:0016740	MF	transferase activity	4.40E-09	2.60E-06
GO:0042578	MF	phosphoric ester hydrolase activity	6.60E-09	2.90E-06
GO:0016791	MF	phosphatase activity	2.60E-08	9.20E-06

NV, non-vernalized samples

2V, samples with two weeks of cold treatment

CC, Cellular component; MF, Molecular function; BP, Biological process

Table IV-7. List of overrepresented GO terms in genes differential expression between 4V and NV

GO accession	Term type	Term	*p* value	FDR
Upregulated (4V > NV) (*p* < 0.0001)				
GO:0009059	BP	macromolecule biosynthetic process	8.00E-08	0.00056
GO:0034645	BP	cellular macromolecule biosynthetic process	1.70E-07	0.00058
GO:0009628	BP	response to abiotic stimulus	3.60E-07	0.00083
GO:0044260	BP	cellular macromolecule metabolic process	5.30E-07	0.00091
GO:0050794	BP	regulation of cellular process	6.50E-07	0.00091
GO:0050789	BP	regulation of biological process	1.00E-06	0.0010
GO:0050896	BP	response to stimulus	1.20E-06	0.0010
GO:0044267	BP	cellular protein metabolic process	1.30E-06	0.0010
GO:0051171	BP	regulation of nitrogen compound metabolic process	1.40E-06	0.0010
GO:0043170	BP	macromolecule metabolic process	1.50E-06	0.0010
GO:0019219	BP	regulation of nucleobase, nucleoside, nucleotide and nucleic acid metabolic process	2.00E-06	0.0012
GO:0080090	BP	regulation of primary metabolic process	2.30E-06	0.0012
GO:0007242	BP	intracellular signaling cascade	2.40E-06	0.0012
GO:0044237	BP	cellular metabolic process	2.40E-06	0.0012
GO:0009987	BP	cellular process	4.90E-06	0.0021
GO:0044249	BP	cellular biosynthetic process	5.40E-06	0.0021
GO:0065007	BP	biological regulation	5.70E-06	0.0021
GO:0010556	BP	regulation of macromolecule biosynthetic process	5.80E-06	0.0021
GO:0009737	BP	response to abscisic acid stimulus	6.00E-06	0.0021
GO:0006351	BP	transcription, DNA-dependent	6.50E-06	0.0021
GO:0006350	BP	transcription	6.80E-06	0.0021
GO:0060255	BP	regulation of macromolecule metabolic process	7.00E-06	0.0021
GO:0032774	BP	RNA biosynthetic process	7.10E-06	0.0021
GO:0006355	BP	regulation of transcription, DNA-dependent	7.70E-06	0.0022
GO:0009058	BP	biosynthetic process	8.00E-06	0.0022
GO:0051716	BP	cellular response to stimulus	8.20E-06	0.0022
GO:0045449	BP	regulation of transcription	8.40E-06	0.0022
GO:0031323	BP	regulation of cellular metabolic process	9.20E-06	0.0022
GO:0019538	BP	protein metabolic process	9.50E-06	0.0022
GO:0051252	BP	regulation of RNA metabolic process	9.60E-06	0.0022
GO:0033554	BP	cellular response to stress	1.30E-05	0.0030
GO:0010467	BP	gene expression	1.40E-05	0.0030
GO:0006950	BP	response to stress	1.50E-05	0.0030
GO:0010468	BP	regulation of gene expression	1.50E-05	0.0030
GO:0050793	BP	regulation of developmental process	1.60E-05	0.0031
GO:0031326	BP	regulation of cellular biosynthetic process	1.70E-05	0.0034
GO:0009889	BP	regulation of biosynthetic process	1.80E-05	0.0034

GO:0019222	BP	regulation of metabolic process	2.00E-05	0.0037
GO:0009719	BP	response to endogenous stimulus	2.10E-05	0.0037
GO:0010033	BP	response to organic substance	2.40E-05	0.0042
GO:0009753	BP	response to jasmonic acid stimulus	3.10E-05	0.0053
GO:0006139	BP	nucleobase, nucleoside, nucleotide and nucleic acid metabolic process	3.40E-05	0.0055
GO:0042221	BP	response to chemical stimulus	3.40E-05	0.0055
GO:0048580	BP	regulation of post-embryonic development	3.70E-05	0.0059
GO:0051239	BP	regulation of multicellular organismal process	4.80E-05	0.0074
GO:0044238	BP	primary metabolic process	5.00E-05	0.0075
GO:0051276	BP	chromosome organization	5.50E-05	0.0081
GO:0009751	BP	response to salicylic acid stimulus	5.70E-05	0.0082
GO:0007005	BP	mitochondrion organization	5.80E-05	0.0082
GO:0043687	BP	post-translational protein modification	5.90E-05	0.0082
GO:0000279	BP	M phase	6.20E-05	0.0084
GO:0009314	BP	response to radiation	6.50E-05	0.0086
GO:0043412	BP	macromolecule modification	7.40E-05	0.0097
GO:0009863	BP	salicylic acid mediated signaling pathway	7.70E-05	0.0098
GO:0071446	BP	cellular response to salicylic acid stimulus	7.70E-05	0.0098
GO:0009725	BP	response to hormone stimulus	7.90E-05	0.0098
GO:0006259	BP	DNA metabolic process	8.20E-05	0.010
GO:0007126	BP	meiosis	9.00E-05	0.010
GO:0006464	BP	protein modification process	9.00E-05	0.010
GO:0051327	BP	M phase of meiotic cell cycle	9.00E-05	0.010
GO:0008509	MF	anion transmembrane transporter activity	2.30E-05	0.013
GO:0005515	MF	protein binding	4.00E-05	0.013
GO:0003676	MF	nucleic acid binding	4.00E-05	0.013
GO:0003677	MF	DNA binding	5.80E-05	0.014
Downregulated (4V < NV) (*p* < 0.00001)				
GO:0044281	BP	small molecule metabolic process	7.50E-26	6.60E-22
GO:0009607	BP	response to biotic stimulus	1.10E-20	4.90E-17
GO:0050896	BP	response to stimulus	7.40E-19	1.70E-15
GO:0006082	BP	organic acid metabolic process	8.90E-19	1.70E-15
GO:0042180	BP	cellular ketone metabolic process	9.70E-19	1.70E-15
GO:0043436	BP	oxoacid metabolic process	1.40E-18	1.80E-15
GO:0019752	BP	carboxylic acid metabolic process	1.40E-18	1.80E-15
GO:0006066	BP	alcohol metabolic process	1.90E-18	2.10E-15
GO:0006950	BP	response to stress	2.20E-18	2.20E-15
GO:0044237	BP	cellular metabolic process	1.50E-17	1.40E-14
GO:0044283	BP	small molecule biosynthetic process	4.00E-17	3.20E-14
GO:0005996	BP	monosaccharide metabolic process	1.90E-16	1.40E-13
GO:0051707	BP	response to other organism	2.40E-16	1.60E-13
GO:0044262	BP	cellular carbohydrate metabolic process	2.60E-16	1.60E-13
GO:0005975	BP	carbohydrate metabolic process	3.60E-16	2.10E-13

GO:0044282	BP	small molecule catabolic process	4.80E-16	2.60E-13
GO:0009987	BP	cellular process	1.20E-15	6.30E-13
GO:0044271	BP	cellular nitrogen compound biosynthetic process	1.80E-15	8.60E-13
GO:0032787	BP	monocarboxylic acid metabolic process	4.20E-15	2.00E-12
GO:0009628	BP	response to abiotic stimulus	4.70E-15	2.10E-12
GO:0034641	BP	cellular nitrogen compound metabolic process	9.60E-15	4.00E-12
GO:0009056	BP	catabolic process	1.00E-14	4.10E-12
GO:0045087	BP	innate immune response	1.50E-14	5.70E-12
GO:0046394	BP	carboxylic acid biosynthetic process	1.70E-14	5.70E-12
GO:0016053	BP	organic acid biosynthetic process	1.70E-14	5.70E-12
GO:0044248	BP	cellular catabolic process	1.70E-14	5.70E-12
GO:0002376	BP	immune system process	2.10E-14	6.60E-12
GO:0006955	BP	immune response	2.10E-14	6.60E-12
GO:0044238	BP	primary metabolic process	2.40E-14	7.10E-12
GO:0051716	BP	cellular response to stimulus	2.40E-14	7.10E-12
GO:0006952	BP	defense response	2.70E-14	7.70E-12
GO:0006519	BP	cellular amino acid and derivative metabolic process	3.60E-14	1.00E-11
GO:0019748	BP	secondary metabolic process	6.40E-14	1.70E-11
GO:0033554	BP	cellular response to stress	1.80E-13	4.60E-11
GO:0009309	BP	amine biosynthetic process	2.40E-13	5.90E-11
GO:0009308	BP	amine metabolic process	2.90E-13	7.00E-11
GO:0009058	BP	biosynthetic process	3.50E-13	8.40E-11
GO:0051649	BP	establishment of localization in cell	4.60E-13	1.10E-10
GO:0051641	BP	cellular localization	5.50E-13	1.20E-10
GO:0008152	BP	metabolic process	8.10E-13	1.80E-10
GO:0010033	BP	response to organic substance	8.90E-13	1.90E-10
GO:0044106	BP	cellular amine metabolic process	1.00E-12	2.10E-10
GO:0046907	BP	intracellular transport	1.30E-12	2.60E-10
GO:0008652	BP	cellular amino acid biosynthetic process	1.40E-12	2.90E-10
GO:0009240	BP	isopentenyl diphosphate biosynthetic process	2.70E-12	5.10E-10
GO:0046490	BP	isopentenyl diphosphate metabolic process	2.70E-12	5.10E-10
GO:0019288	BP	isopentenyl diphosphate biosynthetic process, mevalonate-independent pathway	4.90E-12	9.20E-10
GO:0009651	BP	response to salt stress	5.10E-12	9.30E-10
GO:0044255	BP	cellular lipid metabolic process	5.50E-12	9.80E-10
GO:0065008	BP	regulation of biological quality	5.60E-12	9.80E-10
GO:0051186	BP	cofactor metabolic process	7.30E-12	1.30E-09
GO:0065007	BP	biological regulation	9.40E-12	1.60E-09
GO:0044267	BP	cellular protein metabolic process	1.20E-11	2.00E-09
GO:0016043	BP	cellular component organization	1.20E-11	2.00E-09
GO:0044260	BP	cellular macromolecule metabolic process	1.40E-11	2.20E-09
GO:0006970	BP	response to osmotic stress	1.50E-11	2.40E-09
GO:0019682	BP	glyceraldehyde-3-phosphate metabolic process	1.60E-11	2.50E-09

GO:0006725	BP	cellular aromatic compound metabolic process	1.70E-11	2.60E-09
GO:0008610	BP	lipid biosynthetic process	1.80E-11	2.70E-09
GO:0046483	BP	heterocycle metabolic process	1.90E-11	2.80E-09
GO:0044249	BP	cellular biosynthetic process	2.00E-11	2.80E-09
GO:0006629	BP	lipid metabolic process	2.50E-11	3.50E-09
GO:0009617	BP	response to bacterium	3.00E-11	4.10E-09
GO:0043170	BP	macromolecule metabolic process	3.00E-11	4.10E-09
GO:0042221	BP	response to chemical stimulus	7.70E-11	1.00E-08
GO:0006520	BP	cellular amino acid metabolic process	9.90E-11	1.30E-08
GO:0008299	BP	isoprenoid biosynthetic process	1.60E-10	2.10E-08
GO:0051704	BP	multi-organism process	1.60E-10	2.10E-08
GO:0009814	BP	defense response, incompatible interaction	1.70E-10	2.10E-08
GO:0006720	BP	isoprenoid metabolic process	1.70E-10	2.20E-08
GO:0044272	BP	sulfur compound biosynthetic process	1.80E-10	2.30E-08
GO:0042742	BP	defense response to bacterium	2.40E-10	2.90E-08
GO:0009627	BP	systemic acquired resistance	2.70E-10	3.20E-08
GO:0006090	BP	pyruvate metabolic process	3.90E-10	4.60E-08
GO:0044265	BP	cellular macromolecule catabolic process	4.00E-10	4.70E-08
GO:0009057	BP	macromolecule catabolic process	4.50E-10	5.20E-08
GO:0016054	BP	organic acid catabolic process	5.90E-10	6.60E-08
GO:0046395	BP	carboxylic acid catabolic process	5.90E-10	6.60E-08
GO:0034976	BP	response to endoplasmic reticulum stress	6.00E-10	6.70E-08
GO:0018130	BP	heterocycle biosynthetic process	7.20E-10	7.90E-08
GO:0019538	BP	protein metabolic process	7.90E-10	8.60E-08
GO:0006807	BP	nitrogen compound metabolic process	8.40E-10	8.90E-08
GO:0006996	BP	organelle organization	1.50E-09	1.50E-07
GO:0043412	BP	macromolecule modification	1.50E-09	1.60E-07
GO:0006644	BP	phospholipid metabolic process	1.60E-09	1.70E-07
GO:0009719	BP	response to endogenous stimulus	1.70E-09	1.80E-07
GO:0008104	BP	protein localization	2.00E-09	2.10E-07
GO:0051234	BP	establishment of localization	2.10E-09	2.10E-07
GO:0023052	BP	signaling	2.30E-09	2.30E-07
GO:0009069	BP	serine family amino acid metabolic process	2.40E-09	2.30E-07
GO:0006006	BP	glucose metabolic process	2.90E-09	2.80E-07
GO:0045184	BP	establishment of protein localization	3.00E-09	2.80E-07
GO:0015031	BP	protein transport	3.00E-09	2.80E-07
GO:0051179	BP	localization	3.50E-09	3.30E-07
GO:0006732	BP	coenzyme metabolic process	3.50E-09	3.30E-07
GO:0009310	BP	amine catabolic process	3.80E-09	3.40E-07
GO:0009072	BP	aromatic amino acid family metabolic process	3.80E-09	3.40E-07
GO:0070887	BP	cellular response to chemical stimulus	3.80E-09	3.40E-07
GO:0050832	BP	defense response to fungus	4.00E-09	3.50E-07
GO:0006605	BP	protein targeting	4.10E-09	3.60E-07

GO:0006081	BP	cellular aldehyde metabolic process	5.20E-09	4.50E-07
GO:0016052	BP	carbohydrate catabolic process	5.80E-09	5.00E-07
GO:0019318	BP	hexose metabolic process	6.30E-09	5.30E-07
GO:0006790	BP	sulfur metabolic process	6.90E-09	5.80E-07
GO:0044275	BP	cellular carbohydrate catabolic process	7.60E-09	6.30E-07
GO:0019320	BP	hexose catabolic process	8.30E-09	6.80E-07
GO:0006007	BP	glucose catabolic process	8.30E-09	6.80E-07
GO:0009620	BP	response to fungus	9.00E-09	7.30E-07
GO:0032502	BP	developmental process	9.40E-09	7.60E-07
GO:0006810	BP	transport	9.80E-09	7.80E-07
GO:0008654	BP	phospholipid biosynthetic process	1.00E-08	7.90E-07
GO:0042402	BP	cellular biogenic amine catabolic process	1.00E-08	7.90E-07
GO:0019637	BP	organophosphate metabolic process	1.00E-08	8.10E-07
GO:0006464	BP	protein modification process	1.10E-08	8.60E-07
GO:0043933	BP	macromolecular complex subunit organization	1.30E-08	1.00E-06
GO:0046365	BP	monosaccharide catabolic process	1.50E-08	1.10E-06
GO:0009725	BP	response to hormone stimulus	1.60E-08	1.20E-06
GO:0042445	BP	hormone metabolic process	1.60E-08	1.20E-06
GO:0042446	BP	hormone biosynthetic process	1.70E-08	1.20E-06
GO:0009737	BP	response to abscisic acid stimulus	1.80E-08	1.30E-06
GO:0034613	BP	cellular protein localization	1.80E-08	1.30E-06
GO:0046164	BP	alcohol catabolic process	2.00E-08	1.40E-06
GO:0050789	BP	regulation of biological process	2.10E-08	1.50E-06
GO:0034621	BP	cellular macromolecular complex subunit organization	2.10E-08	1.50E-06
GO:0006886	BP	intracellular protein transport	2.50E-08	1.80E-06
GO:0008219	BP	cell death	2.60E-08	1.80E-06
GO:0071310	BP	cellular response to organic substance	2.60E-08	1.80E-06
GO:0016265	BP	death	2.60E-08	1.80E-06
GO:0006091	BP	generation of precursor metabolites and energy	2.90E-08	2.00E-06
GO:0009791	BP	post-embryonic development	2.90E-08	2.00E-06
GO:0048518	BP	positive regulation of biological process	2.90E-08	2.00E-06
GO:0070727	BP	cellular macromolecule localization	3.00E-08	2.00E-06
GO:0009891	BP	positive regulation of biosynthetic process	3.30E-08	2.10E-06
GO:0031328	BP	positive regulation of cellular biosynthetic process	3.30E-08	2.10E-06
GO:0009893	BP	positive regulation of metabolic process	3.40E-08	2.20E-06
GO:0019438	BP	aromatic compound biosynthetic process	5.00E-08	3.20E-06
GO:0065003	BP	macromolecular complex assembly	5.00E-08	3.20E-06
GO:0009657	BP	plastid organization	5.10E-08	3.20E-06
GO:0000097	BP	sulfur amino acid biosynthetic process	5.40E-08	3.40E-06
GO:0032501	BP	multicellular organismal process	6.00E-08	3.80E-06
GO:0010817	BP	regulation of hormone levels	7.20E-08	4.50E-06
GO:0015979	BP	photosynthesis	7.20E-08	4.50E-06

GO:0051188	BP	cofactor biosynthetic process	8.10E-08	4.90E-06
GO:0034622	BP	cellular macromolecular complex assembly	8.10E-08	4.90E-06
GO:0048583	BP	regulation of response to stimulus	8.20E-08	4.90E-06
GO:0009070	BP	serine family amino acid biosynthetic process	8.80E-08	5.30E-06
GO:0048856	BP	anatomical structure development	9.00E-08	5.40E-06
GO:0031325	BP	positive regulation of cellular metabolic process	9.10E-08	5.40E-06
GO:0007275	BP	multicellular organismal development	1.20E-07	7.10E-06
GO:0006396	BP	RNA processing	1.20E-07	7.20E-06
GO:0051789	BP	response to protein stimulus	1.20E-07	7.20E-06
GO:0016109	BP	tetraterpenoid biosynthetic process	1.80E-07	1.00E-05
GO:0016117	BP	carotenoid biosynthetic process	1.80E-07	1.00E-05
GO:0006461	BP	protein complex assembly	1.80E-07	1.00E-05
GO:0070271	BP	protein complex biogenesis	1.80E-07	1.00E-05
GO:0034050	BP	host programmed cell death induced by symbiont	2.00E-07	1.10E-05
GO:0007242	BP	intracellular signaling cascade	2.10E-07	1.20E-05
GO:0046148	BP	pigment biosynthetic process	2.10E-07	1.20E-05
GO:0012501	BP	programmed cell death	2.40E-07	1.30E-05
GO:0007165	BP	signal transduction	2.40E-07	1.30E-05
GO:0042219	BP	cellular amino acid derivative catabolic process	2.70E-07	1.50E-05
GO:0043623	BP	cellular protein complex assembly	2.90E-07	1.60E-05
GO:0009751	BP	response to salicylic acid stimulus	3.00E-07	1.60E-05
GO:0019725	BP	cellular homeostasis	3.30E-07	1.80E-05
GO:0009626	BP	plant-type hypersensitive response	3.70E-07	2.00E-05
GO:0043687	BP	post-translational protein modification	3.80E-07	2.00E-05
GO:0033036	BP	macromolecule localization	4.00E-07	2.10E-05
GO:0042440	BP	pigment metabolic process	4.20E-07	2.20E-05
GO:0006612	BP	protein targeting to membrane	4.40E-07	2.30E-05
GO:0048519	BP	negative regulation of biological process	4.70E-07	2.40E-05
GO:0080134	BP	regulation of response to stress	4.80E-07	2.50E-05
GO:0006575	BP	cellular amino acid derivative metabolic process	5.00E-07	2.50E-05
GO:0023046	BP	signaling process	5.50E-07	2.80E-05
GO:0023060	BP	signal transmission	5.50E-07	2.80E-05
GO:0009063	BP	cellular amino acid catabolic process	5.60E-07	2.80E-05
GO:0031347	BP	regulation of defense response	5.90E-07	3.00E-05
GO:0009790	BP	embryonic development	6.00E-07	3.00E-05
GO:0022607	BP	cellular component assembly	6.70E-07	3.30E-05
GO:0009605	BP	response to external stimulus	6.70E-07	3.30E-05
GO:0016108	BP	tetraterpenoid metabolic process	6.80E-07	3.30E-05
GO:0016116	BP	carotenoid metabolic process	6.80E-07	3.30E-05
GO:0043090	BP	amino acid import	9.10E-07	4.40E-05
GO:0006873	BP	cellular ion homeostasis	9.50E-07	4.50E-05
GO:0009696	BP	salicylic acid metabolic process	1.00E-06	4.80E-05

GO:0044422	CC	organelle part	7.50E-21	6.50E-18
GO:0044446	CC	intracellular organelle part	2.30E-20	1.00E-17
GO:0005829	CC	cytosol	4.20E-17	1.20E-14
GO:0009507	CC	chloroplast	2.10E-16	4.40E-14
GO:0009536	CC	plastid	4.80E-16	8.30E-14
GO:0044435	CC	plastid part	5.30E-15	7.50E-13
GO:0044434	CC	chloroplast part	1.10E-14	1.30E-12
GO:0016020	CC	membrane	1.90E-12	2.00E-10
GO:0009570	CC	chloroplast stroma	2.10E-12	2.00E-10
GO:0044444	CC	cytoplasmic part	3.70E-12	3.10E-10
GO:0009532	CC	plastid stroma	5.70E-12	4.20E-10
GO:0005737	CC	cytoplasm	5.90E-12	4.20E-10
GO:0005886	CC	plasma membrane	4.30E-11	2.90E-09
GO:0031090	CC	organelle membrane	9.70E-11	5.90E-09
GO:0005911	CC	cell-cell junction	4.40E-09	2.50E-07
GO:0030054	CC	cell junction	6.80E-09	3.60E-07
GO:0009506	CC	plasmodesma	7.50E-09	3.60E-07
GO:0055044	CC	symplast	7.50E-09	3.60E-07
GO:0005794	CC	Golgi apparatus	1.00E-08	4.60E-07
GO:0043234	CC	protein complex	1.90E-08	8.30E-07
GO:0031967	CC	organelle envelope	4.60E-08	1.80E-06
GO:0031975	CC	envelope	4.60E-08	1.80E-06
GO:0044459	CC	plasma membrane part	7.40E-08	2.70E-06
GO:0032991	CC	macromolecular complex	7.40E-08	2.70E-06
GO:0005618	CC	cell wall	1.30E-07	4.60E-06
GO:0044436	CC	thylakoid part	1.60E-07	5.20E-06
GO:0030312	CC	external encapsulating structure	1.60E-07	5.20E-06
GO:0009579	CC	thylakoid	2.50E-07	7.60E-06
GO:0055035	CC	plastid thylakoid membrane	2.80E-07	8.30E-06
GO:0031984	CC	organelle subcompartment	3.40E-07	9.70E-06
GO:0031976	CC	plastid thylakoid	4.40E-07	1.20E-05
GO:0009534	CC	chloroplast thylakoid	4.40E-07	1.20E-05
GO:0009535	CC	chloroplast thylakoid membrane	5.70E-07	1.50E-05
GO:0044425	CC	membrane part	8.30E-07	2.10E-05
GO:0005515	MF	protein binding	6.80E-15	1.10E-11
GO:0003824	MF	catalytic activity	2.70E-10	2.30E-07
GO:0016740	MF	transferase activity	2.20E-08	1.20E-05
GO:0005488	MF	binding	5.70E-08	2.40E-05
GO:0042578	MF	phosphoric ester hydrolase activity	7.80E-08	2.60E-05

NV, non-vernalized samples

4V, samples with four weeks of cold treatment

CC, Cellular component; MF, Molecular function; BP, Biological process

Table IV-8. List of overrepresented GO terms in genes differential expression between 6V and NV

GO accession	Term type	Term	*p* value	FDR
Upregulated (6V > NV) (*p* < 0.0001)				
GO:0009628	BP	response to abiotic stimulus	5.20E-10	3.20E-06
GO:0044267	BP	cellular protein metabolic process	2.60E-09	8.10E-06
GO:0044260	BP	cellular macromolecule metabolic process	7.90E-09	1.60E-05
GO:0009408	BP	response to heat	2.00E-08	3.10E-05
GO:0042221	BP	response to chemical stimulus	2.50E-08	3.10E-05
GO:0009266	BP	response to temperature stimulus	5.10E-08	3.90E-05
GO:0043170	BP	macromolecule metabolic process	5.20E-08	3.90E-05
GO:0009651	BP	response to salt stress	5.90E-08	3.90E-05
GO:0006020	BP	inositol metabolic process	6.10E-08	3.90E-05
GO:0043647	BP	inositol phosphate metabolic process	6.80E-08	3.90E-05
GO:0019538	BP	protein metabolic process	6.90E-08	3.90E-05
GO:0010033	BP	response to organic substance	1.30E-07	6.60E-05
GO:0009058	BP	biosynthetic process	1.80E-07	8.30E-05
GO:0006970	BP	response to osmotic stress	2.10E-07	8.80E-05
GO:0006950	BP	response to stress	2.20E-07	8.80E-05
GO:0009059	BP	macromolecule biosynthetic process	2.40E-07	9.10E-05
GO:0044249	BP	cellular biosynthetic process	4.60E-07	0.00016
GO:0044237	BP	cellular metabolic process	4.80E-07	0.00016
GO:0034645	BP	cellular macromolecule biosynthetic process	4.90E-07	0.00016
GO:0009644	BP	response to high light intensity	6.20E-07	0.00019
GO:0010467	BP	gene expression	1.20E-06	0.00034
GO:0009743	BP	response to carbohydrate stimulus	1.80E-06	0.00052
GO:0044238	BP	primary metabolic process	1.90E-06	0.00052
GO:0042538	BP	hyperosmotic salinity response	2.00E-06	0.00052
GO:0043412	BP	macromolecule modification	2.20E-06	0.00053
GO:0009753	BP	response to jasmonic acid stimulus	2.60E-06	0.00062
GO:0009414	BP	response to water deprivation	2.90E-06	0.00065
GO:0050896	BP	response to stimulus	2.90E-06	0.00065
GO:0010264	BP	myo-inositol hexakisphosphate biosynthetic process	3.40E-06	0.00066
GO:0032958	BP	inositol phosphate biosynthetic process	3.40E-06	0.00066
GO:0033517	BP	myo-inositol hexakisphosphate metabolic process	3.40E-06	0.00066
GO:0006021	BP	inositol biosynthetic process	3.40E-06	0.00066
GO:0019751	BP	polyol metabolic process	3.80E-06	0.00070
GO:0009415	BP	response to water	4.10E-06	0.00074
GO:0007242	BP	intracellular signaling cascade	4.70E-06	0.00083
GO:0009314	BP	response to radiation	5.10E-06	0.00085
GO:0016070	BP	RNA metabolic process	5.10E-06	0.00085
GO:0006457	BP	protein folding	6.40E-06	0.0010

GO:0009737	BP	response to abscisic acid stimulus	6.80E-06	0.0011
GO:0009416	BP	response to light stimulus	1.00E-05	0.0016
GO:0050794	BP	regulation of cellular process	1.00E-05	0.0016
GO:0050789	BP	regulation of biological process	1.30E-05	0.0019
GO:0006979	BP	response to oxidative stress	1.30E-05	0.0019
GO:0051171	BP	regulation of nitrogen compound metabolic process	1.30E-05	0.0019
GO:0006139	BP	nucleobase, nucleoside, nucleotide and nucleic acid metabolic process	1.40E-05	0.0020
GO:0000302	BP	response to reactive oxygen species	1.50E-05	0.0020
GO:0009751	BP	response to salicylic acid stimulus	1.60E-05	0.0020
GO:0006839	BP	mitochondrial transport	1.90E-05	0.0024
GO:0009987	BP	cellular process	1.90E-05	0.0024
GO:0019219	BP	regulation of nucleobase, nucleoside, nucleotide and nucleic acid metabolic process	2.10E-05	0.0026
GO:0031326	BP	regulation of cellular biosynthetic process	2.30E-05	0.0028
GO:0009642	BP	response to light intensity	2.40E-05	0.0028
GO:0009889	BP	regulation of biosynthetic process	2.40E-05	0.0028
GO:0070887	BP	cellular response to chemical stimulus	2.50E-05	0.0028
GO:0031323	BP	regulation of cellular metabolic process	2.50E-05	0.0028
GO:0010468	BP	regulation of gene expression	2.70E-05	0.0030
GO:0006464	BP	protein modification process	2.80E-05	0.0030
GO:0010556	BP	regulation of macromolecule biosynthetic process	2.90E-05	0.0030
GO:0060255	BP	regulation of macromolecule metabolic process	3.00E-05	0.0031
GO:0080090	BP	regulation of primary metabolic process	3.30E-05	0.0034
GO:0006351	BP	transcription, DNA-dependent	3.50E-05	0.0035
GO:0006350	BP	transcription	3.60E-05	0.0036
GO:0051252	BP	regulation of RNA metabolic process	3.70E-05	0.0036
GO:0032774	BP	RNA biosynthetic process	3.80E-05	0.0036
GO:0023052	BP	signaling	3.80E-05	0.0036
GO:0051716	BP	cellular response to stimulus	4.20E-05	0.0039
GO:0033554	BP	cellular response to stress	4.30E-05	0.0040
GO:0006355	BP	regulation of transcription, DNA-dependent	4.60E-05	0.0042
GO:0010200	BP	response to chitin	4.70E-05	0.0042
GO:0045449	BP	regulation of transcription	4.90E-05	0.0043
GO:0019222	BP	regulation of metabolic process	5.10E-05	0.0044
GO:0046173	BP	polyol biosynthetic process	5.80E-05	0.0049
GO:0007165	BP	signal transduction	6.20E-05	0.0052
GO:0006605	BP	protein targeting	7.90E-05	0.0066
GO:0043687	BP	post-translational protein modification	8.60E-05	0.0070
GO:0009610	BP	response to symbiotic fungus	9.10E-05	0.0073
GO:0008152	BP	metabolic process	9.30E-05	0.0074
GO:0009863	BP	salicylic acid mediated signaling pathway	9.50E-05	0.0074
GO:0071446	BP	cellular response to salicylic acid stimulus	9.50E-05	0.0074
GO:0001510	BP	RNA methylation	0.00010	0.0077

GO:0032991	CC	macromolecular complex	1.70E-06	0.0010
GO:0044429	CC	mitochondrial part	5.70E-06	0.0017
GO:0022627	CC	cytosolic small ribosomal subunit	1.00E-05	0.0020
GO:0005740	CC	mitochondrial envelope	2.60E-05	0.0039
GO:0031966	CC	mitochondrial membrane	3.60E-05	0.0039
GO:0015935	CC	small ribosomal subunit	3.90E-05	0.0039
GO:0044446	CC	intracellular organelle part	6.00E-05	0.0049
GO:0044422	CC	organelle part	6.70E-05	0.0049
GO:0043234	CC	protein complex	7.80E-05	0.0052
GO:0016020	CC	membrane	8.80E-05	0.0052
GO:0005634	CC	nucleus	0.00010	0.0056
GO:0003676	MF	nucleic acid binding	3.20E-05	0.027
GO:0003677	MF	DNA binding	9.50E-05	0.040
Downregulated (6V < NV) (*p* < 0.00001)				
GO:0044281	BP	small molecule metabolic process	9.80E-14	7.60E-10
GO:0009607	BP	response to biotic stimulus	9.00E-13	3.50E-09
GO:0010033	BP	response to organic substance	5.70E-12	1.50E-08
GO:0044282	BP	small molecule catabolic process	1.10E-11	2.10E-08
GO:0006952	BP	defense response	2.10E-11	3.30E-08
GO:0051707	BP	response to other organism	5.40E-11	6.30E-08
GO:0044237	BP	cellular metabolic process	5.70E-11	6.30E-08
GO:0050896	BP	response to stimulus	6.50E-11	6.30E-08
GO:0046907	BP	intracellular transport	1.00E-10	8.80E-08
GO:0051641	BP	cellular localization	1.30E-10	9.90E-08
GO:0006950	BP	response to stress	1.40E-10	1.00E-07
GO:0051649	BP	establishment of localization in cell	1.50E-10	1.00E-07
GO:0009987	BP	cellular process	2.20E-10	1.30E-07
GO:0043436	BP	oxoacid metabolic process	2.70E-10	1.40E-07
GO:0019752	BP	carboxylic acid metabolic process	2.70E-10	1.40E-07
GO:0006082	BP	organic acid metabolic process	2.90E-10	1.40E-07
GO:0002376	BP	immune system process	3.30E-10	1.40E-07
GO:0006955	BP	immune response	3.30E-10	1.40E-07
GO:0006519	BP	cellular amino acid and derivative metabolic process	3.70E-10	1.50E-07
GO:0042180	BP	cellular ketone metabolic process	3.80E-10	1.50E-07
GO:0042402	BP	cellular biogenic amine catabolic process	4.20E-10	1.50E-07
GO:0045087	BP	innate immune response	1.50E-09	5.20E-07
GO:0042742	BP	defense response to bacterium	1.80E-09	6.20E-07
GO:0009308	BP	amine metabolic process	2.50E-09	8.00E-07
GO:0044106	BP	cellular amine metabolic process	2.80E-09	8.80E-07
GO:0009617	BP	response to bacterium	3.60E-09	1.10E-06
GO:0048583	BP	regulation of response to stimulus	4.10E-09	1.20E-06
GO:0044283	BP	small molecule biosynthetic process	5.10E-09	1.40E-06
GO:0009056	BP	catabolic process	5.60E-09	1.50E-06

GO:0044248	BP	cellular catabolic process	6.20E-09	1.60E-06
GO:0006576	BP	cellular biogenic amine metabolic process	6.50E-09	1.60E-06
GO:0034613	BP	cellular protein localization	6.90E-09	1.60E-06
GO:0070727	BP	cellular macromolecule localization	6.90E-09	1.60E-06
GO:0044238	BP	primary metabolic process	7.20E-09	1.60E-06
GO:0042219	BP	cellular amino acid derivative catabolic process	8.00E-09	1.80E-06
GO:0042221	BP	response to chemical stimulus	8.30E-09	1.80E-06
GO:0005975	BP	carbohydrate metabolic process	9.20E-09	1.90E-06
GO:0046394	BP	carboxylic acid biosynthetic process	1.00E-08	2.00E-06
GO:0006605	BP	protein targeting	1.00E-08	2.00E-06
GO:0016053	BP	organic acid biosynthetic process	1.00E-08	2.00E-06
GO:0006970	BP	response to osmotic stress	1.10E-08	2.10E-06
GO:0009651	BP	response to salt stress	1.10E-08	2.10E-06
GO:0080134	BP	regulation of response to stress	1.20E-08	2.10E-06
GO:0006886	BP	intracellular protein transport	1.20E-08	2.20E-06
GO:0006725	BP	cellular aromatic compound metabolic process	1.50E-08	2.60E-06
GO:0051234	BP	establishment of localization	1.70E-08	2.90E-06
GO:0034641	BP	cellular nitrogen compound metabolic process	2.10E-08	3.50E-06
GO:0065007	BP	biological regulation	2.80E-08	4.50E-06
GO:0009751	BP	response to salicylic acid stimulus	3.00E-08	4.80E-06
GO:0009719	BP	response to endogenous stimulus	3.30E-08	5.10E-06
GO:0050832	BP	defense response to fungus	3.90E-08	6.00E-06
GO:0006575	BP	cellular amino acid derivative metabolic process	4.20E-08	6.30E-06
GO:0031347	BP	regulation of defense response	4.60E-08	6.70E-06
GO:0051179	BP	localization	4.60E-08	6.70E-06
GO:0044275	BP	cellular carbohydrate catabolic process	5.40E-08	7.50E-06
GO:0016052	BP	carbohydrate catabolic process	5.50E-08	7.60E-06
GO:0006810	BP	transport	5.80E-08	7.90E-06
GO:0044271	BP	cellular nitrogen compound biosynthetic process	6.30E-08	8.40E-06
GO:0016043	BP	cellular component organization	6.60E-08	8.70E-06
GO:0008152	BP	metabolic process	6.90E-08	8.90E-06
GO:0006520	BP	cellular amino acid metabolic process	9.20E-08	1.20E-05
GO:0045184	BP	establishment of protein localization	9.40E-08	1.20E-05
GO:0015031	BP	protein transport	9.40E-08	1.20E-05
GO:0008104	BP	protein localization	1.10E-07	1.30E-05
GO:0006066	BP	alcohol metabolic process	1.10E-07	1.30E-05
GO:0051716	BP	cellular response to stimulus	1.20E-07	1.40E-05
GO:0034621	BP	cellular macromolecular complex subunit organization	1.20E-07	1.40E-05
GO:0019748	BP	secondary metabolic process	1.40E-07	1.60E-05
GO:0050789	BP	regulation of biological process	1.50E-07	1.70E-05
GO:0032787	BP	monocarboxylic acid metabolic process	1.80E-07	2.00E-05

GO:0043933	BP	macromolecular complex subunit organization	1.90E-07	2.10E-05
GO:0048518	BP	positive regulation of biological process	2.20E-07	2.40E-05
GO:0009891	BP	positive regulation of biosynthetic process	3.10E-07	3.20E-05
GO:0031328	BP	positive regulation of cellular biosynthetic process	3.10E-07	3.20E-05
GO:0046395	BP	carboxylic acid catabolic process	3.20E-07	3.30E-05
GO:0016054	BP	organic acid catabolic process	3.20E-07	3.30E-05
GO:0044085	BP	cellular component biogenesis	3.30E-07	3.40E-05
GO:0009310	BP	amine catabolic process	3.50E-07	3.50E-05
GO:0009814	BP	defense response, incompatible interaction	3.50E-07	3.50E-05
GO:0009893	BP	positive regulation of metabolic process	3.90E-07	3.70E-05
GO:0012501	BP	programmed cell death	3.90E-07	3.70E-05
GO:0044262	BP	cellular carbohydrate metabolic process	5.20E-07	4.90E-05
GO:0009309	BP	amine biosynthetic process	5.30E-07	4.90E-05
GO:0031325	BP	positive regulation of cellular metabolic process	5.70E-07	5.20E-05
GO:0044260	BP	cellular macromolecule metabolic process	5.90E-07	5.40E-05
GO:0009057	BP	macromolecule catabolic process	6.60E-07	5.90E-05
GO:0008219	BP	cell death	6.80E-07	6.00E-05
GO:0016265	BP	death	6.80E-07	6.00E-05
GO:0006612	BP	protein targeting to membrane	7.00E-07	6.10E-05
GO:0019438	BP	aromatic compound biosynthetic process	7.40E-07	6.40E-05
GO:0044265	BP	cellular macromolecule catabolic process	7.50E-07	6.40E-05
GO:0043170	BP	macromolecule metabolic process	7.90E-07	6.60E-05
GO:0006569	BP	tryptophan catabolic process	8.30E-07	6.80E-05
GO:0046218	BP	indolalkylamine catabolic process	8.30E-07	6.80E-05
GO:0009058	BP	biosynthetic process	8.60E-07	7.00E-05
GO:0048519	BP	negative regulation of biological process	9.00E-07	7.20E-05
GO:0009725	BP	response to hormone stimulus	9.00E-07	7.20E-05
GO:0009626	BP	plant-type hypersensitive response	9.70E-07	7.70E-05
GO:0005829	CC	cytosol	4.20E-10	2.80E-07
GO:0044422	CC	organelle part	8.70E-08	2.30E-05
GO:0044446	CC	intracellular organelle part	1.00E-07	2.30E-05
GO:0016020	CC	membrane	1.70E-07	2.80E-05
GO:0031090	CC	organelle membrane	2.10E-07	2.80E-05
GO:0003824	MF	catalytic activity	7.20E-07	0.00086

NV, non-vernalized samples

6V, samples with six weeks of cold treatment

CC, Cellular component; MF, Molecular function; BP, Biological process

Table IV-9. List of overrepresented GO terms in genes differential expression between 6V7N and NV

GO accession	Term type	Term	*p* value	FDR
Upregulated (6V7N > NV) (*p* < 0.0001)				
GO:0009056	BP	catabolic process	1.30E-06	0.0063
GO:0009628	BP	response to abiotic stimulus	2.10E-06	0.0063
GO:0044267	BP	cellular protein metabolic process	3.10E-06	0.0063
GO:0019538	BP	protein metabolic process	8.80E-06	0.013
GO:0009408	BP	response to heat	1.60E-05	0.014
GO:0044248	BP	cellular catabolic process	1.70E-05	0.014
GO:0050896	BP	response to stimulus	1.80E-05	0.014
GO:0009314	BP	response to radiation	1.80E-05	0.014
GO:0006950	BP	response to stress	3.00E-05	0.019
GO:0006464	BP	protein modification process	3.10E-05	0.019
GO:0009057	BP	macromolecule catabolic process	4.80E-05	0.026
GO:0043170	BP	macromolecule metabolic process	6.30E-05	0.032
GO:0000302	BP	response to reactive oxygen species	8.80E-05	0.039
GO:0043412	BP	macromolecule modification	8.80E-05	0.039
GO:0016607	CC	nuclear speck	1.90E-05	0.0099
GO:0008270	MF	zinc ion binding	3.90E-07	0.0003
GO:0005342	MF	organic acid transmembrane transporter activity	1.20E-05	0.0031
GO:0046943	MF	carboxylic acid transmembrane transporter activity	1.60E-05	0.0031
GO:0046872	MF	metal ion binding	1.60E-05	0.0031
GO:0043167	MF	ion binding	3.50E-05	0.0044
GO:0043169	MF	cation binding	3.50E-05	0.0044
GO:0016790	MF	thiolester hydrolase activity	7.30E-05	0.0079
Downregulated (6V7N < NV) (*p* < 0.00001)				
GO:0044281	BP	small molecule metabolic process	5.80E-35	5.60E-31
GO:0044237	BP	cellular metabolic process	1.20E-29	5.90E-26
GO:0044267	BP	cellular protein metabolic process	2.70E-29	8.50E-26
GO:0009987	BP	cellular process	3.20E-27	7.60E-24
GO:0046907	BP	intracellular transport	3.00E-25	5.10E-22
GO:0019538	BP	protein metabolic process	3.20E-25	5.10E-22
GO:0044260	BP	cellular macromolecule metabolic process	3.80E-25	5.20E-22
GO:0051649	BP	establishment of localization in cell	9.70E-25	1.20E-21

GO:0043170	BP	macromolecule metabolic process	1.50E-24	1.60E-21
GO:0051641	BP	cellular localization	3.10E-24	2.90E-21
GO:0043412	BP	macromolecule modification	3.70E-24	3.20E-21
GO:0044238	BP	primary metabolic process	7.90E-23	6.30E-20
GO:0042180	BP	cellular ketone metabolic process	8.90E-22	5.70E-19
GO:0043436	BP	oxoacid metabolic process	9.00E-22	5.70E-19
GO:0019752	BP	carboxylic acid metabolic process	9.00E-22	5.70E-19
GO:0009057	BP	macromolecule catabolic process	1.00E-21	6.00E-19
GO:0006082	BP	organic acid metabolic process	1.10E-21	6.00E-19
GO:0050896	BP	response to stimulus	1.50E-21	8.10E-19
GO:0044265	BP	cellular macromolecule catabolic process	2.00E-21	1.00E-18
GO:0016043	BP	cellular component organization	2.20E-21	1.10E-18
GO:0005996	BP	monosaccharide metabolic process	2.50E-21	1.10E-18
GO:0009058	BP	biosynthetic process	2.90E-21	1.20E-18
GO:0044249	BP	cellular biosynthetic process	7.10E-21	2.90E-18
GO:0006807	BP	nitrogen compound metabolic process	1.40E-20	5.50E-18
GO:0009628	BP	response to abiotic stimulus	1.70E-20	6.60E-18
GO:0006066	BP	alcohol metabolic process	1.80E-20	6.70E-18
GO:0008152	BP	metabolic process	2.90E-20	1.00E-17
GO:0009056	BP	catabolic process	7.60E-20	2.60E-17
GO:0044248	BP	cellular catabolic process	2.00E-19	6.50E-17
GO:0044262	BP	cellular carbohydrate metabolic process	3.90E-19	1.20E-16
GO:0009607	BP	response to biotic stimulus	5.30E-19	1.60E-16
GO:0006396	BP	RNA processing	7.10E-19	2.10E-16
GO:0010033	BP	response to organic substance	8.10E-19	2.30E-16
GO:0006464	BP	protein modification process	5.20E-18	1.50E-15
GO:0005975	BP	carbohydrate metabolic process	6.40E-18	1.70E-15
GO:0070887	BP	cellular response to chemical stimulus	9.10E-18	2.40E-15
GO:0051716	BP	cellular response to stimulus	1.30E-17	3.30E-15
GO:0044283	BP	small molecule biosynthetic process	1.50E-17	3.70E-15
GO:0006950	BP	response to stress	3.60E-17	8.90E-15
GO:0006605	BP	protein targeting	4.90E-17	1.20E-14
GO:0045184	BP	establishment of protein localization	7.60E-17	1.70E-14
GO:0015031	BP	protein transport	7.60E-17	1.70E-14
GO:0042221	BP	response to chemical stimulus	9.80E-17	2.20E-14
GO:0071310	BP	cellular response to organic substance	1.20E-16	2.60E-14

GO:0034613	BP	cellular protein localization	2.00E-16	4.10E-14
GO:0006886	BP	intracellular protein transport	2.00E-16	4.20E-14
GO:0070727	BP	cellular macromolecule localization	2.40E-16	4.90E-14
GO:0006139	BP	nucleobase, nucleoside, nucleotide and nucleic acid metabolic process	2.50E-16	5.00E-14
GO:0008104	BP	protein localization	2.70E-16	5.30E-14
GO:0006006	BP	glucose metabolic process	3.20E-16	6.10E-14
GO:0044085	BP	cellular component biogenesis	6.40E-16	1.20E-13
GO:0019318	BP	hexose metabolic process	9.80E-16	1.80E-13
GO:0006996	BP	organelle organization	2.60E-15	4.60E-13
GO:0016052	BP	carbohydrate catabolic process	2.90E-15	5.10E-13
GO:0051234	BP	establishment of localization	3.20E-15	5.40E-13
GO:0001510	BP	RNA methylation	3.20E-15	5.40E-13
GO:0006753	BP	nucleoside phosphate metabolic process	4.00E-15	6.70E-13
GO:0009117	BP	nucleotide metabolic process	5.80E-15	9.60E-13
GO:0034641	BP	cellular nitrogen compound metabolic process	6.80E-15	1.10E-12
GO:0051179	BP	localization	1.00E-14	1.60E-12
GO:0006810	BP	transport	1.20E-14	1.90E-12
GO:0043687	BP	post-translational protein modification	1.90E-14	2.90E-12
GO:0032787	BP	monocarboxylic acid metabolic process	5.30E-14	8.00E-12
GO:0022613	BP	ribonucleoprotein complex biogenesis	6.30E-14	9.40E-12
GO:0042254	BP	ribosome biogenesis	6.70E-14	9.80E-12
GO:0044275	BP	cellular carbohydrate catabolic process	7.70E-14	1.10E-11
GO:0055086	BP	nucleobase, nucleoside and nucleotide metabolic process	8.70E-14	1.20E-11
GO:0046164	BP	alcohol catabolic process	9.70E-14	1.40E-11
GO:0044282	BP	small molecule catabolic process	1.10E-13	1.50E-11
GO:0046365	BP	monosaccharide catabolic process	1.20E-13	1.60E-11
GO:0019320	BP	hexose catabolic process	1.30E-13	1.70E-11
GO:0006007	BP	glucose catabolic process	1.30E-13	1.70E-11
GO:0009451	BP	RNA modification	3.20E-13	4.10E-11
GO:0043414	BP	macromolecule methylation	3.60E-13	4.60E-11
GO:0009791	BP	post-embryonic development	3.60E-13	4.60E-11
GO:0051186	BP	cofactor metabolic process	4.30E-13	5.30E-11
GO:0032259	BP	methylation	5.60E-13	6.70E-11
GO:0046394	BP	carboxylic acid biosynthetic process	5.60E-13	6.70E-11
GO:0016053	BP	organic acid biosynthetic process	5.60E-13	6.70E-11
GO:0007242	BP	intracellular signaling cascade	7.20E-13	8.50E-11

GO:0032502	BP	developmental process	1.20E-12	1.50E-10
GO:0051707	BP	response to other organism	1.50E-12	1.70E-10
GO:0034470	BP	ncRNA processing	1.50E-12	1.70E-10
GO:0006730	BP	one-carbon metabolic process	1.90E-12	2.20E-10
GO:0006090	BP	pyruvate metabolic process	2.40E-12	2.70E-10
GO:0006091	BP	generation of precursor metabolites and energy	2.90E-12	3.20E-10
GO:0016071	BP	mRNA metabolic process	3.30E-12	3.60E-10
GO:0048519	BP	negative regulation of biological process	3.40E-12	3.70E-10
GO:0033036	BP	macromolecule localization	3.60E-12	3.80E-10
GO:0009308	BP	amine metabolic process	3.70E-12	3.90E-10
GO:0061024	BP	membrane organization	4.60E-12	4.80E-10
GO:0016044	BP	cellular membrane organization	4.60E-12	4.80E-10
GO:0006364	BP	rRNA processing	5.00E-12	5.10E-10
GO:0043933	BP	macromolecular complex subunit organization	5.00E-12	5.10E-10
GO:0034660	BP	ncRNA metabolic process	5.50E-12	5.50E-10
GO:0002376	BP	immune system process	6.60E-12	6.40E-10
GO:0006955	BP	immune response	6.60E-12	6.40E-10
GO:0048583	BP	regulation of response to stimulus	6.70E-12	6.50E-10
GO:0016072	BP	rRNA metabolic process	7.50E-12	7.20E-10
GO:0006952	BP	defense response	8.20E-12	7.80E-10
GO:0000956	BP	nuclear-transcribed mRNA catabolic process	8.60E-12	8.00E-10
GO:0006402	BP	mRNA catabolic process	8.60E-12	8.00E-10
GO:0009657	BP	plastid organization	9.10E-12	8.40E-10
GO:0007275	BP	multicellular organismal development	1.00E-11	9.30E-10
GO:0032501	BP	multicellular organismal process	1.00E-11	9.30E-10
GO:0009651	BP	response to salt stress	1.30E-11	1.20E-09
GO:0016070	BP	RNA metabolic process	2.20E-11	2.00E-09
GO:0051789	BP	response to protein stimulus	2.70E-11	2.40E-09
GO:0010467	BP	gene expression	2.90E-11	2.50E-09
GO:0046483	BP	heterocycle metabolic process	3.50E-11	3.00E-09
GO:0034621	BP	cellular macromolecular complex subunit organization	3.60E-11	3.00E-09
GO:0070271	BP	protein complex biogenesis	3.70E-11	3.10E-09
GO:0006461	BP	protein complex assembly	3.70E-11	3.10E-09
GO:0044106	BP	cellular amine metabolic process	4.50E-11	3.70E-09
GO:0023052	BP	signaling	4.60E-11	3.80E-09
GO:0065003	BP	macromolecular complex assembly	6.30E-11	5.20E-09
GO:0006970	BP	response to osmotic stress	8.50E-11	6.90E-09
GO:0023046	BP	signaling process	1.10E-10	8.50E-09

GO:0023060	BP	signal transmission	1.10E-10	8.50E-09
GO:0045087	BP	innate immune response	1.30E-10	1.00E-08
GO:0007165	BP	signal transduction	1.50E-10	1.20E-08
GO:0009309	BP	amine biosynthetic process	1.60E-10	1.30E-08
GO:0044271	BP	cellular nitrogen compound biosynthetic process	2.30E-10	1.80E-08
GO:0043623	BP	cellular protein complex assembly	2.60E-10	2.00E-08
GO:0033554	BP	cellular response to stress	2.60E-10	2.00E-08
GO:0006401	BP	RNA catabolic process	3.10E-10	2.30E-08
GO:0006519	BP	cellular amino acid and derivative metabolic process	3.40E-10	2.60E-08
GO:0016192	BP	vesicle-mediated transport	4.40E-10	3.20E-08
GO:0034622	BP	cellular macromolecular complex assembly	4.60E-10	3.40E-08
GO:0009790	BP	embryonic development	4.60E-10	3.40E-08
GO:0006520	BP	cellular amino acid metabolic process	5.30E-10	3.80E-08
GO:0008652	BP	cellular amino acid biosynthetic process	5.50E-10	3.90E-08
GO:0006412	BP	translation	7.80E-10	5.60E-08
GO:0065007	BP	biological regulation	8.00E-10	5.70E-08
GO:0034976	BP	response to endoplasmic reticulum stress	8.90E-10	6.30E-08
GO:0010027	BP	thylakoid membrane organization	9.50E-10	6.60E-08
GO:0009668	BP	plastid membrane organization	9.50E-10	6.60E-08
GO:0050789	BP	regulation of biological process	1.40E-09	9.70E-08
GO:0009059	BP	macromolecule biosynthetic process	1.90E-09	1.30E-07
GO:0071495	BP	cellular response to endogenous stimulus	2.00E-09	1.30E-07
GO:0051603	BP	proteolysis involved in cellular protein catabolic process	2.10E-09	1.40E-07
GO:0080134	BP	regulation of response to stress	2.30E-09	1.50E-07
GO:0035194	BP	posttranscriptional gene silencing by RNA	3.50E-09	2.30E-07
GO:0006220	BP	pyrimidine nucleotide metabolic process	3.60E-09	2.40E-07
GO:0009416	BP	response to light stimulus	3.80E-09	2.50E-07
GO:0006612	BP	protein targeting to membrane	4.00E-09	2.60E-07
GO:0046777	BP	protein amino acid autophosphorylation	5.60E-09	3.60E-07
GO:0006796	BP	phosphate metabolic process	6.10E-09	3.90E-07
GO:0009165	BP	nucleotide biosynthetic process	6.50E-09	4.10E-07
GO:0006732	BP	coenzyme metabolic process	6.70E-09	4.20E-07
GO:0006793	BP	phosphorus metabolic process	6.90E-09	4.30E-07

GO:0016441	BP	posttranscriptional gene silencing	7.80E-09	4.80E-07
GO:0051788	BP	response to misfolded protein	8.10E-09	5.00E-07
GO:0070647	BP	protein modification by small protein conjugation or removal	8.40E-09	5.20E-07
GO:0048856	BP	anatomical structure development	8.70E-09	5.30E-07
GO:0031347	BP	regulation of defense response	9.10E-09	5.50E-07
GO:0048193	BP	Golgi vesicle transport	1.00E-08	6.30E-07
GO:0009240	BP	isopentenyl diphosphate biosynthetic process	1.50E-08	8.80E-07
GO:0009793	BP	embryonic development ending in seed dormancy	1.50E-08	8.80E-07
GO:0046490	BP	isopentenyl diphosphate metabolic process	1.50E-08	8.80E-07
GO:0044257	BP	cellular protein catabolic process	1.80E-08	1.10E-06
GO:0033365	BP	protein localization in organelle	2.00E-08	1.20E-06
GO:0019288	BP	isopentenyl diphosphate biosynthetic process, mevalonate-independent pathway	2.30E-08	1.30E-06
GO:0006733	BP	oxidoreduction coenzyme metabolic process	2.30E-08	1.30E-06
GO:0016226	BP	iron-sulfur cluster assembly	2.40E-08	1.40E-06
GO:0031163	BP	metallo-sulfur cluster assembly	2.40E-08	1.40E-06
GO:0034645	BP	cellular macromolecule biosynthetic process	2.90E-08	1.60E-06
GO:0070646	BP	protein modification by small protein removal	3.00E-08	1.70E-06
GO:0009314	BP	response to radiation	3.10E-08	1.70E-06
GO:0006221	BP	pyrimidine nucleotide biosynthetic process	3.30E-08	1.90E-06
GO:0009719	BP	response to endogenous stimulus	3.80E-08	2.10E-06
GO:0051168	BP	nuclear export	5.10E-08	2.80E-06
GO:0009218	BP	pyrimidine ribonucleotide metabolic process	5.20E-08	2.80E-06
GO:0046364	BP	monosaccharide biosynthetic process	5.90E-08	3.20E-06
GO:0031047	BP	gene silencing by RNA	6.00E-08	3.30E-06
GO:0019682	BP	glyceraldehyde-3-phosphate metabolic process	6.50E-08	3.50E-06
GO:0051169	BP	nuclear transport	7.10E-08	3.80E-06
GO:0006913	BP	nucleocytoplasmic transport	7.10E-08	3.80E-06
GO:0019748	BP	secondary metabolic process	8.10E-08	4.30E-06
GO:0006739	BP	NADP metabolic process	8.70E-08	4.60E-06
GO:0042742	BP	defense response to bacterium	9.50E-08	5.00E-06
GO:0030163	BP	protein catabolic process	9.70E-08	5.10E-06
GO:0043603	BP	cellular amide metabolic process	9.80E-08	5.10E-06

GO:0048608	BP	reproductive structure development	1.00E-07	5.20E-06
GO:0017038	BP	protein import	1.00E-07	5.20E-06
GO:0019438	BP	aromatic compound biosynthetic process	1.00E-07	5.30E-06
GO:0009743	BP	response to carbohydrate stimulus	1.10E-07	5.40E-06
GO:0006725	BP	cellular aromatic compound metabolic process	1.20E-07	6.00E-06
GO:0022607	BP	cellular component assembly	1.30E-07	6.30E-06
GO:0048367	BP	shoot development	1.30E-07	6.30E-06
GO:0022621	BP	shoot system development	1.30E-07	6.30E-06
GO:0043248	BP	proteasome assembly	1.30E-07	6.60E-06
GO:0051704	BP	multi-organism process	1.40E-07	6.70E-06
GO:0010498	BP	proteasomal protein catabolic process	1.40E-07	6.70E-06
GO:0046496	BP	nicotinamide nucleotide metabolic process	1.60E-07	7.90E-06
GO:0006769	BP	nicotinamide metabolic process	1.60E-07	7.90E-06
GO:0015979	BP	photosynthesis	1.90E-07	9.30E-06
GO:0080129	BP	proteasome core complex assembly	2.00E-07	9.50E-06
GO:0046686	BP	response to cadmium ion	2.20E-07	1.00E-05
GO:0016051	BP	carbohydrate biosynthetic process	2.20E-07	1.10E-05
GO:0019362	BP	pyridine nucleotide metabolic process	2.30E-07	1.10E-05
GO:0006405	BP	RNA export from nucleus	2.40E-07	1.10E-05
GO:0050658	BP	RNA transport	2.40E-07	1.10E-05
GO:0050657	BP	nucleic acid transport	2.40E-07	1.10E-05
GO:0051236	BP	establishment of RNA localization	2.40E-07	1.10E-05
GO:0006403	BP	RNA localization	2.40E-07	1.10E-05
GO:0010629	BP	negative regulation of gene expression	2.60E-07	1.20E-05
GO:0009617	BP	response to bacterium	2.60E-07	1.20E-05
GO:0051188	BP	cofactor biosynthetic process	2.60E-07	1.20E-05
GO:0009627	BP	systemic acquired resistance	2.70E-07	1.20E-05
GO:0016310	BP	phosphorylation	2.80E-07	1.30E-05
GO:0009620	BP	response to fungus	2.90E-07	1.30E-05
GO:0050793	BP	regulation of developmental process	3.00E-07	1.30E-05
GO:0016458	BP	gene silencing	3.20E-07	1.40E-05
GO:0016246	BP	RNA interference	3.20E-07	1.40E-05
GO:0006081	BP	cellular aldehyde metabolic process	3.20E-07	1.40E-05
GO:0010016	BP	shoot morphogenesis	3.20E-07	1.40E-05
GO:0009259	BP	ribonucleotide metabolic process	3.70E-07	1.60E-05
GO:0010605	BP	negative regulation of macromolecule metabolic process	4.00E-07	1.70E-05

GO:0006098	BP	pentose-phosphate shunt	4.10E-07	1.80E-05
GO:0006740	BP	NADPH regeneration	4.10E-07	1.80E-05
GO:0071215	BP	cellular response to abscisic acid stimulus	4.30E-07	1.80E-05
GO:0009066	BP	aspartate family amino acid metabolic process	5.00E-07	2.10E-05
GO:0051239	BP	regulation of multicellular organismal process	5.60E-07	2.40E-05
GO:0048585	BP	negative regulation of response to stimulus	5.90E-07	2.50E-05
GO:0009696	BP	salicylic acid metabolic process	6.60E-07	2.80E-05
GO:0010154	BP	fruit development	6.60E-07	2.80E-05
GO:0009626	BP	plant-type hypersensitive response	6.60E-07	2.80E-05
GO:0009220	BP	pyrimidine ribonucleotide biosynthetic process	6.70E-07	2.80E-05
GO:0002252	BP	immune effector process	6.80E-07	2.80E-05
GO:0035195	BP	gene silencing by miRNA	7.00E-07	2.90E-05
GO:0000338	BP	protein deneddylation	7.30E-07	3.00E-05
GO:0010388	BP	cullin deneddylation	7.30E-07	3.00E-05
GO:0048316	BP	seed development	7.30E-07	3.00E-05
GO:0048518	BP	positive regulation of biological process	8.00E-07	3.20E-05
GO:0034050	BP	host programmed cell death induced by symbiont	8.10E-07	3.30E-05
GO:0044255	BP	cellular lipid metabolic process	8.40E-07	3.30E-05
GO:0009892	BP	negative regulation of metabolic process	8.50E-07	3.40E-05
GO:0048523	BP	negative regulation of cellular process	8.70E-07	3.40E-05
GO:0010608	BP	posttranscriptional regulation of gene expression	8.90E-07	3.50E-05
GO:0005515	MF	protein binding	2.60E-15	5.00E-12
GO:0016740	MF	transferase activity	3.00E-10	2.90E-07
GO:0003735	MF	structural constituent of ribosome	7.20E-10	4.50E-07
GO:0003824	MF	catalytic activity	2.30E-09	1.10E-06
GO:0005198	MF	structural molecule activity	6.40E-08	2.40E-05
GO:0042578	MF	phosphoric ester hydrolase activity	1.20E-07	3.70E-05
GO:0005488	MF	binding	1.40E-07	3.70E-05
GO:0016772	MF	transferase activity, transferring phosphorus-containing groups	1.60E-07	3.70E-05
GO:0016301	MF	kinase activity	4.80E-07	9.90E-05
GO:0000166	MF	nucleotide binding	6.30E-07	0.00012

NV, non-vernalized samples

6V7N, samples with six weeks of cold treatment followed by seven days in the normal growth conditions

CC, Cellular component; MF, Molecular function; BP, Biological process

Chapter V

General Discussion

In this dissertation, we found two *FRI* paralogs (*FRIa, FRIb*) in the *B. rapa* and confirmed, BrFRIb acts as a positive activator of *FLC,* when transformed *B. rapa* gene *BrFRIb* into early flowering *A. thaliana*, and plant shows late flowering through triggered the expression of *AtFLC*. This confirmed *BrFRIb* has an *FLC* triggering function (Chapter II). In the absence of *AtFRI* in *A. thaliana* confirming early flowering due to low expression of *AtFLC*. We also confirmed that *BrFLC1, BrFLC2,* and *BrFLC3* act as floral repressors by producing transgenic plants overexpressing each *FLC* gene (Chapter II) and finding a delay in flowering. We also examined the relationship between flowering time after 4 weeks of cold treatment (vernalization requirement) and total amount of expression of four *BrFLC* (*BrFLC*s) in nine *B. rapa* lines. Before cold exposures, *BrFLC*s expression varied between lines and late flowering *B. rapa* lines showed higher expression levels of *BrFLC*s except for one line (BRA2209). In this late flowering line (BRA2209), repression rate of *BrFLC*s expression after vernalization is lower, leading to higher *BrFLC*s expression levels after cold treatment compared with early flowering lines. From these results, I suggested that high levels of the total amount of *BrFLC* expression before cold exposure and/or the repression rate after cold exposure could be associated with a high vernalization requirement (Chapter II), i.e. the levels of *FLC* are critical.

Histone modification mechanism is an important for controlling expression levels of genes which I found conserved between two species *A. thaliana* and *B. rapa*. In different accessions total amount of *BrFLC* expression were also varied and high levels of the total amount of *BrFLCs* expression were observed before cold exposure indicating the association with high vernalization requirement (Chapter II). Before exposure to cold, an active histone mark H3K4me3 accumulation were found in the nucleation site of *BrFLC2*, *BrFLC3*, and *BrFLC5,* while *BrFLC1* had both H3K4me3 and H3K36me3 modifications (Kawanabe et al. 2016), which is responsible for high *FLC*s expression. During vernalization, depending on the duration of cold treatment expression of all four *BrFLCs* expression were repressed, and maintaining silencing were associated with the accumulation of H3K27me3 around the nucleation region of all *BrFLC*s. After return to warm condition, H3K27me3 accumulation were spreading across the whole of the four *BrFLC* genes, and all four *BrFLC*s maintaining stably silenced (Chapter III). This evidence indicates like *A. thaliana*, PHD-PRC2 is

essential for inducing stable epigenetic repression which recruited to the gene regions of the *BrFLC*s. ChIP-seq experiments were showed like *BrFLC*s only very few genes showed spreading of H3K27me3, suggesting that this epigenetic changes in vernalization is specific to only a few genes including four *BrFLC* genes (Chapter III). This discussion indicates that similar to *Arabidopsis*, epigenetic histone modification plays an important role in changing the expression of *BrFLC* genes under vernalization in *B. rapa*. We also compared the level of the repressive histone markH3K27me3 between lines, between tissues, or between before and after vernalization by chromatin immunoprecipitation sequencing (ChIP-seq) at whole genome levels. About 90% of the same genes had H3K27me3 in the two *B. rapa* lines examined, while there is greater variation between different tissues, indicating that H3K27me3 distribution is conserved between lines but differs between tissues within a line (Chapter III). In *B. rapa*, among the four *BrFLC* paralogs, only *BrFLC2* had a COOLAIR-like transcript, BrFLC2as, and there were no lncRNA transcripts like COLDAIR and COLRWRAP in any of the four *BrFLC*s (Shea et al. 2019). In *A. thaliana*, COLDAIR and COLDWRAP recruit PHD-PRC2, which catalyses the marking of the gene with the histone repressive mark H3K27me3. However, I showed H3K27me3 accumulation in all four *BrFLC* paralogs in spite of lacking COLDAIR-like transcript (Chapter III).

We did the transcriptome analysis with different durations of vernalization treatments in *B. rapa* and found most genes were downregulated following cold treatment. *BrFLC* expression decreased and expression of genes known to transmit the vernalisation state *BrVIN3* and *BrSOC1* were induced during cold treatment (Chapter IV). During cold treatment, some flowering pathway genes showed different expression patterns between paralogs and some genes whose orthologous genes in *A. thaliana* were unchanged showed change of expression in *B. rapa*. From this result, I suggested that Chinese cabbage's flowering pathway is different and more complex than in *A. thaliana* (Chapter IV).

In conclusion, according to above discussion accumulation of H3K27me3 was confirmed in all *BrFLC* genes, suggesting that PHD-PRC2 is recruited to the nucleation regions of all *BrFLC*s. In *Arabidopsis*, COLDAIR may function for the recruitment of PRC2 to *FLC* locus by vernalization known as vernalization response element (VRE), whereas PHD-PRC2 complex is recruited in *B. rapa* without COLDAIR. So, it is unknown how the PHD-PRC2 complex is recruited at the *BrFLC* locus, and it is likely *B. rapa* VREs are important for PHD-PRC2 recruitment. Further analysis will be required to determine the function of lncRNA for the recruitment of PHD-PRC2 to the nucleation regions of all *BrFLC* genes.

Acknowledgements

Firstly, I would like to express my deepest gratitude to Associate Professor Dr. Ryo Fujimoto, Laboratory of Horticultural Breeding and Propagation, Graduate School of Agricultural Science, Kobe University, for give me a chance to study in his group in Japan, for his kindness, for his continuous guidance and encouragement throughout this work. He also gave me the chance to interact with researchers at national and international academic societies.

I am very grateful to Professor Dr Takeshi Takasaki-Yasuda and Professor Dr. Hitoshi Nakayashiki for their kind review of this thesis and for valuable comments and suggestions.

I would like to thank Ms. Tomoko Kusumi for her technical assistance.

I am very thankful to Chris A Helliwell, Daniel J Shea, Elizabeth S Dennis, Etsuko Itabashi, Hasan Mehraj, Junji Miyazaki, Keiichi Okazaki, Kenji Osabe, Motoaki Seki, Motoki Shimizu, Namiko Nishida, Naomi Miyaji, Satoko Takada, Satoshi Takahashi, Tomohiro Kakizaki, Weiwei Deng, William James Peacock, Yutaka Suzuki as co-authors.

I am also very thankful to all students of this laboratory for their continuous supports doing experiments and for helpful discussions and for response to various question and accompanied and encouragement during these three years.

I would like to thank to Ministry of Education, Culture, Sports, Science and Technology of Japan for financial supports.

At last but not least, I always thank to my family member specially to my daughter for their kind support and understanding.

Publications List

Peer-reviewed papers

1. Satoko Takada#, **Ayasha Akter#**, Etsuko Itabashi, Namiko Nishida, Daniel J Shea, Naomi Miyaji, Hasan Mehraj, Kenji Osabe, Motoki Shimizu, Takeshi Takasaki-Yasuda, Tomohiro Kakizaki, Keiichi Okazaki, Elizabeth S Dennis, Ryo Fujimoto. The role of *FRIGIDA* and *FLOWERING LOCUS C* genes in flowering time of *Brassica rapa* leafy vegetables. Scientific Reports. 9 (1): 13843, Sep, 2019. # Co-first author.
2. **Ayasha Akter**, Satoshi Takahashi, Weiwei Deng, Daniel J Shea, Etsuko Itabashi, Motoki Shimizu, Naomi Miyaji, Kenji Osabe, Namiko Nishida, Yutaka Suzuki, Chris A Helliwell, Motoaki Seki, William James Peacock, Elizabeth S Dennis, Ryo Fujimoto. The histone modification H3 lysine 27 tri-methylation has conserved gene regulatory roles in the triplicated genome of *Brassica rapa* L. DNA Research. 26 (5): 433-443, Oct, 2019.
3. **Ayasha Akter**, Junji Miyazaki, Daniel J Shea, Namiko Nishida, Satoko Takada, Naomi Miyaji, Hasan Mehraj, Motoki Shimizu, Md Asad-ud Doullah, Takeshi Takasaki-Yasuda, Keiichi Okazaki, Ryo Fujimoto. Gene expression analysis in response to vernalization in Chinese cabbage (*Brassica rapa* L.). The Horticulture Journal. In press (UTD-150), Feb, 2020.

Books

1. **Ayasha Akter**, Namiko Nishida, Satoko Takada, Etsuko Itabashi, Kenji Osabe, Daniel J Shea, Ryo Fujimoto. Genetic and Epigenetic Regulation of Vernalization in Brassicaceae. In: MA El-Esawi (Ed.) Brassica Germplasm: Characterization, Breeding and Utilization. IntechOpen, London, UK. pp.75, 03, 2018.
2. Honghao Lv, Naomi Miyaji, Kenji Osabe, **Ayasha Akter,** Hasan Mehraj, Daniel J. Shea and Ryo Fujimoto. 2020. The importance of genetic and epigenetic research in the Brassica vegetables in the face of climate change. In: Kole C. (eds) Genomic designing of climate-smart vegetable crops. Springer, Chapter 3, pp. 161-255, 03, 2020.
3. Takumi Okamoto, Xiaochun Wei, Hasan Mehraj, Mohammad Rashed Hossain, **Ayasha Akter,** Naomi Miyaji, Yoshinobu Takada, Jong-In Park, Ryo Fujimoto, Ill-Sup Nou and Masao Watanabe. 2020. Chinese Cabbage (*Brassica rapa* L. var. *pekinensis*) Breeding: Application of Molecular Technology. In: JM Al-Khayri (eds) Advances in Plant Breeding Strategies: Vegetable Crops - Fruits, Leaves, Stems. Springer. (In press).

References

Aikawa, S., M. J. Kobayashi, A. Satake, K. K. Shimizu and H. Kudoh. 2010. Robust control of the seasonal expression of the *Arabidopsis FLC* gene in a fluctuating environment. Proc. Natl. Acad. Sci. U. S. A. 107: 11632-11637.

Akter, A., S. Takahashi, W. Deng, D. J. Shea, E. Itabashi, M. Shimizu, N. Miyaji, K. Osabe, N. Nishida, Y. Suzuki, C. A. Helliwell, M. Seki, W. J. Peacock, E. S. Dennis and R. Fujimoto. 2019. The histone modification H3 lysine 27 tri-methylation has conserved gene regulatory roles in the triplicated genome of *Brassica rapa* L.. DNA Res. 26: 433-443.

Alvarez-Buylla, E. R., S. J. Liljegren, S. Pelaz, S. E. Gold, C. Burgeff, G. S. Ditta, F. Vergara-Silva and M. F. Yanofsky. 2000. MADS-box gene evolution beyond flowers: expression in pollen, endosperm, guard cell, roots and trichomes. Plant J. 24: 1-11.

Andrés, F. and G. Coupland. 2012. The genetic basis of flowering responses to seasonal cues. Nat. Rev. Genet. 13: 627-639.

Angel, A., J. Song, C. Dean and M. Howard. 2011. A polycomb-based switch underlying quantitative epigenetic memory. Nature 476: 105-108.

Ansorge, W. J. 2009. Next-generation DNA sequencing techniques. N. Biotechnol. 25: 195-203.

Bastow, R., J. S. Mylne, C. Lister, Z. Lippman, R. A. Martienssen and C. Dean. 2004. Vernalization requires epigenetic silencing of *FLC* by histone methylation. Nature 427: 164-167.

Berke, L. and B. Snel. 2014. The histone modification H3K27me3 is retained after gene duplication and correlates with conserved noncoding sequences in *Arabidopsis*. Genome Biol. Evol. 6: 572-579.

Berke, L., G. F. Sanchez-Perez, and B. Snel. 2012. Contribution of the epigenetic mark H3K27me3 to functional divergence after whole genome duplication in *Arabidopsis*. Genome Biol. 13: R94.

Birve, A., A. K. Sengupta, D. Beuchle, J. Larsson, J. A. Kennison, Å. Rasmuson-Lestander and J. Müller. 2001. *Su(z)12*, a novel *Drosophila* Polycomb group gene that is conserved in vertebrates and plants. Development 128: 3371-3379.

Bloomer, R. H. and C. Dean. 2017. Fine-tuning timing: natural variation informs the mechanistic basis of the switch to flowering in *Arabidopsis thaliana*. J. Exp. Bot. 68: 5439-5452.

Bouyer, D., F. Roudier, M. Heese, E.D. Andersen, D. Gey, M.K. Nowack, J. Goodrich, J.P. Renou, P.E. Grini, V. Colot and A. Schnittger .2011. Polycomb repressive complex 2 controls the embryo-to-seedling phase transition. PLoS Genet. 7: e1002014.

Buzas, D. M., M. Robertson, E. J. Finnegan, and C. A. Helliwell. 2011. Transcription-dependence of histone H3 lysine 27 trimethylation at the Arabidopsis polycomb target gene *FLC*. Plant J. 65: 872-881.

Chen, X. and D. X. Zhou. 2013. Rice epigenomics and epigenetics: challenges and opportunities. Curr. Opin. Plant Biol. 16: 164-169.

Cheng, F., J. Wu and X. Wang. 2014. Genome triplication drove the diversification of *Brassica* plants. Hort. Res. 1: 14024.

Cheng, F., J. Wu, L. Fang, S. Sun, B. Liu, K. Lin, G. Bonnema and X. Wang. 2012. Biased gene fractionation and dominant gene expression among the subgenomes of *Brassica rapa*. PLoS One 7: e36442.

Chin, K., T. A. DeFalco, W. Moeder and K. Yoshioka. 2013. The Arabidopsis cyclic nucleotide-gated ion channels AtCNGC2 and AtCNGC4 work in the same signaling pathway to regulate pathogen defense and floral transition. Plant Physiol. 163: 611-624.

Choi, K., J. Kim, H.J. Hwang, S.Y. Kim, C. Park, S.Y. Kim and I. Lee. 2011. The FRIGIDA complex activates transcription of *FLC*, a strong flowering repressor in *Arabidopsis*, by recruiting chromatin modification factors. Plant Cell. 23: 289-303.

Chouard, P. 1960. Vernalization and its relations to dormancy. Annu. Rev. Plant Physiol. 11: 191-238.

Clough, S. J. and A. F. Bent. 1998. Floral dip: a simplified method for *Agrobacterium* mediated transformation of *Arabidopsis thaliana*. Plant J. 16: 735-743.

Corbesier, L. and G. Coupland. 2005. Photoperiodic flowering of *Arabidopsis*: Integrating genetic and physiological approaches to characterization of the floral stimulus. Plant Cell Environ. 28: 54-66.

Coustham, V, P. Li, A. Strange, C. Lister, J. Song and C. Dean. 2012. Quantitative modulation of Polycomb silencing underlies natural variation in vernalization. Science 337: 584-587.

De, Lucia, F., P. Crevillen, A. M. Jones, T. Greb and C. Dean. 2008. A PHD-polycomb repressive complex 2 triggers the epigenetic silencing of *FLC* during vernalization. Proc. Natl. Acad. Sci. U.S.A. 105: 16831-16836.

Deng, W., H. Ying, C. A. Helliwell, J. M. Taylor, W. J. Peacock and E. S. Dennis. 2011. *FLOWERING LOCUS C* (*FLC*) regulates development pathways throughout the life cycle of *Arabidopsis*. Proc. Natl. Acad. Sci. U. S. A. 108: 6680-6685.

Deng, W., D. M. Buzas, H. Ying, M. Robertson, J. Taylor, W. J. Peacock, E. S. Dennis and C. Helliwell. 2013. Arabidopsis polycomb repressive complex 2 binding sites contain putative GAGA factor binding motifs within coding regions of genes. BMC Genomics, 14: 593.

Dennis, E. S. and W. J. Peacock. 2007. Epigenetic regulation of flowering. Curr. Opin. Plant Biol. 10: 520-527.

Diaz, A., K. Park, D. A. Lim and J. S. Song. 2012. Normalization, bias correction, and peak calling for ChIP-seq. Stat. Appl. Genet. Mol. Biol. 11: Article 9.

Du, Z., X. Zhou, Y. Ling, Z. Zhang and Z. Su. 2010. agriGO: a GO analysis toolkit for the agricultural community. Nucleic Acids Res. 38: W64-W70.

Falik, O., I. Hoffmann and A. Novoplansky. 2014. Say it with flowers: Flowering acceleration by root communication. Plant Signal. Behav. 9: e28258.

Finnegan, E. J. and E. S. Dennis. 2007. Vernalization-induced trimethylation of histone H3 lysine 27 at *FLC* is not maintained in mitotically quiescent cells. Curr. Biol. 17: 1978-1983.

Friend, D. J. C. 1985. *Brassica*. Harlevy AH, editor. Handbook of Flowering. CRC Press. pp. 44-77.

Fuchs, J., D. Demidov, A. Houben and I. Schubert. 2006. Chromosomal histone modification patterns-from conservation to diversity. Trends Plant Sci. 11: 199-208.

Fujimoto, R., T. Sasaki, R. Ishikawa, K. Osabe, T. Kawanabe and E.S. Dennis. 2012. Molecular mechanisms of epigenetic variation in plants. Int. J. Mol. Sci. 13: 9900-9922.

Fujimoto, R., J. M. Taylor, S. Shirasawa, W. J. Peacock and E. S. Dennis. 2012. Heterosis of *Arabidopsis* hybrids between C24 and Col is associated with increased photosynthesis capacity. Proc. Natl. Acad. Sci. U.S.A. 109: 7109-7114.

Fujimoto, R., T. Sasaki and T. Nishio. 2006. Characterization of DNA methyltransferase genes in *Brassica rapa*. Genes Genet. Syst. 81: 235-242.

Fujimoto, R., T. Sasaki, R. Ishikawa, K. Osabe, T. Kawanabe and E. S. Dennis. 2012. Molecular mechanisms of epigenetic variation in plants. Int. J. Mol. Sci. 13: 9900-9922.

Gazzani, S., A. R. Gendall, C. Lister, and C. Dean. 2003. Analysis of the molecular basis of flowering time variation in Arabidopsis accessions. Plant Physiol. 132: 1107-1114.

Gendall, A. R., Y. Y. Levy, A. Wilson and C. Dean. 2001. The *VERNALIZATION 2* gene mediates the epigenetic regulation of vernalization in *Arabidopsis*. Cell 107: 525-535.

Greb, T., J. S. Mylne, P. Crevillen, N. Geraldo, H. An, A. R. Gendall and C. Dean. 2007. The PHD finger protein VRN5 functions in the epigenetic silencing of *Arabidopsis FLC*. Curr. Biol. 17: 73-78.

Groszmann, M., I. K. Greaves, N. Albert, R. Fujimoto, C. A. Helliwell, E.S. Dennis and W. J. Peacock. 2011. Epigenetics in plants-vernalisation and hybrid vigour. Biochim. Biophy. Acta. 1809: 427-437.

Gu, X., C. Le, Y. Wang, Z. Li, D. Jiang, Y. Wang and Y. He. 2013. *Arabidopsis* FLC clade members form flowering-repressor complexes coordinating responses to endogenous and environmental cues. Nat. Commun. 4: 1947.

He, G., X. Zhu, A. A. Elling, L. Chen, X. Wang, L. Guo, M. Liang, H. He, H. Zhang, F. Chen and Y. Qi. 2010. Global epigenetic and transcriptional trends among two rice subspecies and their reciprocal hybrids. Plant Cell 22: 17-33.

He, Y. and R. M. Amasino. 2005. Role of chromatin modification in flowering-time control. Trends Plant Sci. 10: 30–35.

Helliwell, C.A., C.C. Wood, M. Robertson, W.J. Peacock and E.S. Dennis. 2006. The Arabidopsis FLC protein interacts directly *in vivo* with *SOC1* and *FT* chromatin and is part of a high-molecular-weight protein complex. Plant J. 46: 183-192.

Helliwell, C.A., R. S. Anderssen, M. Robertson, and E. J. Finnegan. 2015. How is *FLC* repression initiated by cold ? Trends Plant Sci. 20: 76-82.

Henderson, I. R. and C. Dean. 2004. Control of *Arabidopsis* flowering: The chill before the bloom. Development 131: 3829-3838.

Heo, J. B. and S. Sung. 2011. Vernalization-mediated epigenetic silencing by a long intronic noncoding RNA. Science 331: 76-79.

Hossain, M. M., H. Inden and T. Asahira. 1990. Seed vernalized interspecific hybrids through in vitro ovule culture in *Brassica*. Plant Sci. 68: 95-102.

Huang, F., T. Liu and X. Hou. 2018b. Isolation and functional characterization of a floral repressor, *BcMAF1*, from Pak-choi (*Brassica rapa* ssp. *chinensis*). Front. Plant Sci. 9: 290.

Huang, F., T. Liu, J. Tang, W. Duan and X. Hou. 2019. BcMAF2 activates *BcTEM1* and represses flowering in Pak-choi (*Brassica rapa* ssp. *chinensis*). Plant Mol. Biol. 100: 19-32.

Huang, F., X. Wu, X. Hou, S. Shao and T. Liu. 2018a. Vernalization can regulate flowering time through microRNA mechanism in *Brassica rapa*. Physiol. Plant. 164: 204-215.

Irwin, J. A., E. Soumpourou, C. Lister, J. D. Ligthart, S. Kennedy and C. Dean. 2016. Nucleotide polymorphism affecting *FLC* expression underpins heading date variation in horticultural brassicas. Plant J. 87: 597-605.

Irwin, J. A., C. Lister, E. Soumpourou, Y. Zhang, E.C. Howell, G. Teakle and C. Dean. 2012. Functional alleles of the flowering time regulator *FRIGIDA* in the *Brassica oleracea* genome. BMC Plant Biol. 12: 21.

Itabashi, E., K. Osabe, R. Fujimoto and T. Kakizaki. 2018. Epigenetic regulation of agronomical traits in Brassicaceae. Plant Cell Rep. 37: 87-101.

Ito H, T. Saito and T. Hatayama. 1966. Time and temperature factors for the flower formation in cabbage II. The site of vernalization and the nature of vernalization sensitivity. Tohoku. J. Agri. Res. 17: 1-15.

Johanson, U., J. West, C. Lister, S. Michaels, R. Amasino and C. Dean. 2000. Molecular analysis of *FRIGIDA*, a major determinant of natural variation in *Arabidopsis* flowering time. Science 290: 344-347.

Jung, W. Y., A. Lee, J. S. Moon, Y. S. Kim, and H. S. Cho. 2018. Genome-wide identification of flowering time genes associated with vernalization and the regulatory flowering networks in Chinese cabbage. Plant Biotechnol. Rep. 12: 347-363.

Kakizaki, T., T. Kato, N. Fukino, M. Ishida, K. Hatakeyama and S. Matsumoto. 2011. Identification of quantitative trait loci controlling late bolting in Chinese cabbage (*Brassica rapa* L.) parental line Nou 6 gou. Breed. Sci. 61: 151-159.

Kawamura, K., T. Kawanabe, M. Shimizu, A. J. Nagano, N. Saeki, K. Okazaki, M. Kaji, E. S. Dennis, K. Osabe and R. Fujimoto. 2016. Genetic distance of inbred lines of Chinese cabbage and its relationship to heterosis. Plant Gene 5: 1-7.

Kawanabe, T., K. Osabe, E. Itabashi, K. Okazaki, E. S. Dennis and R. Fujimoto. 2016. Development of primer sets that can verify the enrichment of histone modifications, and their application to examining vernalization-mediated chromatin changes in *Brassica rapa* L. Genes Genet. Syst. 91: 1-10.

Kim, D. H. and S. Sung. 2017. Vernalization-triggered intragenic chromatin loop formation by long noncoding RNAs. Dev Cell 40: 302-312.

Kim, D. H. and S. Sung. 2010. The Plant Homeo Domain finger protein, VIN3-LIKE 2, is necessary for photoperiod-mediated epigenetic regulation of the floral repressor, MAF5. Proc. Natl. Acad. Sci. U. S. A. 107: 17029-17034.

Kim, D. H. and S. Sung. 2014. Genetic and epigenetic mechanisms underlying vernalization. The Arabidopsis Book 12: e0171.

Kim, D. H., M.R. Doyle, S. Sung and R. M. Amasino. 2009. Vernalization: winter and the timing of flowering in plants. Annu. Rev. Cell Dev. Biol. 25, 277-299.

Kim, D., B. Langmead, and S. L. Salzberg. 2015. HISAT: a fast spliced aligner with low memory requirements. Nat. Methods 12: 357-360.

Kim, D., G. Pertea, C. Trapnell, H. Pimentel, R. Kelley and S. L. Salzberg. 2013. TopHat2: accurate alignment of transcriptomes in the presence of insertions, deletions and gene fusions. Genome Biol. 14: R36.

Kim, S. Y., B. S. Park, S. J. Kwon, J. Kim, M. H. Lim, Y. D. Park, D. Y. Kim, S. C. Suh, Y. M. Jin, J. H. Ahn and Y. H. Lee. 2007. Delayed flowering time in *Arabidopsis* and *Brassica rapa* by the overexpression of *FLOWERING LOCUS C (FLC)* homologs isolated from Chinese cabbage (*Brassica rapa* L. ssp. *pekinensis*). Plant Cell Rep. 26: 327-336.

Kitamoto, N, S. Yui, K. Nishikawa, Y. Takahata and S. Yokoi. 2014. A naturally occurring long insertion in the first intron in the *Brassica rapa FLC2* gene causes delayed bolting. Euphytica 196: 213-223.

Kitamoto, N., K. Nishikawa, Y. Tanimura, S. Urushibara, T. Matsuura, S. Yokoi, Y. Takahata and S Yui. 2017. Development of late-bolting F1 hybrids of Chinese cabbage (*Brassica rapa* L.) allowing early spring cultivation without heating. Euphytica 213:292.

Ko, J. H., I. Mitina, Y. Tamada, Y. Hyun, Y. Choi, R.M. Amasino, B. Noh and Y. S. Noh. 2010. Growth habit determination by the balance of histone methylation activities in *Arabidopsis*. EMBO J. 29: 3208-3215.

Kole, C., P Quijada, S. D. Michaels, R. M. Amasino and T. C. Osborn. 2001. Evidence for homology of flowering-time genes *VFR2* from *Brassica rapa* and *FLC* from *Arabidopsis thaliana*. Theor. Appl. Genet. 102: 425-430.

Kole, C., P. Quijada, S. D. Michaels, R. M. Amasino, T. C. Osborn. 2001. Evidence for homology of flowering-time genes *VFR2* from *Brassica rapa* and *FLC* from *Arabidopsis thaliana*. Theor. Appl. Genet. 102 :425-430.

Lafos, M., P. Kroll, M. L. Hohenstatt, F. L. Thorpe, O. Clarenz and D. Schubert. 2011, Dynamic regulation of H3K27 trimethylation during *Arabidopsis* differentiation. PLoS Genet. 7: e1002040.

Le Corre, V., F. Roux and X. Reboud. 2002. DNA polymorphism at the *FRIGIDA* gene in *Arabidopsis thaliana*: extensive nonsynonymous variation is consistent with local selection for flowering time. Mol. Biol. Evol. 19: 1261-1271.

Lee, I. and R. M. Amasino. 1995. Effect of vernalization, photoperiod, and light quality on the flowering phenotype of Arabidopsis plants containing the *FRIGIDA* gene. Plant Physiol. 108: 157-162.

Leijten, W., R. Koes, I. Roobeek and G. Frugis. 2018. Translating flowering time from *Arabidopsis thaliana* to Brassicaceae and Asteraceae crop species. Plants 7: E111.

Levy, Y. Y., S. Mesnage, J. S. Mylne, A.R. Gendall and C. Dean. 2002. Multiple roles of *Arabidopsis VRN1* in vernalization and flowering time control. Science 297:243-246.

Li, X., S. Zhang, J. Bai and Y. He. 2016. Tuning growth cycles of *Brassica* crops via natural antisense transcripts of *BrFLC*. Plant Biotechnol. J. 14: 905-914.

Li, F., H. Kitashiba, K. Inaba and T. Nishio. 2009. A *Brassica rapa* linkage map of EST-based SNP markers for identification of candidate genes controlling flowering time and leaf morphological traits. DNA Res. 16: 311-323.

Lin, S. I., J. G. Wang, S. Y. Poon, C. L. Su, S. S. Wang and T. J. Chiou. 2005. Differential regulation of *FLOWERING LOCUS C* expression by vernalization in cabbage and Arabidopsis. Plant Physiol. 137: 1037-1048.

Liu, C., F. Lu, X. Cui and X. Cao. 2010. Histone methylation in higher plants. Annu. Rev. Plant Biol. 61: 395-420.

Liu, C., S. Wang, W. Xu and X. Liu. 2017. Genome-wide transcriptome profiling of radish (*Raphanus sativus* L.) in response to vernalization. PLoS One 12: e0177594.

Lo, C. C. and P. S. Chain. 2014. Rapid evaluation and quality control of next generation sequencing data with FaQCs. BMC Bioinformatics 15: 366.

Long, W., X. Zou and X. Zhang. 2015.Transcriptome analysis of canola (*Brassica napus*) under salt stress at the germination stage. PLoS One 10: e0116217.

Lou, P., J. Zhao, J. S. Kim, S. Shen, D. P. Del Carpio, X. Song, M. Jin, D. Vreugdenhil, X. Wang, M. Koornneef and G. Bonnema. 2007. Quantitative trait loci for flowering time and morphological traits in multiple populations of *Brassica rapa*. J. Exp. Bot. 58: 4005-4016.

Lyons, R., A. Rusu, J. Stiller, J. Powell, J. M. Manners and K. Kazan. 2015. Investigating the association between flowering time and defense in the *Arabidopsis thaliana-Fusarium oxysporum* interaction. PLoS One 10: e0127699.

Makarevitch, I., S. R. Eichten, R. Briskine, A. J. Waters, O. N. Danilevskaya, R. B. Meeley, C. L. Myers, M. W. Vaughn and N. M. Springer. 2013. Genomic distribution of maize facultative heterochromatin marked by trimethylation of H3K27. Plant Cell 25: 780-793.

Más P., P. F. Devlin, S. Panda and S. A. Kay. 2000. Functional interaction of phytochrome B and cryptochrome 2. Nature 408 :207-211.

Méndez-Vigo, B., F. X. Picó, M. Ramiro, J. M. Martínez-Zapater and C. Alonso-Blanco. 2011. Altitudinal and climatic adaptation is mediated by flowering traits and *FRI, FLC*, and *PHYC* genes in Arabidopsis. Plant Physiol. 157: 1942-1955.

Michaels, S. D. and R. M. Amasino. 1999. *FLOWERING LOCUS C* encodes a novel MADS domain protein that acts as a repressor of flowering. Plant Cell 11: 949-956.

Michaels, S. D. and R. M. Amasino. 2001. Loss of *FLOWERING LOCUS C* activity eliminates the late-flowering phenotype of *FRIGIDA* and autonomous pathway mutations but not responsiveness to vernalization. Plant Cell 13: 935-941.

Michaels, S. D. and R. M. Amasino.1999. *FLOWERING LOCUS C* encodes a novel MADS domain protein that acts as a repressor of flowering. Plant Cell 11: 949-956.

Miyaji, N., M. Shimizu, J. Miyazaki, K. Osabe, M. Sato, Y. Ebe, S. Takada, M. Kaji, E. S. Dennis, R. Fujimoto and K. Okazaki. 2017. Comparison of transcriptome profiles by *Fusarium oxysporum* inoculation between Fusarium yellows resistant and susceptible lines in *Brassica rapa* L. Plant Cell Rep. 36: 1841-1854.

Moghaddam, A. M., F. Roudier, M. Seifert, C. Bérard, M. L. Magniette, R. K. Ashtiyani, A. Houben, V. Colot, and M. F. Mette. 2011. 2011. Additive inheritance of histone modifications in *Arabidopsis thaliana* intra-specific hybrids. Plant J. 67: 691-700.

Mortazavi, A., B. A. Williams, K. McCue, L. Schaeffer and B. Wold. 2008. Mapping and quantifying mammalian transcriptomes by RNA-Seq. Nat. Methods 5: 621-628.

Mylne J. S., L. Barrett, F. Tessadori, S. Mesnage, L. Johnson, Y. V. Bernatavichute, S. E. Jacobsen, P. Fransz and C. Dean. 2006. LHP1, the *Arabidopsis* homologue of HETEROCHROMATIN PROTEIN1, is required for epigenetic silencing of *FLC*. Proc. Natl. Acad. Sci. U.S.A. 103: 5012-5017.

Nagano, A. J., M. N. Honjo, M. Mihara, M. Sato and H. Kudoh. 2015. Detection of plant viruses in natural environments by using RNA-Seq. Methods Mol. Biol. 1236: 89-98.

Oh, S., H. Zhang, P. Ludwig and S. van Nocker. 2004. A mechanism related to the yeast transcriptional regulator Paf1c is required for expression of the Arabidopsis *FLC/MAF* MADS box gene family. Plant Cell 16: 2940-2953.

Okazaki, K., K. Sakamoto, R. Kikuchi, A. Saito, E. Togashi, Y. Kuginuki, S. Matsumoto and M. Hirai. 2007. Mapping and characterization of *FLC* homologs and QTL analysis of flowering time in *Brassica oleracea*. Theor. Appl. Genet. 114: 595-608.

Osborn, T. C., C. Kole, I. A. P. Parkin, A. G. Sharpe, M. Kuiper, D. J. Lydiate and M. Trick. 1997. Comparison of flowering time genes in *Brassica rapa*, *B. napus* and *Arabidopsis thaliana*. Genetics 146: 1123-1129.

Pouteau, S. and C. Albertini. 2009. The significance of bolting and floral transitions as indicators of reproductive phase change in *Arabidopsis*. J. Exp. Bot. 60: 3367- 3377.

Quadrana, L. and V. Colot, 2016. Plant transgenerational epigenetics. Annu. Rev. Genet. 50: 467-491.

Raman, H., R. Raman, N. Coombes, J. Song, R. Prangnell, C. Bandaranayake, R. Tahira,V. Sundaramoorthi, A. Killian, J. Meng, E. S. Dennis and S. Balasubramanian. 2016. Genome-wide association analyses reveal complex genetic architecture underlying natural variation for flowering time in canola. Plant Cell Environ. 39: 1228-1239.

Ratcliffe, O. J., R. W. Kumimoto, B. J. Wong and J. L. Riechmann. 2003. Analysis of the Arabidopsis MADS AFFECTING FLOWERING gene family: MAF2 prevents vernalization by short periods of cold. Plant Cell 15: 1159-1169.

Ratcliffe, O. J., G. C. Nadzan, T. L. Reuber and J. L. Riechmann. 2001. Regulation of flowering in *Arabidopsis* by an *FLC* homologue. Plant Physiol. 126: 122-132.

Razi, H., E.C. Howell, H. J. Newbury and M. J. Kearsey. 2008. Does sequence polymorphism of *FLC* paralogues underlie flowering time QTL in *Brassica oleracea*? Theor. Appl. Genet. 116: 179-192.

Richards E. J. 2011. Natural epigenetic variation in plant species: A view from the field. Curr. Opin. Plant Biol. 14: 204-209.

Risk, J. M., R. E. Laurie, R. C. Macknight, and C. L. Day. 2010. FRIGIDA and related proteins have a conserved central domain and family specific N-and C-terminal regions that are functionally important. Plant Mol. Biol. 73: 493-505.

Saeki, N., T. Kawanabe, H. Ying, M. Shimizu, M. Kojima, H. Abe, K. Okazaki, M. Kaji, J. M. Taylor, H. Sakakibara, W. J. Peacock, E. S. Dennis and R. Fujimoto. 2016. Molecular and cellular characteristics of hybrid vigour in a commercial hybrid of Chinese cabbage. BMC Plant Biol. 16: 45.

Saitou, N. and M. Nei. 1987.The neighbor-joining method: a new method for reconstructing phylogenetic trees. Mol. Biol. Evol. 4: 406-425.

Schiessl, S. V., B. Huettel, D. Kuehn, R. Reinhardt and R. J. Snowdon. 2017. Flowering time gene variation in *Brassica* species shows evolutionary principles. Front. Plant Sci. 8: 1742.

Schranz, M. E., P. Quijada, S. B. Sung, L. Lukens, R. Amasino and T. C. Osborn. 2002. Characterization and effects of the replicated flowering time gene *FLC* in *Brassica rapa*. Genetics 162: 1457-1468.

Scortecci, K. C., S. D. Michaels and R. M. Amasino. 2001. Identification of a MADS-box gene, *FLOWERING LOCUS M*, that represses flowering. Plant J. 26: 229-236.

Scortecci, K., S. D. Michaels and R. M. Amasino. 2003. Genetic interactions between *FLM* and other flowering-time genes in *Arabidopsis thaliana*. Plant Mol. Biol. 52: 915-922.

Searle, I., Y. He, F. Turck, C. Vincent, F. Fornara, S. Kröber, R. A. Amasino and G. Coupland. 2006. The transcription factor *FLC* confers a flowering response to vernalization by repressing meristem competence and systemic signaling in *Arabidopsis*. Genes Dev. 20: 898-912.

Shea, D. J., N. Nishida, S. Takada, E. Itabashi, S. Takahashi, A. Akter, N. Miyaji, K. Osabe, H. Mehraj, M. Shimizu, M. Seki, T. Kakizaki, K. Okazaki, E. S. Dennis and R. Fujimoto. 2019. Long noncoding RNAs in *Brassica rapa* L. following vernalization. Sci. Rep. 9: 9302.

Shea, D. J., E. Itabashi, S. Takada, E. Fukai, T, Kakizaki, R. Fujimoto and K. Okazaki. 2018. The role of *FLOWERING LOCUS C* in vernalization of *Brassica*: the importance of vernalization research in the face of climate change. Crop Pasture Sci. 69: 30-39.

Shea, D. J., M. Shimizu, E. Itabashi, N. Miyaji, J. Miyazaki, K. Osabe, M. Kaji, K. Okazaki and R. Fujimoto. 2018. Genome re-sequencing, SNP analysis, and genetic mapping of the parental lines of a commercial F_1 hybrid cultivar of Chinese cabbage. Breed. Sci. 68: 375-380.

Shea, D. J., Y. Tomaru, E. Itabashi, Y. Nakamura, T. Miyazaki, T. Kakizaki, T.N. Naher, M. Shimizu, R. Fujimoto, E. Fukai, and K. Okazaki. 2018. The production and characterization of a *BoFLC2* introgressed *Brassica rapa* by repeated backcrossing to an F_1. Breed. Sci. 68: 316-325.

Sheldon C. C., A. B. Conn, E. S. Dennis, W. J. Peacock 2002. Different regulatory regions are required for the vernalization-induced repression of *FLOWERING LOCUS C* and for the epigenetic maintenance of repression. Plant Cell 14: 2527-2537.

Sheldon, C. C., E. J. Finnegan, E. S. Dennis and W. J. Peacock. 2006. Quantitative effects of vernalization on *FLC* and *SOC1* expression. Plant J. 45: 871-883.

Sheldon, C. C., E. J. Finnegan, W. J. Peacock and E. S. Dennis. 2009. Mechanisms of gene repression by vernalization in Arabidopsis. Plant J. 59: 488-498.

Sheldon, C. C., J. E. Burn, P. P. Perez, J. Metzger, J. A. Edwards, W. J. Peacock and E. S. Dennis. 1999. The *FLF* MADS box gene: a repressor of flowering in Arabidopsis regulated by vernalization and methylation. Plant Cell 11: 445-458.

Sheldon, C. C., D. T. Rouse, E. J. Finnegan, W. J. Peacock and E. S. Dennis. 2000. The molecular basis of vernalization: the central role of *FLOWERING LOCUS C* (*FLC*). Proc. Natl. Acad. Sci. U.S.A. 97: 3753-3758.

Shimizu, M., R. Fujimoto, H. Ying, Z. J. Pu, Y. Ebe, T. Kawanabe, N. Saeki, J. M. Taylor, M. Kaji, E. S. Dennis and K. Okazaki. 2014. Identification of candidate genes for fusarium yellows resistance in Chinese cabbage by differential expression analysis. Plant Mol. Biol. 85: 247-257.

Shindo C., M. J. Aranzana, C. Lister, C. Baxter, C. Nicholls, M. Nordborg and C. Dean. 2005. Role of *FRIGIDA* and *FLOWERING LOCUS C* in determining variation in flowering time of Arabidopsis. Plant Physiol. 138 :1163-1173.

Simpson, G. G. 2004. The autonomous pathway: Epigenetic and post-transcriptional gene regulation in the control of *Arabidopsis* flowering time. Curr. Opin. Plant Biol. 7 :570-574.

Srikanth, A. and M. Schmid. 2011. Regulation of flowering time: All roads lead to Rome. Cell. Mol. Life Sci. 68: 2013-2037.

Su, T., W. Wang, P. Li, B. Zhang, P. Li, X. Xin, H. Sun, Y. Yu, D. Zhang, X. Zhao, C. Wen, G. Zhou, Y. Wang, H. Zheng, S. Yu and F, Zhang. 2018. A genomic variation map provides insights into the genetic basis of spring Chinese cabbage (*Brassica rapa* ssp. *pekinensis*) selection. Mol. Plant 11: 1360-1376.

Sun, M., X. Qi, L. Hou, X. Xu, Z. Zhu and M. Li. 2015. Gene expression analysis of pak choi in response to vernalization. PLoS One 10: e0141446.

Sung, S. and R. M. Amasino. 2004. Vernalization in *Arabidopsis thaliana* is mediated by the PHD finger protein VIN3. Nature 427: 159-164.

Sung S., Y. He, T.W. Eshoo, Y. Tamada, L. Johnson, K. Nakahigashi, K. Goto, S. E. Jacobsen and R. M. Amasino. 2006. Epigenetic maintenance of the vernalized state in *Arabidopsis thaliana* requires LIKE HETEROCHROMATIN PROTEIN 1. Nat Genet. 38: 706-710

Sung, S. and R. M. Amasino. 2004. Vernalization in *Arabidopsis thaliana* is mediated by the PHD finger protein VIN3. Nature 427: 159-164.

Swiezewski, S., F. Liu, A. Magusin and C. Dean. 2009. Cold-induced silencing by long antisense transcripts of an *Arabidopsis* Polycomb target. Nature 462: 799-802.

Swindell, W. R., M. Huebner and A. P. Weber. 2007. Transcriptional profiling of Arabidopsis heat shock proteins and transcription factors reveals extensive overlap between heat and non-heat stress response pathways. BMC Genomics 8: 125.

Tadege, M., C. C. Sheldon, C. A. Helliwell, P. Stoutjesdijk, E. S. Dennis and W. J. Peacock. 2001. Control of flowering time by *FLC* orthologues in *Brassica napus*. Plant J. 28: 545-553.

Takada, S., A. Akter, E. Itabashi, N. Nishida, D. J. Shea, N. Miyaji, H. Mehraj, K. Osabe, M. Shimizu, T. Takasaki-Yasuda, T. Kakizaki, K. Okazaki, E. S. Dennis and R. Fujimoto. 2019. The role of *FRIGIDA* and *FLOWERING LOCUS C* genes in flowering time of *Brassica rapa* leafy vegetables. Sci. Rep. 9: 13843.

Takahashi, S., K. Osabe, Fukushima, S. Takuno, N. Miyaji, M. Shimizu, T. Takasaki-Yasuda, Y. Suzuki, E.S. Dennis, M. Seki and R. Fujimoto. 2018. Genome-wide characterization of DNA methylation, small RNA expression, and histone H3 lysine nine di-methylation in *Brassica rapa* L.. DNA Res. 25: 511-520.

Takahashi, S., N. Fukushima, Osabe, E. Itabashi, M. Shimizu, N. Miyaji, T. Takasaki-Yasuda, Y. Suzuki, M. Seki and R. Fujimoto. 2018. Identification of DNA methylated regions by using methylated DNA immunoprecipitation sequencing in *Brassica rapa*. Crop Pasture Sci. 69: 107-120.

Tang, H., M. R. Woodhouse, F, Cheng, J. C. Schnable, B. S. Pedersen, G. Conant, X. Wang, M. Freeling, J. C. Pires. 2012. Altered patterns of fractionation and exon deletions in *Brassica rapa* support a two-step model of paleohexaploidy. Genetics 190: 1563-1574.

Teutonico, R. A. and T. C. Osborn. 1996. Mapping of RFLP and quantitative trait loci in *Brassica rapa* and comparison to linkage maps of *B. napus*, *B. oleracea* and *Arabidopsis*. Theor. Appl. Genet. 89: 885-894.

Tong, C., X. Wang, J. Yu, J. Wu, W. Li, J. Huang, C. Dong, W. Hua and S. Liu. 2013. Comprehensive analysis of RNA-seq data reveals the complexity of the transcriptome in *Brassica rapa*. BMC Genomics 14: 689.

Trapnell, C., A. Roberts, L. Goff, G. Pertea, D. Kim, D. R. Kelley, H. Pimentel, S. L. Salzberg, J. L. Rinn and L. Pachter. 2012. Differential gene and transcript expression analysis of RNA-seq experiments with TopHat and Cufflinks. Nat. Protoc. 7: 562-578.

Tsai, M. C., O. Manor, Y. Wan, N. Mosammaparast, J. K. Wang, F. Lan, Y. Shi, E. Segal, H. Y. Chang. 2010. Long noncoding RNA as modular scaffold of histone modification complexes. Science 329: 689-693.

Turck, F., F. Roudier, S. Farrona, M. L. Martin-Magniette, E. Guillaume, N. Buisine, S. Gagnot, R. A. Martienssen, G. Coupland and V. Colot. 2007. Arabidopsis TFL2/LHP1 specifically associates with genes marked by trimethylation of histone H3 lysine 27. PLoS Genet. 3: e86.

UN: 1935. Genome analysis in *Brassica* with special reference to the experimental formation of *B. napus* and peculiar mode of fertilization. Jpn. J. Bot. 7: 389-452.

Wang, N., W. Qian, I. Suppanz, L. Wei, B. Mao, Y. Long, J. Meng, A. E. Müller and C. Jung. 2011. Flowering time variation in oilseed rape (*Brassica napus* L.) is associated with allelic variation in the *FRIGIDA* homologue *BnaA.FRI.a*. J. Exp. Bot. 62: 5641-5658.

Wang, R., S. Farrona, C. Vincent, A. Joecker, H. Schoof, F. Turck, C. Alonso-Blanco, G. Coupland and M. C. Albani. 2009. *PEP1* regulates perennial flowering in *Arabis alpina*. Nature. 459: 423-427.

Wang, A., J. Hu, X. Huang, X. Li, G. Zhou and Z. Yan. 2016. Comparative transcriptome analysis reveals heat-responsive genes in Chinese cabbage (*Brassica rapa* ssp. *chinensis*). Front. Plant Sci. 7: 939.

Wang, J., Y. Qiu, F. Cheng, X. Chen, X. Zhang, H. Wang, J. Song, M. Duan, H. Yang and X. Li. 2017. Genome-wide identification, characterization, and evolutionary analysis of flowering genes in radish (*Raphanus sativus* L.). BMC Genomics 18: 981.

Wang, X., H. Wang, J. Wang, R. Sun, J. Wu, S. Liu, Y. Bai, J. H. Mun, I. Bancroft, F. Cheng, S. Huang, X. Li, W. Hua, J. Wang, X. Wang, M. Freeling, J. C. Pires, A. H. Paterson, B. Chalhoub, B. Wang, A. Hayward, A. G. Sharpe, B. S. Park, B. Weisshaar, B. Liu, B. Li, B. Liu, C. Tong, C. Song, C. Duran, C. Peng, C. Geng, C. Koh, C. Lin, D. Edwards, D. Mu, D. Shen, E. Soumpourou, F. Li, F. Fraser, G. Conant, G. Lassalle, G. J. King, G. Bonnema, H. Tang, H. Wang, H. Belcram, H. Zhou, H. Hirakawa, H. Abe, H. Guo, H. Wang, H. Jin, I. A. Parkin, J. Batley, J. S. Kim, J. Just, J. Li, J. Xu, J. Deng, J. A. Kim, J. Li, J. Yu, J. Meng, J. Wang, J. Min, J. Poulain, J. Wang, K. Hatakeyama, K. Wu, L. Wang, L. Fang, M. Trick, M. G. Links, M. Zhao, M. Jin, N. Ramchiary, N. Drou, P. J. Berkman, Q. Cai, Q. Huang, R. Li, S. Tabata, S. Cheng, S. Zhang, S. Zhang, S. Huang, S. Sato, S. Sun, S. J. Kwon, S. R. Choi, T. H. Lee, W. Fan, X. Zhao, X. Tan, X. Xu, Y. Wang, Y. Qiu, Y. Yin, Y. Li, Y. Du, Y. Liao, Y. Lim, Y. Narusaka, Y. Wang, Z. Wang, Z. Li, Z. Wang, Z. Xiong and Z. Zhang. 2011. The genome of the mesopolyploid crop species *Brassica rapa*. Nat. Genet. 43: 1035-1039.

Weinhofer, I., Hehenberger, E., Roszak, P., Hennig, L. and Köhler, C. 2010, H3K27me3 profiling of the endosperm implies exclusion of polycomb group protein targeting by DNA methylation. PLoS Genet. 6: e1001152.

Whittaker, C. and C. Dean. The *FLC* locus: 2017. A platform for discoveries in epigenetics and adaptation. Ann. Rev. Cell Dev. Biol. 33: 555-575.

Wood, C. C., M. Robertson, G. Tanner, W. J. Peacock, E. S. Dennis and C. A. Helliwell. 2006. The *Arabidopsis thaliana* vernalization response requires a polycomb-like protein complex that also includes VERNALIZATION INSENSITIVE 3. Proc. Natl. Acad. Sci. U. S. A. 103: 14631-14636.

Xiao, D., J. J. Zhao, X. L. Hou, R. K. Basnet, D. P. D. Carpio, N. W. Zhang, J. Bucher, K. Lin, F. Cheng, X. W. Wang and G. Bonnema. 2013.The *Brassica rapa FLC* homologue *FLC2* is a key regulator of flowering time, identified through transcriptional co-expression networks. J. Exp. Bot. 64: 4503-4516.

Xiao, D., J. J. Zhao, X.L. Hou, R. K. Basnet, D. P. Carpio, N. W. Zhang, J. Bucher, K. Lin, F. Cheng, X. W. Wang and G. Bonnema.2013. The *Brassica rapa FLC* homologue *FLC2* is a key regulator of flowering time, identified through transcriptional co-expression networks. J. Exp. Bot. 64: 4503-4516.

Xiao, J., Lee, U. S. and Wagner, D. 2016. Tug of war: adding and removing histone lysine methylation in *Arabidopsis*. Curr. Opin. Plant Biol. 34: 41-53.

Xing, M., H. Lv, J. Ma, D. Xu, H. Li, L. Yang, J. Kang, X. Wang and Z. Fang. 2016. Transcriptome profiling of resistance to *Fusarium oxysporum* f. sp. *conglutinans* in cabbage (*Brassica oleracea*) roots. PLoS One 11: e0148048.

Yong, H. Y., Z. Zou, E. P. Kok, B. H. Kwan, K. Chow, S. Nasu, M. Nanzyo, H. Kitashiba and T. Nishio. 2014. Comparative transcriptome analysis of leaves and roots in response to sudden increase in salinity in *Brassica napus* by RNA-seq. BioMed Res. Int. 2014: 1–19.

Zhang, H. and S. van Nocker. 2002. The *VERNALIZATION INDEPENDENCE 4* gene encodes a novel regulator of *FLOWERING LOCUS C*. Plant J. 31: 663-667.

Zhang, X., O Clarenz, Cokus, Y. V. Bernatavichute, M. Pellegrini, J. Goodrich and S.E. Jacobsen. 2007. Whole-genome analysis of histone H3 lysine 27 trimethylation in *Arabidopsis*. PLoS Biol. 5: e129.

Zhao, J., V, Kulkarni, Liu N, Del Carpio DP, Bucher J, Bonnema G. *BrFLC2*(*FLOWERING LOCUS C*) as a candidate gene for a vernalization response QTL in *Brassica rapa*. J. Exp. Bot. 61: 1817-1825.

Zhao, J., V. Kulkarni, N. Liu, D. P. Del Carpio, J. Bucher and G. Bonnema. 2010. *BrFLC2* (*FLOWERING LOCUS C*) as a candidate gene for a vernalization response QTL in *Brassica rapa*. J. Exp. Bot. 61: 1817-1825.

Zheng, B. and Chen, X. 2011. Dynamics of histone H3 lysine 27 trimethylation in plant development. Curr. Opin. Plant Biol. 14: 123-129.

Zhu, A., Greaves, I. K., Dennis, E. S. and Peacock, W. J. 2017. Genome-wide analyses of four major histone modifications in Arabidopsis hybrids at the germinating seed stage. BMC Genomics 18: 137.

Zou, X., X. Tan, C. Hu, L. Zeng, G. Lu, G. Fu, Y. Cheng and X. Zhang. 2013. The transcriptome of *Brassica napus* L. roots under waterlogging at the seedling stage. Int. J. Mol. Sci. 14: 2637-2651.